Mediators of Inflammation

Inflammatory Response to Traumatic Injury: Clinical and Animal Researches in Inflammation

Guest Editors: Huang-Ping Yu, Irshad H. Chaudry, Mashkoor A. Choudhry, Chung-Hsi Hsing, Fu-Chao Liu, and Zhengyuan Xia

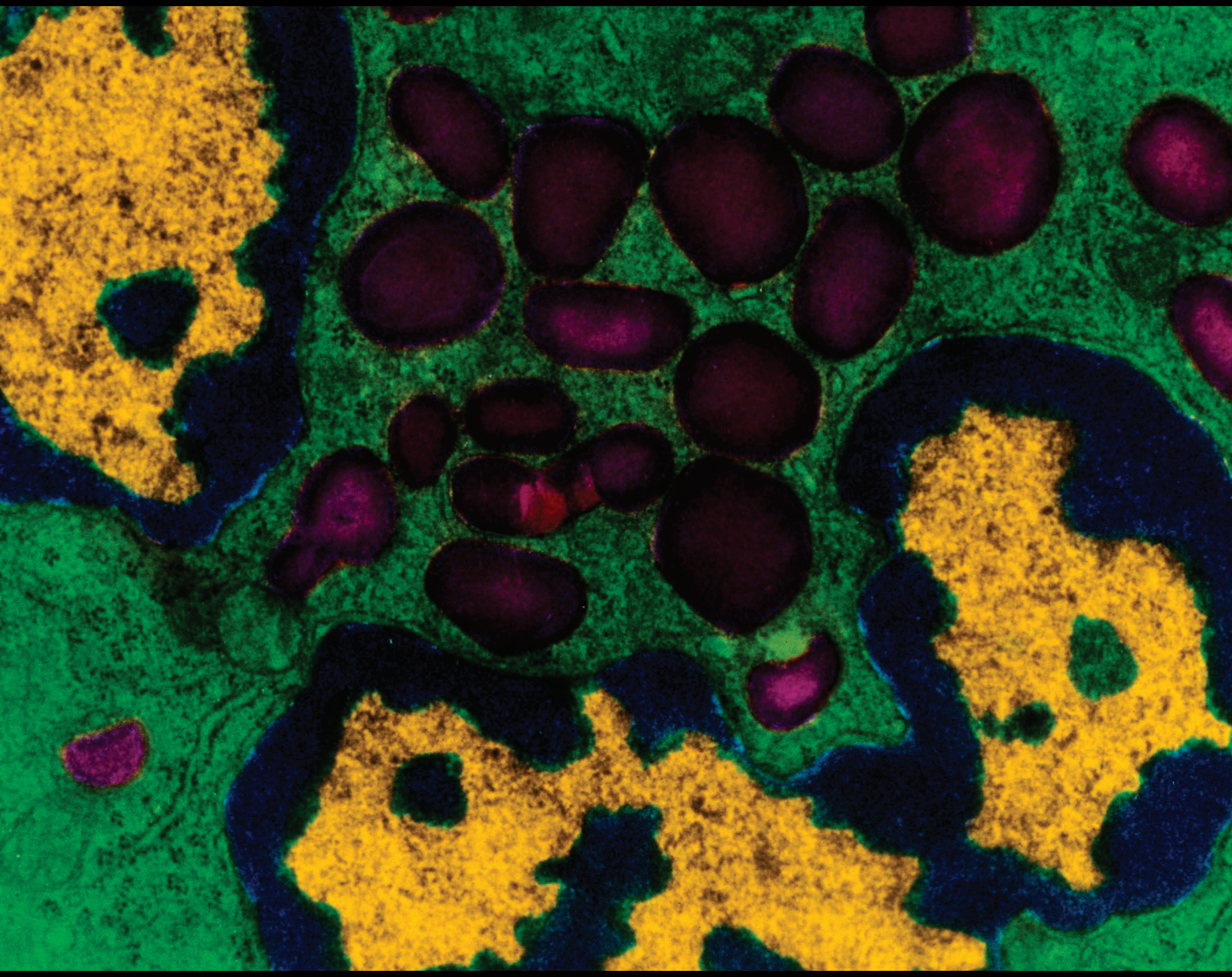

Inflammatory Response to Traumatic Injury: Clinical and Animal Researches in Inflammation

Inflammatory Response to Traumatic Injury: Clinical and Animal Researches in Inflammation

Guest Editors: Huang-Ping Yu, Irshad H. Chaudry, Mashkoor A. Choudhry, Chung-Hsi Hsing, Fu-Chao Liu, and Zhengyuan Xia

Editorial Board

Contents

Hindawi Publishing Corporation
Mediators of Inflammation
Volume 2015, Article ID 729637, 2 pages
http://dx.doi.org/10.1155/2015/729637

Editorial

Inflammatory Response to Traumatic Injury: Clinical and Animal Researches in Inflammation

Huang-Ping Yu,[1,2] Irshad H. Chaudry,[3] Mashkoor A. Choudhry,[4] Chung-Hsi Hsing,[5] Fu-Chao Liu,[1,2] and Zhengyuan Xia[6]

[1]*Department of Anesthesiology, Chang Gung Memorial Hospital, Taoyuan 333, Taiwan*
[2]*College of Medicine, Chang Gung University, Taoyuan 333, Taiwan*
[3]*Department of Surgery and Center for Surgical Research, University of Alabama at Birmingham, Birmingham, AL 35294, USA*
[4]*Department of Surgery, Loyola University Chicago Health Sciences Campus, Maywood, IL 60153, USA*
[5]*Department of Anesthesiology, Chi Mei Medical Center, Tainan 710, Taiwan*
[6]*Department of Anesthesiology, University of Hong Kong, Pokfulam, Hong Kong*

Correspondence should be addressed to Huang-Ping Yu; yuhp2001@adm.cgmh.org.tw

Received 2 June 2015; Accepted 2 June 2015

Inflammatory response is usually associated with various traumatic insults. In addition, traumatic injury produces excessive proinflammatory mediators and subsequent activating or recruiting immune cells into the target organs and results in systemic inflammatory response. However, the complex pathways and mechanisms of inflammatory responses on traumatic injury have not been clearly elucidated. The aim of this special issue is to describe the role of inflammation in traumatic injury, providing an up-to-date viewpoint for therapeutic approaches.

Patients after tangential excision surgery usually suffered from tremendous pain, which leads to anxiety, emergency, agitation, and inflammatory reaction. W. Geng et al. showed that preoperative administration of flurbiprofen axetil decreased postoperative tramadol consumption and the visual analog scale after surgery. In addition, flurbiprofen axetil attenuated emergency agitation score and Ramsay score after extubation and reduced the systemic levels of proinflammatory cytokines tumor necrosis factor-α and interleukin-6 after the operation. The adverse events induced by intubation and extubation may cause intracranial hemorrhage and increase of intracranial pressure, especially in posterior fossa surgery patients. C. Tang et al. suggested that I-gel combined with tracheal intubation could reduce the stress response of posterior fossa surgery patients. Plasma β-endorphin, cortisol, interleukin-6, tumor necrosis factor-α, malondialdehyde concentrations, and blood glucose were decreased in I-gel facilitated endotracheal tube intubation group. Utilization of I-gel combined with endotracheal tube in posterior fossa surgery may lower inflammatory and oxidative response.

Y. Chen et al. reported that sepsis-induced acute intestinal injury was attenuated by dexmedetomidine treatment. The protective effects of dexmedetomidine on sepsis-induced injury may be associated with the inhibition of inflammation via modulating toll-like receptor 4 pathway. Inhalation anesthetics isoflurane may inhibit hypoxia pulmonary vasoconstriction. In addition, dexmedetomidine can reduce the dose of isoflurane inhalation and potentiate hypoxia pulmonary vasoconstriction. R. Xia et al. reported that dexmedetomidine could augment hypoxia pulmonary vasoconstriction and improve oxygenation during one-lung ventilation through inhibiting oxidative stress and increasing nitric oxide release. Histone deacetylases modulate cytokine synthesis and release. Trichostatin A, a histone deacetylase inhibitor, is documented to be anti-inflammatory and neuroprotective. C.-H. Hsing et al. indicated that trichostatin A reduced lipopolysaccharide-induced neuroinflammation and cognitive dysfunction. J.-A. Lin et al. first identified the effects of

bone components on toll-like receptor 4 surface expression. Toll-like receptor 4 surface expression in human monocytes was used as the main target to assess immune dysfunction following bone component exposure. They found that bone component exposure downregulated toll-like receptor 4 surface expression. Perinatal insults and subsequent neuroinflammation is the major mechanism of neonatal brain injury. C.-Y. Chen et al. reported that hypoxic preconditioning conferred strong neuroprotection, likely through suppression of glial activation and subsequent inflammatory responses after hypoxia-ischemia insults in neonatal rats.

The elderly hip fracture is one of the most common injuries and represents a high incidence of complications and mortality. L. Gan et al. examined the influence of immediate surgery on systemic inflammatory response and lung injury induced by elderly hip fracture. They found that the elderly hip fracture could result in systemic inflammatory response and lung injury. In addition, the proximal femoral intramedullary pinning surgery following hip fracture aggravated the above pathological states by increasing the mitochondrial DNA release. Cardiopulmonary bypass induces neutrophil activation and release of matrix metalloproteinases-9, contributing to postoperative pulmonary infiltration and dysfunction. T.-C. Lin et al. reported that elective cardiac surgery with cardiopulmonary bypass induced short-term elevation of plasma metalloproteinases-9 concentrations within 24 hours. However, increase of neutrophils and reduced oxygenation are not correlated with cardiopulmonary bypass time and postoperative pulmonary dysfunction. Y. Tian et al. suggested that combination of 3-day captopril treatment and isoflurane preconditioning additively attenuated myocardial ischemia reperfusion by reducing oxidative stress and inflammation. Acute kidney injury is a frequent and severe complication during sepsis. Though fluid resuscitation is the main therapy, heart failure is usually lethal for those patients receiving large volumes of fluids. Y. Wang et al. reported that single small-volume resuscitation with hydroxyethyl starch and hypertonic saline hydroxyethyl starch could attenuate endotoxemia-induced kidney injury.

Resveratrol, a natural polyphenolic compound of grape and red wine, owns potential anti-inflammatory effects, which results in the reduction of cytokines overproduction, the inhibition of neutrophil activity, and the alteration of adhesion molecules expression. Resveratrol has been shown to reduce organ damage following traumatic and shock-like states. Such protective phenomenon is reported to be implicated in a variety of intracellular signaling pathways including the activation of estrogen receptor, the regulation of the sirtuin 1/nuclear factor-kappa B and mitogen-activated protein kinases/hemeoxygenase-1 pathway, and the mediation of proinflammatory cytokines, reactive oxygen species formation and reaction. F.-C. Liu et al. reviewed the organ-protective and anti-inflammatory effects of resveratrol in trauma-hemorrhagic injury. S. Hamaguchi et al. reported elevated circulating free DNA levels during early-phase sepsis might represent a candidate biomarker for the severity of sepsis. In addition, regulatory T cells suppress excessive immune responses and are potential therapeutic targets in autoimmune disease and organ transplantation rejection. C. Jun et al. found that recruitment of regulatory T cells into the kidney was related to the recovery of renal function after ischemia–reperfusion injury.

Together, the reviews, research articles, and clinical studies that are featured in this special issue enhance our knowledge base of inflammation in traumatic injury.

Huang-Ping Yu
Fu-Chao Liu
Chung-Hsi Hsing
Zhengyuan Xia
Mashkoor A. Choudhry
Irshad H. Chaudry

Hindawi Publishing Corporation
Mediators of Inflammation
Volume 2015, Article ID 632592, 11 pages
http://dx.doi.org/10.1155/2015/632592

Research Article

Hypoxic Preconditioning Suppresses Glial Activation and Neuroinflammation in Neonatal Brain Insults

Chien-Yi Chen,[1,2] Wei-Zen Sun,[3] Kai-Hsiang Kang,[4] Hung-Chieh Chou,[2] Po-Nien Tsao,[2] Wu-Shiun Hsieh,[2] and Wen-Mei Fu[4]

[1]*Graduate Institute of Clinical Medicine, National Taiwan University College of Medicine, Taipei, Taiwan*
[2]*Departments of Pediatrics, National Taiwan University Hospital and National Taiwan University College of Medicine, Taipei, Taiwan*
[3]*Department of Anesthesiology, National Taiwan University Hospital and National Taiwan University College of Medicine, Taipei, Taiwan*
[4]*Department of Pharmacology, College of Medicine, National Taiwan University, No. 1 Jen Ai Road, Section 1, Taipei 10051, Taiwan*

Correspondence should be addressed to Wen-Mei Fu; wenmei@ntu.edu.tw

Received 20 December 2014; Accepted 3 March 2015

Academic Editor: Zhengyuan Xia

Perinatal insults and subsequent neuroinflammation are the major mechanisms of neonatal brain injury, but there have been only scarce reports on the associations between hypoxic preconditioning and glial activation. Here we use neonatal hypoxia-ischemia brain injury model in 7-day-old rats and *in vitro* hypoxia model with primary mixed glial culture and the BV-2 microglial cell line to assess the effects of hypoxia and hypoxic preconditioning on glial activation. Hypoxia-ischemia brain insult induced significant brain weight reduction, profound cell loss, and reactive gliosis in the damaged hemisphere. Hypoxic preconditioning significantly attenuated glial activation and resulted in robust neuroprotection. As early as 2 h after the hypoxia-ischemia insult, proinflammatory gene upregulation was suppressed in the hypoxic preconditioning group. *In vitro* experiments showed that exposure to 0.5% oxygen for 4 h induced a glial inflammatory response. Exposure to brief hypoxia (0.5 h) 24 h before the hypoxic insult significantly ameliorated this response. In conclusion, hypoxic preconditioning confers strong neuroprotection, possibly through suppression of glial activation and subsequent inflammatory responses after hypoxia-ischemia insults in neonatal rats. This might therefore be a promising therapeutic approach for rescuing neonatal brain injury.

1. Introduction

Hypoxia-ischemia injury is the final common mechanism in different kinds of brain damage resulting from trauma. Hypoxia-ischemia injury is also the major cause of brain damage in neonates [1]. The incidence of hypoxia-ischemia encephalopathy is about 2.5 per 1,000 live births, and significant neurologic morbidity occurs in as many as 50–75% of these infants [2]. Long-term consequences, including cerebral palsy, cognitive deficits, seizure disorders, intellectual deficits, and behavioral problems, are lifelong and devastating [3]. To date, it is still a big challenge to protect the newborn brain from hypoxia-ischemia injury.

Pathophysiological features of cerebral hypoxia-ischemia are unique to the immature brain and provide the potential for clinical intervention [4]. Multiple mechanisms are involved in the pathogenesis of neonatal hypoxia-ischemia brain injury, including oxidative stress, apoptosis, and excitotoxicity. There is growing evidence to demonstrate the pivotal role of inflammation [1]. The inflammatory cascade is characterized by a rapid activation of resident microglial cells and infiltration of peripheral leukocytes into the injured parenchyma [5–7]. Astroglial cells are also activated and play a significant and sustained role in inflammation following brain trauma and hypoxia-ischemia. Once activated, these inflammatory cells contribute to neuronal damage through the release of cytotoxic mediators, including cytokines, chemokines, reactive oxygen species, adhesion molecules, and matrix metalloproteins [8]. Therapeutic approaches targeting anti-inflammation can diminish brain injury in

animal models of neonatal insults, such as antineutrophil serum [9], IL-1 receptor antagonists [10], and the microglial inhibitor minocycline [11].

Hypoxic preconditioning, or hypoxia-induced tolerance, refers to a brief period of hypoxia that protects against an otherwise lethal insult occurring minutes, hours, or days later [12]. Gidday et al. [13] were the first to show the neuroprotective effect of hypoxic preconditioning in neonatal brain injury. They found a dramatic neuroprotective effect when 7-day-old rats were exposed to 8% oxygen (hypoxic admixture) for 3 hours, followed by combined hypoxia-ischemia (8% oxygen plus carotid artery occlusion) 24 hours later. Several subsequent studies further examined the underlying mechanisms, including the roles of the adenosine A1 receptor [14], vascular endothelial growth factor (VEGF) [15], erythropoietin (EPO) [16], nitric oxide synthase (NOS) [17], hypoxia-inducible factor (HIF) [18], glycogen [19], and others [20]. Most of these studies focused on neuronal [21] and vascular structure [22], but the role of glial cells in hypoxic preconditioning was seldom explored. The beneficial effects of hypoxic preconditioning might involve counter-regulation of glial activation and subsequent inflammatory processes following the cerebral hypoxia-ischemia insult. In this study, we examined whether hypoxic preconditioning renders glial cells hyporesponsive due to hypoxia-ischemia induced activation. The anti-inflammatory effect of hypoxic preconditioning in glial cells was studied both *in vivo* and *in vitro*.

2. Materials and Methods

2.1. Animals. All experiments were performed in accordance with the National Institutes of Health Guidelines on Laboratory Animal Welfare and were approved by the Animal Care and Use Committee of the College of Medicine, National Taiwan University. Ten to twelve Sprague-Dawley pups per dam were used in this study and housed in institutional standard cages on a 12-hour light/12-hour dark cycle, with *ad libitum* access to water and food. The pups were housed with their dams until weaning on postnatal day 21 (P21). Only male rat pups were used in this study.

2.2. Hypoxic Preconditioning in Rat Pups. A modified Rice-Vannucci model was used for the induction of hypoxia-ischemia (HI) brain damage in 7-day-old (P7) neonatal rats [23]. P7 rats were anesthetized with isoflurane (3.5% for induction and 1.5% for maintenance) in a mixture of nitrogen and oxygen, delivered via a facial mask. The right common carotid artery was dissected and cut between double ligatures of Prolene sutures (6-0). After anesthesia and surgery, the animals were allowed to recover for at least 1 h. The litters were then placed in a 3.0-liter airtight plastic box submerged in a 37°C water bath and flushed for 2 h with a humidified mixture of 8% oxygen and 92% nitrogen, delivered at a rate of 2 L/min. After hypoxia-ischemia, the pups were returned to and kept with their dams (HI group). Hypoxia preconditioning (HP) was performed as described by Gidday et al. [13]. Six-day-old (P6) Sprague-Dawley rats were exposed to 8% oxygen for 3 h followed by a combined hypoxia-ischemia insult 1 day later, as described above (HP + HI group). Sham-operated controls received anesthesia and neck incision without carotid artery ligation and did not receive the hypoxia insult (sham group).

2.3. Hemispheric Weight Reduction. On day 14 after birth (P14), the pups were anaesthetized with isoflurane and decapitated and the brains were removed ($n = 6$ in each group). After removal of the brainstem and cerebellum, the forebrain was sectioned at the midline, and both hemispheric weights were determined. A previous study showed that the extent of unilateral reduction in hemispheric weight is highly correlated with biochemical, electrophysiological, and morphometric markers of tissue injury, in the same animal model [24]. Therefore, the percentage reduction in hemispheric weight was used as a measurement of cerebral injury in this study, calculated as (left hemisphere weight − right hemisphere weight)/left hemisphere weight.

2.4. Nissl and Immunohistochemistry Staining. Brains were collected 24 h after HI injury (P8) for immunohistochemistry assessment of glial activation and Nissl staining was performed for evaluation of structural and cellular damage ($n = 5$ in each group). The pups were anaesthetized with isoflurane and perfused transcardially with ice-cold saline followed by 4% paraformaldehyde in 0.1 M phosphate-buffered saline (PBS). Brains were then removed, postfixed overnight in 4% paraformaldehyde, and then transferred into a 30% sucrose solution for 72 h. At this time, brains were embedded and frozen in Neg-50 (Richard-Allan Scientific, Thermo Fisher Scientific, Kalamazoo, MI, USA) for storage at −80°C. Coronal sections were cut at 20 μm on a Leica cryostat and collected serially onto gelatin-coated slides for storage at −80°C.

For Nissl staining, the brain sections were rinsed with PBS twice and then stained with 0.1% cresyl violet solution for 5 min. After rinsing quickly in distilled water, the sections were dehydrated in 100% alcohol for 10 min, cleared in xylene, and then mounted with permanent mounting medium.

Immunohistochemistry was performed to identify activated microglia and macrophages using the marker CD11b, and glial fibrillary acidic protein (GFAP) was used as a marker of activated astrocytes. Briefly, sections were thawed and treated with 3% hydrogen peroxide for 30 min. After blocking in 4% nonfat milk containing 0.4% Triton X-100 for 60 min at room temperature, the sections were incubated overnight at 4°C with primary antibodies against CD11b (1 : 200; Serotec, Oxford, UK) and GFAP (1 : 500; Lab Vision Corporation). Sections were then washed several times in PBS and incubated with a biotinylated secondary antibody and then treated using an avidin-biotin complex kit (ABC kit; Vector Laboratories. Burlingame, California). Finally, the labeling was detected by treatment with 0.01% hydrogen peroxide and 0.05% 3,3′-diaminobenzidine (DAB; Sigma, St. Louis, MO, USA). The DAB reaction was stopped by rinsing tissues in PBS. Labeled tissue sections were then mounted and analyzed under a bright-field microscope.

Table 1: List of primers used for RT-PCR.

Gene name	Accession number	Sequence	Position	Product length
iNOS	NM_010927.2	F 5′-CCTTGTTCAGCTACGCCTTC-3′	1841–1860	573 bp
		R 5′-GGCTGGACTTTTCACTCTGC-3′	2413–2394	
COX-2	NM_011198.3	F 5′-TGATGACTGCCCAACTCCCATG-3′	527–547	723 bp
		R 5′-AATGTTGAAGGTGTCCGGCAGC-3′	1249–1228	
TNF-α	NM_013693.2	F 5′-TCAGCCTCTTCTCATTCCTGC-3′	254–274	203 bp
		R 5′-TTGGTGGTTTGCTACGACGTG-3′	456–436	
IL-1β	NM_008361.3	F 5′-CTCCATGAGCTTTGTACAAGG-3′	545–565	245 bp
		R 5′-TGCTGATGTACCAGTTGGGG-3′	789–770	
GAPDH	XM_001478528.1	F 5′-ACCACAGTCCATGCCATCAC-3′	579–598	452 bp
		R 5′-TCCACCACCCTGTTGCTGTA-3′	1030–1011	

2.5. Hypoxia and Reoxygenation in a Mixed Primary Glial Culture and Microglial BV-2 Cell Line. Primary glial cultures were prepared according to a previous report [25]. In brief, mixed glial cultures were prepared using brains of 1-day-old pups from Sprague-Dawley rats. After anesthesia, the pups were decapitated, cerebral hemispheres were harvested, and the meninges removed. Minced pooled tissue was then digested with 0.25% trypsin, centrifuged, and dissociated into a single-cell suspension by gentle trituration. After filtration, the cells were seeded at a density of 1×10^7 cells into 75 cm^2 flasks in Dulbecco's modified Eagle's medium (DMEM; Gibco, Grand Island, NY, USA) containing 10% heat-inactivated fetal bovine serum (FBS; Gibco), 2 mM L-glutamine, 1 mM sodium pyruvate, 100 mM nonessential amino acids, 100 U/mL penicillin, and 100 mg/mL streptomycin. Cell cultures were maintained at 37°C in a humidified atmosphere of 5% CO_2 and 95% air, and medium was replenished twice a week. These cells were used for experiments after reaching confluence (7-8 days).

The murine BV-2 cell line was cultured in DMEM with 10% FBS at 37°C in a humidified incubator in 5% CO_2 and 95% air. Confluent cultures were passaged by trypsinization. All the cells were plated on 12-well plates at a density of 2.5×10^5 cells/well for nitrite assays or on 6-well plates at a density of 5×10^5 cells/well for reverse transcriptase-polymerase chain reaction (RT-PCR). The cells were then cultured for 2 days before experimental treatment.

Hypoxia/reoxygenation was performed as previously described with some modifications [25]. To generate the hypoxic condition, the cultures were gassed with 0.5% O_2, 94.5% N_2, and 5% CO_2 (Ruskinn Hypoxic Gas Mixer, Model INVIVO2 200, serial number BBD902300), and control cultures were incubated under normoxic conditions for the same duration. After the indicated hypoxic period, reoxygenation was performed by transferring the cells into a regular normoxic incubator (95% air, 5% CO_2), and cells were incubated for another 24 h for nitrite assays. For RT-PCR, total RNA was extracted from the cells after termination of hypoxia, using the same method outlined above.

2.6. Cell Viability and Nitrite Assays. Cell viability was assessed by the 3-(4,5-dimethylthiazol-2-yl)-5-(3-carboxymethoxyphenyl)-2-(4-sulfophenyl)-2H-tetrazolium (MTT) assay. Cells cultured in 12-well plates were exposed to hypoxia (0.5, 1, 2, and 4 h) or lipopolysaccharide (1 μM). After incubation for 24 h, 20 μL CellTiter 96 AQueous One Solution Reagent (Promega, Madison, WI, USA) was added to culture wells for 30 min. One hundred microliters of the culture medium from each well was transferred to an ELISA 96-well plate, and absorbance at 490 nm was measured with a 96-well plate reader. The absorbance at 490 nm is directly proportional to the number of living cells in culture.

Accumulation of nitrite in the medium was determined using a colorimetric assay with Griess reagent. Briefly, 100 μL of culture supernatant reacted with an equal volume of Griess reagent (one part 0.1% naphthylethylenediamine and one part 1% sulfanilamide in 5% H_3PO_4) in 96-well cell culture plates for 10 min at room temperature in the dark. Nitrite concentrations were determined by using standard solutions of sodium nitrite prepared in cell culture medium. The absorbance at 550 nm was determined using a microplate reader (BioTek, Winooski, VT, USA).

2.7. Reverse Transcriptase-Polymerase Chain Reaction. Total RNA was extracted from brain tissue homogenates ($n = 4$ in each group) or cell culture ($n = 5$ in each group) using an RNeasy mini Kit (Qiagen, Valencia, CA, USA). Two micrograms of RNA was used for RT-PCR. The reaction mixture contained 1 μg Oligo $(dT)_{15}$ Primer, 0.02 mM deoxynucleotide triphosphate (dNTP), 40 U RNase Inhibitor, 100 U M-MLV Reverse Transcriptase, and 5x Reaction Buffer (Promega Corporation, Madison, WI, USA). PCR was performed using an initial step of denaturation (5 min at 94°C), 25 cycles of amplification (94°C for 30 s, 55°C for 30 s, and 72°C for 30 s), and an extension (72°C for 7 min). PCR products were analyzed on 1.5% agarose gels. The mRNA of glyceraldehyde 3-phosphate dehydrogenase (GAPDH) served as the internal control for sample loading and mRNA integrity. All of the mRNA levels were normalized to the level of GAPDH expression. The oligonucleotide primers are shown in Table 1.

2.8. Detection of Inflammatory Mediators by ELISA. Two major proinflammatory cytokines, tumor necrosis factor-alpha (TNF-α) and interleukin-1 beta (IL-1β), were detected using ELISA kits (R&D Systems, Minneapolis, MN, USA),

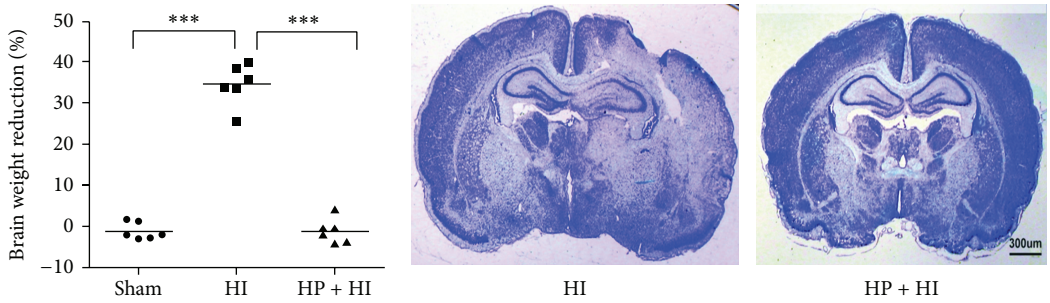

Figure 1: Hypoxia preconditioning exerts significant neuroprotection in neonatal hypoxia-ischemia brain injury. (a) The ratio of hemispheric brain weight reduction measured 7 days after hypoxia-ischemia injury was significantly reduced in the hypoxia preconditioning group (HP + HI), compared with the hypoxia-ischemia only (HI) group. (b) Nissl stained frozen sections showed extensive brain damage in the ipsilateral hemisphere 24 h after hypoxia-ischemia injury (HI, left panel), which was attenuated by hypoxia preconditioning (HP + HI, right panel).

according to the manufacturer's instructions. Briefly, pups were sacrificed by decapitation at 2, 6, 12, 24, and 72 h after HI ($n = 4$ for each time point per group) and protein samples of the ipsilateral hemispheric cortex from each pup were collected. All protein concentrations were determined by the Bradford method (Bio-Rad Bulletin 1177, Bio-Rad Laboratories, Hercules, CA, USA). Data were acquired using a 96-well plate reader (BioTek). The cytokine content is expressed as pg cytokines/mg protein.

2.9. Statistical Analysis. Data are presented as mean ± SEM. The comparisons for brain weight reduction were performed by one-way analysis of variance (ANOVA). The mRNA levels and protein concentrations at different time points were analyzed by two-way ANOVA to compare the HI and HP + HI groups. Individual groups were then compared using Bonferroni's post hoc tests, as appropriate. Statistical analyses were performed using Prism GraphPad v.5.0 (GraphPad Software, San Diego, CA, USA), with a significance level of $P < 0.05$.

3. Results

3.1. Hypoxia Preconditioning Is Neuroprotective and Attenuates Microglial and Astroglial Activation after a Hypoxia-Ischemia Insult in Neonatal Rats. The mean ratio of brain weight reduction of the right hemisphere, measured 7 days after right carotid artery ligation and exposure to 2 h of hypoxia in the HI group, was 34.6 ± 2.1%; this reduction was significantly greater than in the HP + HI group. The ratio of brain weight reduction was not statistically different between HP + HI and sham groups. The percentages for brain weight reduction are individually illustrated in Figure 1(a). Twenty-four hours after the hypoxia-ischemia insult, Nissl stained coronal sections at the level of the dorsal hippocampus demonstrated widespread injury in the right hemisphere of the HI group (Figure 1(b)). The numbers of normal-appearing neurons in neocortex, hippocampus, and striatum were also markedly decreased in the HI group. In contrast, brain weight reductions were significantly attenuated, and there was a marked increase in the number of normal-appearing neurons in rats that underwent 3 h of hypoxia preconditioning 24 h before hypoxia-ischemia injury (HP + HI group). The brain sections in the HP + HI group also showed minimal morphological damage. Hypoxia preconditioning in P7 rats provided nearly complete neuroprotection against hypoxia-ischemia injury, based on morphological indicators.

To identify the effect of hypoxia preconditioning on glial response after hypoxia-ischemia injury, we used CD11b immunostaining to determine microglial activation and GFAP immunostaining to determine astrocytic activation (Figure 2). Twenty-four hours after hypoxia-ischemia injury in the HI group, numerous CD11b-positive microglia and GFAP-positive astroglia were observed in the ipsilateral hemisphere. These cells were scattered throughout the entire cortex and hippocampus. Most microglia were round-shaped with thick processes, and these cells were considered to be in an activated state. The reactive astroglia were also detected in the ipsilateral hemisphere and had a similar spatial distribution to the activated microglia. In the HP + HI group, the numbers of CD11b-positive microglia and GFAP-positive astroglia were much less than in the HI group. The morphology of microglia in the HP + HI group was also different to the HI group. The CD11b-positive cells in the ipsilateral hemisphere of rats from the HP + HI group (Figure 2, second lane) and in the contralateral hemispheres of the HI rats (not shown) appeared as ramified microglia, indicative of the resting state. These results demonstrate that the activation of microglia and astroglia following neonatal hypoxia-ischemia injury was attenuated by hypoxia preconditioning.

3.2. Hypoxia Preconditioning Suppresses Hypoxia-Ischemia Injury-Induced Inflammation in Neonatal Brain. We next examined the effect of hypoxia preconditioning on the inflammatory response induced by hypoxia-ischemia injury. Comparing the mRNA levels of the right cortex in the HP + HI group with the HI group, inducible NOS (iNOS) and IL-1β upregulation were significantly reduced as early as 2 h after the hypoxia-ischemia insult (Figure 3(a)). Six hours after the hypoxia-ischemia insult, mRNA expression of all inflammatory mediators was markedly increased in

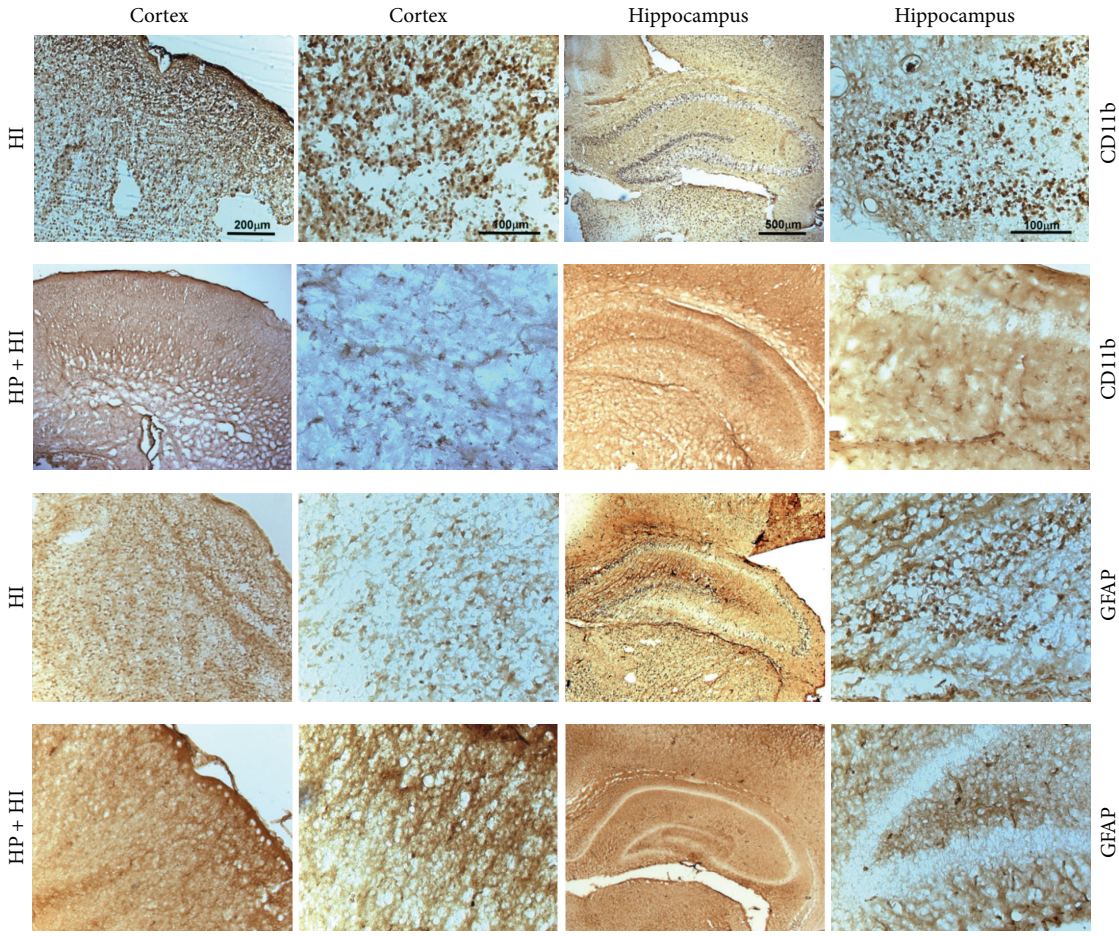

Figure 2: Hypoxia preconditioning inhibits microglial and astroglial activation in neonatal hypoxia-ischemia brain injury. Hypoxia-ischemia (HI) significantly induced microglial (first panel, CD11b) and astroglial activation (third panel, GFAP) in the cerebral cortex and hippocampus, which was correlated with neuronal damage (as shown in Figure 1). Hypoxia preconditioning (HP + HI) diminished the activation of microglial (second panel, CD11b) and astroglial cells (fourth panel, GFAP) after hypoxia-ischemia injury. Based on morphological observations, most microglial cells in the representative section were in an activated state in HI group, but a ramified form (resting state) in the HP + HI group.

the HI group. Hypoxia preconditioning significantly suppressed upregulation of the cytokine genes, TNF-α and IL-1β, at 6 h. Hypoxia preconditioning also suppressed COX-2 upregulation 6 h after hypoxia-ischemia injury in the HP + HI group (but this only reached marginal significance; $P = 0.08$). We thus extracted total protein from the right cortex and further evaluated TNF-α and IL-1β protein expression by ELISA at different time points (Figure 3(b)). The levels of TNF-α were very low in the sham group (0.08 ± 0.02 pg/mg protein) and were increased markedly at 2 h after the hypoxia-ischemia insult (1.65 ± 0.32 pg/mg protein, HI group). These levels peaked at 6 h (3.42 ± 0.88 pg/mg protein, HI group) and were decreased after 12 h. Hypoxia preconditioning resulted in a significant reduction of the TNF-α level at 6 h (1.16 ± 0.04 pg/mg protein, HP + HI group). The level of IL-1β was also very low at baseline (0.71 ± 0.1 pg/mg protein, sham group), slightly increased 2 h after the hypoxia-ischemia insult (3.15 ± 0.52 pg/mg protein, HI group), and markedly elevated 6 h after the hypoxia-ischemia insult (25.97 ± 3.89 pg/mg protein, HI group). Hypoxia preconditioning before the hypoxia-ischemia insult markedly decreased the IL-1β levels at 6 h (10.19 ± 1.47 pg/mg protein, HP + HI group). Therefore, hypoxia preconditioning was able to suppress the hypoxia-ischemia injury-induced inflammatory response in neonatal rat brain.

3.3. Hypoxia Preconditioning Suppresses Hypoxia-Induced Glial Cell Activation In Vitro. To further clarify the role of glial cells in the anti-inflammatory mechanisms of hypoxia preconditioning, we next examined the glial response to hypoxia preconditioning at the cellular level. Firstly, nitrite production and cell viability after hypoxia exposure for different time durations were determined in a primary mixed glial culture and in the microglial cell line, BV-2 (Figure 4). Exposure to hypoxic conditions for less than 1 h did not increase nitrite production in either the primary mixed glial culture or the BV-2 cell line. However, nitrite production increased as hypoxia duration increased, for exposure times exceeding 1 h. Cell viability was not significantly changed, except for 8 h of hypoxia.

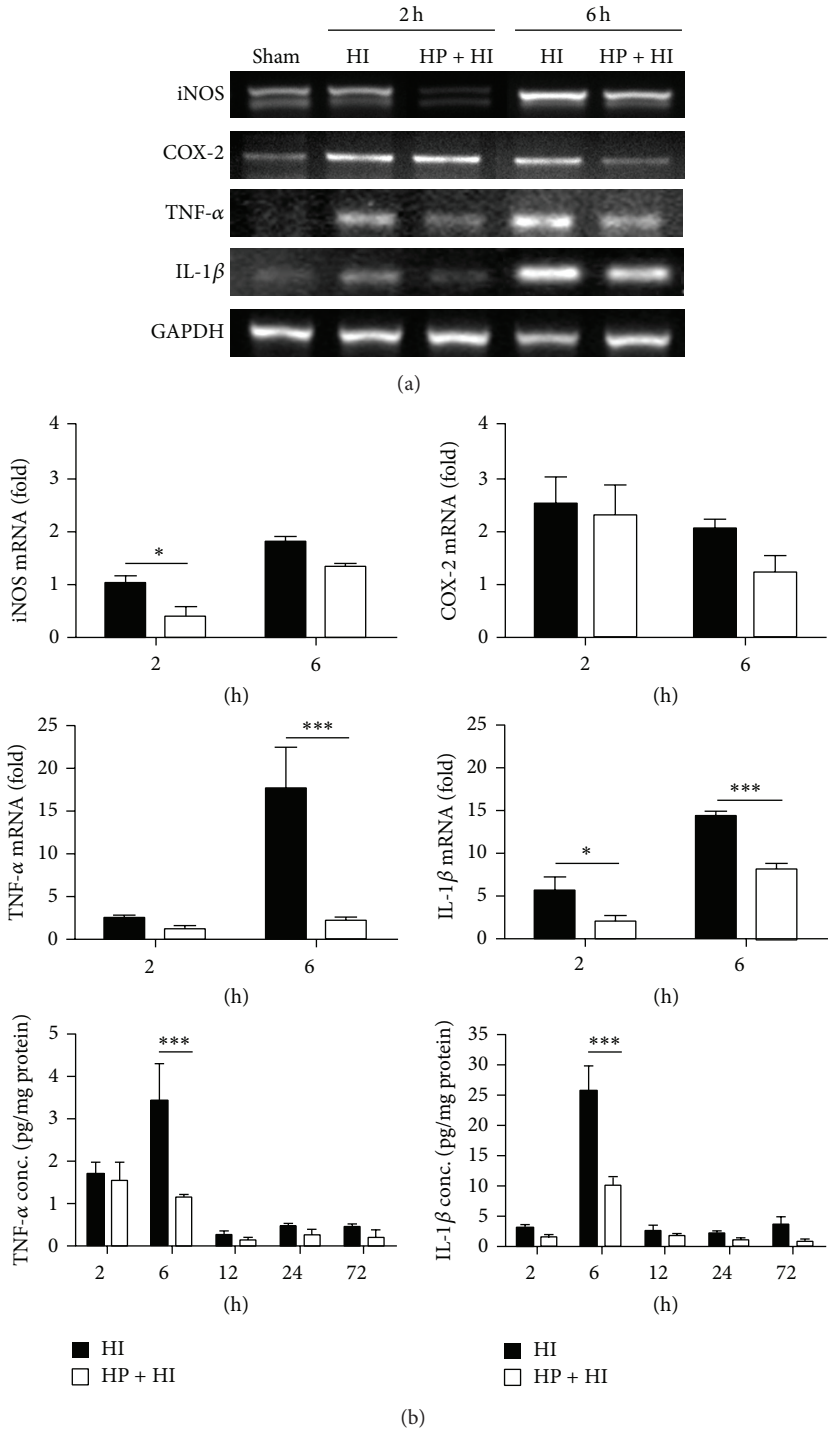

Figure 3: Hypoxia preconditioning reduces proinflammatory gene expression in neonatal hypoxia-ischemia brain injury. (a) The mRNA levels of inducible nitric oxide synthase (iNOS), cyclooxygenase-2 (COX-2), tumor necrosis factor-alpha (TNF-α), and interleukin-1 beta (IL-1β) in the ipsilateral cerebral cortex from neonatal rats were determined at 2 and 6 h after hypoxia-ischemia (HI) injury ($n = 4$ in each group). The gene expression levels were upregulated by HI injury, especially at 6 h after injury. Hypoxia preconditioning (HP + HI) was able to significantly suppress these responses. (b) The protein concentrations of TNF-α and IL-1β were determined by ELISA at different time points ($n = 4$ in each group). The suppression of inflammatory mediators in the HP + HI group was significant at 6 h after HI. ((a), (b)) Data represented as the mean ± standard error of the mean (SEM). $^{*}P < 0.05$ compared with HI, $^{***}P < 0.001$ compared with HI, and $P = 0.08$ for COX-2 mRNA level at 6 h for HP + HI group compared with HI group.

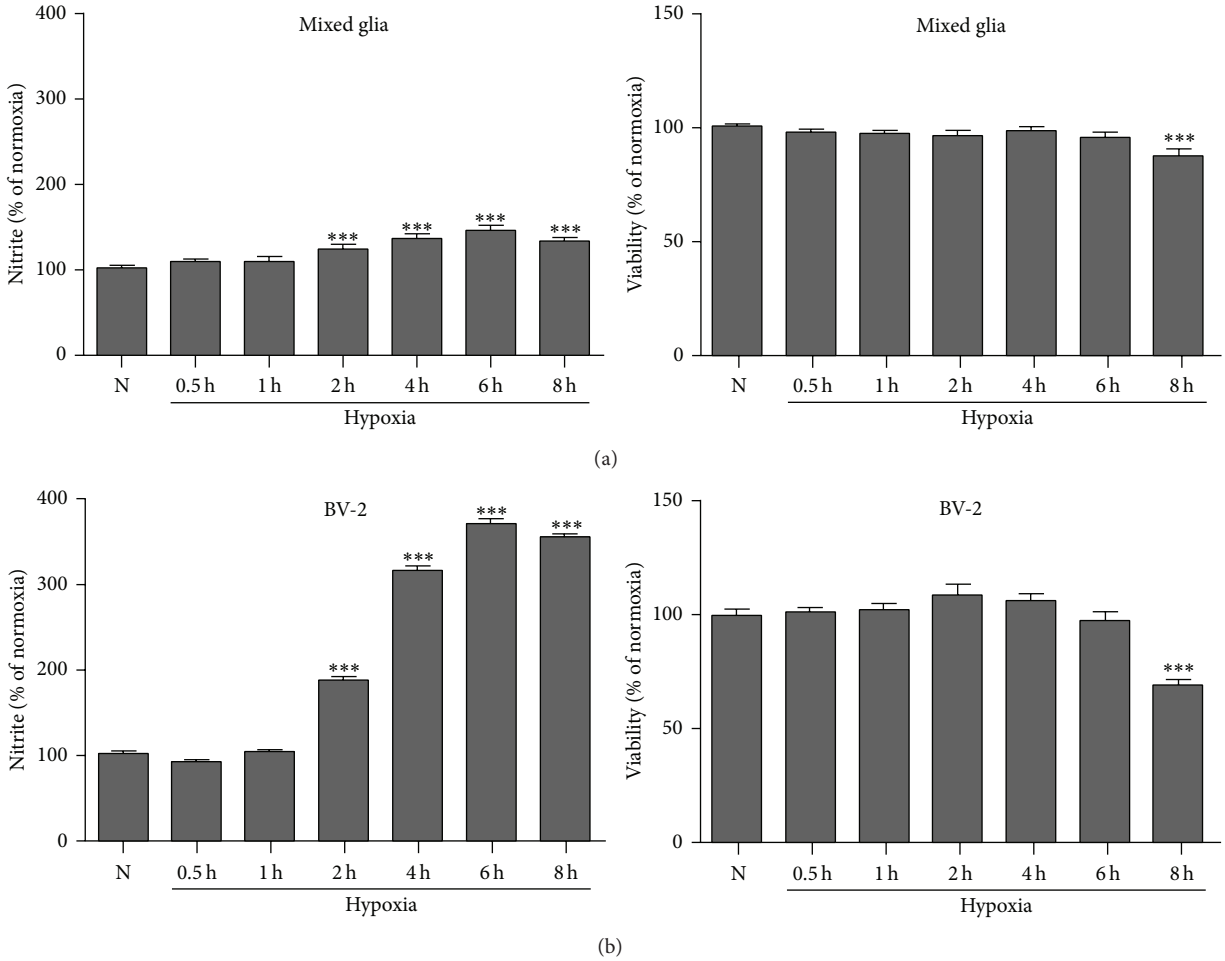

Figure 4: Hypoxia insult induces glial activation in cultured glial cells without reducing cell viability. Nitrite production and cell viability were determined in a primary mixed glial culture (a) and in the BV-2 microglial cell line (b) after exposure to hypoxia, at various time intervals (as indicated). Hypoxia durations up to 6 h increased nitrite production in a time-dependent manner without reducing cell viability. Hypoxia exposure for 8 h was able to induce a low level of cell death. The data represent the mean ± standard error of the mean (SEM), based on five independent experiments in each group. ((a), (b)) $^{***}P < 0.001$ compared with HI group.

We then used mixed primary glial cultures to investigate the effect of hypoxia preconditioning. The cells were preexposed to hypoxia for 0.5, 1, or 2 h and then returned to the normoxia incubator. Twenty-four hours later, these cells were incubated in a hypoxia chamber again for 4 h, which mimics the *in vivo* model of hypoxia preconditioning. The production of nitrite after reoxygenation was decreased significantly by hypoxia preconditioning for 0.5 h, but not for 1 or 2 h (Figure 5(a)), and cell viability stayed the same. The expression of proinflammatory genes was also evaluated by RT-PCR (Figure 5(b)). Hypoxia preconditioning for 0.5 h significantly suppressed the expression of COX-2 genes. These results indicate that hypoxia preconditioning for 0.5 h exerts the most pronounced effect on suppression of inflammatory mediators in primary mixed glial cultures. To examine the response of isolated microglia, the same experimental protocol was also applied in the BV-2 microglial cell line. The levels of nitrite were decreased significantly by 0.5–2 h hypoxia preconditioning (Figure 6(a)). The expression levels of TNF-α (Figure 6(b)) and IL-1β (Figure 6(c)) were suppressed by 0.5 h hypoxia preconditioning in the BV-2 cell line.

4. Discussion

There is emerging evidence indicating that inflammatory processes play a pivotal role in the pathogenesis of neonatal brain injury [5, 9, 26]. In the present study, we found that the inflammatory cascade was initiated with the release of proinflammatory mediators within hours after exposure to a hypoxia-ischemia insult. The expression of proinflammatory genes increased as early as 2 hours after hypoxia-ischemia in the neonatal brain. The expression levels of TNF-α and IL-1β were even more significant 6 hours after the hypoxia-ischemia insult. The inflammatory events were accompanied by activation of resident glial cells. Twenty-four hours after the hypoxia-ischemia insult, extensive activation and proliferation of microglial and astroglial cells were noted in the cortex and hippocampus, with associated tissue damage. The astrocytes were hypertrophic and the microglial cells

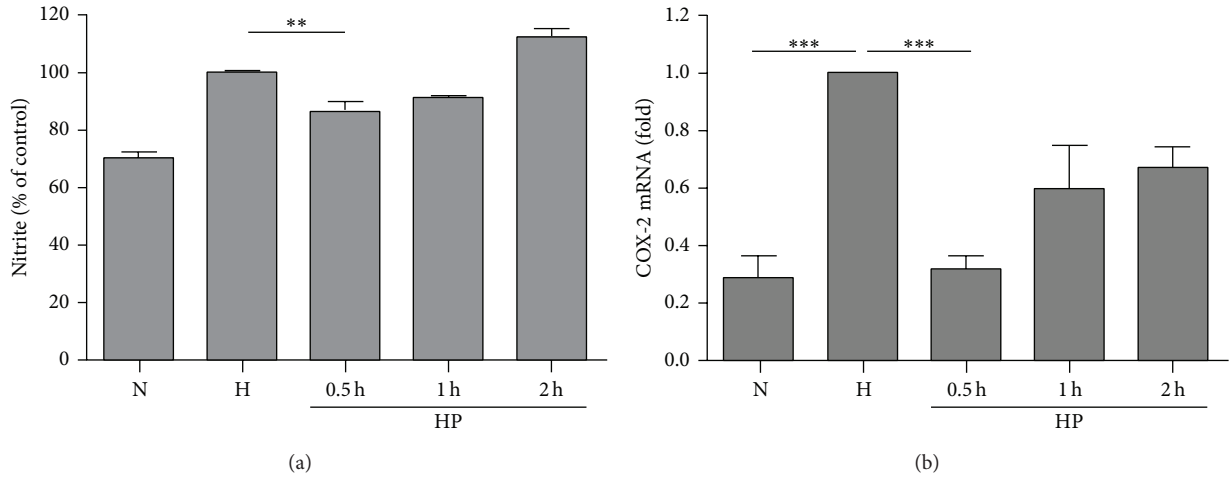

Figure 5: Hypoxia preconditioning suppresses prolonged hypoxia-induced inflammation in primary mixed glial culture. (a) Brief hypoxia exposure for 0.5 h before prolonged hypoxia damage (4 h) significantly reduced the production of nitrite. $^{**}P < 0.01$ compared with hypoxia control. (b) mRNA expression of cyclooxygenase-2 (COX-2) was also significantly suppressed by brief hypoxic preconditioning for 0.5 h. $^{***}P < 0.001$ compared with normoxia and hypoxia control. ((a), (b)) The data represent the mean ± standard error of the mean (SEM), based on five independent experiments in each group.

also appeared in their activated state, with an enlarged cell body and shorter but thicker cellular processes. Activation of glial cells enhances the inflammatory process and further exacerbates brain damage.

Our finding in the present study also complements the previous inference that 3 hours of hypoxia exposure, 24 hours before the hypoxia-ischemia insult, markedly reduces neonatal brain injury [13, 18, 27]. In our study, hypoxia preconditioning provides robust endogenous neuroprotection. Compared to the nonischemic left cerebral hemisphere, the brain weight reduction for the injured right hemisphere was 34.6%. However, hypoxia preconditioning 1 day before hypoxia-ischemia injury completely rescued right hemispheric structural damage, as illustrated in Figure 1. The left brain hemisphere in the HI group was exposed to only 2 hours of hypoxic gas without disruption of carotid artery blood flow. Based on the results of Nissl staining in the left hemisphere of the HI group, which revealed normal structure and cellularity, it could be argued that hypoxic preconditioning *per se* did not cause structural damage in normal rats, which is compatible with evidence from previous studies [13, 23]. Since the structural neuroprotective effect of hypoxia preconditioning is quite striking, further identification of the underlying mechanism may have an important role in the development of therapeutic strategies. Several pathways have been linked with hypoxia preconditioning in neurons [15, 21], but only a few studies assessed the role of glial cells [7, 28]. Our study demonstrates that hypoxia preconditioning attenuates activation and infiltration of microglial and astroglial cells after hypoxia-ischemia in neonatal brain. Most microglial cells in the ipsilateral cortex and hippocampus remained in the resting form in the hypoxia preconditioning group.

Hypoxia-ischemia-induced expression for iNOS, COX-2, TNF-α, and IL-1β was also significantly suppressed after hypoxia preconditioning treatment. The results suggest that hypoxia preconditioning also exerted anti-inflammatory effects in neonates that were subsequently exposed to a hypoxia-ischemia insult, through inhibition of glial activation. Whether all types of cerebral preconditioning share the same molecular mechanism is not yet clear and will need further investigation [29]. Rosenzweig et al. [30] demonstrated that LPS preconditioning suppressed neutrophil infiltration into the brain and microglial/macrophage activation in the ischemic hemisphere. The expression of TNF-α and production of reactive oxygen species were also reduced [31]. Similar to ischemic and LPS preconditioning, we have also demonstrated in this study that hypoxia preconditioning was able to suppress the cellular inflammatory response after exposure to global cerebral insults. Diminished activation of glial cell responses, which ordinarily exacerbates ischemic injury, may contribute to the neuroprotection conferred by hypoxia preconditioning.

It may be argued that a diminished inflammatory reaction arises from a reduction in neuronal damage and is not a direct cellular response. We thus developed an *in vitro* model of hypoxia preconditioning to assess the cellular response. In a mixed glial culture, a prior exposure to brief hypoxia 24 hours before the prolonged hypoxia insult significantly reduced the production of inflammatory mediators (such as nitrite) and the expression of the inflammatory related gene, COX-2. Our results also showed that a longer period of hypoxia preconditioning had less of an anti-inflammatory effect, which implies the importance of selecting the appropriate duration for hypoxia preconditioning. The induction of proinflammatory cytokine genes, including TNF-α and IL-1β, was not as prominent as for the *in vivo* model. The difference in cytokine response may be due to the recruitment of circulating white blood cells. In the animal model, hypoxia-ischemia will induce migration and infiltration of circulating macrophages

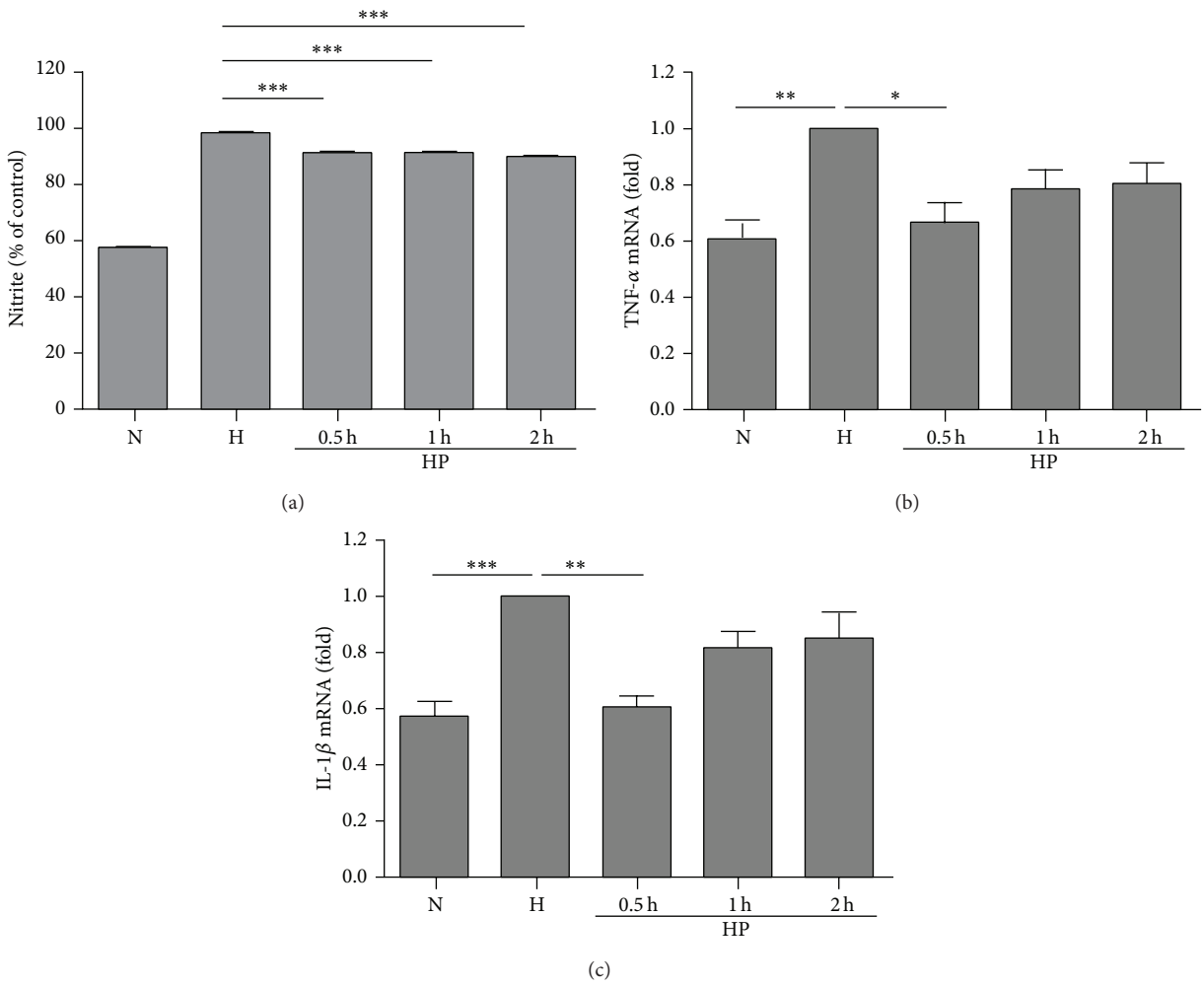

Figure 6: Hypoxia preconditioning suppresses prolonged hypoxia-induced inflammation in the BV-2 microglial cell line. (a) Brief hypoxia exposure (0.5, 1, and 2 h) before prolonged hypoxia damage (4 h) significantly reduced the production of nitrite. $^{***}P < 0.001$ compared with hypoxia control. (b) mRNA expression of tumor necrosis factor-alpha (TNF-α) was suppressed by brief hypoxia preconditioning. $^{**}P < 0.01$ compared with normoxia control and $^{*}P < 0.05$ compared with hypoxia control. (c) mRNA expression of interleukin-1 beta (IL-1β) was also suppressed by brief hypoxia preconditioning. $^{***}P < 0.001$ compared with normoxia control and $^{**}P < 0.01$ compared with hypoxia control. ((a), (b), (c)) The data represent the mean ± standard error of the mean (SEM), based on five independent experiments in each group.

and monocytes, further increasing proinflammatory cytokine release [32]. The major cell type in mixed glial culture is astroglia, which might have a lower production of cytokines. Thus, we further evaluated the microglial response to hypoxia preconditioning using the microglial cell line, BV-2. The production of nitrite and expression of TNF-α and IL-1β were all significantly increased after hypoxia exposure for 4 hours, and hypoxia preconditioning for the optimal duration (0.5 h) was able to attenuate the activation effects. Again, longer durations of hypoxia preconditioning decreased the anti-inflammation effects, as in primary mixed glia cultures.

Glial cells, in particular astrocytes, are usually viewed as supporters of neuronal function. However, numerous studies are increasingly demonstrating the important role of glial cells in preserving brain function under physiological and pathological conditions [33]. The generation of anti-inflammatory cytokines and trophic factors by preconditioned astrocytes might also contribute to neuroprotection [34]. The suppression of glial cell activation and subsequent inflammatory reactions, as shown in the present study, might contribute to the cerebral protective effects of hypoxia preconditioning.

The results of the present study can also be extrapolated to other mechanisms of neonatal brain injury. An increasing body of evidence has demonstrated a link between inflammation and long-term brain dysfunction. A recent meta-analysis of 26 articles has shown a positive association between infection and cerebral palsy, in both preterm and full-term infants [35]. In addition, the expression levels of inflammatory cytokines and chemokines in amniotic fluids and cord blood have been shown to correlate with neonatal brain injury and later developmental disability [36, 37]. In preventing these consequences, induction of an endogenous anti-inflammatory response by hypoxia preconditioning may be beneficial to protect neurons from brain damage.

5. Conclusions

In conclusion, hypoxic preconditioning induced significant neuroprotection against neonatal hypoxia-ischemia brain insults and suppressed astroglial and microglial activation in the ischemic cortex and hippocampus. Pretreatment with sublethal exposure to hypoxia before prolonged hypoxia injury prevented the cellular inflammatory response in the primary glial culture and microglial cell line BV-2. These results further address the importance of anti-inflammatory strategies in preventing neonatal brain injury.

Conflict of Interests

The authors declare that there is no conflict of interests regarding the publication of this paper.

Acknowledgments

The authors would like to thank the Second Core Lab of the Department of Medical Research of National Taiwan University Hospital for technical assistance. This work was partially supported by National Taiwan University Hospital, Taiwan, Grant nos. NTUH.96-M-041 and UN104-020. The authors also would like to thank Dr. Chih-Peng Lin, Department of Anesthesiology, National Taiwan University Hospital, for helping to prepare the revised paper.

References

[1] D. M. Ferriero, "Neonatal brain injury," *The New England Journal of Medicine*, vol. 351, no. 19, pp. 1985–1995, 2004.

[2] J. Y. Yager, E. A. Armstrong, and A. M. Black, "Treatment of the term newborn with brain injury: simplicity as the mother of invention," *Pediatric Neurology*, vol. 40, no. 3, pp. 237–243, 2009.

[3] J. J. Volpe, *Neurology of the Newborn*, Saunders/Elsevier, Philadelphia, Pa, USA, 5th edition, 2008.

[4] A. J. du Plessis and J. J. Volpe, "Perinatal brain injury in the preterm and term newborn," *Current Opinion in Neurology*, vol. 15, no. 2, pp. 151–157, 2002.

[5] A. McRae, E. Gilland, E. Bona, and H. Hagberg, "Microglia activation after neonatal hypoxic-ischemia," *Developmental Brain Research*, vol. 84, no. 2, pp. 245–252, 1995.

[6] J. A. Ivacko, R. Sun, and F. S. Silverstein, "Hypoxic-ischemic brain injury induces an acute microglial reaction in perinatal rats," *Pediatric Research*, vol. 39, no. 1, pp. 39–47, 1996.

[7] C. Kaur, G. Rathnasamy, and E.-A. Ling, "Roles of activated microglia in hypoxia induced neuroinflammation in the developing brain and the retina," *Journal of Neuroimmune Pharmacology*, vol. 8, no. 1, pp. 66–78, 2013.

[8] F. Stigger, G. Lovatel, M. Marques et al., "Inflammatory response and oxidative stress in developing rat brain and its consequences on motor behavior following maternal administration of LPS and perinatal anoxia," *International Journal of Developmental Neuroscience*, vol. 31, no. 8, pp. 820–827, 2013.

[9] S. Hudome, C. Palmer, R. L. Roberts, D. Mauger, C. Housman, and J. Towfighi, "The role of neutrophils in the production of hypoxic-ischemic brain injury in the neonatal rat," *Pediatric Research*, vol. 41, no. 5, pp. 607–616, 1997.

[10] D. Martin, N. Chinookoswong, and G. Miller, "The interleukin-1 receptor antagonist (rhIL-1ra) protects against cerebral infarction in a rat model of hypoxia-ischaemia," *Experimental Neurology*, vol. 130, no. 2, pp. 362–367, 1994.

[11] K. L. Arvin, B. H. Han, Y. Du, S.-Z. Lin, S. M. Paul, and D. M. Holtzman, "Minocycline markedly protects the neonatal brain against hypoxic-ischemic injury," *Annals of Neurology*, vol. 52, no. 1, pp. 54–61, 2002.

[12] R. A. Stetler, R. K. Leak, Y. Gan et al., "Preconditioning provides neuroprotection in models of CNS disease: paradigms and clinical significance," *Progress in Neurobiology*, vol. 114, pp. 58–83, 2014.

[13] J. M. Gidday, J. C. Fitzgibbons, A. R. Shah, and T. S. Park, "Neuroprotection from ischemic brain injury by hypoxic preconditioning in the neonatal rat," *Neuroscience Letters*, vol. 168, no. 1-2, pp. 221–224, 1994.

[14] M. A. Pérez-Pinźon, P. L. Mumford, M. Rosenthal, and T. J. Sick, "Anoxic preconditioning in hippocampal slices: role of adenosine," *Neuroscience*, vol. 75, no. 3, pp. 687–694, 1996.

[15] Y. Feng, P. G. Rhodes, and A. J. Bhatt, "Hypoxic preconditioning provides neuroprotection and increases vascular endothelial growth factor A, preserves the phosphorylation of Akt-Ser-473 and diminishes the increase in caspase-3 activity in neonatal rat hypoxic-ischemic model," *Brain Research*, vol. 1325, pp. 1–9, 2010.

[16] M. Bernaudin, A.-S. Nedelec, D. Divoux, E. T. MacKenzie, E. Petit, and P. Schumann-Bard, "Normobaric hypoxia induces tolerance to focal permanent cerebral ischemia in association with an increased expression of hypoxia-inducible factor-1 and its target genes, erythropoietin and VEGF, in the adult mouse brain," *Journal of Cerebral Blood Flow & Metabolism*, vol. 22, no. 4, pp. 393–403, 2002.

[17] J. M. Gidday, A. R. Shah, R. G. Maceren et al., "Nitric oxide mediates cerebral ischemic tolerance in a neonatal rat model of hypoxic preconditioning," *Journal of Cerebral Blood Flow and Metabolism*, vol. 19, no. 3, pp. 331–340, 1999.

[18] M. Bergeron, J. M. Gidday, A. Y. Yu, G. L. Semenza, D. M. Ferriero, and F. R. Sharp, "Role of hypoxia-inducible factor-1 in hypoxia-induced ischemic tolerance in neonatal rat brain," *Annals of Neurology*, vol. 48, no. 3, pp. 285–296, 2000.

[19] R. M. Brucklacher, R. C. Vannucci, and S. J. Vannucci, "Hypoxic preconditioning increases brain glycogen and delays energy depletion from hypoxia-ischemia in the immature rat," *Developmental Neuroscience*, vol. 24, no. 5, pp. 411–417, 2002.

[20] H.-S. Sun, B. Xu, W. Chen et al., "Neuronal K(ATP) channels mediate hypoxic preconditioning and reduce subsequent neonatal hypoxic-ischemic brain injury," *Experimental Neurology*, vol. 263, pp. 161–171, 2015.

[21] S. G. Benitez, A. E. Castro, S. I. Patterson, E. M. Muñoz, and A. M. Seltzer, "Hypoxic preconditioning differentially affects GABAergic and glutamatergic neuronal cells in the injured cerebellum of the neonatal rat," *PLoS ONE*, vol. 9, no. 7, Article ID e102056, 2014.

[22] A. Boroujerdi and R. Milner, "Defining the critical hypoxic threshold that promotes vascular remodeling in the brain," *Experimental Neurology*, vol. 263, pp. 132–140, 2015.

[23] J. E. Rice III, R. C. Vannucci, and J. B. Brierley, "The influence of immaturity on hypoxic-ischemic brain damage in the rat," *Annals of Neurology*, vol. 9, no. 2, pp. 131–141, 1981.

[24] P. Andine, M. Thordstein, I. Kjellmer et al., "Evaluation of brain damage in a rat model of neonatal hypoxic-ischemia," *Journal of Neuroscience Methods*, vol. 35, no. 3, pp. 253–260, 1990.

[25] D.-Y. Lu, W.-H. Yu, W.-L. Yeh et al., "Hypoxia-induced matrix metalloproteinase-13 expression in astrocytes enhances permeability of brain endothelial cells," *Journal of Cellular Physiology*, vol. 220, no. 1, pp. 163–173, 2009.

[26] H. Hagberg, E. Gilland, E. Bona et al., "Enhanced expression of interleukin (IL)-1 and IL-6 messenger RNA and bioactive protein after hypoxia-ischemia in neonatal rats," *Pediatric Research*, vol. 40, no. 4, pp. 603–609, 1996.

[27] R. C. Vannucci, J. Towfighi, and S. J. Vannucci, "Hypoxic preconditioning and hypoxic-ischemic brain damage in the immature rat: Pathologic and metabolic correlates," *Journal of Neurochemistry*, vol. 71, no. 3, pp. 1215–1220, 1998.

[28] E. Suryana and N. M. Jones, "The effects of hypoxic preconditioning on white matter damage following hypoxic-ischaemic injury in the neonatal rat brain," *International Journal of Developmental Neuroscience*, vol. 37, pp. 69–75, 2014.

[29] N. Zhang, X. Zhang, X. Liu et al., "Chrysophanol inhibits NALP3 inflammasome activation and ameliorates cerebral ischemia/reperfusion in mice," *Mediators of Inflammation*, vol. 2014, Article ID 370530, 12 pages, 2014.

[30] H. L. Rosenzweig, N. S. Lessov, D. C. Henshall, M. Minami, R. P. Simon, and M. P. Stenzel-Poore, "Endotoxin preconditioning prevents cellular inflammatory response during ischemic neuroprotection in mice," *Stroke*, vol. 35, no. 11, pp. 2576–2581, 2004.

[31] H. Y. Lin, C. C. Huang, and K. F. Chang, "Lipopolysaccharide preconditioning reduces neuroinflammation against hypoxic ischemia and provides long-term outcome of neuroprotection in neonatal rat," *Pediatric Research*, vol. 66, no. 3, pp. 254–259, 2009.

[32] D. Amantea, G. Nappi, G. Bernardi, G. Bagetta, and M. T. Corasaniti, "Post-ischemic brain damage: pathophysiology and role of inflammatory mediators," *The FEBS Journal*, vol. 276, no. 1, pp. 13–26, 2009.

[33] G. Trendelenburg and U. Dirnagl, "Neuroprotective role of astrocytes in cerebral ischemia: focus on ischemic preconditioning," *Glia*, vol. 50, no. 4, pp. 307–320, 2005.

[34] J. M. Gidday, "Cerebral preconditioning and ischaemic tolerance," *Nature Reviews Neuroscience*, vol. 7, no. 6, pp. 437–448, 2006.

[35] Y. W. Wu and J. M. Colford Jr., "Chorioamnionitis as a risk factor for cerebral palsy: a meta-analysis," *The Journal of the American Medical Association*, vol. 284, no. 11, pp. 1417–1424, 2000.

[36] R. Romero, R. Gomez, J. H. Choi, and I. O. Kim, "Amniotic fluid inflammatory cytokines (interleukin-6, interleukin-1beta, and tumor necrosis factor-alpha), neonatal brain white matter lesions, and cerebral palsy," *The American Journal of Obstetrics and Gynecology*, vol. 177, no. 1, pp. 19–26, 1997.

[37] T. Kaukola, E. Satyaraj, D. D. Patel et al., "Cerebral palsy is characterized by protein mediators in cord serum," *Annals of Neurology*, vol. 55, no. 2, pp. 186–194, 2004.

Hindawi Publishing Corporation
Mediators of Inflammation
Volume 2015, Article ID 587378, 11 pages
http://dx.doi.org/10.1155/2015/587378

Research Article

The Immediate Intramedullary Nailing Surgery Increased the Mitochondrial DNA Release That Aggravated Systemic Inflammatory Response and Lung Injury Induced by Elderly Hip Fracture

Li Gan,[1,2] Jianfeng Zhong,[1,2] Ruhui Zhang,[3] Tiansheng Sun,[1,2] Qi Li,[1] Xiaobin Chen,[2] and Jianzheng Zhang[2]

[1]*Department of Orthopaedics, Zhujiang Hospital, Southern Medical University, Guangzhou, Guangdong 510282, China*
[2]*Department of Orthopaedics, Beijing Army General Hospital, Beijing 100700, China*
[3]*Department of Respiratory Diseases, Chronic Airways Diseases Laboratory, Nanfang Hospital, Southern Medical University, Guangzhou, Guangdong 510282, China*

Correspondence should be addressed to Tiansheng Sun; hamyyj@126.com and Qi Li; 260693016@qq.com

Received 12 December 2014; Revised 8 February 2015; Accepted 20 February 2015

Academic Editor: Chung-Hsi Hsing

Conventional concept suggests that immediate surgery is the optimal choice for elderly hip fracture patients; however, few studies focus on the adverse effect of immediate surgery. This study aims to examine the adverse effect of immediate surgery, as well as to explore the meaning of mtDNA release after trauma. In the experiment, elderly rats, respectively, received hip fracture operations or hip fracture plus intramedullary nail surgery. After fracture operations, the serum mtDNA levels as well as the related indicators of systemic inflammatory response and lung injury significantly increased in the rats. After immediate surgery, the above variables were further increased. The serum mtDNA levels were significantly related with the serum cytokine (TNF-α and IL-10) levels and pulmonary histological score. In order to identify the meaning of mtDNA release following hip fracture, the elderly rats received injections with mtDNA. After treatment, the related indicators of systemic inflammatory response and lung injury significantly increased in the rats. These results demonstrated that the immediate surgery increased the mtDNA release that could aggravate systemic inflammatory response and lung injury induced by elderly hip fracture; serum mtDNA might serve as a potential biomarker of systemic inflammatory response and lung injury following elderly hip fracture.

1. Introduction

Hip fracture is the most serious consequence of falling in the elderly; 87% to 96% of hip fracture patients are 65 years of age or older, and hip fractures are associated with numerous complications and increased mortality [1, 2]. The overall in-hospital mortality of elderly patients with hip fracture is nearly 5.0% [3]. The major causes of the high mortality are complications associated with the fracture event [4]. Of these complications, lung infection is the most common cause of mortality [1]. Traditionally, long-term bed rest is considered the main risk factor for the development of lung infections and death, and early and ultraearly surgery in hip fracture patients can reduce the postoperative complications and mortality associated with long-term best rest [5–8]. However, our recent studies have demonstrated that hip fracture in the elderly can induce systemic inflammatory responses and lung injury, which increase the risk of pulmonary infection and death during the postinjury period [9–11]. In addition, damage control orthopedics (DCO) findings suggest that immediate definitive fixation of long-bone fractures can be detrimental to patients who are physiologically unstable [12, 13].

Therefore, it is necessary to confirm the influence of immediate surgery on systemic inflammatory responses and lung injury after hip fracture in elderly patients.

Mitochondria are evolutionary endosymbionts that were derived from bacteria [14] and therefore contain bacterial molecular motifs. Previous studies have implicated mitochondrial damage-associated molecular patterns (DAMPs) with sterile inflammation [15–18]. In addition, mtDNA has been detected in the plasma of trauma patients and causes functionally important immune consequences [19–21]. However, the role of mtDNA remains uncertain in systemic inflammatory responses and lung injury induced by hip fracture in the elderly. Our study aimed to investigate the patterns of mtDNA release in a fracture model and a fracture plus surgery model as well as to evaluate the relationship between mtDNA and posttraumatic inflammation. Understanding the relationship between mtDNA and posttraumatic inflammation may help elucidate the underlying pathophysiological mechanisms through which trauma induces SIRS and may facilitate the identification of novel therapeutic targets. In addition, understanding the patterns of mtDNA release may help to predict the occurrence of posttraumatic inflammation.

2. Materials and Methods

This paper consisted of two parts. In the first part, we studied the influence of immediate surgery on the elderly hip fracture rats. In the second part, we investigated the effects of serum mtDNA on the elderly rats.

2.1. Animals. Twenty- to 23-month-old rats are considered elderly [22]. A total of 85 elderly male Sprague-Dawley (SD) rats (age: 22-23 months; weight: 450–550 g) were purchased from Beijing Haiwang Experimental Animal Center and were housed in a climate-controlled barrier facility with 12 h light/dark cycles at 24 ± 2°C and free access to food and water for a period of at least 1 week prior to the experimental procedures; the rats were then maintained at the Beijing Military Generational Hospital. The experiments were performed according to the guidelines for Experimental Animal Care and Use approved by the Beijing Military General Hospital Ethics Committee (Permit number: 20140218).

2.2. Grouping of Animals. In order to study the influence of immediate surgery on the elderly hip fracture rats, in the first part of the experiment, 60 elderly rats were randomly divided into three groups. The sham group ($n = 20$) only received anesthesia, the fracture group ($n = 20$) received anesthesia and underwent hip fracture operations, and the fracture plus surgery group ($n = 20$) underwent proximal femoral intramedullary nail surgery in addition to receiving anesthesia and undergoing hip fracture operations.

2.3. Fracture Model. The rats in the fracture group and the fracture plus surgery group were anesthetized with 10% chloral hydrate (3.5 mL kg^{-1}, i.p.) and then placed in a prone position on the base of a blunt guillotine ramming apparatus. Rats were fixed after the proximal femur was identified and marked. The 500 g blunt guillotine was lifted to a 15 cm height and was allowed to fall freely along the axis. The force of the falling object resulted in a unilateral closed proximal femoral fracture (hip fracture).

2.4. Proximal Femoral Intramedullary Pinning Surgery. The surgery was performed immediately after fracture according to Sears et al. [23]. Prophylactic preoperative antibiotics (gentamicin, 5 mg/kg) were administered before incision. A proximal lateral femoral incision (approximately 0.5 cm) was made, and the fracture ends were exposed. A 1.25 mm Kirschner wire was retrogradely inserted into the proximal femoral medullary cavity using a drill, and the proximal part of the pin emerged from the piriform fossa. The proximal portion of the pin was connected to the drill, and the distal femoral medullary cavity was entered. Fracture reduction was performed during the insertion of the Kirschner wire. The proximal portion of the pin was cut, and the incision was closed with 3-0 polyglycolic acid sutures. The animals in the fracture group and the fracture plus surgery group were administered Buprenex (buprenorphine, 0.1 mg/kg) every 10–12 h for pain control.

2.5. Collection of Samples. The rats were sacrificed at 8, 24, 48, and 72 h after treatment. Each thorax was opened rapidly; subsequently, blood samples were collected by heart puncture and were centrifuged at 3000 rpm for 10 min to separate the serum from cellular blood components. The serum was stored at −80°C for the later mtDNA and cytokine assays. Lung tissues were quickly harvested. The left trachea was exposed, and the bronchoalveolar lavage fluid was collected three times through a tracheal cannula with autoclaved PBS that was instilled up to a total volume of 1.0 mL and then centrifuged at 3000 rpm for 10 min. The supernatant was frozen at −80°C until the subsequent cytokine and protein assays. The right middle lung lobes were removed for the MPO and NE assays. The rest of the right lung was fixed immediately in 10% formalin and stored at 4°C for subsequent histological observation and pathological scoring.

2.6. Histological Analysis. Lung specimens were embedded in paraffin. Tissue sections (5–8 μm) were prepared and stained with hematoxylin and eosin (H&E). Briefly, 3 slices were randomly selected from each rat, and 3 fields of each slice were reviewed under a microscope (100x magnification, Olympus DP71, Tokyo, Japan). All slides were examined and scored by an experienced pathologist (Ru Hui) who was blinded to the experimental groups based on the lung injury scoring system [24]. The score was based on categories of inflammatory cell infiltration, pulmonary edema, congestion, and intra-alveolar hemorrhage that were graded on a scale of normal (0), mild (1), moderate (2), or severe (3) injury, with a maximum possible score of 12.

2.7. Protein Assay. The total protein concentration in the BALF was determined using a BCA protein assay kit (Pierce

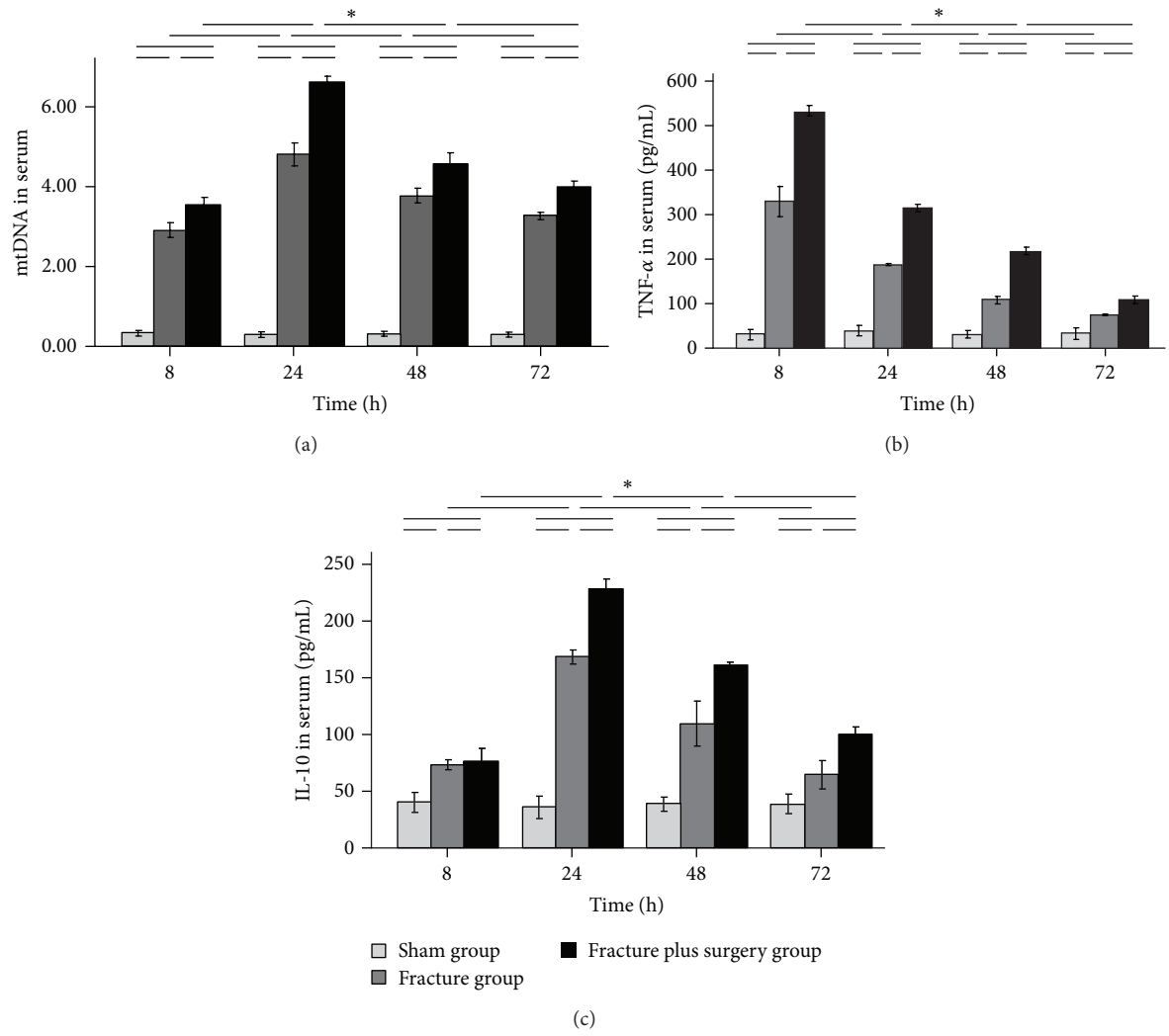

Figure 1: Time course of serum mtDNA (a), TNF-α (b), and IL-10 (c) levels. Results are expressed as mean ± standard error. $^{*}P < 0.05$ when compared to other groups.

Biotechnology, USA) following the manufacturer's instructions.

2.8. Cytokines Assay. The cytokines (TNF-α and IL-10) in the serum and BALF were measured using an enzyme-linked immunosorbent assay (ELISA) system (R&D Systems, USA) following the manufacturer's instructions.

2.9. MPO and NE Activity Assay. The right middle lung lobes were placed in 1 mL of homogenization buffer (4°C). Samples were homogenized and incubated at 4°C for 1 h. The final homogenate was centrifuged at 10,000 rpm for 15 min. Tissue supernatants were used for the determination of MPO and NE activity. MPO activity was measured using an MPO kit (Miltenyi Biotec, Germany) according to the manufacturer's instructions. NE activity was determined using a quantitative sandwich enzyme immunoassay (R&D Systems, USA) following the manufacturer's instructions.

2.10. Serum mtDNA Isolation. Serum was extracted before the blood samples were incubated at 37°C for 1 h and centrifuged at 2500 rpm for 10 min. Serum DNA was extracted from 200 μL of serum using a QIAamp Blood Mini Kit based on affinity columns (Qiagen, Hilden, Germany) according to the manufacturer's recommendations.

2.11. FQ-PCR. MtDNA gene primers were designed according to a previous study [25]: forward, CAGCCGCTATTAAAGGTTCG; and reverse, CCTGGATTACTCCGGTCTGA. The product size was 79 bp. The mtDNA plasmid was constructed using a TA cloning kit as follows: the purified PCR products were linked into the pMD18-T vector (TaKaRa, Japan), and the connective product was transformed to DH5α

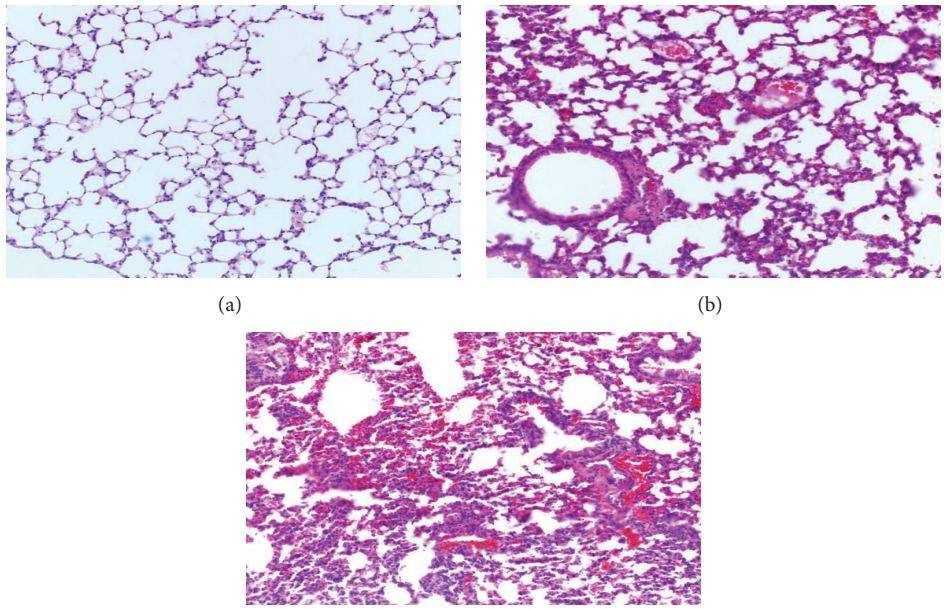

(a) (b) (c)

Figure 2: Representative H&E sections of pulmonary tissues (magnification, 100x). After treatment, the sham group (a) had no obvious inflammation; the fracture group (b) and the fracture plus surgery group (c) showed typical symptoms of acute lung injury.

competent *Escherichia coli*. The positive *E. coli* clones were screened and enriched, and then mtDNA was extracted from the plasmid and measured. A standard curve was generated by six dilutions of DNA (rang 10^2–10^7 copies/μL) using an ABI 7500 sequence detection system (ABI, USA). FQ-PCR reactions were conducted in 96-well plates within a total volume of 20 μL/well containing the following reagents: SYBR Premix Ex Taq II (2x): 10 μL; forward primer: 0.8 μL; reverse primer: 0.8 μL; ROX reference Dye II (50x): 0.4 μL; DNA: 2 μL; and ddH_2O: 6 μL. The PCR kit was purchased from TaKaRa Company (TaKaRa, Japan). The PCR reaction was conducted using the following conditions: 95°C for 30 s, followed by 95°C for 5 s and 60°C for 34 s, repeated for 40 cycles. Each sample and DNA standard was analyzed in duplicate, and the mean value was used for quantification. Only standard curves with a coefficient of correlation >0.96 were accepted.

2.12. Rat Femur mtDNA Preparation. In order to identify the effects of serum mtDNA on the elderly rats, in the second part of the experiment, 5 elderly rats were sacrificed by cervical dislocation, their femurs were collected, and the femoral mitochondria was isolated using a mitochondrial isolation kit (Pierce, USA) according to the manufacturer's instructions. Subsequently, the mitochondrial pellets were resuspended in Hanks' balanced salt solution (HBSS) (Gibco Life Technologies, USA). After a protease inhibitor cocktail (1 : 100) (Qiagen, USA) was added, the suspension was sonicated on ice (VCX130-Vibra Cell, USA) at 100% amplitude 10 times for 30 s each with 30 s intervals. The mtDNA was isolated by centrifugation at 15,000 ×g for 10 min at 4°C followed by centrifugation at 100,000 ×g at 4°C for 30 min. The mtDNA were extracted from the isolated mitochondrial pellets using the DNeasy Blood and Tissue Kit (Qiagen) following manufacturer's instructions. The purity and concentrations of the mtDNA were determined by FQ-PCR and spectrophotometry, respectively.

2.13. mtDNA Inoculation of Animals. 20 elderly rats were randomly divided into control group and mtDNA group. The control group ($n = 10$) received intravenous injections with 1 mL PBS; the mtDNA group ($n = 10$) received injections with 1 mL of 10 μg/mL mtDNA. The mtDNA concentration was selected according to our previous experiments [21]. After 24 h, the animals were sacrificed by cervical dislocation, and then specimens were collected and detected as the first part.

2.14. Statistical Analysis. Data are presented as the means ± standard deviation. All data were analyzed by SPSS software (version 13.0). One-way ANOVA with Bonferroni post hoc tests were performed to compare the data from all groups at each monitoring point. Quantitative data were compared between two groups using the t-test. To evaluate the predictive value of mtDNA and cytokines (TNF-α and IL-10), a linear regression analysis was applied to measure the relationships between pulmonary histological score and the mtDNA and cytokine levels. A P value of less than 0.05 was considered statistically significant.

3. Results

3.1. The Influence of Immediate Surgery on Elderly Hip Fracture Rats

3.1.1. Changes of mtDNA, TNF-α, and IL-10 Levels in Serum. The serum mtDNA, TNF-α, and IL-10 levels in the fracture

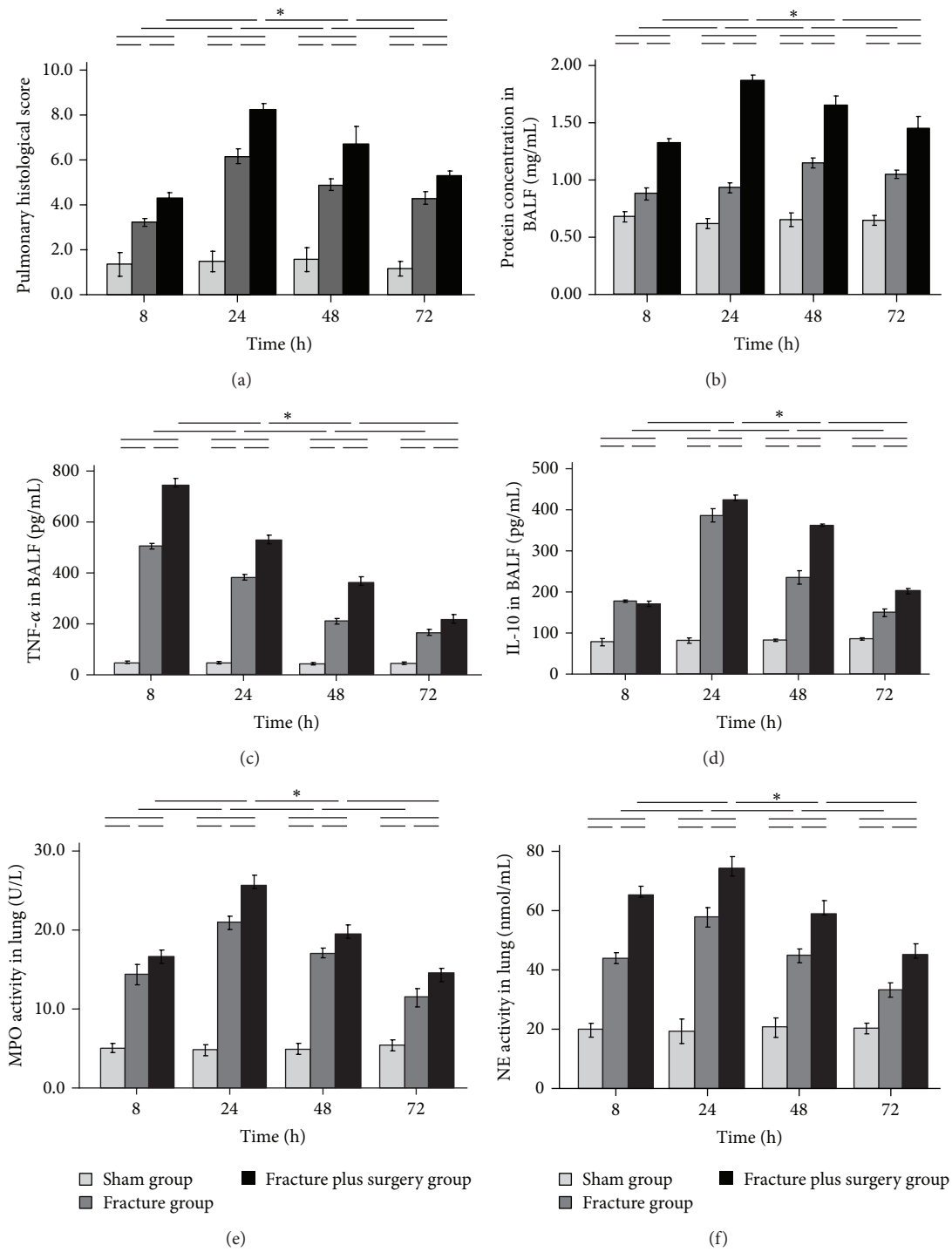

Figure 3: Time course of the pulmonary histological score (a), the protein (b), TNF-α (c), and IL-10 (d) concentrations in BALF and the lung tissue MPO (e) and NE (f) activity. Results are expressed as mean ± standard error. $^{*}P < 0.05$ when compared to other groups.

group and the fracture plus surgery group increased rapidly after treatment, peaked at 24 h (with the exception of TNF-α, which peaked at 8 h), and were significantly higher than those in the sham group at all time points (all $P < 0.05$). Compared with the fracture group, at 8, 24, 48, and 72 h after treatment, the above variables were higher in the fracture plus surgery group (all $P < 0.05$) (Figure 1).

3.1.2. Pulmonary Changes. As shown in Figure 2(a), the lung tissue structure of the sham group was clear, and

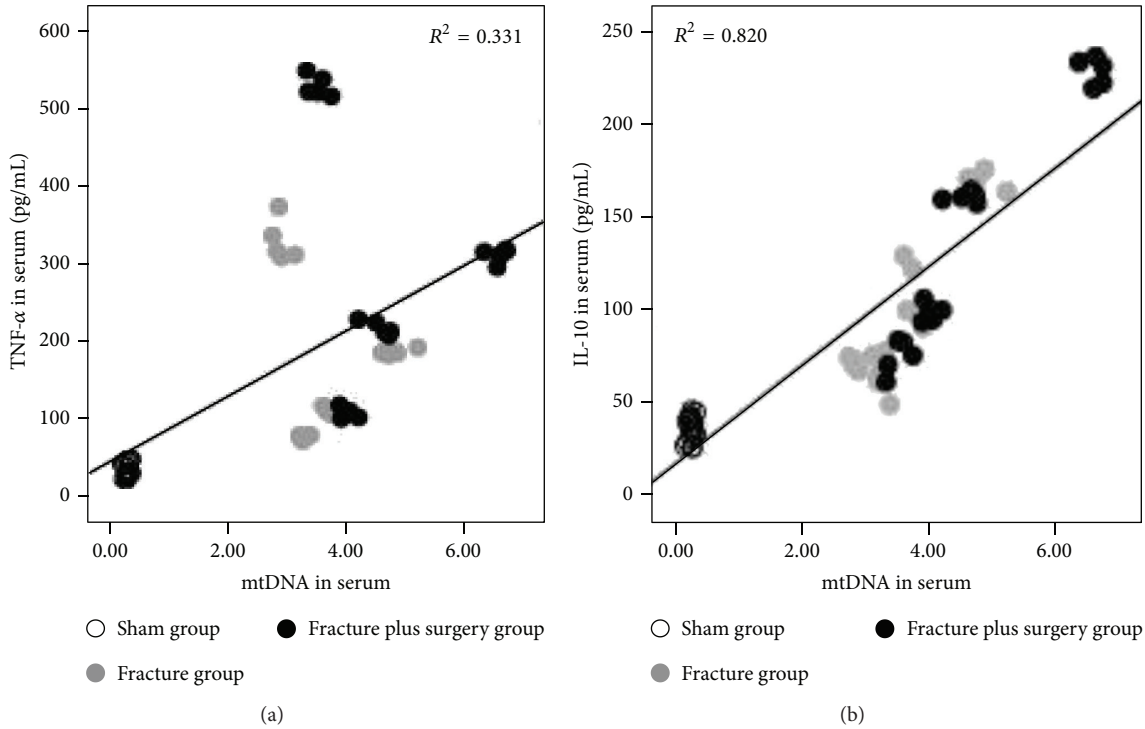

Figure 4: Scatter plots and regression lines showed that the serum TNF-α (a) and IL-10 (b) concentrations exhibited a significant relationship with the serum mtDNA levels.

the alveolar walls were normal without significant inflammatory corpuscle infiltration after treatment. However, the pulmonary tissue slices of the fracture group (Figure 2(b)) and the fracture plus surgery group (Figure 2(c)) exhibited increased congestion, pulmonary edema, polymorphonuclear and mononuclear cell infiltrates, and damaged alveolar architecture.

As shown in Figure 3, at 8, 24, 48, and 72 h after treatment, the pulmonary histological score, the cytokine (TNF-α and IL-10) and protein concentrations in BALF, and the lung tissue MPO and NE activity of the fracture group and the fracture plus surgery group increased rapidly after treatment, peaked at 24 h (except TNF-α, which peaked at 8 h), and were higher than the respective values in the sham group at all time points (all $P < 0.05$). Compared with the fracture group, at 8, 24, 48, and 72 h after treatment, the above variables were higher in the fracture plus surgery group (all $P < 0.05$).

3.2. The Results of the Linear Regression Analysis. The results of the linear regression analysis revealed that the serum mtDNA levels exhibited a significant relationship with the serum TNF-α ($B = 0.004$, $P = 0.000$) and IL-10 ($B = 0.025$, $P = 0.000$) concentrations (Figure 4), and the serum mtDNA ($B = 0.863$, $P = 0.000$) and IL-10 ($B = 0.010$, $P = 0.001$) levels were significantly correlated with the pulmonary histological score (serum TNF-α levels were removed; $P = 0.180$) (Figure 5).

3.3. The Effects of Serum mtDNA on the Elderly Rats. As shown in Figure 6(a), the lung tissue structure of the control group had no obvious manifestation of inflammation. However, the pulmonary tissue slices of the mtDNA group (Figure 6(b)) showed typical manifestations of acute lung injury. At 24 h after treatment, the serum TNF-α (Figure 7(a)) and IL-10 (Figure 7(b)) levels, the pulmonary histological score (Figure 7(c)), the protein (Figure 7(d)), TNF-α (Figure 7(e)), and IL-10 (Figure 7(f)) concentrations in BALF, and the lung tissue MPO (Figure 7(g)) and NE (Figure 7(h)) activity in the mtDNA group were significantly higher than the respective values in the control group (all $P < 0.05$).

4. Discussion

There is indisputable evidence that trauma can trigger an inflammatory response [26]. However, not all traumas result in an uncontrolled systemic inflammatory response. When trauma induces a host defense response, which is defined as systemic inflammatory response syndrome (SIRS) and is characterized by local and systemic release of proinflammatory cytokines, anti-inflammatory mediators are produced (compensatory anti-inflammatory response syndrome, CARS) to inhibit SIRS. Only when the organisms are overwhelmed by trauma is the balance broken, and an imbalance in the immune responses leads to the development of multiorgan failure (MOF) [27–30]. The lungs are the first and primary target organ to be affected in the postinjury period, and lung injury caused by posttraumatic inflammatory reactions increases mortality risk [23, 31, 32]. Recently, a number of studies have reported that the elderly

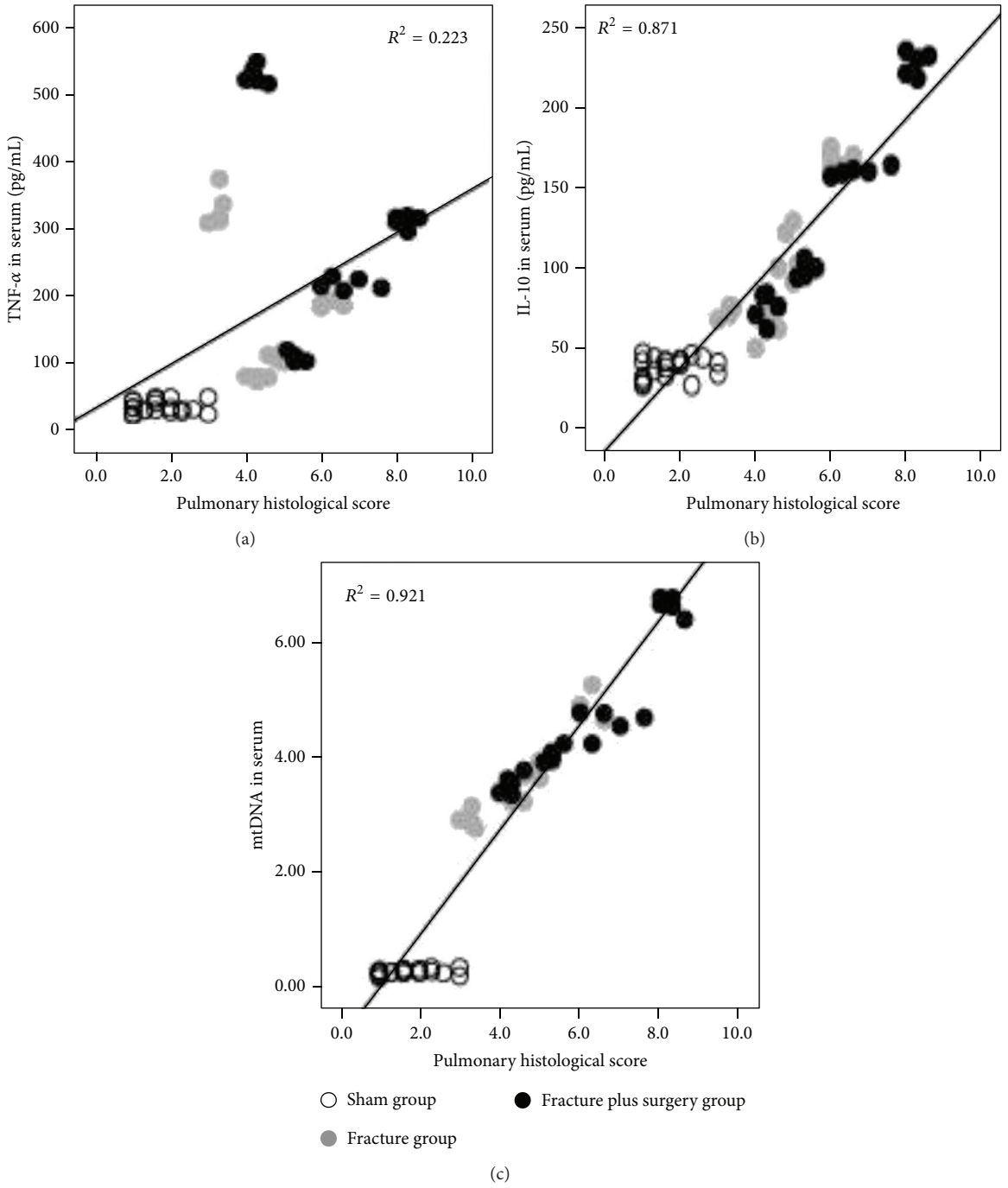

Figure 5: Scatter plots and regression lines showed that the serum TNF-α (a) level was not significantly correlated with the pulmonary histological score; however, the serum IL-10 (b) and mtDNA (c) levels exhibited a significant relationship with the pulmonary histological score.

possess a reduced physiological reserve and are more vulnerable to posttraumatic inflammatory reactions; even minor trauma can cause severe autodestructive proinflammatory cytokine release that is uncompensated by anti-inflammatory mediators [33–35]. This is consistent with our experimental results. In our experiment, compared with the sham group, at 8, 24, 48, and 72 h after treatment, the serum TNF-α and IL-10 levels, the pulmonary histological score, the cytokine (TNF-α and IL-10) and protein concentrations in the BALF, and the lung tissue MPO and NE activities were significantly increased in the fracture group. These findings suggest that hip fracture resulted in significant systemic inflammation and lung injury in the elderly rats.

Elderly trauma patients require special treatment because of their higher mortality rate following trauma, even minor trauma [36–38]. Surgical and clinical dogma states that if, at

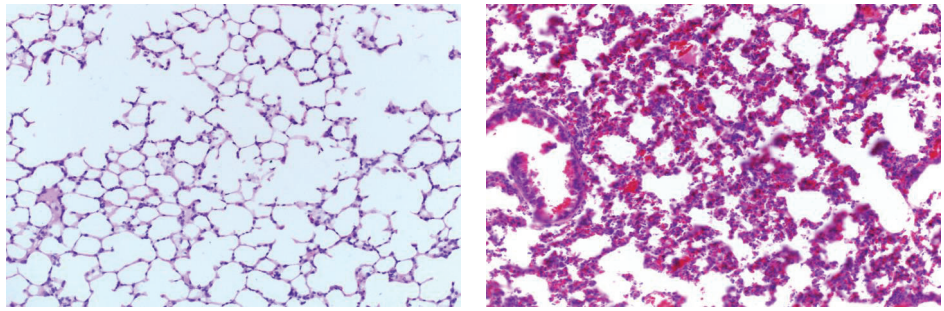

(a) (b)

Figure 6: Representative H&E sections of pulmonary tissues (magnification, 100x). After treatment, the control group (a) had no obvious inflammation and the mtDNA (b) showed typical symptoms of acute lung injury.

all possible, any patient with a hip fracture should undergo surgical fixation as soon as possible because any delay in surgery is thought to increase the risk of complications and death [6, 7, 39, 40]. However, hip fracture in the elderly can induce systemic inflammatory responses and lung injury, which increase the risk of pulmonary infection and death during the postinjury period [9–11]. In addition, the DCO proposes that immediate definitive fixation of long-bone fractures can be detrimental to patients who are physiologically unstable [12, 13]. Therefore, the adverse effects of immediate surgery are worth investigating. In our experiment, compared with the fracture group, the serum TNF-α and IL-10 levels, the pulmonary histological score, the cytokine (TNF-α and IL-10) and protein concentrations in the BALF, and the lung tissue MPO and NE activity were significantly increased in the fracture plus surgery group. These findings indicate that immediate intramedullary nailing surgery aggravated the systemic inflammatory reaction and lung injury induced by elderly hip fracture.

Previous studies have reported that elderly hip fracture induces a systemic inflammatory response and lung injury and increases the incidence of complications and mortality in elderly patients [1, 9, 11, 30, 32, 35]. Any neglect or misdiagnosis of this condition may produce disastrous results. Early diagnosis and evaluation of the systemic inflammatory response and lung injury after trauma are crucial for timely correction of this complicated syndrome. Potential biomarkers include acute phase proteins, cytokines, and chemokines [41–44]; however, none of these markers are sufficiently specific due to overlap with other inflammatory diseases [45–47]. Ideal biomarkers with higher sensitivity and specificity remain to be identified.

Recent studies have demonstrated that mtDNA is a critical activator of inflammation and the innate immune system. The release of mtDNA by cellular injury is a key link between trauma, inflammation, and SIRS [20, 48, 49]. A previous study reported that mtDNA from femoral reamings activated inflammation [18]. Our previous study also indicated that mtDNA induces a systemic inflammatory response and lung injury [21]. Therefore, we hypothesized that circulating mtDNA levels are associated with the systemic inflammatory response and lung injury induced by elderly hip fracture and might serve as a viable biomarker for the inflammatory response.

In the first part of our study, at 8, 24, 48, and 72 h after treatment, compared with the sham group, the serum mtDNA levels were significantly increased in the fracture group and the fracture plus surgery group; the serum mtDNA levels of the fracture plus surgery group were higher than those in the fracture group. It indicated that hip fracture releases mtDNA into the circulation; the immediate intramedullary nailing surgery increases the release of mtDNA. In addition, the results of the linear regression analysis revealed that the serum mtDNA levels were significantly correlated with serum cytokine (TNF-α and IL-10) levels and the pulmonary histological score. Compared with serum cytokines (TNF-α and IL-10), serum mtDNA was more closely correlated with the pulmonary histological score, indicating that the increasing release of mtDNA may be the reason of immediate intramedullary nailing surgery aggravating the systemic inflammatory response and lung injury induced by hip fracture in the elderly.

In order to identify the effects of serum mtDNA on the rats, the second part of our study was carried out. The result showed that the serum TNF-α and IL-10 levels, the pulmonary histological score, the cytokine (TNF-α and IL-10) and protein concentrations in the BALF, and the lung tissue MPO and NE activity were significantly increased in the rats which received mtDNA injections. It indicated that the mtDNA could cause systemic inflammation and lung injury in the elderly rats.

In general, hip fracture induces substantial mtDNA release, systemic inflammatory response, and lung injury in the elderly. Immediate intramedullary nailing surgery could aggravate the above pathological states. Serum mtDNA exhibited a significant relationship with posttraumatic inflammation and can serve as a potential biomarker of the systemic inflammatory response and lung injury following hip fracture in the elderly. Further study will define the value of serum mtDNA in the early diagnosis and prognosis of

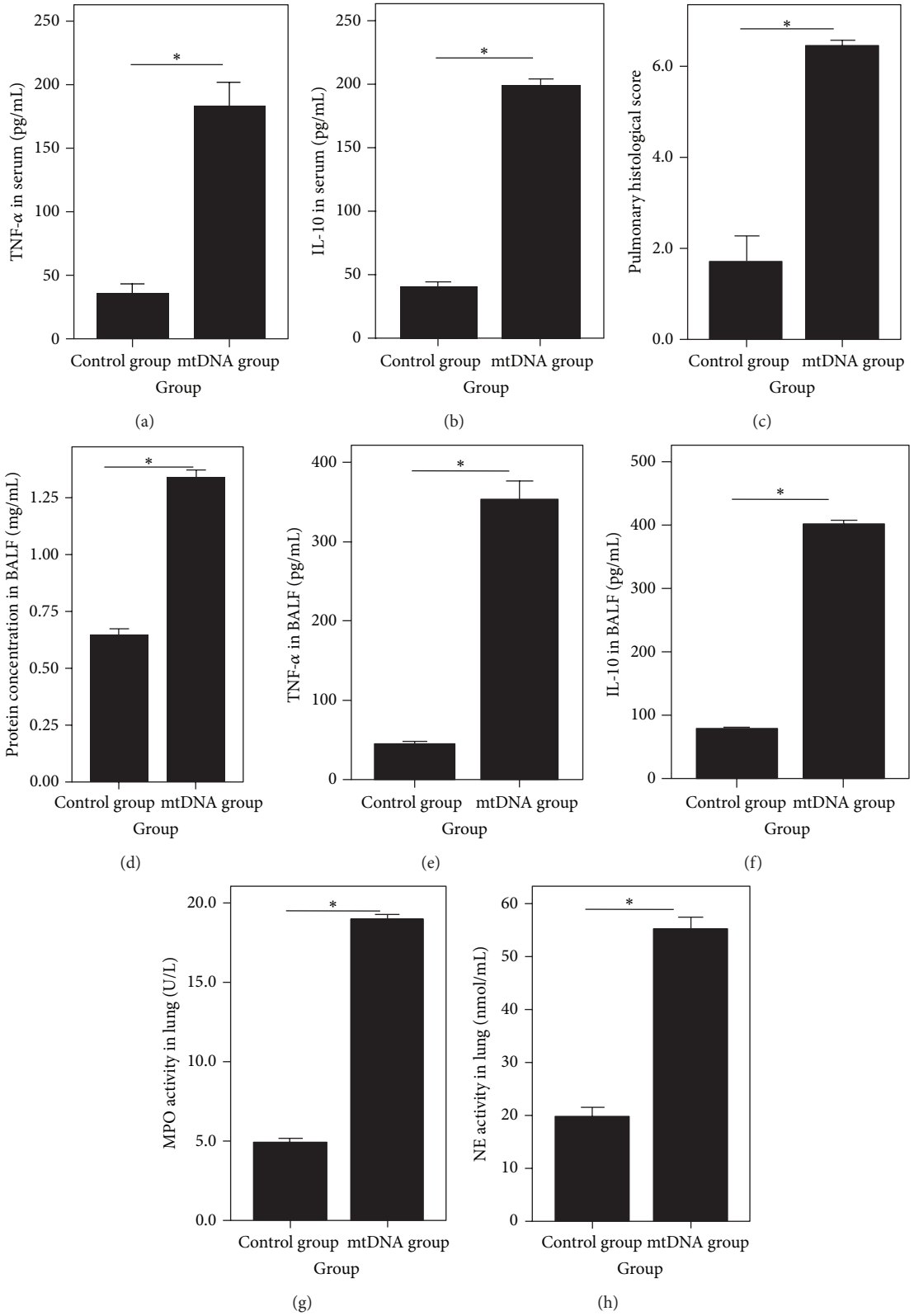

Figure 7: The serum TNF-α (a) and IL-10 (b) levels, the pulmonary histological score (c), the protein (d), TNF-α (e) and IL-10 (f) concentrations in BALF, and the lung tissue MPO (g) and NE (h) activity. Results are expressed as mean ± standard error. $^{*}P < 0.05$ when compared to other groups.

posttraumatic inflammation and may aid in the evaluation of the physical condition of trauma patients and inform the proper surgical approach.

Ethical Approval

Our experiments have abided by the statement of ethical standards for manuscripts submitted to Mediators of Inflammation.

Conflict of Interests

The authors declare that there is no conflict of interests regarding the publication of this paper.

Authors' Contribution

Li Gan, Jianfeng Zhong, and Ruhui Zhang contributed equally to this paper.

References

[1] J. J. W. Roche, R. T. Wenn, O. Sahota, and C. G. Moran, "Effect of comorbidities and postoperative complications on mortality after hip fracture in elderly people: prospective observational cohort study," *British Medical Journal*, vol. 331, no. 7529, pp. 1374–1376, 2005.

[2] C. B. Wang, C. F. J. Lin, W. M. Liang et al., "Excess mortality after hip fracture among the elderly in Taiwan: a nationwide population-based cohort study," *Bone*, vol. 56, no. 1, pp. 147–153, 2013.

[3] K. Alzahrani, R. Gandhi, A. Davis, and N. Mahomed, "In-hospital mortality following hip fracture care in southern Ontario," *Canadian Journal of Surgery*, vol. 53, no. 5, pp. 294–298, 2010.

[4] P. Vestergaard, L. Rejnmark, and L. Mosekilde, "Increased mortality in patients with a hip fracture-effect of pre-morbid conditions and post-fracture complications," *Osteoporosis International*, vol. 18, no. 12, pp. 1583–1593, 2007.

[5] S. Haleem, L. Lutchman, R. Mayahi, J. E. Grice, and M. J. Parker, "Mortality following hip fracture: trends and geographical variations over the last 40 years," *Injury*, vol. 39, no. 10, pp. 1157–1163, 2008.

[6] N. Simunovic, P. J. Devereaux, S. Sprague et al., "Effect of early surgery after hip fracture on mortality and complications: systematic review and meta-analysis," *Canadian Medical Association Journal*, vol. 182, no. 15, pp. 1609–1616, 2010.

[7] C. E. Uzoigwe, H. G. F. Burnand, C. L. Cheesman, D. O. Aghedo, M. Faizi, and R. G. Middleton, "Early and ultra-early surgery in hip fracture patients improves survival," *Injury*, vol. 44, no. 6, pp. 726–729, 2013.

[8] C. L. Daugaard, H. L. Jorgensen, T. Riis, J. B. Lauritzen, B. R. Duus, and S. Van Der Mark, "Is mortality after hip fracture associated with surgical delay or admission during weekends and public holidays? A retrospective study of 38,020 patients," *Acta Orthopaedica*, vol. 83, no. 6, pp. 609–613, 2012.

[9] T. Sun, X. Wang, Z. Liu, S. Liu, and J. Zhang, "Patterns of cytokine release and evolution of remote organs from proximal femur fracture in COPD rats," *Injury*, vol. 42, no. 8, pp. 825–832, 2011.

[10] T. Sun, X. Wang, Z. Liu, X. Chen, and J. Zhang, "Plasma concentrations of pro- and anti-inflammatory cytokines and outcome prediction in elderly hip fracture patients," *Injury*, vol. 42, no. 7, pp. 707–713, 2011.

[11] H. Zhang, T. Sun, Z. Liu, J. Zhang, X. Wang, and J. Liu, "Systemic inflammatory responses and lung injury following hip fracture surgery increases susceptibility to infection in aged rats," *Mediators of Inflammation*, vol. 2013, Article ID 536435, 12 pages, 2013.

[12] P. F. Stahel, W. R. Smith, and E. E. Moore, "Current trends in resuscitation strategy for the multiply injured patient," *Injury*, vol. 40, supplement 4, pp. S27–S35, 2009.

[13] F. Hildebrand, P. Giannoudis, C. Kretteck, and H.-C. Pape, "Damage control: extremities," *Injury*, vol. 35, no. 7, pp. 678–689, 2004.

[14] L. Sagan, "On the origin of mitosing cells," *Journal of Theoretical Biology*, vol. 14, no. 3, pp. 225–274, 1967.

[15] J. Pugin, "How tissue injury alarms the immune system and causes a systemic inflammatory response syndrome," *Annals of Intensive Care*, vol. 2, article, 2012.

[16] V. M. Stoecklein, A. Osuka, and J. A. Lederer, "Trauma equals danger-damage control by the immune system," *Journal of Leukocyte Biology*, vol. 92, no. 3, pp. 539–551, 2012.

[17] X. Gu, Y. Yao, G. Wu, T. Lv, L. Luo, and Y. Song, "The plasma mitochondrial dna is an independent predictor for post-traumatic systemic inflammatory response syndrome," *PLoS ONE*, vol. 8, no. 8, Article ID e72834, 2013.

[18] C. J. Hauser, T. Sursal, E. K. Rodriguez, P. T. Appleton, Q. Zhang, and K. Itagaki, "Mitochondrial damage associated molecular patterns from femoral reamings activate neutrophils through formyl peptide receptors and P44/42 MAP kinase," *Journal of Orthopaedic Trauma*, vol. 24, no. 9, pp. 534–538, 2010.

[19] Q. Zhang, K. Itagaki, and C. J. Hauser, "Mitochondrial DNA is released by shock and activates neutrophils via p38 map kinase," *Shock*, vol. 34, no. 1, pp. 55–59, 2010.

[20] Q. Zhang, M. Raoof, Y. Chen et al., "Circulating mitochondrial DAMPs cause inflammatory responses to injury," *Nature*, vol. 464, no. 7285, pp. 104–107, 2010.

[21] J.-Z. Zhang, Z. Liu, J. Liu, J.-X. Ren, and T.-S. Sun, "Mitochondrial DNA induces inflammation and increases TLR9/NF-κB expression in lung tissue," *International Journal of Molecular Medicine*, vol. 33, no. 4, pp. 817–824, 2014.

[22] H.-J. He, Y. Wang, Y. Le et al., " Surgery up regulates high mobility group box-1 and disrupts the blood-brain barrier causing cognitive dysfunction in aged rats," *CNS Neuroscience and Therapeutics*, vol. 18, no. 12, pp. 994–1002, 2012.

[23] B. W. Sears, D. Volkmer, S. Yong et al., "Binge alcohol exposure modulates rodent expression of biomarkers of the immunoinflammatory response to orthopaedic trauma," *The Journal of Bone and Joint Surgery—American Volume*, vol. 93, no. 8, pp. 739–749, 2011.

[24] J. Deree, J. Martins, T. de Campos et al., "Pentoxifylline attenuates lung injury and modulates transcription factor activity in hemorrhagic shock," *Journal of Surgical Research*, vol. 143, no. 1, pp. 99–108, 2007.

[25] J. Ellinger, D. C. Müller, S. C. Müller et al., "Circulating mitochondrial DNA in serum: a universal diagnostic biomarker for patients with urological malignancies," *Urologic Oncology*, vol. 30, no. 4, pp. 509–515, 2012.

[26] S. Hirsiger, H.-P. Simmen, C. M. L. Werner, G. A. Wanner, and D. Rittirsch, "Danger signals activating the immune response

after trauma," *Mediators of Inflammation*, vol. 2012, Article ID 315941, 10 pages, 2012.

[27] M. Keel and O. Trentz, "Pathophysiology of polytrauma," *Injury*, vol. 36, no. 6, pp. 691–709, 2005.

[28] P.-B. Xu, J.-S. Lou, Y. Ren, C.-H. Miao, and X.-M. Deng, "Gene expression profiling reveals the defining features of monocytes from septic patients with compensatory anti-inflammatory response syndrome," *Journal of Infection*, vol. 65, no. 5, pp. 380–391, 2012.

[29] T. Visser, J. Pillay, L. Koenderman, and L. P. H. Leenen, "Post-injury immune monitoring: can multiple organ failure be predicted?" *Current Opinion in Critical Care*, vol. 14, no. 6, pp. 666–672, 2008.

[30] J. J. Hoth, J. D. Wells, S. E. Jones, B. K. Yoza, and C. E. McCall, "Complement mediates a primed inflammatory response after traumatic lung injury," *Journal of Trauma and Acute Care Surgery*, vol. 76, no. 3, pp. 601–609, 2014.

[31] S. F. Monaghan, R. K. Thakkar, D. S. Heffernan et al., "Mechanisms of indirect acute lung injury: a novel role for the coinhibitory receptor, programmed death-1," *Annals of Surgery*, vol. 255, no. 1, pp. 158–164, 2012.

[32] S. Tiansheng, C. Xiaobin, L. Zhi, W. Xiaowei, L. Guang, and Z. Liren, "Is damage control orthopedics essential for the management of bilateral femoral fractures associated or complicated with shock? an animal study," *Journal of Trauma—Injury, Infection and Critical Care*, vol. 67, no. 6, pp. 1402–1411, 2009.

[33] C. Forasassi, J.-L. Golmard, E. Pautas, F. Piette, I. Myara, and A. Raynaud-Simon, "Inflammation and disability as risk factors for mortality in elderly acute care patients," *Archives of Gerontology and Geriatrics*, vol. 48, no. 3, pp. 406–410, 2009.

[34] R. M. Smith, "Immunity, trauma and the elderly," *Injury*, vol. 38, no. 12, pp. 1401–1404, 2007.

[35] Q. Zhu, X. Qian, S. Wang et al., "A comparison of elderly and adult multiple organ dysfunction syndrome in the rat model," *Experimental Gerontology*, vol. 41, no. 8, pp. 771–777, 2006.

[36] P. Tornetta III, H. Mostafavi, J. Riina et al., "Morbidity and mortality in elderly trauma patients," *Journal of Trauma—Injury, Infection and Critical Care*, vol. 46, no. 4, pp. 702–706, 1999.

[37] S. M. Henry, A. N. Pollak, A. L. Jones, S. Boswell, and T. M. Scalea, "Pelvic fracture in geriatric patients: a distinct clinical entity," *Journal of Trauma*, vol. 53, no. 1, pp. 15–20, 2002.

[38] C. S. Roberts, H.-C. Pape, A. L. Jones, A. L. Malkani, J. L. Rodriguez, and P. V. Giannoudis, "Damage control orthopaedics: evolving concepts in the treatment of patients who have sustained orthopaedic trauma," *Instructional course lectures*, vol. 54, pp. 447–462, 2005.

[39] L. Moja, A. Piatti, V. Pecoraro et al., "Timing matters in hip fracture surgery: patients operated within 48 hours have better outcomes. A meta-analysis and meta-regression of over 190,000 patients," *PLoS ONE*, vol. 7, no. 10, Article ID e46175, 2012.

[40] E. I. O. Vidal, D. C. Moreira-Filho, R. S. Pinheiro et al., "Delay from fracture to hospital admission: a new risk factor for hip fracture mortality?" *Osteoporosis International*, vol. 23, no. 12, pp. 2847–2853, 2012.

[41] A. J. Rogers and M. A. Matthay, "Applying metabolomics to uncover novel biology in ARDS," *The American Journal of Physiology—Lung Cellular and Molecular Physiology*, vol. 306, no. 11, pp. L957–L961, 2014.

[42] M. Bhargava and C. H. Wendt, "Biomarkers in acute lung injury," *Translational Research*, vol. 159, no. 4, pp. 205–217, 2012.

[43] L. J. M. Cross and M. A. Matthay, "Biomarkers in acute lung injury: insights into the pathogenesis of acute lung injury," *Critical Care Clinics*, vol. 27, no. 2, pp. 355–377, 2011.

[44] R. D. Fremont, T. Koyama, C. S. Calfee et al., "Acute lung injury in patients with traumatic injuries: utility of a panel of biomarkers for diagnosis and pathogenesis," *Journal of Trauma—Injury, Infection and Critical Care*, vol. 68, no. 5, pp. 1121–1127, 2010.

[45] J. Pugin, "Biomarkers of sepsis: is procalcitonin ready for prime time?" *Intensive Care Medicine*, vol. 28, no. 9, pp. 1203–1204, 2002.

[46] E. B. Yan, L. Satgunaseelan, E. Paul et al., "Post-traumatic hypoxia is associated with prolonged cerebral cytokine production, higher serum biomarker levels, and poor outcome in patients with severe traumatic brain injury," *Journal of Neurotrauma*, vol. 31, no. 7, pp. 618–629, 2014.

[47] V. Ciriello, S. Gudipati, P. Z. Stavrou, N. K. Kanakaris, M. C. Bellamy, and P. V. Giannoudis, "Biomarkers predicting sepsis in polytrauma patients: current evidence," *Injury*, vol. 44, no. 12, pp. 1680–1692, 2013.

[48] L. V. Collins, S. Hajizadeh, E. Holme, I.-M. Jonsson, and A. Tarkowski, "Endogenously oxidized mitochondrial DNA induces in vivo and in vitro inflammatory responses," *Journal of Leukocyte Biology*, vol. 75, no. 6, pp. 995–1000, 2004.

[49] S.-Y. Seong and P. Matzinger, "Hydrophobicity: an ancient damage-associated molecular pattern that initiates innate immune responses," *Nature Reviews Immunology*, vol. 4, no. 6, pp. 469–478, 2004.

Hindawi Publishing Corporation
Mediators of Inflammation
Volume 2015, Article ID 601083, 6 pages
http://dx.doi.org/10.1155/2015/601083

Clinical Study

Flurbiprofen Axetil Enhances Analgesic Effects of Sufentanil and Attenuates Postoperative Emergence Agitation and Systemic Proinflammation in Patients Undergoing Tangential Excision Surgery

Wujun Geng,[1] Wandong Hong,[2] Junlu Wang,[1] Qinxue Dai,[1] Yunchang Mo,[1] Kejian Shi,[1] Jiehao Sun,[1] Jinling Qin,[1] Mei Li,[3] and Hongli Tang[1]

[1]*Department of Anesthesiology, First Affiliated Hospital of Wenzhou Medical University, Wenzhou, Zhejiang 325000, China*
[2]*Department of Gastroenterology, First Affiliated Hospital of Wenzhou Medical University, Wenzhou, Zhejiang 325000, China*
[3]*Department of Anesthesia, Guangdong Provincial People's Hospital and Guangdong Academy of Medical Sciences, Guangzhou 510000, China*

Correspondence should be addressed to Hongli Tang; tanghongliok@126.com

Received 9 January 2015; Accepted 16 February 2015

Academic Editor: Huang-Ping Yu

Objective. Our present study tested whether flurbiprofen axetil could reduce perioperative sufentanil consumption and provide postoperative analgesia with decrease in emergency agitation and systemic proinflammatory cytokines release. *Methods*. Ninety patients undergoing tangential excision surgery were randomly assigned to three groups: (1) preoperative dose of 100 mg flurbiprofen axetil and a postoperative dose of 2 μg/kg sufentanil and 10 mL placebo by patient-controlled analgesia (PCA) pump, (2) preoperative dose of 100 mg flurbiprofen axetil and a postoperative dose of 2 μg/kg sufentanil and 100 mg flurbiprofen axetil by PCA pump, and (3) 10 mL placebo and a postoperative dose of 2 μg/kg sufentanil and 10 mL placebo by PCA pump. *Results*. Preoperative administration of flurbiprofen axetil decreased postoperative tramadol consumption and the visual analog scale at 4, 6, 12, and 24 h after surgery, which were further decreased by postoperative administration of flurbiprofen axetil. Furthermore, flurbiprofen axetil attenuated emergency agitation score and Ramsay score at 0, 5, and 10 min after extubation and reduced the TNF-α and interleukin- (IL-) 6 levels at 24 and 48 h after the operation. *Conclusion*. Flurbiprofen axetil enhances analgesic effects of sufentanil and attenuates emergence agitation and systemic proinflammation in patients undergoing tangential excision surgery.

1. Introduction

Burn patients usually suffered from tremendous pain [1–3], especially after tangential excision surgery. Good postoperative analgesia may help reduce pain related multiple problems, such as anxiety, emergency agitation, and lack of confidence in medical team [4]. Moreover, burn patients are predisposed to sepsis and multiple organ failure [5, 6]. These are major complications associated with burn trauma and the activation of a proinflammatory cascade after burn injury appears to be important in their development [7, 8]. Therefore, effective modulation of pain relief and the postoperative systemic inflammatory response should be beneficial to the patients who received tangential excision surgery.

Flurbiprofen axetil, which is incorporated in lipid microspheres, is a nonsteroidal anti-inflammatory drug (NSAID) with high affinity to the site of surgical incision and inflammatory tissues [9]. NSAIDs exert their analgesic effect not only through peripheral inhibition of prostaglandin synthesis but also through a variety of other peripheral and central mechanisms that augments the peripheral mechanism [10]. NSAIDs and opioid drugs are known to possess synergistic analgesic effects. It has been reported that pretreatment

with flurbiprofen axetil enhances analgesic effect of fentanyl and reduces fentanyl concentration required for immobility under propofol anesthesia [11, 12]. Further studies show that preoperative intravenous administration of flurbiprofen axetil reduces postoperative pain in patients undergoing radical resection of esophageal carcinoma, postmastectomy, spinal fusion, and thyroid gland surgery [13–17] and relieves cancer related multiple breakthrough pain [18]. However, there are a few reports on whether preoperative flurbiprofen axetil can reduce perioperative opioid consumption and postoperative emergency agitation and pain after tangential excision surgery. In the present study, we hypothesized that preoperative flurbiprofen axetil can reduce perioperative sufentanil consumption and provide postoperative analgesia with decrease in emergency agitation and systemic proinflammatory cytokines release in patients undergoing tangential excision surgery.

2. Materials and Methods

2.1. Patients' Selection. This randomized, double-blind, and placebo-controlled clinical study (clinical trial registration number: ChiCTR-IPR-15005830) was approved by the Ethics Committee of the Wenzhou Medical University, and informed consent was obtained from the patients prior study enrollment. Ninety patients undergoing tangential excision surgery were involved in this study. The inclusion criteria were (1) American Society of Anesthesiologists (ASA) I-II and (2) age 25–55 years. The exclusion criteria were (1) patients with a history of allergic reaction to NSAIDs or opioid drugs, (2) patients with any contraindications for the use of NSAIDs, (3) patient with infections and inhalation injury, (4) patients with severe hepatic, renal, cardiovascular, or psychological disorders, and (5) patients with mental illness, neuromuscular diseases, language disorders, and immunodeficiency diseases.

2.2. Study Design. On the day before the surgery, all the patients were instructed about the study protocol and the use of visual analog scale (VAS) and the patient-controlled analgesia (PCA) pump. Patients who were unable to use the VAS and the PCA pump were excluded. The patients undergoing tangential excision surgery were randomly divided into three groups ($n = 30$ in each group). Group A patients received a preoperative dose of 100 mg [11] flurbiprofen axetil (Taide pharmaceutical Co., Beijing, China) by intravenous administration and a postoperative dose of 2 μg/kg sufentanil (Renfu Pharmaceutical Co., Yichang, China) and 10 mL placebo (intralipid) and normal saline (total volume, 100 mL) by PCA pump. Group B patients received a preoperative dose of 100 mg flurbiprofen axetil by intravenous administration and a postoperative dose of 2 μg/kg sufentanil and 100 mg flurbiprofen axetil and normal saline (total volume, 100 mL) by PCA pump. Group C patients received 10 mL placebo by intravenous administration and a postoperative dose of 2 μg/kg sufentanil and 10 mL placebo and normal saline (total volume, 100 mL) by PCA pump. Preoperative flurbiprofen axetil/placebo was administrated 15 min before the induction of anesthesia.

2.3. Anesthesia and Analgesia Procedures. All patients involved in the study received intramuscular injections of diazepam 10 mg and atropine 0.5 mg at 30 min before anesthesia. On arrival at the operating room, standard monitors including pulse oximetry, electrocardiogram, and noninvasive arterial blood pressure were applied. General anesthesia was induced with midazolam 0.05 mg/kg, etomidate 0.1 mg/kg, propofol 2 mg/kg, sufentanil 0.5 μg/kg, and cisatracurium 2 mg/kg. Propofol 4–12 mg/kg/h and remifentanil 5–40 μg/kg/h were infused through micro pumps to maintain anesthesia. These drugs' dose was adjusted according to the change of hemodynamics. The neuromuscular blockade was maintained by intermittent injection of cisatracurium as required.

After the surgery, all the patients received patient-controlled intravenous analgesia (PCIA) when extubated and then were transferred to the postanesthesia recovery room. No other analgesics were given during the perioperative period. A physician who was blinded to the group assignment assessed spontaneous postsurgical pain intensity at rest using VAS at 1, 2, 4, 6, 12, 24, and 48 hours after the operation.

2.4. Assessment of Emergence Agitation Score and the Ramsay Calm Score. Another physician who was blinded to the group assignment assessed emergence agitation score and the Ramsay calm score at 0, 5, 10, 30, and 60 min after extubation. The emergence agitation score is assessed as follows: 0 points is cooperation, 1 point is physical restlessness when stimulated, 2 points is slight physical restlessness without stimulation, and 3 points is fierce struggling and difficult to control. The Ramsay calm score is assessed as 1 point is anxiety, 2 points is cooperation, 3 points is drowsiness but obedience to instructions, 4 points is asleep but can wake up easily, 5 points is asleep but can react to strong stimulation, and 6 points is deeply asleep and cannot be woken up (2–4 points display sedation well; 5-6 points display over sedation).

2.5. Determination of the Levels of Systemic Proinflammatory Cytokines. Blood (2 mL) was collected from the central vein before induction of anesthesia, at the end of operation, and 24 h and 48 h after the surgery. Plasma was separated by centrifugation at 3000 rpm for 10 min and stored at −70°C for further analysis. Plasma inflammatory cytokines tumor necrosis factor- (TNF-) a and IL-6 levels were measured, using the commercially available human ELISA kit (Jiancheng Co., Nanjing, China) as described [19]. All steps involved were operated according to the manufacturers' instructions.

2.6. Statistical Analysis. Statistical analysis was performed using SPASS 16.0 software. Values were expressed as mean ± SD, with one-way ANOVA and q test used among the groups and chi-square test used on counting data. $P < 0.05$ was considered statistically significant.

3. Results

Ninety patients were involved in the present study. One patient from group A did not have his scheduled surgery;

Table 1: General data of the three groups (mean ± SD).

Items	Group A ($n = 29$)	Group B ($n = 30$)	Group C ($n = 28$)
Gender (M/F)	17/12	19/11	16/12
Age (years)	41.2 ± 7.1	39.2 ± 8.3	40.6 ± 6.9
Weight (kg)	62.3 ± 11.8	66.2 ± 13.1	65.8 ± 10.6
Height (cm)	166 ± 7	167 ± 5	165 ± 8
Operation time (min)	112.8 ± 24.5	118.3 ± 27.8	116.7 ± 21.2
Blood loss (mL)	386 ± 107	413 ± 125	409 ± 114
Postoperative sufentanil (analgesic) dose (μg)	125.6 ± 23.5	132.4 ± 26.3	130.6 ± 21.2
Postoperative tramadol requirement dose (mg)	147.7 ± 30.3*	68.5 ± 20.4$^{**\#}$	230.5 ± 39.6

$^{*}P < 0.05$, $^{**}P < 0.05$ versus group C, $^{\#}P < 0.05$ versus group A.

Table 2: Emergence agitation score among the three groups (mean ± SD).

Groups	Time after extubation (min)				
	0	5	10	30	60
A ($n = 29$)	1.33 ± 0.41	1.01 ± 0.52	0.87 ± 0.16	0.58 ± 0.62	0.00 ± 0.00
B ($n = 30$)	1.31 ± 0.32	0.97 ± 0.47	0.84 ± 0.09	0.55 ± 0.64	0.00 ± 0.00
C ($n = 28$)	2.82 ± 0.21*	2.71 ± 0.45*	2.07 ± 0.51*	0.60 ± 0.28	0.00 ± 0.00

$^{*}P < 0.05$ versus groups A and B.

two patients from group C were excluded because of postoperative transfer to another hospital. As shown in Table 1, there were no significant differences among the three groups in terms of gender, weight, height, operation time, and blood loss. In addition, heart rate, arterial blood pressures, pulse oximetry, and fluid administration were not significantly different among the three groups ($P > 0.05$). Postoperative tramadol consumption in group A was significantly lower than that in group C but significantly higher than that in group B ($P < 0.05$).

VAS data are presented in Figure 1. There were no significant differences among groups A, B, and C at 1 and 2 h after surgery ($P > 0.05$). VAS in groups A and B were significantly lower than that in group C at 4, 6, 12, and 24 h after surgery ($P < 0.05$), and the VAS in group B is also significantly lower than that of group A at 4, 6, 12, and 24 h after surgery ($P < 0.05$). Further, the VAS in group C is significantly higher than that in group B at 48 h after the surgery ($P < 0.05$), but without significant increase as compared with that of group A ($P > 0.05$).

To further investigate the efficacy of flurbiprofen axetil, we assessed the emergence agitation score and Ramsay calm score. As shown in Tables 2 and 3, the emergency agitation score and Ramsay score at 0, 5 and 10 min after extubation in groups A and B were significantly lower than that in group C. There was no significant difference between groups A and B at 0, 5, and 10 min after extubation, and no significant difference among the three groups at 30 minutes and 60 minutes after extubation was observed.

Then, we investigate the anti-inflammatory effects of flurbiprofen axetil in patients undergoing tangential excision surgery. As shown in Tables 4 and 5, operation significantly increased the plasma levels of TNF-α and IL-6, which was significantly decreased by preoperative administration of flurbiprofen axetil at 24 and 48 h after the operation.

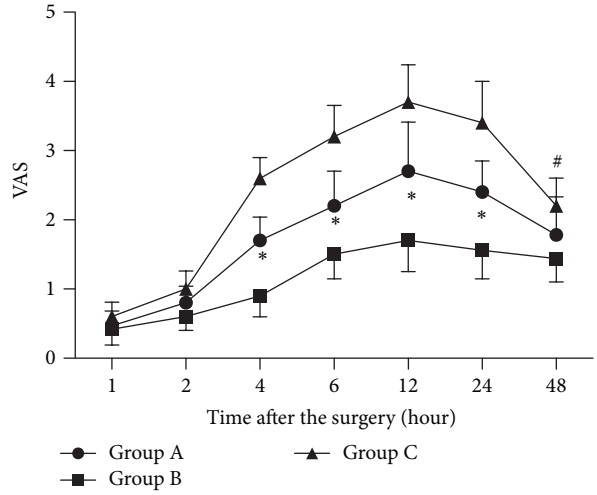

Figure 1: Visual analog pain scale: patients rated their levels of pain on the 0–10 cm VAS (0 cm = no pain to 10 cm = the worst possible pain). $^{*}P < 0.05$ versus other groups, $^{\#}P < 0.05$ group C versus group B.

Postoperative administration of flurbiprofen axetil further significantly reduced the plasma levels of TNF-α and IL-6 ($P < 0.05$, group A versus group B) at 24 and 48 h after the operation.

4. Discussion

In the present study, we demonstrated that flurbiprofen axetil improves analgesic effects of sufentanil. This is well supported by our results showing that preoperative administration of flurbiprofen axetil decreased the VAS at 4, 6, 12, and 24 h after surgery, and the VAS was further decreased by

Table 3: Ramsay calm score among the three groups (mean ± SD).

Groups	Time after extubation (min)				
	0	5	10	30	60
A ($n = 29$)	2.24 ± 0.34	2.38 ± 0.43	2.02 ± 0.65	2.01 ± 0.21	2.00 ± 0.00
B ($n = 30$)	2.31 ± 0.72	2.21 ± 0.44	2.77 ± 0.38	1.93 ± 0.22	2.00 ± 0.00
C ($n = 28$)	3.47 ± 0.26*	3.36 ± 0.36*	3.85 ± 0.22*	1.92 ± 0.34	2.00 ± 0.00

$^{*}P < 0.05$ versus groups A and B.

Table 4: Plasma level of TNF-α (pg/mL) among the three groups (mean ± SD).

Groups	Before induction of anesthesia	Time after operation (h)		
		0	24	48
A ($n = 29$)	547.56 ± 36.73	956.42 ± 32.19	780.62 ± 35.71$^{*\$}$	738.37 ± 27.85$^{\$}$
B ($n = 30$)	570.91 ± 31.53	961.45 ± 34.17	658.87 ± 28.35$^{**\#\$}$	612.64 ± 21.31$^{*\#\$}$
C ($n = 28$)	554.64 ± 37.36$^{\$}$	948.35 ± 39.78	890.68 ± 31.72	806.10 ± 32.62

$^{*}P < 0.05$, $^{**}P < 0.05$ versus group C; $^{\#}P < 0.05$ versus group A.
$^{\$}P < 0.05$ versus all the other time points in the patients of the same group.

Table 5: Plasma level of IL-6 (pg/mL) among the three groups (mean ± SD).

Groups	Before induction of anesthesia	Time after operation (h)		
		0	24	48
A ($n = 29$)	220.33 ± 13.16	359.45 ± 17.36	283.38 ± 12.32$^{*\$}$	263.31 ± 19.20$^{\$}$
B ($n = 30$)	218.68 ± 15.42	351.38 ± 16.38	236.67 ± 13.49$^{**\#\$}$	229.38 ± 15.49$^{*\#\$}$
C ($n = 28$)	225.73 ± 14.18$^{\$}$	349.95 ± 17.81	327.28 ± 20.18	289.38 ± 17.73

$^{*}P < 0.05$, $^{**}P < 0.05$ versus group C; $^{\#}P < 0.05$ versus group A.
$^{\$}P < 0.05$ versus all the other time points in the patients of the same group.

postoperative administration of flurbiprofen axetil in PCIA pump, which is associated with lower postoperative tramadol consumption. Furthermore, flurbiprofen axetil attenuated postoperative emergence agitation and reduced the systemic levels of proinflammatory cytokines. To the best of our knowledge, this is the first study to investigate the efficiency of flurbiprofen axetil on postoperative pain and emergence agitation.

Emergence agitation is a postanesthetic complication that interferes with a patient's recovery and presents a challenge in terms of assessment and management. It mainly occurs within 15 min after extubation [20]. Although the pathophysiology mechanisms of this complication are very complicated, much evidence indicates the involvement of pain stimulus [21–23]. Thus, all kinds of analgesics [24, 25] have been used in experimental and clinical studies to manage the occurrence of emergence agitation, among which were preemptive analgesics such as dexmedetomidine, clonidine, opioids, ketorolac, and lornoxicam. Our present study further confirmed that modulation of postoperative pain relief attenuates emergence agitation. This is evidenced by flurbiprofen axetil mediated reduction in emergence agitation score and Ramsay calm score at 0, 5, and 10 min after extubation.

Preemptive analgesia, a new concept to enhance the postoperative analgesia, is to give a first dose of analgesics before pain stimulation. Nevertheless, some clinical studies have conflicting results regarding the efficacy of preemptive analgesia [26]. However, Mihara and colleagues [27] evaluated the efficacy of flurbiprofen axetil for postoperative pain management after laparoscopic colectomy, and the conclusion was satisfactory. Similar to other studies [15, 28], our present study suggested preoperative administration of flurbiprofen axetil had preemptive analgesia effects, which was supported by the results that flurbiprofen axetil decreased the VAS at 4, 6, 12, and 24 h after surgery and postoperative tramadol consumption. Furthermore, postoperative administration of flurbiprofen axetil in PCIA pump enhanced the analgesic effects of sufentanil.

The burn patient's pain, infection, and other factors weaken the body's immune status and predispose the patients to sepsis and multiple organ failure [5, 6]. The proinflammatory cytokines after burn injury play an important role in the development of these complications. TNF-α is believed to be the initiating cytokine that induces a cascade of secondary cytokines and humoral factors that can lead to local and systemic sequelae [29]. Moreover, TNF-α is a potent mediator of the shock-like state associated with thermal injury and sepsis [30]. In the present study, tangential excision surgery significantly increased the plasma levels of TNF-α and IL-6, which was decreased by preoperative administration of flurbiprofen axetil, and further reduced by postoperative

administration of flurbiprofen axetil at 24 and 48 h after the operation.

The NSAIDs are associated with many adverse effects, including reducing platelet aggregation, renal and gastrointestinal mucosal injury. In our present study, there were no adverse effects found in any of the involved patients, which might be due to the relatively short period of flurbiprofen axetil administration in the current study. However, there are still several limitations in the current study, such as psychosocial characteristics, educational background, and preoperative pathology of the patients that were not controlled, and it is also not well known in our study whether pain relief attenuates the postoperative systemic inflammatory response, or the decrease of inflammatory response reduces postoperative pain.

5. Conclusion

In summary, the results of current study demonstrate that flurbiprofen axetil can enhance analgesic effects of sufentanil and attenuate emergence agitation, which was associated with decrease of systemic proinflammatory cytokines release in patients undergoing tangential excision surgery. Our data suggest that intravenous flurbiprofen axetil may be useful approaches to reduce postoperative pain and emergence agitation in burn patients.

Conflict of Interests

The authors declare no conflict of interests regarding the publication of this paper.

Authors' Contribution

Wujun Geng and Hongli Tang wrote the paper. Wandong Hong, Junlu Wang, Qinxue Dai, Yunchang Mo, Kejian Shi, Jiehao Sun, Jinling Qin, and Mei Li researched data. Wujun Geng and Hongli Tang designed the study, reviewed the data, and revised the paper. Wujun Geng, Wandong Hong, and Junlu Wang contributed equally to this work.

Acknowledgment

This study was supported by grants from Science and Technology Bureau project of Wenzhou city (Y20140567, Y20140547).

References

[1] R. J. A. de Castro, P. C. Leal, and R. K. Sakata, "Pain management in burn patients," *Revista Brasileira de Anestesiologia*, vol. 63, no. 1, pp. 149–158, 2013.

[2] H. Gamst-Jensen, P. N. Vedel, V. O. Lindberg-Larsen, and I. Egerod, "Acute pain management in burn patients: appraisal and thematic analysis of four clinical guidelines," *Burns*, vol. 40, no. 8, pp. 1463–1469, 2014.

[3] L. Yuxiang, Z. Lingjun, T. Lu et al., "Burn patients' experience of pain management: a qualitative study," *Burns*, vol. 38, no. 2, pp. 180–186, 2012.

[4] F. M. Ardabili, S. Purhajari, T. Najafi Ghezeljeh, and H. Haghani, "The effect of shiatsu massage on pain reduction in burn patients," *World Journal of Plastic Surgery*, vol. 3, no. 2, pp. 115–118, 2014.

[5] M. G. Jeschke, R. Pinto, R. Kraft et al., "Morbidity and survival probability in burn patients in modern burn care," *Critical Care Medicine*, 2015.

[6] K. Shimizu, H. Ogura, T. Asahara et al., "Gut microbiota and environment in patients with major burns—a preliminary report," *Burns*, 2014.

[7] M. G. Schwacha, "Macrophages and post-burn immune dysfunction," *Burns*, vol. 29, no. 1, pp. 1–14, 2003.

[8] C. C. Finnerty, M. G. Jeschke, D. N. Herndon et al., "Temporal cytokine profiles in severely burned patients: a comparison of adults and children," *Molecular Medicine*, vol. 14, no. 9-10, pp. 553–560, 2008.

[9] K. Mikawa, K. Nishina, N. Maekawa, M. Shiga, and H. Obara, "Dose-response of flurbiprofen on postoperative pain and emesis after paediatric strabismus surgery," *Canadian Journal of Anaesthesia*, vol. 44, no. 1, pp. 95–98, 1997.

[10] J. N. Cashman, "The mechanisms of action of NSAIDs in analgesia," *Drugs*, vol. 52, no. 5, pp. 13–23, 1996.

[11] Z.-F. Liu, X.-Q. Chai, and K.-Z. Chen, "Flurbiprofen axetil enhances analgesic effect of fentanyl associated with increase in β-endorphin levels," *Journal of Anesthesia*, vol. 25, no. 5, pp. 679–684, 2011.

[12] M. Kodaka, M. Tsukakoshi, H. Miyao, K. Tsuzaki, J. Ichikawa, and M. Komori, "The fentanyl concentration required for immobility under propofol anesthesia is reduced by pretreatment with flurbiprofen axetil," *Canadian Journal of Anesthesia*, vol. 60, no. 12, pp. 1204–1211, 2013.

[13] Y. Wang, H.-B. Zhang, B. Xia, G.-M. Wang, and M.-Y. Zhang, "Preemptive analgesic effects of flurbiprofen axetil in patients undergoing radical resection of esophageal carcinoma via the left thoracic approach," *Chinese Medical Journal*, vol. 125, no. 4, pp. 579–582, 2012.

[14] Y. Wen, M. Wang, J. Yang et al., "A comparison of fentanyl and flurbiprofen axetil on serum VEGF-C, TNF-α, and IL-1ß concentrations in women undergoing surgery for breast cancer," *Pain Practice*, 2014.

[15] M. Sun, Q. Liao, L. Wen, X. Yan, F. Zhang, and W. Ouyang, "Effect of perioperative intravenous flurbiprofen axetil on chronic postmastectomy pain," *Journal of Central South University. Medical Sciences*, vol. 38, no. 7, pp. 653–660, 2013.

[16] K. Yamashita, M. Fukusaki, Y. Ando et al., "Preoperative administration of intravenous flurbiprofen axetil reduces postoperative pain for spinal fusion surgery," *Journal of Anesthesia*, vol. 20, no. 2, pp. 92–95, 2006.

[17] Z. Zhang, H. Zhao, C. Wang, F. Han, and G. Wang, "Lack of preemptive analgesia by intravenous flurbiprofen in thyroid gland surgery: a randomized, double-blind and placebo-controlled clinical trial," *International Journal of Medical Sciences*, vol. 8, no. 5, pp. 433–438, 2011.

[18] J. Hao, K. Wang, Y. Shao, X. Cheng, and Z. Yan, "Intravenous flurbiprofen axetil to relieve cancer-related multiple breakthrough pain: a clinical study," *Journal of Palliative Medicine*, vol. 16, no. 2, pp. 190–192, 2013.

[19] S. Lei, W. Su, H. Liu et al., "Nitroglycerine-induced nitrate tolerance compromises propofol protection of the endothelial cells against TNF-α: the role of PKC-β_2 and nadph oxidase," *Oxidative Medicine and Cellular Longevity*, vol. 2013, Article ID 678484, 9 pages, 2013.

[20] T. Voepel-Lewis, S. Malviya, and A. R. Tait, "A prospective cohort study of emergence agitation in the pediatric postanesthesia care unit," *Anesthesia and Analgesia*, vol. 96, no. 6, pp. 1625–1630, 2003.

[21] M. B. Mohkamkar, F. M. Farhoudi, A. M. Alam-Sahebpour, S.-A. Mousavi, S. Khani, and S. Shahmohammadi, "Postanesthetic emergence agitation in pediatric patients under general anesthesia," *Iranian Journal of Pediatrics*, vol. 24, no. 2, pp. 184–190, 2014.

[22] S. Dahmani, H. Delivet, and J. Hilly, "Emergence delirium in children: an update," *Current Opinion in Anaesthesiology*, vol. 27, no. 3, pp. 309–315, 2014.

[23] D. Yu, W. Chai, X. Sun, and L. Yao, "Emergence agitation in adults: risk factors in 2,000 patients," *Canadian Journal of Anesthesia*, vol. 57, no. 9, pp. 843–848, 2010.

[24] K. Peng, S. R. Wu, F. H. Ji, and J. Li, "Premedication with dexmedetomidine in pediatric patients: a systematic review and meta-analysis," *Clinics*, vol. 69, no. 11, pp. 777–786, 2014.

[25] D. Costi, A. M. Cyna, S. Ahmed et al., "Effects of sevoflurane versus other general anaesthesia on emergence agitation in children," *The Cochrane Database of Systematic Reviews*, vol. 9, Article ID CD007084, 1996.

[26] C. Vanlersberghe, M. H. Lauwers, and F. Camu, "Preoperative ketorolac administration has no preemptive analgesic effect for minor orthopaedic surgery," *Acta Anaesthesiologica Scandinavica*, vol. 40, no. 8, pp. 948–952, 1996.

[27] R. Mihara, M. Soen, H. Kusaka et al., "Effect of continuous intravenous infusion of flurbiprofen axetil and tramadol hydrochloride for postoperative pain management of laparoscopic colectomy," *The Japanese Journal of Anesthesiology*, vol. 60, no. 12, pp. 1364–1369, 2011.

[28] L. Zhang, J. Zhu, L. Xu et al., "Efficacy and safety of flurbiprofen axetil in the prevention of pain on propofol injection: a systematic review and meta-analysis," *Medical Science Monitor*, vol. 20, pp. 995–1002, 2014.

[29] P. F. Piguet, G. E. Grau, and P. Vassalli, "Tumor necrosis factor and immunopathology," *Immunologic Research*, vol. 10, no. 2, pp. 122–140, 1991.

[30] M. A. Marano, L. L. Moldawer, Y. Fong et al., "Cachectin/TNF production in experimental burns and Pseudomonas infection," *Archives of Surgery*, vol. 123, no. 11, pp. 1383–1388, 1988.

Hindawi Publishing Corporation
Mediators of Inflammation
Volume 2015, Article ID 341740, 5 pages
http://dx.doi.org/10.1155/2015/341740

Research Article

Matrix Metalloproteinase-9 Production following Cardiopulmonary Bypass Was Not Associated with Pulmonary Dysfunction after Cardiac Surgery

Tso-Chou Lin,[1] Feng-Yen Lin,[2,3] Yi-Wen Lin,[4] Che-Hao Hsu,[1] Go-Shine Huang,[1] Zhi-Fu Wu,[1] Yi-Ting Tsai,[4] Chih-Yuan Lin,[4] Chi-Yuan Li,[5,6] and Chien-Sung Tsai[4]

[1]*Department of Anesthesiology, Tri-Service General Hospital, National Defense Medical Center, Taipei, Taiwan*
[2]*Department of Internal Medicine, School of Medicine, College of Medicine, Taipei Medical University, Taipei, Taiwan*
[3]*Division of Cardiology, Department of Internal Medicine, Taipei Medical University Hospital, Taipei, Taiwan*
[4]*Division of Cardiovascular Surgery, Department of Surgery, Tri-Service General Hospital, National Defense Medical Center, Taipei, Taiwan*
[5]*Graduate Institute of Clinical Medical Sciences, China Medical University, Taichung, Taiwan*
[6]*Department of Anesthesiology, China Medical University Hospital, Taichung, Taiwan*

Correspondence should be addressed to Chien-Sung Tsai; sung1500@mail.ndmctsgh.edu.tw

Received 5 December 2014; Revised 8 February 2015; Accepted 9 February 2015

Academic Editor: Zhengyuan Xia

Background. Cardiopulmonary bypass (CPB) causes release of matrix metalloproteinase- (MMP-) 9, contributing to pulmonary infiltration and dysfunction. The aims were to investigate MMP-9 production and associated perioperative variables and oxygenation following CPB. *Methods*. Thirty patients undergoing elective cardiac surgery were included. Arterial blood was sampled at 6 sequential points (before anesthesia induction, before CPB and at 2, 4, 6, and 24 h after beginning CPB) for plasma MMP-9 concentrations by ELISA. The perioperative laboratory data and variables, including bypass time, PaO_2/FiO_2, and extubation time, were also recorded. *Results*. The plasma MMP-9 concentrations significantly elevated at 2–6 h after beginning CPB ($P < 0.001$) and returned to the preanesthesia level at 24 h ($P = 0.23$), with predominant neutrophil counts after surgery ($P < 0.001$). The plasma MMP-9 levels at 4 and 6 h were not correlated with prolonged CPB time and displayed no association with postoperative PaO_2/FiO_2, regardless of reduced ratio from preoperative 342.9 ± 81.2 to postoperative 207.3 ± 121.3 mmHg ($P < 0.001$). *Conclusion*. Elective cardiac surgery with CPB induced short-term elevation of plasma MMP-9 concentrations within 24 hours, however, without significant correlation with CPB time and postoperative pulmonary dysfunction, despite predominantly increased neutrophils and reduced oxygenation.

1. Introduction

Cardiopulmonary bypass (CPB) induces a systemic inflammatory response [1] and the following postoperative pulmonary dysfunction [2]. After initiating CPB, blood cells are activated by contact with artificial surfaces of circuits and direct contact of air and damaged tissues, resulting in release of various proinflammatory cytokines. The cessation of alveolar ventilation and ischemia-reperfusion injury leads to neutrophil activation [3] and trafficking to lung [4] and entrapment in the pulmonary capillaries. The released proteolytic enzymes, such as matrix metalloproteinase- (MMP-) 9, degrade alveolar basement membrane and matrix [5], facilitating neutrophil transmigration and protein extravasation into the interstitial tissue of lung [6]. Consequently, injury to the alveolar endothelium and alveolar-capillary barrier dysfunction as central events in the pathogenesis of acute lung injury [7] are manifested with postoperative pulmonary edema and abnormal gas exchange after cardiac surgery with CPB.

The MMPs are a family of more than 25 species of zinc-dependent proteases that are essential for normal tissue remodeling in processes including bone growth, wound healing, and reproduction [5]. Among them, elevated MMP-9 concentration has been a risk factor for future myocardial infarction [8] or coronary revascularization [9] and heart failure [10] by myocardial remodeling [11] after acute myocardial infarction, in addition to acute lung injury [12] and chronic obstructive pulmonary disease [13]. Some clinical studies demonstrated increased MMP-9 levels following CPB for cardiac surgery [14, 15], however, with scarce evidence of correlation with postoperative pulmonary dysfunction, except in rat models with CPB-induced [16] or pancreatitis-associated [17] lung injury. We therefore hypothesized that MMP-9 activation following CPB may contribute to postoperative pulmonary dysfunction. The aims of this study were to investigate MMP-9 concentrations following CPB and analyze the association with perioperative variables and postoperative pulmonary parameters PaO_2/FiO_2 among patients undergoing elective cardiac surgery.

2. Materials and Methods

2.1. Participants. The study was approved by the ethics committee (TSGHIRB-1-101-05-115) and written informed consent was obtained from 30 patients undergoing elective cardiac surgery. Patients with cancers, patients with autoimmune diseases, patients receiving steroids, and patients with preoperative respiratory or hepatic failure were excluded.

2.2. Perioperative Management. In the operation room, patients were premedicated with fentanyl and midazolam for arterial catheterization. General anesthesia was induced with fentanyl 1.5–3 μg/kg, propofol 0.5–1.5 mg/kg, and cisatracurium 0.1–0.2 mg/kg and maintained with sevoflurane or isorfluane after tracheal intubation. A pulmonary artery catheter was placed through right internal jugular vein and transesophageal echocardiography was used to monitor real-time cardiac performance throughout the whole procedure. Routine median sternotomy and standard cardiopulmonary bypass (Sarns 8000, Terumo, Ann Arbor, MI) with an extracorporeal membrane oxygenator (Capiox SX 18, Terumo, Ann Arbor, MI) were carried out in sequence to maintain the body temperature at 28–30°C during surgery. The perfusionist adjusted sevoflurane or isoflurane concentration on the vaporizer to keep mean arterial blood pressure between 50 and 80 mmHg during bypass period. Following standard rewarming and deairing, the pump was weaned at the end of the procedure. Routine inotropic support including dopamine or dobutamine infusion was added for acceptable cardiac output, if necessary. All patients were transferred to the cardiovascular surgical ICU with endotracheal intubation after surgery.

2.3. Blood Samples and Data Collection. Each 20 mL of arterial blood was sampled from the arterial line at 6 sequential time points (before induction, just before CPB, and at 2 h, 4 h, 6 h, and 24 h after beginning CPB) into EDTA-containing tubes. After immediate centrifugation of blood samples at speed 1500 rpm for 10 min at room temperature, the plasma samples were divided into Eppendorf tubes and frozen at −70°C for later plasma MMP-9 concentration testing.

Arterial blood gas analysis was routinely examined perioperatively and immediately upon ICU admission by GEM Premier 3000 (Instrumentation Laboratory, Lexington, MA). Perioperative variables, including general anesthesia, operation, and bypass times, as well as preoperative and postoperative laboratory data, were also recorded. The ratio of arterial oxygen tension (PaO_2, expressed in mmHg) to inspired oxygen fraction (FiO_2) was also calculated before and after operation, as well as before extubation. The severity of hypoxemia is defined as mild ($200 < PaO_2/FiO_2 \leq 300$ mmHg), moderate ($100 < PaO_2/FiO_2 \leq 200$ mmHg), and severe ($PaO_2/FiO_2 \leq 100$ mmHg) by the Berlin definition of acute respiratory distress syndrome [18].

2.4. Enzyme-Linked Immunosorbent Assay (ELISA). The protein concentrations of MMP-9 in the plasma were measured by using the commercially available DuoSet ELISA development kits (R&D Systems Inc., McKinley Place N.E., Minneapolis, USA) according to the manufacturer's protocol (MMP9 catalog number DY911). The absorbance of the color at 450 nm was recorded using a TECAN Sunrise ELISA Reader (Tecan Group Ltd., Männedorf, Switzerland).

2.5. Statistical Analysis. The results were analyzed through SPSS software version 17 (SPSS, Chicago, IL). The demographic data, perioperative variables, postoperative leukocyte counts, arterial blood gas data, and plasma MMP-9 concentrations were presented as mean ± SD. The correlation between MMP-9 concentrations, CPB time, and pulmonary PaO_2/FiO_2 ratios was analyzed by paired t-test or Pearson correlation analysis. P value <0.05 was considered statistically significant.

3. Results

Demographic data of 30 patients were summarized in Table 1, with mean CPB time 120.8 ± 52.4 min. The postoperative white blood cell and neutrophil counts increased significantly (Table 2), whereas lymphocyte and platelet counts decreased, as compared with the preoperative data ($P < 0.001$). The blood glucose levels were significantly elevated from 135.7 ± 37.1 (range 83–221) to 210.2 ± 44.1 (range 126–338) mg/dL postoperatively ($P < 0.001$). To examine alveolar oxygen exchange, PaO_2/FiO_2 ratio was calculated. There were only 12 patients having a preoperative ratio within 200–300 mmHg (mild hypoxemia), while turning to 3 patients with ratio ≤100 mmHg (severe hypoxemia), 16 within 100–200 mmHg (moderate hypoxemia), and 6 within 200–300 mmHg (mild hypoxemia) postoperatively. The mean PaO_2/FiO_2 ratio reduced from preoperative 342.9 ± 81.2 (range 232.0–563.0) to postoperative 207.3 ± 121.3 (range 67.0–538.3) mmHg ($P < 0.001$) ($n = 30$) but recovered before extubation 325.7 ± 129.8 (range 156.0–597.5) mmHg ($P = 0.456$), with extubation time 38.0 ± 28.6 (range 3.5–140) hours after arriving at ICU

Table 1: Demographic data and perioperative variables ($n = 30$).

Gender (male/female)	23/7	
Age, year	60.0 ± 10.5	(33–80)
Height, cm	163.9 ± 7.3	(148–179)
Weight, kg	68.1 ± 13.7	(43–104)
Body mass index, kg/cm^2	25.3 ± 4.4	(17.2–37.3)
General anesthesia time, min	345.6 ± 75.1	(237–495)
Operation time, min	290.3 ± 67.3	(184–441)
Cardiopulmonary bypass time, min	120.8 ± 52.4	(49–281)
Aortic clamp time, min	75.2 ± 35.2	(16–167)
Ischemic heart disease	15	
Coronary artery graft	2.7 ± 0.6	(1–3)
Valvular heart disease	12	
Heart tumor	2	
Atrial septal defect	1	
Hypertension	20	
Diabetes mellitus	10	

The data were presented as mean ± SD (range).

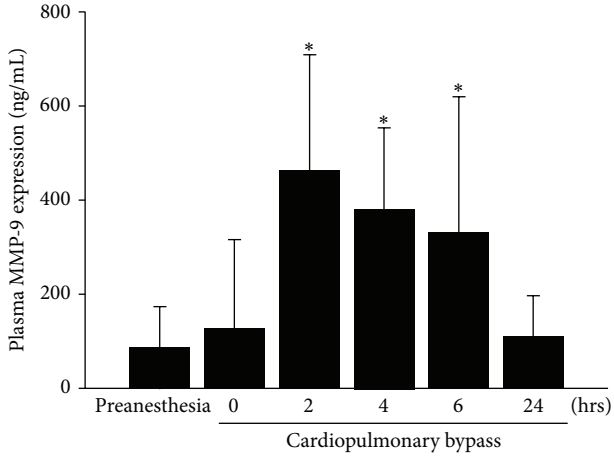

Figure 1: Plasma matrix metalloproteinase-9 concentrations increased significantly at 2–6 hours after beginning cardiopulmonary bypass ($n = 30$), as compared with the preanesthesia level (all $P < 0.001$). The level returned closely to the preanesthesia level at 24 hours ($P = 0.23$).

($n = 27$), except for 3 patients with pneumonia or mediastinitis-related septic shock, and expired at postoperative 10, 25, and 31 days in the ICU. The mean ICU stay ($n = 27$) was 3.5 ± 1.4 (range 2–9) days, with mean hospital stay 11.7 ± 3.9 (range 7–23) days after surgery.

As shown in Figure 1, the plasma MMP-9 levels ($n = 30$) rose significantly at 2, 4, and 6 hours after the start of CPB, with 462.6 ± 247.2 (range 65.5–1102.4), 381.1 ± 174.3 (range 144.1–843.8), and 331.4 ± 288.4 (range 19.9–1266.4) ng/mL, respectively, as compared with 85.7 ± 88.8 ng/mL before anesthesia induction (all $P < 0.001$). The mean level returned closely to the preanesthesia value at 24 hours after the start of CPB (109.3 ± 88.6 ng/mL, $P = 0.23$).

Using Pearson correlation analysis, plasma MMP-9 concentrations at 4 and 6 hours after initiation of CPB were not correlated with CPB time ($P = 0.60$ and 0.83, resp.). Besides, the MMP-9 levels at 4 hours displayed no differences between patients with less or more than 121 min CPB time (376.6 ± 193.3 versus 388.8 ± 143.9 ng/mL, $P = 0.86$). To test the MMP-9 effect on pulmonary dysfunction, the MMP-9 levels at 4 and 6 hours were not associated with postoperative PaO_2/FiO_2 ratio ($P = 0.63$ and 0.48, resp.) and neither was CPB time for PaO_2/FiO_2 ($P = 0.25$).

4. Discussion

In this study, elective cardiac surgery with CPB induced a transient elevation of MMP-9 concentrations at 2–6 hours after beginning CPB, with a mean CPB time of 120.8 minutes. However, the MMP-9 levels at 4 and 6 hours were not correlated with the bypass time and postoperative PaO_2/FiO_2 ratio, despite predominant increase of neutrophil counts upon arriving at ICU, mostly at 4 hours after beginning CPB.

CPB causes a systemic inflammatory response, including activation of neutrophils [3], which are chemoattracted to the inflammatory site. Degranulation of the inflammatory mediators from neutrophils, such as reactive oxygen species and proinflammatory cytokines, could cause pulmonary dysfunction after cardiac surgery by augmenting both neutrophil-pulmonary endothelial adhesion and change of alveolar-endothelial permeability [19]. Also, MMP-9 is degranulated from neutrophils to degrade type IV collagen, the major constituent of basement membrane, and to facilitate neutrophil extravasation. In a canine myocardial ischemia/reperfusion model, infiltrating neutrophils are an early source of MMP-9 after reperfusion [20]. Our previous study [14] demonstrated that intracellular MMP-9 protein and mRNA expression of neutrophils increased after beginning CPB, consistent with the increase of plasma MMP-9 concentrations during cardiac surgery. In this study, we demonstrated a similar trend of MMP-9 production following cardiac surgery and tried to analyze the correlation between MMP-9 concentration and CPB time. With a mean 2-hour bypass period, most cardiac operations in this study were finished 2 hours thereafter. Therefore, blood samples obtained upon arriving at the ICU (mostly 4–6 hours after beginning CPB) could be an indicator for ongoing MMP-9 overproduction or remission after surgery. Among our patients, the MMP-9 concentrations at 4–6 hours were not correlated with CPB time, indicating rapid remission of MMP-9 production after elective cardiac surgery with relative shorter CPB time, despite significant increase of neutrophil counts after surgery.

Cardiac surgery using CPB may cause postoperative pulmonary dysfunction, including acute lung injury and/or acute respiratory distress syndrome (ARDS) [2]. According to the 2012 Berlin definition of ARDS [18], the severity of pulmonary dysfunction is updated by degree of hypoxemia as mild ($200 < PaO_2/FiO_2 \leq 300$ mmHg), moderate ($100 < PaO_2/FiO_2 \leq 200$ mmHg), and severe ($PaO_2/FiO_2 \leq 100$ mmHg). In our patients, postoperative depression of oxygenation was observed, including reduced PaO_2/FiO_2 ratio and patients shifting from preoperative mild hypoxemia ($n = 12$) to postoperative severe ($n = 3$), moderate

Table 2: Perioperative laboratory data and variables.

	Preoperative	Postoperative	*P* value
White blood cell count, /mm^3	7,500 ± 2,300	11,500 ± 4,000	<0.001
N ratio, %	65.4 ± 8.6	86.3 ± 5.5	<0.001
L ratio, %	22.9 ± 8.5	7.8 ± 3.2	<0.001
Neutrophil count, /mm^3	5,000 ± 2,000	10,000 ± 3,700	<0.001
Lymphocyte count, /mm^3	1,600 ± 600	800 ± 300	<0.001
Platelet, /mm^3	229.8 ± 70.7	152.4 ± 38.7	<0.001
Hemoglobin, g/dL	13.0 ± 2.0	10.2 ± 1.5	<0.001
BUN, mg/dL	21.4 ± 14.5	18.2 ± 10.2	0.101
Creatinine, mg/dL	2.0 ± 2.9	1.6 ± 1.9	0.202
AST, U/L	29.9 ± 22.2	40.7 ± 16.8	0.002
ALT, U/L	29.0 ± 23.0	21.0 ± 8.7	0.027
Glucose, mg/dL	135.7 ± 37.1	210.2 ± 44.1	<0.001
Lactate, mmol/L	1.0 ± 0.4	3.2 ± 1.9	<0.001
Base excess, mmol/L	2.2 ± 1.9	0.1 ± 4.1	0.012
HCO_3^-, mmol/L	25.7 ± 2.2	25.2 ± 3.5	0.466
Troponin-I, ng/mL		3.7 ± 2.8	
B-type natriuretic peptide, pg/mL		213.1 ± 242.2	
Cardiac index, L/min/m^2		3.3 ± 1.1	
PaO_2/FiO_2 ratio, mmHg	342.9 ± 81.2	207.3 ± 121.3	<0.001
PaO_2/FiO_2 ratio before extubation		325.7 ± 129.8	0.456*
Extubation time, hours		38.0 ± 28.6	
ICU stay, days		3.5 ± 1.4	
Hospital stay, days		11.7 ± 3.9 (7–23)	

*Compared with the preoperative data.

($n = 16$), and mild ($n = 6$) hypoxemia. Based on the previous evidence of predominant neutrophil recruitment and activation following CPB [6, 14], neutrophil-mediated MMP-9 activation [14, 20], and MMP-involved acute lung injury [7, 12], we hypothesized that MMP-9 activation may contribute to pulmonary dysfunction following CPB, which could be manifested by reduced PaO_2/FiO_2 ratio. Eventually, our results demonstrated transient enhancement of MMP-9 concentrations at 4–6 hours following CPB, which, however, was not correlated with reduced postoperative PaO_2/FiO_2, indicating clinically short-term and insignificant influence on pulmonary function in our patients with elective cardiac surgery.

Two limitations should be addressed. First, only the plasma MMP-9 concentrations and clinical parameters were analyzed during the acute phase in this study, needing further ex vivo or experimental data to verify the biological changes of acute lung injury and the following myocardial remodeling. Second, limited case number in this study may diminish the clinical manifestation and its significance of correlation. More participants with various groups of severity are needed to verify MMP-9 as a clinical indicator for pulmonary dysfunction after cardiac surgery.

In conclusion, we identified that elective cardiac surgery with CPB induced a short-term elevation of MMP-9 concentrations at 2–6 hours after beginning CPB, with predominant increase of neutrophils. The postoperative MMP-9 levels upon arriving at ICU were not correlated with bypass time and reduced oxygenation after cardiac surgery.

Conflict of Interests

The authors declare that there is no conflict of interests regarding the publication of this paper.

Authors' Contribution

Chi-Yuan Li and Chien-Sung Tsai contributed equally to this work.

Acknowledgments

The authors gratefully acknowledge the research assistants, Jui-Chi Tsai, Ph.D., and Hsin-Hua Chung, for laboratory analysis. Grant support from Taiwan Ministry of Science and Technology (NSC102-2314-B-016-026 and MOST 103-2314-B-016-022-MY3) and Tri-Service General Hospital (TSGH-C103-028 and TSGH-C95-46) is also acknowledged.

References

[1] O. J. Warren, A. J. Smith, C. Alexiou et al., "The inflammatory response to cardiopulmonary bypass: part 1—mechanisms of

pathogenesis," *Journal of Cardiothoracic and Vascular Anesthesia*, vol. 23, no. 2, pp. 223–231, 2009.

[2] E. Apostolakis, K. S. Filos, E. Koletsis, and D. Dougenis, "Lung dysfunction following cardiopulmonary bypass," *Journal of Cardiac Surgery*, vol. 25, no. 1, pp. 47–55, 2010.

[3] M. Kolackova, J. Krejsek, V. Svitek et al., "The effect of conventional and mini-invasive cardiopulmonary bypass on neutrophil activation in patients undergoing coronary artery bypass grafting," *Mediators of Inflammation*, vol. 2012, Article ID 152895, 8 pages, 2012.

[4] J. Rossaint, C. Berger, H. van Aken et al., "Cardiopulmonary bypass during cardiac surgery modulates systemic inflammation by affecting different steps of the leukocyte recruitment cascade," *PLoS ONE*, vol. 7, no. 9, Article ID e45738, 2012.

[5] R. P. Iyer, N. L. Patterson, G. B. Fields, and M. L. Lindsey, "The history of matrix metalloproteinases: milestones, myths, and misperceptions," *The American Journal of Physiology—Heart and Circulatory Physiology*, vol. 303, no. 8, pp. H919–H930, 2012.

[6] T. Kotani, Y. Kotake, H. Morisaki et al., "Activation of a neutrophil-derived inflammatory response in the airways during cardiopulmonary bypass," *Anesthesia and Analgesia*, vol. 103, no. 6, pp. 1394–1399, 2006.

[7] Y. Aschner, R. L. Zemans, C. M. Yamashita, and G. P. Downey, "Matrix metalloproteinases and protein tyrosine kinases: potential novel targets in acute lung injury and ARDS," *Chest*, vol. 146, no. 4, pp. 1081–1091, 2014.

[8] B. J. Jefferis, P. Whincup, P. Welsh et al., "Prospective study of matrix metalloproteinase-9 and risk of myocardial infarction and stroke in older men and women," *Atherosclerosis*, vol. 208, no. 2, pp. 557–563, 2010.

[9] K.-F. Wang, P.-H. Huang, C.-H. Chiang et al., "Usefulness of plasma matrix metalloproteinase-9 level in predicting future coronary revascularization in patients after acute myocardial infarction," *Coronary Artery Disease*, vol. 24, no. 1, pp. 23–28, 2013.

[10] D. R. Wagner, C. Delagardelle, I. Ernens, D. Rouy, M. Vaillant, and J. Beissel, "Matrix metalloproteinase-9 is a marker of heart failure after acute myocardial infarction," *Journal of Cardiac Failure*, vol. 12, no. 1, pp. 66–72, 2006.

[11] F. G. Spinale, "Myocardial matrix remodeling and the matrix metalloproteinases: influence on cardiac form and function," *Physiological Reviews*, vol. 87, no. 4, pp. 1285–1342, 2007.

[12] A. Davey, D. F. McAuley, and C. M. O'Kane, "Matrix metalloproteinases in acute lung injury: mediators of injury and drivers of repair," *European Respiratory Journal*, vol. 38, no. 4, pp. 959–970, 2011.

[13] B. Brajer, H. Batura-Gabryel, A. Nowicka, B. Kuznar-Kaminska, and A. Szczepanik, "Concentration of matrix metalloproteinase-9 in serum of patients with chronic obstructive pulmonary disease and a degree of airway obstruction and disease progression," *Journal of Physiology and Pharmacology*, vol. 59, supplement 6, pp. 145–152, 2008.

[14] T.-C. Lin, C.-Y. Li, C.-S. Tsai et al., "Neutrophil-mediated secretion and activation of matrix metalloproteinase-9 during cardiac surgery with cardiopulmonary bypass," *Anesthesia and Analgesia*, vol. 100, no. 6, pp. 1554–1560, 2005.

[15] H. F. Galley, G. D. Macaulay, and N. R. Webster, "Matrix metalloproteinase-9, tissue inhibitor of metalloproteinase-1 and tumour necrosis factor α release during cardiopulmonary bypass," *Anaesthesia*, vol. 57, no. 7, pp. 659–662, 2002.

[16] C. Wang, D. Li, Y. Qian, J. Wang, and H. Jing, "Increased matrix metalloproteinase-9 activity and mRNA expression in lung injury following cardiopulmonary bypass," *Laboratory Investigation*, vol. 92, no. 6, pp. 910–916, 2012.

[17] T. Keck, J. H. Balcom IV, C. Fernandez-del Castillo, B. A. Antoniu, and A. L. Warshaw, "Matrix metalloproteinase-9 promotes neutrophil migration and alveolar capillary leakage in pancreatitis-associated lung injury in the rat," *Gastroenterology*, vol. 122, no. 1, pp. 188–201, 2002.

[18] V. M. Ranieri, G. D. Rubenfeld, B. T. Thompson et al., "Acute respiratory distress syndrome: the Berlin definition," *Journal of the American Medical Association*, vol. 307, no. 23, pp. 2526–2533, 2012.

[19] R. Wynne and M. Botti, "Postoperative pulmonary dysfunction in adults after cardiac surgery with cardiopulmonary bypass: clinical significance and implications for practice," *The American Journal of Critical Care*, vol. 13, no. 5, pp. 384–393, 2004.

[20] M. Lindsey, K. Wedin, M. D. Brown et al., "Matrix-dependent mechanism of neutrophil-mediated release and activation of matrix metalloproteinase 9 in myocardial ischemia/reperfusion," *Circulation*, vol. 103, no. 17, pp. 2181–2187, 2001.

Hindawi Publishing Corporation
Mediators of Inflammation
Volume 2015, Article ID 163140, 11 pages
http://dx.doi.org/10.1155/2015/163140

Research Article

Histone Deacetylase Inhibitor Trichostatin A Ameliorated Endotoxin-Induced Neuroinflammation and Cognitive Dysfunction

Chung-Hsi Hsing,[1,2,3] Shih-Kai Hung,[4,5] Yeong-Chang Chen,[1,2] Tsui-Shan Wei,[1] Ding-Ping Sun,[6] Jhi-Joung Wang,[1,2] and Ching-Hua Yeh[7]

[1]*Department of Medical Research, Chi Mei Medical Center, Tainan 710, Taiwan*
[2]*Department of Anesthesiology, Chi Mei Medical Center, Tainan 710, Taiwan*
[3]*Department of Anesthesiology, Taipei Medical University, Taipei 110, Taiwan*
[4]*Department of Radiation Oncology, Buddhist Dalin Tzu Chi General Hospital, Chiayi 622, Taiwan*
[5]*School of Medicine, Tzu Chi University, Hualien 970, Taiwan*
[6]*Department of Surgery, Chi Mei Medical Center, Tainan 710, Taiwan*
[7]*Department of Medicinal Botanicals and Health Applications, Da-Yeh University, Changhua 515, Taiwan*

Correspondence should be addressed to Ching-Hua Yeh; judyyeh@mail.dyu.edu.tw

Received 6 January 2015; Revised 25 March 2015; Accepted 25 March 2015

Academic Editor: Zhengyuan Xia

Excessive production of cytokines by microglia may cause cognitive dysfunction and long-lasting behavioral changes. Activating the peripheral innate immune system stimulates cytokine secretion in the central nervous system, which modulates cognitive function. Histone deacetylases (HDACs) modulate cytokine synthesis and release. Trichostatin A (TSA), an HDAC inhibitor, is documented to be anti-inflammatory and neuroprotective. We investigated whether TSA reduces lipopolysaccharide- (LPS-) induced neuroinflammation and cognitive dysfunction. ICR mice were first intraperitoneally (i.p.) injected with vehicle or TSA (0.3 mg/kg). One hour later, they were injected (i.p.) with saline or *Escherichia coli* LPS (1 mg/kg). We analyzed the food and water intake, body weight loss, and sucrose preference of the injected mice and then determined the microglia activation and inflammatory cytokine expression in the brains of LPS-treated mice and LPS-treated BV-2 microglial cells. In the TSA-pretreated mice, microglial activation was lower, anhedonia did not occur, and LPS-induced cognitive dysfunction (anorexia, weight loss, and social withdrawal) was attenuated. Moreover, mRNA expression of HDAC2, HDAC5, indoleamine 2,3-dioxygenase (IDO), TNF-α, MCP-1, and IL-1β in the brain of LPS-challenged mice and in the LPS-treated BV-2 microglial cells was lower. TSA diminished LPS-induced inflammatory responses in the mouse brain and modulated the cytokine-associated changes in cognitive function, which might be specifically related to reducing HDAC2 and HDAC5 expression.

1. Introduction

The loss of intellectual functions such as thinking, remembering, learning, and the activities of daily living is called *cognitive dysfunction*. The forms of cognitive dysfunction are seen in illnesses such as Alzheimer's and infectious diseases. In cognitive disorders, neurodegeneration and neuroinflammation have been implicated [1–3]. Neuroinflammation has been associated with altered neural circuitry after trauma and in neurodegenerative diseases, which suggests that the central nervous system (CNS) is involved in changing cognitive function by directly and indirectly affecting neurons [4, 5]. Communication between the immune system and the CNS is necessary and is a response to immune-induced immunological, physiological, and behavioral changes [6]. Proinflammatory cytokines and endotoxins induce a sickness behavior syndrome [7–9]. Proinflammatory cytokines such as tumor necrosis factor- (TNF-) α, interleukin- (IL-) 1β,

and monocyte chemotactic protein- (MCP-) 1 in the brain are partially responsible for the behavioral symptoms of, for example, anorexia, social withdrawal, and anhedonia [10–13]. Activation of the peripheral innate immune system stimulates cytokine secretion in the CNS. These cytokines modulate the behavioral symptoms of sickness. The overexpression of inflammatory cytokines in the brain is associated with cognitive dysfunction, sickness behavior, and depression [14–16].

Microglia are one of two major innate types of immune cell in the CNS and mediate its immune responses, in particular to lipopolysaccharide (LPS). Activated microglia produce antigens, inflammatory cytokines, and phagocytosis. Limiting microglial activity is considered beneficial for neuroinflammatory changes [17–19].

Changes in gene expression in the brain are important in normal aging and in neurodegenerative disease-induced cognitive deficits. The posttranslational modification of various histones is involved in regulating and silencing gene expression. Histone acetylation is controlled by histone acetyl transferases (HATs), general transcription factors and histone deacetylases (HDACs), and suppressed gene transcription [20, 21]. HDACs and HDAC inhibitors modulate cytokine synthesis and release [22–24]. There are four classes of human HDACs [24]. Classes I and II are involved in brain disease [20]. HDAC inhibitors are both anticancer and anti-inflammatory agents. Several HDAC inhibitors have been reported as neuroprotective in rat models [25, 26]. Nonselective HDAC inhibitors such as trichostatin A (TSA) inhibit all Class I and Class II HDACs and induce histone acetylation. TSA regulates the cytokine expression in the LPS-mediated inflammatory response [22, 24]. Although TSA is anti-inflammatory [27], its role in LPS-induced neuroinflammation and cognitive dysfunction is unclear.

We investigated the effects of TSA in LPS-induced neuroinflammation and cognitive dysfunction and, in particular, whether TSA reduces that inflammation and dysfunction.

2. Materials and Methods

2.1. Animals. CD-1 (ICR) BR strain adult and juvenile mice (male, 8 weeks old, and 30–35 g) were purchased from BioLasco (Charles River Laboratories). All mice were housed individually in polypropylene cages and maintained in a temperature-controlled room (22 ± 2°C) on a 12 h light/dark cycle with *ad libitum* access to rodent chow and water except during the behavior-observation tests. At the end of each study, the mice were examined postmortem for signs of diseases such as splenomegaly or tumors. Data from mice determined to be unhealthy were excluded from analysis. All procedures were in accordance with the Taiwan National Institute of Health Guidelines for the Care and Use of Laboratory Animals and the Chi Mei Foundation Medical Center Animal Use Policy. Chi Mei Medical Center approved the animal care protocol for the experiments in this study.

2.2. Cell Culture. BV-2 microglial cell lines were cultured in RPMI 1640 supplemented with 10% fetal bovine serum (FBS) and antibiotics. The cells were maintained at 37°C in a humidified atmosphere and 5% CO_2, and the growth medium was refreshed every two days until confluence. Cultures were washed twice and supplemented with medium containing experimental conditions.

2.3. Behavior Tests. Locomotor activity and social exploratory behavior were measured as previously described [10]. In brief, the mice were handled for 2 min each day for 5 days before experimentation to adapt them to routine handling. Tests were done during the dark phase (between 0800 and 1700) of the photoperiod under infrared lighting to aid video recording.

2.4. Locomotor Activity. The mice were maintained in their home cage, and locomotor activity was video-recorded during 3 min tests. On the video recordings, cages were divided into six identical rectangles and a trained observer who was blinded to experimental treatments determined the incidence of line crossing within 3 min.

2.5. Sucrose Preference. This test was done as previously described [9]. To assess sucrose preference, the mice were provided with two solutions, water or freshly prepared 2% sucrose, in 50 mL conical tubes with stoppers fitted with ball-type sipper tubes. Before the test, all the mice were adjusted to the two-bottle choice test to reduce their reactions to novelty and to ensure stability of the sucrose consumption baseline. To avoid any place preference, the relative location (left or right) of the sucrose bottle was changed whenever fluid intake was measured. Fluid consumption was measured by weighing bottles before and after each test session. The habituation period lasted until a stable sucrose intake level was reached. All the mice drank both the water and the 2% sucrose solution but preferred drinking the sucrose over the water (data not shown). On the day of the sucrose preference test, mice were deprived of fluid and food for 2 h before the test [11]. At the start of the dark phase of the photoperiod (0800), drinking water and the 2% sucrose solution were placed in the home cage for 9 h, 15 h, and 24 h, respectively. At the end of each testing period, the fluid content of the conical tubes was measured and sucrose preference was determined using the equation: sucrose intake/total fluid intake (water + sucrose intake) × 100% [8].

2.6. RNA Extraction and Reverse Transcriptase-Polymerase Chain Reaction (RT-PCR). Total RNA from cultured BV-2 cells and from the cortex and hippocampus of the mice brains was extracted using Trizol reagent (Invitrogen, Carlsbad, CA, USA) as previously described [12]. Total mRNA (2 μg) was synthesized to cDNA using reverse transcriptase kits (Clontech, BD Biosciences, Palo Alto, CA, USA) according to the manufacturer's protocol. Briefly, RNA samples were heated with RNase-free H_2O and random primers at 70°C for 3 min and immediately cooled on ice. A mixture containing deoxyribonucleoside triphosphate (dNTP), 5× first-strand buffer, dithiothreitol (DTT), and MMLV (Moloney Murine Leukemia Virus) reverse transcriptase was subsequently gently mixed and then incubated at 42°C for 60 min.

The reaction was then terminated by heating the mixture to 70°C for 15 min. RT-PCR was done on a thermal cycler (Applied Biosystems, Foster City, CA, USA) using 2x Taq DNA Polymerase Master Mix (Bioman Scientific Co., Jhonghe City, New Taipei City, Taiwan). The sequences of primers used in this experiment were as follows:

mouse HDAC2:

forward: 5′-GCG TAC AGT CAA GGA GGC GGC-3′;
reverse: 5′-CCC CAG CAA CTG AAC CAC CCG-3′;

mouse HDAC5:

forward: 5′-CCT CAG CCT GGC CAC TGT GC-3′;
reverse: 5′-TGT CCA CCC CAA TGC CCC CA-3′;

mouse TNF-α:

forward: 5′-GAG TGA CAA GCC TGT AGC CCA-3′;
reverse: 5′-CCC TTC TCC AGC TGG AAG A-3′;

mouse IL-1β:

forward: 5′-GTG GCT GTG GAG AAG CTG TGG C-3′;
reverse: 5′-TGG GTC CGA CAG CAC GAG GC-3′;

mouse MCP-1:

forward: 5′-AGG TCC CTG TCA TGC TTC TG-3′;
reverse: 5′-GCT GCT GGT GAT CCT CTT GT-3′;

mouse indoleamine 2,3-dioxygenase (IDO):

forward: 5′-GAA GGA TCC TTG AAG ACC AC-3′;
reverse: 5′-GAA GCT GCG ATT TCC ACC AA-3′;

mouse β-actin transcript (internal control):

forward: 5′-GGG AAT GGG TCA GAA GGA CT-3′;
reverse: 5′-TTT GAT GTC ACG CAC GAT TT-3′.

β-actin, the housekeeping gene, was used to normalize all test genes. The data were analyzed using ImageJ software (version 1.41o) (National Institutes of Health, Bethesda, MD) (http://rsbweb.nih.gov/ij/), and results are expressed as fold differences.

2.7. Immunohistochemical Staining. Twenty-four hours after LPS administration, the mice were briefly anesthetized with isoflurane and then killed using cervical dislocation. The cortex and hippocampus of each mouse brain were fixed with 3.7% formaldehyde. All specimens were embedded in paraffin and sliced into 4 μm thick sections. Sections were deparaffinized and then rehydrated, antigens were retrieved, and endogenous peroxidase activity was quenched using 3% hydrogen peroxide in PBS. After the sections had been blocked with an IHC blocking reagent (Background Sniper; Biocare Medical, Concord, CA, USA) for 1 h, they were incubated with anti-Iba1 (1 : 800 dilution) (Biocare Medical), anti-HDAC2 (1 : 200 dilution) or anti-HDAC5 (1 : 200 dilution) (Abcam, Cambridge, MA) rabbit anti-mouse antibodies in blocking reagent at 4°C overnight. Slides were then washed in PBS, incubated with species-specific biotinylated secondary antibody (1 : 200) for 30 min, washed with PBS again, amplified consecutively with Avidin horseradish peroxidase (HRP) (Vector Laboratories, Burlingame, CA, USA), and visualized by incubating them with 3,3′-diaminobenzidine tetrahydrochloride (Sigma-Aldrich, St. Louis, MO, USA). All slides were counterstained with hematoxylin (Mayer's; Thermo Shandon, Pittsburgh, PA, USA), dehydrated, and mounted. For negative Controls, the procedure omitted the primary antibody.

2.8. Enzyme-Linked Immunosorbent Assays (ELISAs). Cell culture supernatants were collected and the levels of TNF-α, IL-1β, and MCP-1 (R&D Systems, Minneapolis, MN, USA) were measured using ELISA kits according to the manufacturer's instructions. All samples were run in triplicate. After the reaction, plates were washed and 100 μL of *o*-phenylenediamine substrate (Sigma-Aldrich) was added to each well. Plates were incubated for 30 min at room temperature, after which 50 μL of 4 N sulfuric acid was added to each well. The plates were read at 490 nm on a microplate reader (Spectra MAX 340PC), and the data were analyzed.

2.9. Western Blotting. Harvested cells were lysed with a buffer containing 1% Triton X-100, 50 mM of Tris (pH 7.5), 10 mM of ethylenediamine tetraacetic acid (EDTA), 0.02% of sodium azide, and a protease inhibitor cocktail (Roche Boehringer Mannheim Diagnostics, Mannheim, Germany). After one freeze-thaw cycle, cell lysates were centrifuged at 13,000 rpm for 20 min at 4°C. The lysates were boiled in sample buffer for 5 min. Protein samples (30 μg/lane) were loaded on SDS-PAGE (sodium dodecyl sulfate polyacrylamide gel electrophoresis) and electrotransferred to a polyvinylidene fluoride (PVDF) membrane (Millipore, Billerica, MA, USA). Nonspecific bindings were blocked by incubating the membrane with 5% skim milk in Tris-buffered saline (TBS) containing 0.1% Tween 20 (TBST) for 2 h. The membranes were then hybridized with primary antibodies: inducible Iba1 (1 : 1000) (Biocare Medical), acetyl histone H3 (Lys9) (1 : 500) (Millipore), and β-actin (1 : 20000) (Sigma-Aldrich) at 4°C overnight. The membranes were then washed with 0.1% TBST and incubated with a 1 : 5000 dilution of species-specific HRP-conjugated secondary antibodies (Santa Cruz

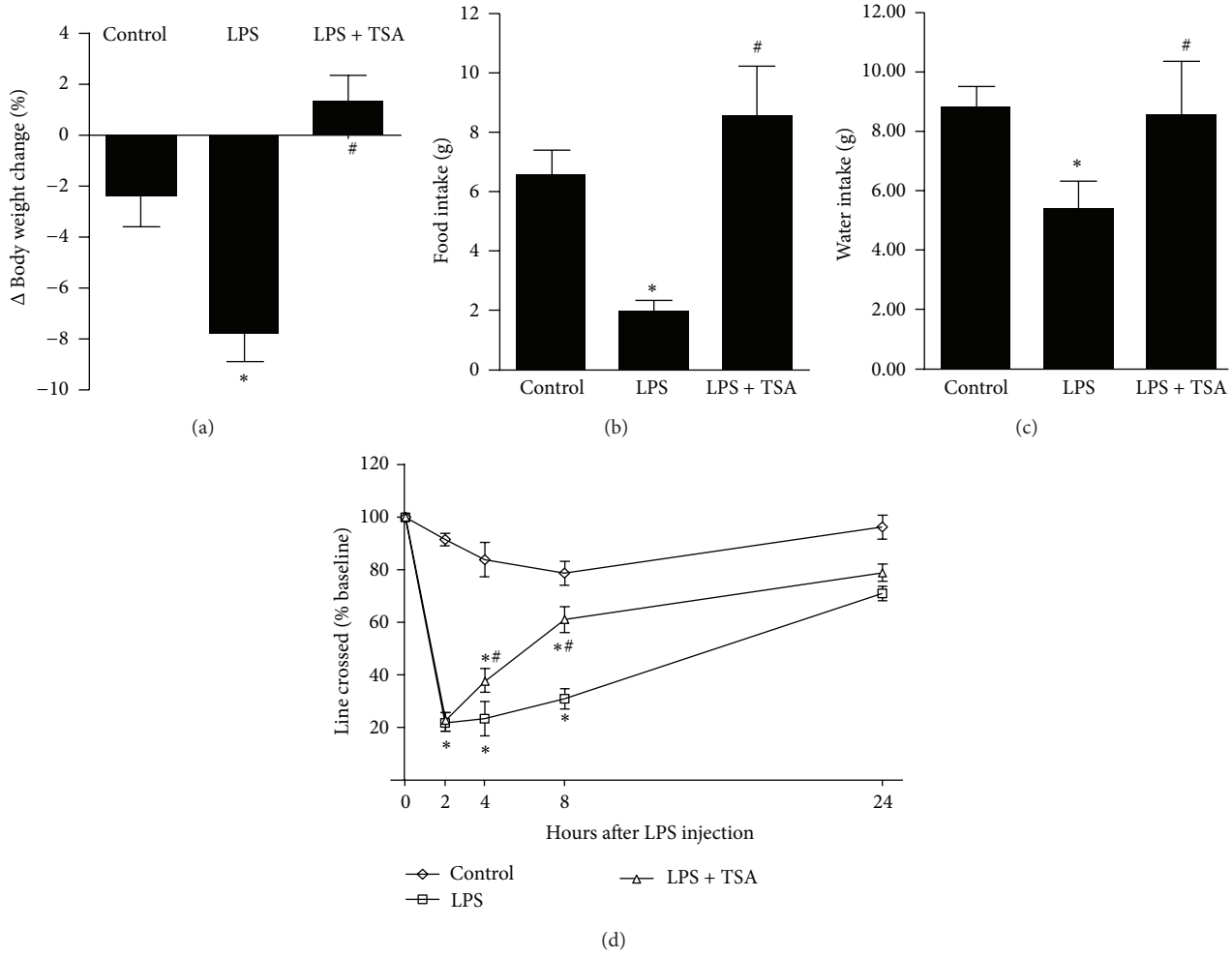

Figure 1: TSA facilitated the recovery from LPS-induced anorexia and increased line crossing (locomotor activity). Mice were pretreated with saline (Controls) or TSA (0.3 mg/kg) for 1 h and then intraperitoneally challenged with saline or *E. coli* LPS (1 mg/kg). (a) Body weight, (b) food intake, and (c) water intake were measured before an LPS injection and then again 24 h later. (d) Line crossing was measured before the LPS injection and then again 2, 4, 8, and 24 h later. Bars and graphs present means ± SEM ($n = 6$). $^{*}P < 0.05$ compared with the Control group; $^{\#}P < 0.05$ compared with the LPS-only group.

Biotechnology, Santa Cruz, CA, USA) at room temperature for 1 h. After they had been washed, the membranes were soaked in electrochemiluminescence (ECL) solution (PerkinElmer Life Sciences, Boston, MA, USA) for 1 min and then exposed to X-ray film (BioMax; Eastman Kodak, Rochester, NY, USA). The relative signal intensity was also quantified using ImageJ 1.41o.

2.10. Experimental Protocols. For *in vitro* studies, TSA (Cayman Chemical, Ann Arbor, MI, USA) and *E. coli* LPS (serotype O55:B5; Sigma-Aldrich) were prepared in isotonic PBS. BV-2 cells were washed and replenished with medium containing TSA (10 ng/mL). One hour later, LPS 50 ng/mL was added to the culture medium and incubated for 4 h. Total protein was collected from cell homogenates and determined using a kit (DC Protein Assay; Bio-Rad Laboratories, Hercules, CA, USA). Total RNA was isolated using Trizol reagent and the HDAC2, HDAC5, TNF-α, IL-1β, MCP-1, and IDO were assayed using RT-PCR.

For *in vivo* experiments, TSA and LPS were dissolved in pyrogen-free isotonic, sterile saline. In the first experiment, adult male ICR mice were injected (i.p.) with vehicle or TSA (0.3 mg/kg/body wt). One hour later, they were injected (i.p.) with saline or LPS (1 mg/kg) and asphyxiated 24 h later ($n = 6$ in each group). The dose of LPS was chosen because it caused a proinflammatory cytokine response in the brain and mild temporary sickness behavior [28]. Their brains were removed and dissected. The cortex was stored at −80°C and the hippocampus was fixed with 3.7% formaldehyde. Total RNA was isolated from these regions using Trizol. HDAC2, HDAC5, TNF-α, IL-1β, MCP-1, and IDO were assayed using RT-PCR.

In the second experiment, adult male ICR mice were treated with saline or TSA and then LPS, as described above ($n = 6$ in each group). Their motivation to engage in social

behavior was determined immediately before the injection of saline or LPS, and again 2, 4, 8, and 24 h later. Body weight, food, and water intake were measured at each time point over the 24 h period. Anhedonia was evaluated using sucrose preference 26–47 h after the saline or LPS injection.

2.11. Statistical Analysis. Data were analyzed using SAS/STAT (SAS Institute, Cary, NC, USA) Generalized Linear Model (GENMOD) procedures. Data were subjected to Kruskal–Wallis ANOVA (analysis of variance) to determine significant main effects and interactions between main factors. When appropriate, a post hoc Tukey test was used to determine whether treatment means were significantly different from one another ($P < 0.05$). All data are means ± SEM (standard error of the mean).

3. Results

3.1. Effects of TSA on LPS-Treated Mice with Cognitive Dysfunction. LPS-only-treated mice (LPS) lost significantly ($P < 0.05$) more body weight than did the saline-treated Controls and LPS + TSA-treated mice gained weight (Figure 1(a)). Food intake was significantly lower in the LPS group than in the Control group but significantly higher in the LPS + TSA group than in the LPS group (Figure 1(b)). Water intake was significantly lower in the LPS group than in the Control group but significantly higher in the LPS + TSA group than in the LPS group (Figure 1(c)). Eight hours after the mice in each group had been injected with the group treatment (saline [Control], LPS-only, or LPS + TSA) the number of line crossings in 3 min by each mouse was counted and compared with the number at baseline: there was a 20% decrease in saline-pretreated Controls, a 40% decrease in TSA-pretreated mice ($P < 0.05$), and an 80% decrease in LPS-only-treated mice ($P < 0.05$) (Figure 1(d)).

The effect of TSA on LPS-induced anhedonia was determined using a sucrose preference test. Between 35 and 47 h after the LPS challenge, sucrose preference was significantly lower in the LPS-only-treated group (Figure 2).

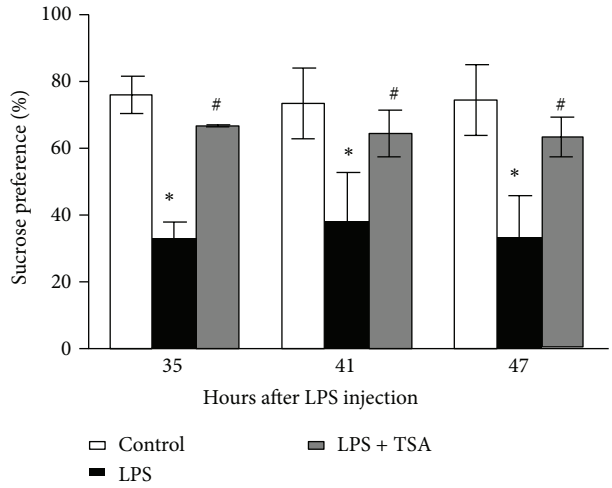

Figure 2: TSA inhibited LPS-induced anhedonia. Mice were pretreated with saline (Controls) or TSA (0.3 mg/kg) for 1 h and then intraperitoneally challenged with saline or *E. coli* LPS (1 mg/kg). The sucrose preference was determined 35 to 47 h after LPS injection. Bars represent the mean ± SEM ($n = 6$). $^{*}P < 0.05$ compared with the Control group; $^{\#}P < 0.05$ compared with the LPS-only group.

3.2. Neuroinflammation Was Significantly Lower in LPS + TSA-Treated Mice Than in LPS-Only-Treated Mice. Mice pretreated with saline (Control) or TSA (0.3 mg/kg) were challenged with saline or LPS (1 mg/kg). Twenty-four hours later, the mice were killed and their cortex and hippocampus were collected. RT-PCR showed that their HDAC2 and HDAC5 mRNA expression levels were higher in the LPS-only-challenged mice. In the mice pretreated with TSA, HDAC2 and HDAC5 mRNA levels were significantly lower in both brain regions (Figure 3(a)). A histological examination showed that HDAC2 and HDAC5 levels were significantly higher in the cortex of LPS-only-challenged mice than in Control mice and in mice that had been pretreated with TSA (Figure 3(b)). HDAC inhibitors modulate cytokine synthesis and release [22–24]; we thus determined the effects of TSA on LPS-induced cytokines expression. After 24 h of LPS challenge, the expressions of TNF-α, IL-1β, MCP-1, and IDO mRNA in cortex and hippocampus were significantly higher than in Control mice. These increases were reduced in the mice pretreated with TSA (Figure 4).

3.3. TSA Inhibits LPS-Induced Microglia Activation. Microglia mediate cytokines expression in CNS and limiting microglial activity is considered beneficial for neuroinflammation [17–19]. We next determined the effects of TSA on LPS-induced microglia activation. A histological examination showed that Iba1 levels were significantly higher in the hippocampus and cortex of LPS-only-challenged mice, which were reduced in mice pretreated with TSA (Figure 5(a)). In the *in vitro* experiment, Iba1 protein expression was significantly higher in LPS-only-treated BV-2 microglial cells than in PBS Control and in LPS + TSA-treated cells (Figure 5(b)).

3.4. Cytokine Expression in LPS + TSA-Treated BV-2 Microglial Cells Was Significantly Lower Than in LPS-Only-Treated Cells. In LPS-only-treated stimulated BV-2 cells, RT-PCR showed that HDAC2 and HDAC5 mRNA levels were significantly higher than in Control cells and in LPS + TSA-treated cells (Figure 6(a)). Moreover, TSA also induced acetyl histone H3 expression in LPS-treated BV-2 cells (Figure 5(b)). We also detected the expression levels of LPS-induced neuroinflammation mediators: TNF-α, IL-1β, MCP-1, and IDO. RT-PCR showed that TNF-α, IL-1β, MCP-1, and IDO mRNA were significantly higher in LPS-only-treated BV-2 cells than in Control cells and in LPS + TSA-treated cells (Figure 6(b)). We determined the protein levels of these cytokines' expression using ELISA. TNF-α, IL-1β, and MCP-1 concentrations in cultured supernatants of LPS-only-treated BV-2 cells were also significantly higher in LPS-only-treated BV-2 cells than in Control cells and in LPS + TSA-treated cells (Figure 6(c)).

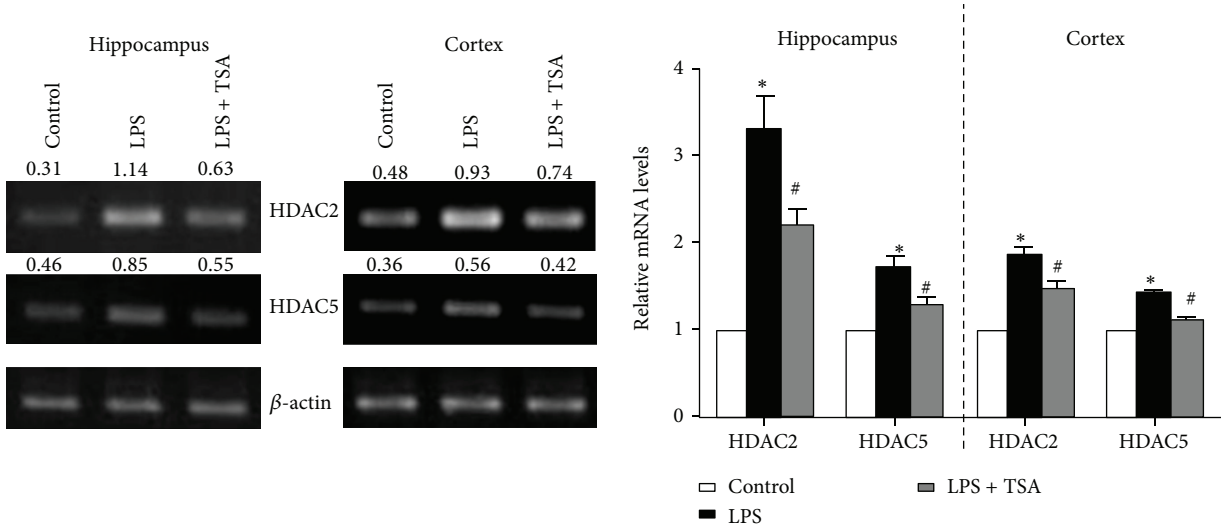

(a)

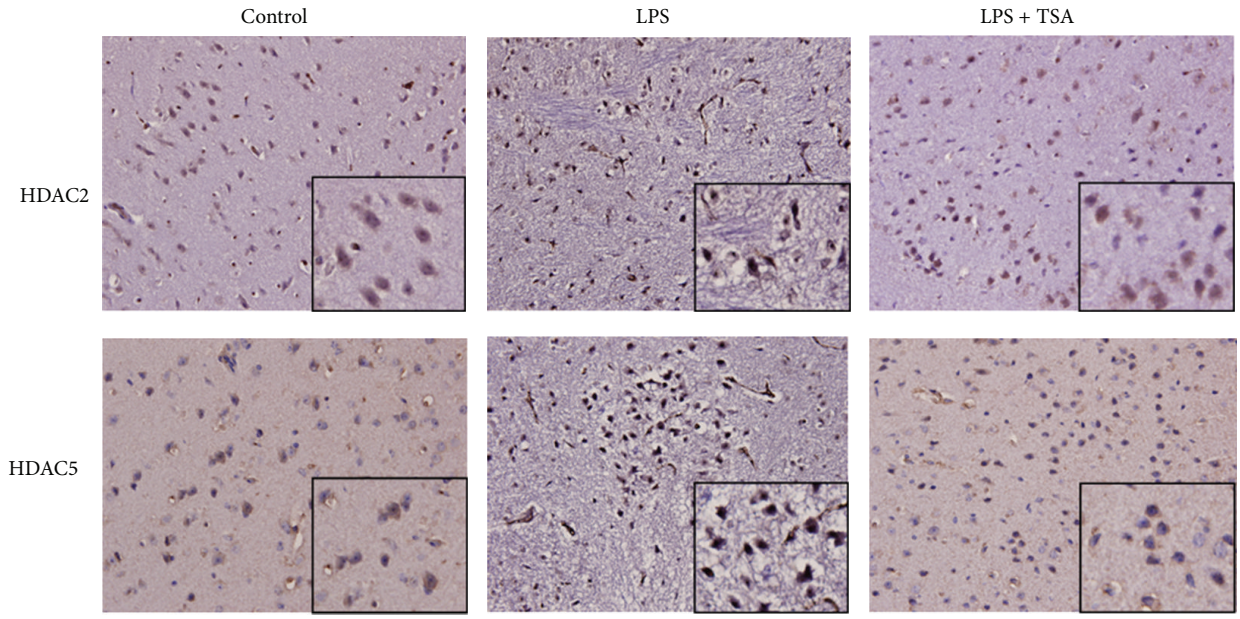

(b)

Figure 3: TSA attenuated LPS-induced HDAC2 and HDAC5 expression in the hippocampus and cortex of mice. Mice were pretreated with saline (Controls) or TSA (0.3 mg/kg) for 1 h and then intraperitoneally challenged with saline or *E. coli* LPS (1 mg/kg) ($n = 6$ in each group). (a) HDAC2 and HDAC5 mRNA were detected using RT-PCR. The right panel shows the quantification of mRNA expression from six independent experiments. $^{*}P < 0.05$ compared with the Control group; $^{\#}P < 0.05$ compared with the LPS-only group. (b) Immunohistochemical staining showed that HDAC2 and HDAC5 expression were increased in the cortex of mice after being LPS challenged, which were reduced in LPS + TSA mice.

4. Discussion

The present study showed that TSA effectively facilitated recovery from LPS-induced anorexia and inhibited anhedonia and increased the number of line crossings. Our *in vivo* and *in vitro* experiments showed that LPS increased HDAC2, HDAC5, TNF-α, IL-1β, MCP-1, and IDO expression and that TSA treatment decreased their expression. Previous studies [1–3, 10, 16] showed that neuroinflammation is associated with myriad complications: cognitive dysfunction, prolonged sickness behavior, and depressive-like behavior. After inducing anorexia and anhedonia via LPS administration, we used a locomotor activity and sucrose preference to assess behavior. Because of facility limit, we did not perform passive avoidance test (PAT) and Morris water maze (MWM) test to further evaluate mice behavior changes. Nevertheless, we determined the histology and gene expression changes which were related to neuroinflammation as well as cognitive dysfunction. All these changes were consistent in behavior experiments in this study.

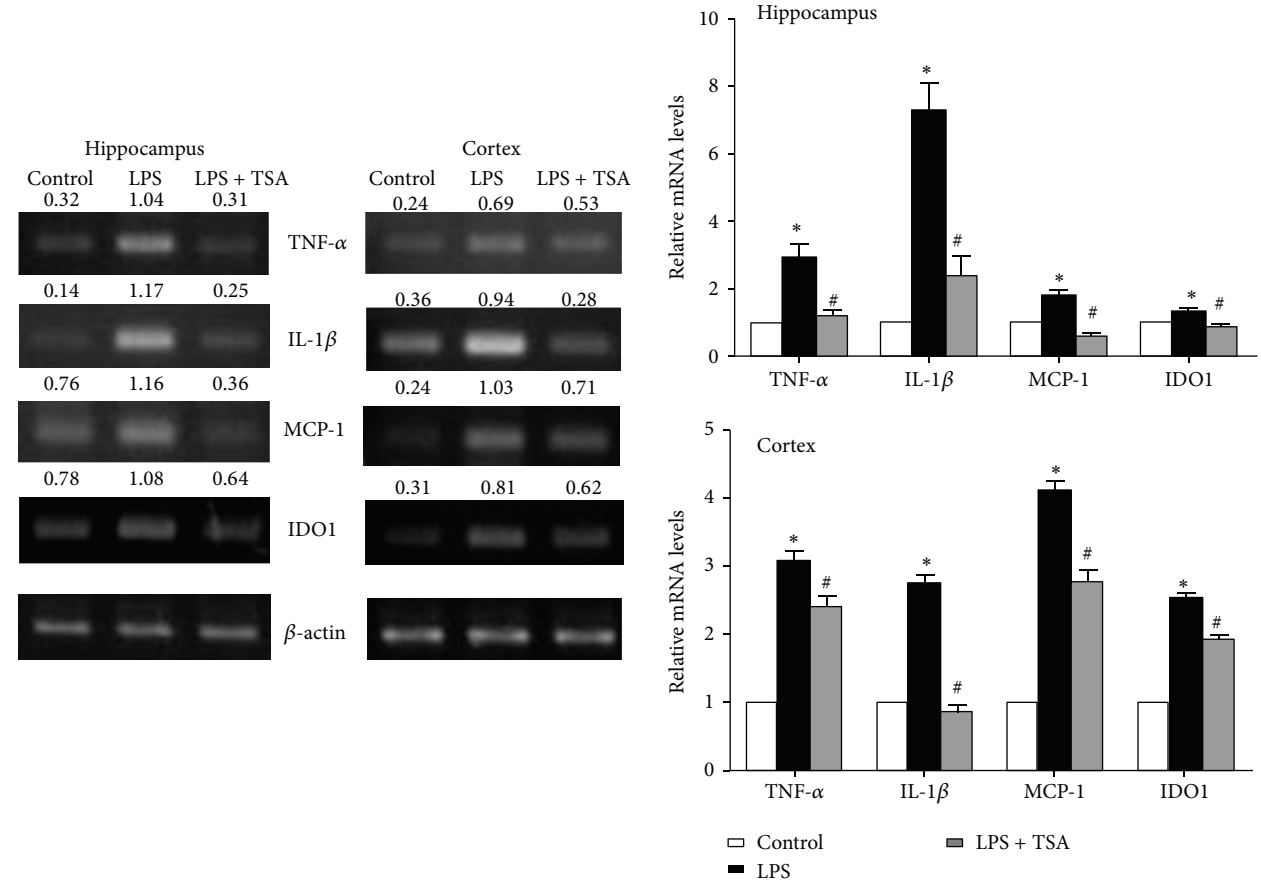

Figure 4: TSA attenuated LPS-induced cytokine mRNA expression in the hippocampus and cortex of mice. Mice were pretreated with saline (Controls) or TSA (0.3 mg/kg) for 1 h and then intraperitoneally challenged with saline or *E. coli* LPS (1 mg/kg) ($n = 6$ in each group). After 24 h they had been treated with LPS, TNF-α, IL-1β, MCP-1, and IDO mRNA expression in the hippocampus and cortex of mice determined using RT-PCR. The lower panel shows the quantification of mRNA expression from six independent experiments. $^{*}P < 0.05$ compared with the Control group; $^{\#}P < 0.05$ compared with the LPS-only group.

Changes caused by histone acetylation are associated with cognitive function [29, 30]. HDAC inhibitors have been used to treat some brain disorders, for example, psychiatric diseases, cognitive impairment, and cognitive decline. HDAC inhibitors were neuroregenerative and neuroprotective in animal models of several neurological diseases [20]. Previous studies [30] showed that SAHA, an HDAC inhibitor, improved memory formation in a mouse model of neurodegeneration. The present study showed that TSA facilitated recovery from LPS-induced cognitive dysfunction.

HDAC Classes I and II are involved in brain disease [20]. HDAC1 has neuroprotective function but a previous study showed that it did not affect cognitive function in neuron-specific HDAC1 deletion mice [20, 30]. HDAC7 plays an important role in vascular endothelium but loss of HDAC7 does not affect brain disorders [20, 31]. Histone acetylation and memory formation ability were reduced in HDAC2-overexpressing mice (Class I group). Hippocampal overexpression of HDAC5 in mice (Class II group) induced depression-like behavior [30, 32]. HDAC inhibitors can facilitate learning and memory formation, which suggests that higher levels of histone acetylation are important for memory formation [33]. We found that TSA increased acetyl histone H3 expression in LPS-challenged microglial cells. HDAC2 and HDAC5 mRNA expression were also reduced by TSA in our *in vivo* and *in vitro* experiments.

In neurodegenerative or neuroinflammatory diseases, CNS has more activated microglia and higher levels of proinflammatory cytokines such as TNF-α, IL-1β, and IDO [13, 34]. In brain, the expression of IL-1β and other proinflammatory cytokines mRNAs are induced by systemically administering LPS, which affect cognitive dysfunction. Other studies [35, 36] have shown that IDO-mediated tryptophan metabolism is involved in neuroinflammatory disease. Inhibiting IDO activation prevents LPS-induced symptoms of depression, for example, anhedonia [16, 37]. We found that TSA reduced the levels of the proinflammatory cytokine TNF-α, IL-1β, and IDO expression in LPS-challenged mice brain and LPS-treated BV-2 cells.

HDAC activation modulates inflammation and immune cell activation [23]. LPS induces HDAC and proinflammatory cytokine expression in mouse microglia, and the cytokine

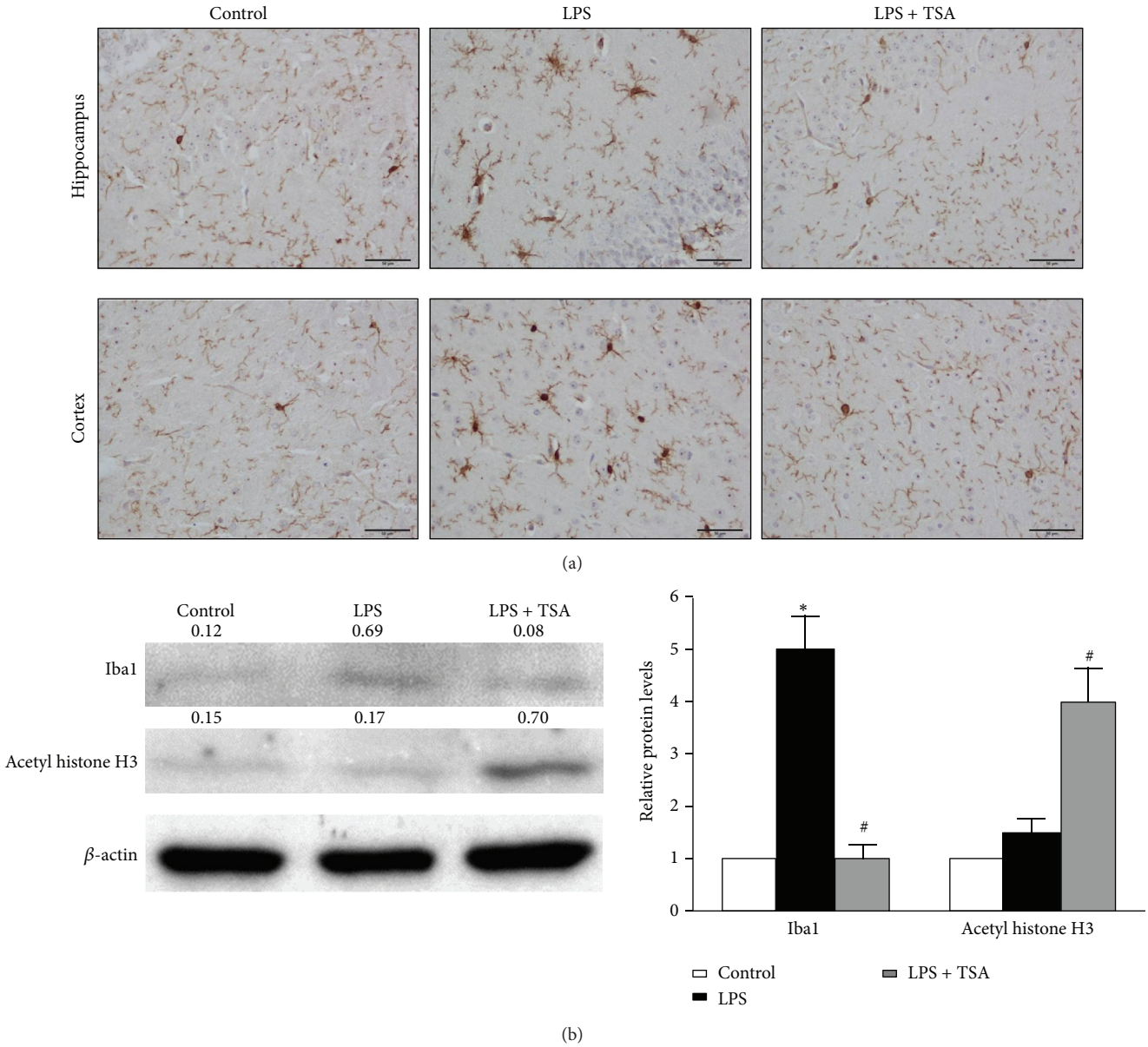

Figure 5: TSA reduced the LPS-induced activation of microglial cells in mice and BV-12 cells. (a) Mice were pretreated with saline (Controls) or TSA (0.3 mg/kg) for 1 h and then intraperitoneally challenged with saline or *E. coli* LPS (1 mg/kg). Immunohistochemistry staining shows that Iba1 expression in the hippocampus and the cortex of mice was higher after 24 h of LPS challenge than in Control and LPS + TSA mice. (b) One hour after BV-2 cells had been pretreated with TSA (10 ng/mL), they were treated with LPS. Four hours later, the protein was collected. Western blotting shows Iba1 and acetyl histone H3 expression in BV-2 cells. The right panel shows the quantification of protein expression from three independent experiments. $^{*}P < 0.05$ compared with the Control group; $^{\#}P < 0.05$ compared with the LPS-only group.

expression is reduced by HDAC inhibitors [22]. The mechanism of HDAC and HDAC inhibitors on reducing proinflammatory cytokines in microglia is not fully understood. HDAC inhibitors are used for cancer therapy because they regulate gene transcription [38]. HDAC inhibitors induce or repress gene expression because acetylation markedly affects the function of nonhistone proteins, particularly reversibly acetylated transcription factors. The effects of HDAC inhibitors on inflammatory gene expression are based on the cell type and the stimulus [25, 27]. Previous studies report that TSA upregulates and downregulates different genes in the same cells. TSA increases LPS-stimulated IL-8 expression but inhibits IL-12 p40 expression in BEAS-2B cells [39]. HDAC inhibitors VPA and SAHA inhibit inflammatory cytokines but increase lymphocyte apoptosis and, dose-dependently, increase H3 acetylation [40]. We found that TSA reduced HDAC2 and HDAC5 mRNA expression and increased H3 acetylation in LPS-treated mice and cells. The TSA reduced LPS-induced proinflammatory cytokine expression. We also found that TSA treatment reduced the activation of microglia

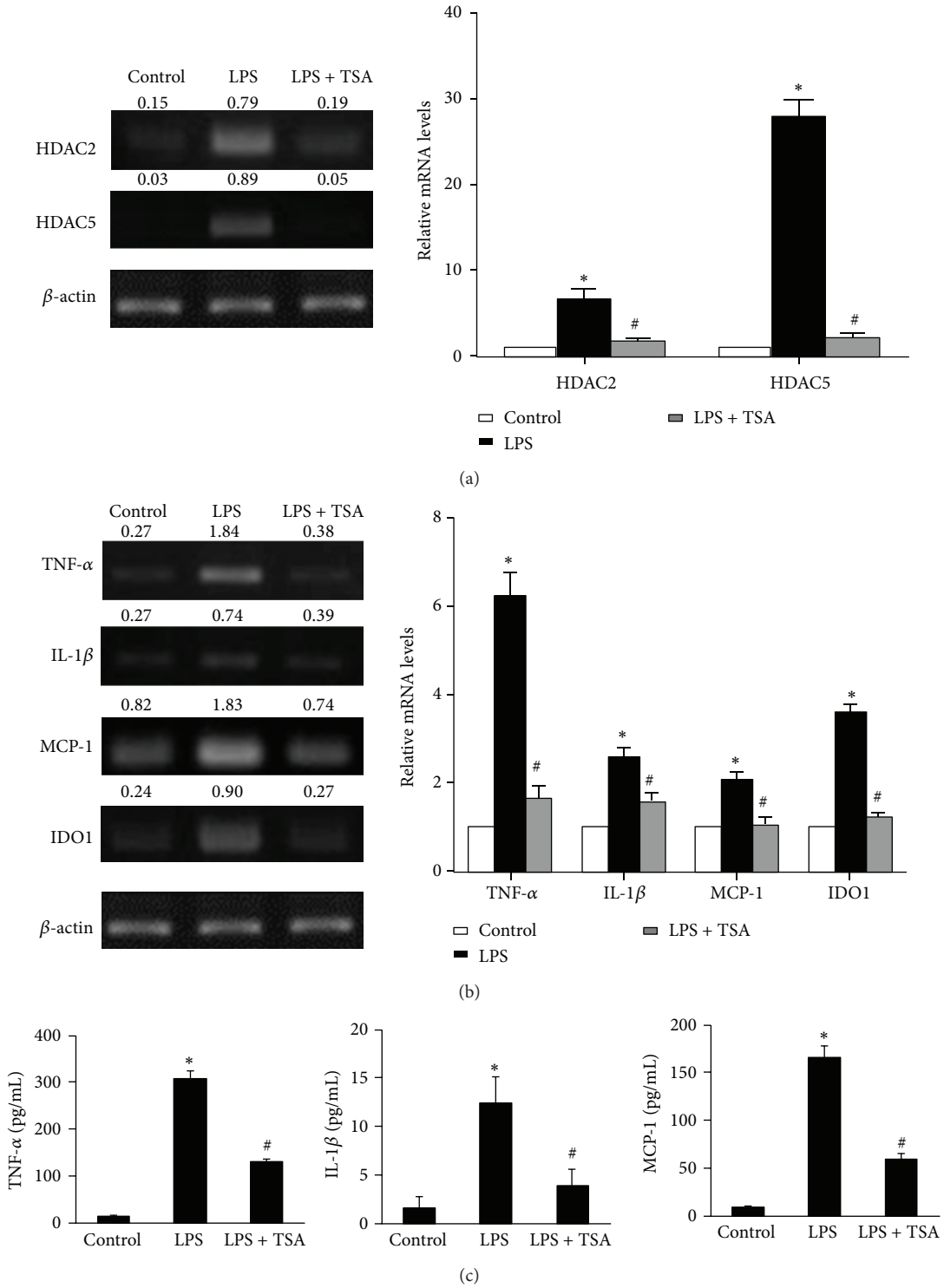

Figure 6: TSA reduced the LPS-induced mRNA expression levels of HDACs and cytokines in BV-2 cells. One hour after BV-2 cells had been pretreated with saline or TSA (10 ng/mL), they were treated with saline or LPS for 4 hours as indicated. (a) HDAC2 and HDAC5 and (b) TNF-α, IL-1β, MCP-1, and IDO mRNA expression were determined using RT-PCR. The right panel shows the quantification of mRNA expression from three independent experiments. (c) The protein levels of TNF-α, IL-1β, and MCP-1 in supernatants of the cultured BV-2 cells were determined using ELISA. Data are means ± SEM ($n = 3$ in each group). $^{*}P < 0.05$ compared with the Control group; $^{\#}P < 0.05$ compared with the LPS-only group.

in LPS-challenged mice and BV-2 cells. Taking all our results together, TSA reduced HDAC and cytokine expression in LPS-treated mice and microglial cells. TSA facilitated recovery from LPS-induced cognitive dysfunction in mice. The effect of TSA on reducing LPS-induced neuroinflammation may be involved in the epigenetic regulation of cytokine expression. The regulatory mechanism that TSA uses to inhibit HDAC and cytokine expression requires additional investigation.

This study showed that TSA decreased LPS-induced sickness behavior symptoms (e.g., anorexia and anhedonia) and reduced microglia activation and neuroinflammatory cytokines production. These findings showed that TSA can be used to mitigate cytokine expression in the brain and beneficially affect mood, motivation, and behavior. We conclude that TSA can be a beneficial part of a pharmacological strategy to decrease infection-induced cognitive dysfunction and neuroinflammation.

Disclosure

The authors confirm that all data underlying the findings are fully available without restriction.

Conflict of Interests

The authors have declared that no competing interests exist.

Acknowledgments

This work was supported by Grants NSC101-2314-B-384-003-MY3 from the Taiwan National Science Council and MOST 103-2320-B-212-001 from Taiwan Ministry of Science and Technology.

References

[1] Y. Xu, J. Yan, P. Zhou et al., "Neurotransmitter receptors and cognitive dysfunction in Alzheimer's disease and Parkinson's disease," *Progress in Neurobiology*, vol. 97, no. 1, pp. 1–13, 2012.

[2] Y. Wan, J. Xu, D. Ma, Y. Zeng, M. Cibelli, and M. Maze, "Postoperative impairment of cognitive function in rats: a possible role for cytokine-mediated inflammation in the hippocampus," *Anesthesiology*, vol. 106, no. 3, pp. 436–443, 2007.

[3] N. Terrando, C. Monaco, D. Ma, B. M. J. Foxwell, M. Feldmannc, and M. Maze, "Tumor necrosis factor-alpha triggers a cytokine cascade yielding postoperative cognitive decline," *Proceedings of the National Academy of Sciences of the United States of America*, vol. 107, no. 47, pp. 20518–20522, 2010.

[4] J. C. M. Schlachetzki and M. Hüll, "Microglial activation in Alzheimer's disease," *Current Alzheimer Research*, vol. 6, no. 6, pp. 554–563, 2009.

[5] M. C. Morganti-Kossmann, L. Satgunaseelan, N. Bye, and T. Kossmann, "Modulation of immune response by head injury," *Injury*, vol. 38, no. 12, pp. 1392–1400, 2007.

[6] K. W. Kelley, R. M. Bluthé, R. Dantzer et al., "Cytokine-induced sickness behavior," *Brain, Behavior, and Immunity*, vol. 17, supplement 1, pp. S112–S118, 2003.

[7] R. Dantzer and K. W. Kelley, "Twenty years of research on cytokine-induced sickness behavior," *Brain, Behavior, and Immunity*, vol. 21, no. 2, pp. 153–160, 2007.

[8] L. L. Skalisz, V. Beijamini, S. L. Joca, M. A. B. F. Vital, C. Da Cunha, and R. Andreatini, "Evaluation of the face validity of reserpine administration as an animal model of depression-Parkinson's disease association," *Progress in Neuro-Psychopharmacology and Biological Psychiatry*, vol. 26, no. 5, pp. 879–883, 2002.

[9] F. Frenois, M. Moreau, J. O'Connor et al., "Lipopolysaccharide induces delayed FosB/DeltaFosB immunostaining within the mouse extended amygdala, hippocampus and hypothalamus, that parallel the expression of depressive-like behavior," *Psychoneuroendocrinology*, vol. 32, no. 5, pp. 516–531, 2007.

[10] J. Abraham, S. Jang, J. P. Godbout et al., "Aging sensitizes mice to behavioral deficits induced by central HIV-1 gp120," *Neurobiology of Aging*, vol. 29, no. 4, pp. 614–621, 2008.

[11] T. K. S. Craft and A. C. DeVries, "Role of IL-1 in poststroke depressive-like behavior in mice," *Biological Psychiatry*, vol. 60, no. 8, pp. 812–818, 2006.

[12] S. Layé, P. Parnet, E. Goujon, and R. Dantzer, "Peripheral administration of lipopolysaccharide induces the expression of cytokine transcripts in the brain and pituitary of mice," *Molecular Brain Research*, vol. 27, no. 1, pp. 157–162, 1994.

[13] R. Dantzer, J. C. O'Connor, G. G. Freund, R. W. Johnson, and K. W. Kelley, "From inflammation to sickness and depression: when the immune system subjugates the brain," *Nature Reviews Neuroscience*, vol. 9, no. 1, pp. 46–56, 2008.

[14] J. Chen, J. B. Buchanan, N. L. Sparkman, J. P. Godbout, G. G. Freund, and R. W. Johnson, "Neuroinflammation and disruption in working memory in aged mice after acute stimulation of the peripheral innate immune system," *Brain, Behavior, and Immunity*, vol. 22, no. 3, pp. 301–311, 2008.

[15] Y. Huang, C. J. Henry, R. Dantzer, R. W. Johnson, and J. P. Godbout, "Exaggerated sickness behavior and brain proinflammatory cytokine expression in aged mice in response to intracerebroventricular lipopolysaccharide," *Neurobiology of Aging*, vol. 29, no. 11, pp. 1744–1753, 2008.

[16] J. P. Godbout, M. Moreau, J. Lestage et al., "Aging exacerbates depressive-like behavior in mice in response to activation of the peripheral innate immune system," *Neuropsychopharmacology*, vol. 33, no. 10, pp. 2341–2351, 2008.

[17] G. A. Garden and T. Möller, "Microglia biology in health and disease," *Journal of Neuroimmune Pharmacology*, vol. 1, no. 2, pp. 127–137, 2006.

[18] A. D. Kraft and G. J. Harry, "Features of microglia and neuroinflammation relevant to environmental exposure and neurotoxicity," *International Journal of Environmental Research and Public Health*, vol. 8, no. 7, pp. 2980–3018, 2011.

[19] K. Saijo and C. K. Glass, "Microglial cell origin and phenotypes in health and disease," *Nature Reviews Immunology*, vol. 11, no. 11, pp. 775–787, 2011.

[20] A. Fischer, F. Sananbenesi, A. Mungenast, and L.-H. Tsai, "Targeting the correct HDAC(s) to treat cognitive disorders," *Trends in Pharmacological Sciences*, vol. 31, no. 12, pp. 605–617, 2010.

[21] C. L. Peterson and M.-A. Laniel, "Histones and histone modifications," *Current Biology*, vol. 14, no. 14, pp. R546–R551, 2004.

[22] V. Kannan, N. Brouwer, U.-K. Hanisch, T. Regen, B. J. L. Eggen, and H. W. G. M. Boddeke, "Histone deacetylase inhibitors suppress immune activation in primary mouse microglia,"

Journal of Neuroscience Research, vol. 91, no. 9, pp. 1133–1142, 2013.

[23] S. J. Shuttleworth, S. G. Bailey, and P. A. Townsend, "Histone Deacetylase inhibitors: new promise in the treatment of immune and inflammatory diseases," *Current Drug Targets*, vol. 11, no. 11, pp. 1430–1438, 2010.

[24] H.-S. Suh, S. Choi, P. Khattar, N. Choi, and S. C. Lee, "Histone deacetylase inhibitors suppress the expression of inflammatory and innate immune response genes in human microglia and astrocytes," *Journal of Neuroimmune Pharmacology*, vol. 5, no. 4, pp. 521–532, 2010.

[25] M. A. Halili, M. R. Andrews, L. I. Labzin et al., "Differential effects of selective HDAC inhibitors on macrophage inflammatory responses to the Toll-like receptor 4 agonist LPS," *Journal of Leukocyte Biology*, vol. 87, no. 6, pp. 1103–1114, 2010.

[26] H. J. Kim, M. Rowe, M. Ren, J. S. Hong, P. S. Chen, and D. M. Chuang, "Histone deacetylase inhibitors exhibit anti-inflammatory and neuroprotective effects in a rat permanent ischemic model of stroke: multiple mechanisms of action," *Journal of Pharmacology and Experimental Therapeutics*, vol. 321, no. 3, pp. 892–901, 2007.

[27] I. M. Adcock, "HDAC inhibitors as anti-inflammatory agents," *British Journal of Pharmacology*, vol. 150, no. 7, pp. 829–831, 2007.

[28] J.-L. Bret-Dibat and R. Dantzer, "Cholecystokinin receptors do not mediate the suppression of food- motivated behavior by lipopolysaccharide and interleukin-1 beta in mice," *Physiology and Behavior*, vol. 69, no. 3, pp. 325–331, 2000.

[29] J. M. Levenson, K. J. O'Riordan, K. D. Brown, M. A. Trinh, D. L. Molfese, and J. D. Sweatt, "Regulation of histone acetylation during memory formation in the hippocampus," *The Journal of Biological Chemistry*, vol. 279, no. 39, pp. 40545–40559, 2004.

[30] J.-S. Guan, S. J. Haggarty, E. Giacometti et al., "HDAC2 negatively regulates memory formation and synaptic plasticity," *Nature*, vol. 459, no. 7243, pp. 55–60, 2009.

[31] C. L. Benn, R. Butler, L. Mariner et al., "Genetic knock-down of HDAC7 does not ameliorate disease pathogenesis in the R6/2 mouse model of Huntington's disease," *PLoS ONE*, vol. 4, no. 6, Article ID e5747, 2009.

[32] N. M. Tsankova, O. Berton, W. Renthal, A. Kumar, R. L. Neve, and E. J. Nestler, "Sustained hippocampal chromatin regulation in a mouse model of depression and antidepressant action," *Nature Neuroscience*, vol. 9, no. 4, pp. 519–525, 2006.

[33] S. Peleg, F. Sananbenesi, A. Zovoilis et al., "Altered histone acetylation is associated with age-dependent memory impairment in mice," *Science*, vol. 328, no. 5979, pp. 753–756, 2010.

[34] J. M. Rubio-Perez and J. M. Morillas-Ruiz, "A review: inflammatory process in Alzheimer's disease, role of cytokines," *The Scientific World Journal*, vol. 2012, Article ID 756357, 15 pages, 2012.

[35] A.-M. van Dam, M. Brouns, S. Louisse, and F. Berkenbosch, "Appearance of interleukin-1 in macrophages and in ramified microglia in the brain of endotoxin-treated rats: a pathway for the induction of non-specific symptoms of sickness?" *Brain Research*, vol. 588, no. 2, pp. 291–296, 1992.

[36] R. Dantzer, "Cytokine-induced sickness behavior: where do we stand?" *Brain, Behavior, and Immunity*, vol. 15, no. 1, pp. 7–24, 2001.

[37] J. C. O'Connor, M. A. Lawson, C. André et al., "Lipopolysaccharide-induced depressive-like behavior is mediated by indoleamine 2,3-dioxygenase activation in mice," *Molecular Psychiatry*, vol. 14, no. 5, pp. 511–522, 2009.

[38] D. R. Walkinshaw and X.-J. Yang, "Histone deacetylase inhibitors as novel anticancer therapeutics," *Current Oncology*, vol. 15, no. 5, pp. 70–76, 2008.

[39] K. Iwata, K. Tomita, H. Sano, Y. Fujii, A. Yamasaki, and E. Shimizu, "Trichostatin A, a histone deacetylase inhibitor, down-regulates interleukin-12 transcription in SV-40-transformed lung epithelial cells," *Cellular Immunology*, vol. 218, no. 1-2, pp. 26–33, 2002.

[40] R. Glauben, A. Batra, I. Fedke et al., "Histone hyperacetylation is associated with amelioration of experimental colitis in mice," *Journal of Immunology*, vol. 176, no. 8, pp. 5015–5022, 2006.

Hindawi Publishing Corporation
Mediators of Inflammation
Volume 2015, Article ID 360973, 8 pages
http://dx.doi.org/10.1155/2015/360973

Research Article

Protective Effect of $CXCR3^+CD4^+CD25^+Foxp3^+$ Regulatory T Cells in Renal Ischemia-Reperfusion Injury

Cao Jun,[1] Li Qingshu,[2] Wei Ke,[1] Li Ping,[1] Dong Jun,[1] Luo Jie,[1] and Min Su[1]

[1] *Department of Anesthesiology, The First Affiliated Hospital of Chongqing Medical University, No. 1 Youyi Road, Yuzhong District, Chongqing 400016, China*
[2] *Department of Pathology, Chongqing Medical University, Chongqing 400016, China*

Correspondence should be addressed to Min Su; minsu89011068@163.com

Received 12 August 2014; Revised 7 October 2014; Accepted 12 October 2014

Academic Editor: Huang-Ping Yu

Regulatory T cells (Tregs) suppress excessive immune responses and are potential therapeutic targets in autoimmune disease and organ transplantation rejection. However, their role in renal ischemia-reperfusion injury (IRI) is unclear. Levels of Tregs and expression of CXCR3 in Tregs were analyzed to investigate their function in the early phase of renal IRI. Mice were randomly divided into Sham, IRI, and anti-CD25 (PC61) + IRI groups. The PC61 + IRI group was established by i.p. injection of PC61 monoclonal antibody (mAb) to deplete Tregs before renal ischemia. $CD4^+CD25^+Foxp3^+$ Tregs and CXCR3 on Tregs were analyzed by flow cytometry. Blood urea nitrogen (BUN), serum creatinine (Scr) levels, and tubular necrosis scores, all measures of kidney injury, were greater in the IRI group than in the Sham group. Numbers of Tregs were increased at 72 h after reperfusion in kidney. PC61 mAb preconditioning decreased the numbers of Tregs and aggravated kidney injury. There was no expression of CXCR3 on Tregs in normal kidney, while it expanded at 72 h after reperfusion and inversely correlated with BUN, Scr, and kidney histology score. This indicated that recruitment of Tregs into the kidney was related to the recovery of renal function after IRI and CXCR3 might be involved in the migration of Tregs.

1. Introduction

Ischemia-reperfusion injury (IRI) is a common and important clinical problem in many different organs. It has a critical role in the pathogenesis of acute renal failure and graft rejection, is associated with increased morbidity and mortality, and is closely related to the development of chronic kidney disease [1, 2].

Increasing numbers of studies implicate important roles for immune and inflammatory pathways in IRI [3, 4]. The activation and accumulation of neutrophils and macrophages in the innate immune phase had been thought to be the prime cellular mediator of microvascular plugging and local tissue damage in the IRI model [5]. There was a viewpoint that both T and B cells constituted the primary mediators of the adaptive immune response and did not play a role in the acute phase of IRI. However, recent data have challenged this assumption and demonstrate an important modulatory role of T cells in IRI [6–8].

Regulatory T cells (Tregs), a subset of $CD4^+$T cells, suppress excessive immune responses. This population of cells is commonly identified by their expression of CD4 and CD25 on the cell surface and their upregulation of the transcription factor forkhead box P3 (FoxP3) [9]. Multiple mechanisms of action for Tregs have been reported [10], such as direct cell-cell contact, depletion of interleukin- (IL-) 2, release of soluble inhibitory factors like IL-10 or transforming growth factor-β, and hydrolysis of ATP to adenosine, which exhibit direct immunosuppressive effects. Furthermore, Tregs have the ability to traffic to areas of inflammation to regulate immune reactions [11]. Previous studies have demonstrated that the chemokine receptor CXCR3 plays an important role in Treg cell recruitment in transplantation rejection [12] and inflammatory reactions [13]. In the present study, the levels of Tregs and the expression of CXCR3 on Tregs were measured to investigate the role of $CXCR3^+$ Tregs in renal IRI.

2. Materials and Methods

2.1. Animals. Male C57BL/6J mice, aged 8 to 12 weeks and weighing 20 to 25 g, were obtained from the Animal Center of Chongqing Medical University. One week before the experiments, animals were housed in a specific pathogen-free laboratory in an acclimatized room at standard room conditions (25°C, 55% humidity) with regular 12 h/12 h light/dark cycles. They were fed with a standard diet and had free access to tap water. All experiments were conducted in accordance with the Declaration of Helsinki (1964) and the "Principles of Laboratory Animal Care" NIH Publication vol. 25, no. 28, revised 1996. The study was performed under the Reduction, Replacement, and Refinement principle. All experimental procedures involving animals were approved by the Animal Ethics and Use Committee of Chongqing Medical University.

2.2. Experimental Groups. Mice were randomly divided into three groups: Sham ($n = 16$), IRI ($n = 16$), and PC61 + IRI ($n = 16$), where PC61 is a monoclonal antibody (mAb) to CD25. It has been reported that PC61 has no effect on renal function in normal or Sham mice [14], which we confirmed in a preliminary study. Thus, we did not have an additional experimental group in which Sham mice were administered the mAb.

2.2.1. Sham Group. Sham animals underwent the same surgical procedure without clamping of the renal pedicles. Eight mice were sacrificed at 24 h and 72 h after the operation.

2.2.2. IRI Group. Microvascular clamps were placed on both renal pedicles for 45 min. The clamps were removed, and the wounds were sutured. Eight mice were sacrificed at 24 h and 72 h after IRI.

2.2.3. PC61 + IRI Group. Depletion of Tregs was performed by i.p. injection with 250 μg of anti-CD25 (PC61) mAb (eBioscience; San Diego, CA, USA) at 24 h before renal ischemia [15]. Eight mice were sacrificed at 24 h and 72 h after IRI.

2.3. Experimental Protocol. The animals were anaesthetized with i.p. administration of 10% ketamine mixed with 2% xylazine. The renal pedicles were bluntly dissected. Microvascular clamps were placed on both renal pedicles for 45 min. The clamps were removed, and the wounds were sutured. The animals were placed on a heating pad and monitored visually until they were completely awake. After the operation, the animals were left to recover at room temperature, with immediate and unrestricted access to food and water. In the first 24 h after the surgery, the animals were treated with 2 μg of tramadol hydrochloride per g of body weight every 8 h for postoperative analgesia. Mice were sacrificed at 24 h and 72 h after IRI, and blood samples were collected from the inferior vena cava. Blood urea nitrogen (BUN) and serum creatinine (Scr) levels were measured to evaluate renal function. Half of the left kidney was dissected at each time point for histology assessment. The other half of the left kidney and the right kidney were homogenized, and the leukocytes within the tissue were isolated. The numbers of $CD4^+CD25^+Foxp3^+$ Tregs and $CXCR3^+CD4^+CD25^+Foxp3^+$ Tregs in kidney tissue were analyzed by flow cytometry. The correlation of these populations with BUN, Scr, and tubular necrosis score was calculated.

2.4. BUN and Scr Measurements. Whole blood (0.6 mL) was collected and the serum was isolated for BUN and Scr measurements with a Hitachi 747 automatic analyzer (Hitachi; Tokyo, Japan).

2.5. Flow Cytometry. Kidney tissue was disrupted mechanically in 10 mL of RPMI 1640 medium supplemented with 5% of newborn calf serum using a homogenizer. To remove debris, samples were passed through a 100 μm cell strainer with 50 mL of RPMI 1640 medium at 4°C. Leukocytes were isolated by centrifugation-suspension in Percoll at 4°C. Multiple-color immunofluorescence staining was analyzed using a FACS flow cytometer (FACSCalibur; BD Biosciences; Franklin Lakes, NJ, USA). The fluorochrome-conjugated monoclonal antibodies anti-CD4 Percp (RM 4-5), anti-CXCR3 PE (1C6/CXR3), anti-CD25 FITC (PC61.5), and anti-Foxp3 Alexa 647 (259D/C7) were purchased from eBioscience. Surface staining was used for detection of CD4, CD25, and CXCR3 whereas intracellular staining was used for detection of Foxp3 at 4°C. Data were analyzed by using FlowJo for Windows (Version 7.2.5; Ashland, OR, USA).

2.6. Kidney Histology. Paraformaldehyde-fixed and paraffin-embedded 4 μm sections were stained with hematoxylin-eosin (H&E). Damaged tubules were identified by the presence in the cortex of diffuse tubular dilatation, intraluminal casts, and/or tubular cell blebbing, vacuolization, and detachment, as assessed in a blinded fashion by a renal pathologist in ten high-power fields (400x magnification) per section. The percentages of histological changes in the kidney tissue were scored using a semiquantitative scale designed to evaluate the degree of tubular necrosis as follows [16, 17]: 0 = normal kidney; 1 = minimal necrosis (5% involvement); 2 = mild necrosis (5–25% involvement); 3 = moderate necrosis (25–50% involvement); 4 = severe necrosis (50–75% involvement); and 5 = most severe necrosis (>75% involvement).

2.7. Statistical Analysis. Comparisons between multiple groups were performed by a one-way analysis of variance test followed by the Kruskal-Wallis test where appropriate. Significance for differences between independent groups was determined using the Mann-Whitney U test. Spearman's rank correlation was applied for detecting correlation between different study parameters. Two-tailed P values < 0.05 were considered to be significant. For statistical analyses, GraphPad Prism version 5.0 was used (GraphPad Software; San Diego, CA, USA).

3. Results

3.1. Renal Function Assessment after IRI. BUN and Scr levels were both greater in the IRI group than in the Sham group

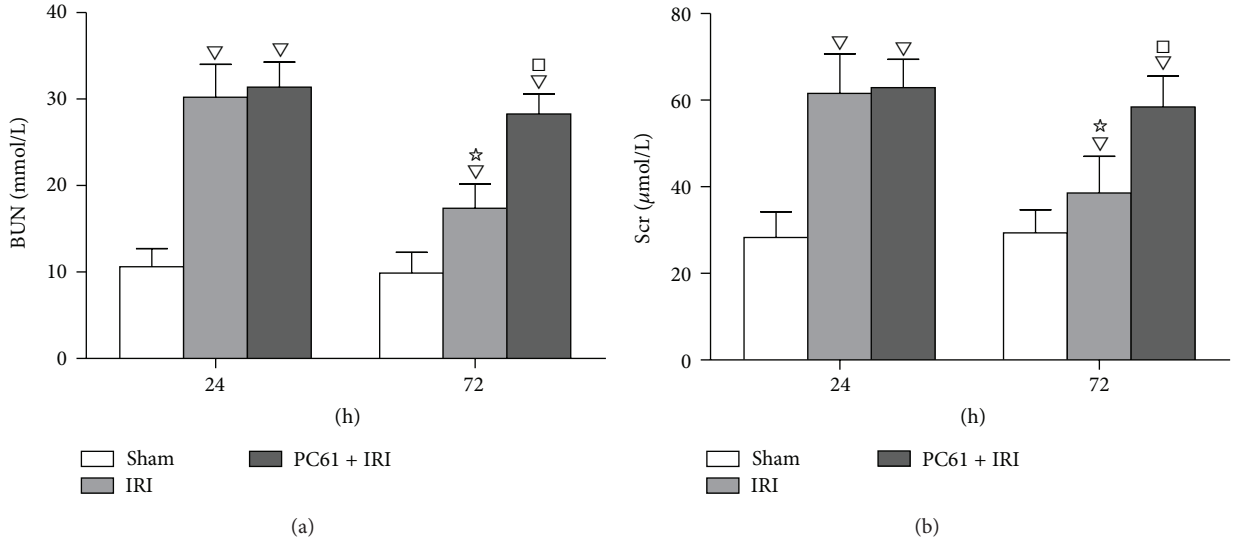

Figure 1: BUN and Scr levels at 24 h and 72 h after reperfusion. (a) Concentrations of BUN. (b) Concentrations of Scr. Values of the bar graphs represent the mean ± SD ($n = 8$ per group). Compared with the Sham group, $^{\triangledown}P < 0.05$; compared with the IRI group at 24 h after reperfusion, $^{\star}P < 0.05$; compared with the IRI group at 72 h after reperfusion, $^{\square}P < 0.05$.

at 24 h (30.2 ± 3.8 mmol/L *versus* 10.6 ± 2.1 mmol/L and 61.6 ± 9.1 μmol/L *versus* 28.3 ± 5.9 μmol/L, resp., $P < 0.05$) and at 72 h (17.4 ± 2.8 mmol/L *versus* 9.9 ± 2.4 mmol/L and 38.6 ± 8.4 μmol/L *versus* 29.4 ± 5.3 μmol/L, resp., $P < 0.05$) after reperfusion. However, the BUN and Scr concentrations were decreased at 72 h compared with those at 24 h in the IRI group ($P < 0.05$), although both concentrations were still greater than those in the Sham group ($P < 0.05$). With PC61 mAb administration before renal ischemia, BUN and Scr levels were greater at 72 h (28.3 ± 2.3 mmol/L *versus* 17.4 ± 2.8 mmol/L and 58.4 ± 7.2 μmol/L *versus* 38.6 ± 8.4 μmol/L, resp., $P < 0.05$) but not at 24 h after reperfusion as compared with the IRI group (Figure 1).

3.2. Kidney Histology. Kidney tissue structure was normal in the Sham group, with only a few swollen renal tubular epithelial cells. After IRI or PC61 treatment, a large number of tubular epithelial cells swelled, parts of the cells shrunk and had dark nuclei, the basal membrane was fractured due to cell necrosis and abscission, and cellular debris and casts were seen in the enlarged lumen. The tubular necrosis score in the IRI group was greater than that in the Sham group at 24 h and 72 h after reperfusion ($P < 0.05$). With PC61 mAb administration before renal ischemia, the score was greater at 72 h (4.25 ± 0.46 *versus* 3.70 ± 0.56, $P < 0.05$) but not at 24 h as compared with the IRI group (Figure 2).

3.3. Changes of $CD4^+CD25^+Foxp3^+$ Tregs and $CXCR3^+CD4^+CD25^+Foxp3^+$ Tregs in the Kidney after Reperfusion. There was almost no detectable expression of $CD4^+CD25^+Foxp3^+$ Tregs in kidney from the Sham group or IRI group at 24 h after reperfusion. The numbers of $CD4^+CD25^+Foxp3^+$ Tregs were increased more than 20-fold at 72 h in the IRI group as compared with the Sham group or that at 24 h in the IRI group ($P < 0.05$). The administration of PC61 mAb depleted Tregs in the kidneys (Figure 3(a)).

There was no detectable expression of $CXCR3^+CD4^+CD25^+Foxp3^+$ Tregs in the kidney from the Sham group or the IRI group at 24 h after reperfusion. The numbers of $CXCR3^+CD4^+CD25^+Foxp3^+$ Tregs were increased more than 10-fold at 72 h in the IRI group as compared with the Sham group or 24 h in the IRI group ($P < 0.05$). Administration of PC61 mAb effectively depleted the above population of cells in the kidneys (Figure 3(b)).

Representative dot plots of $CD4^+CD25^+Foxp3^+$ Tregs in the kidney from the Sham group and the IRI group were shown in Figures 3(c) and 3(d). There was almost no detectable expression of $CD4^+CD25^+Foxp3^+$ Tregs in the Sham group or at 24 h in the IRI group. In contrast, the percentage of this population in $CD4^+$ T cells in the IRI group expanded significantly at 72 h.

Because there were no $CXCR3^+CD4^+CD25^+$ Tregs detected in the kidney from the Sham group or IRI group at 24 h, only the dot plots from the IRI group at 72 h after reperfusion were shown in Figure 3(e). The proportion of $CXCR3^+CD4^+CD25^+$ Tregs in $CD4^+CD25^+Foxp3^+$ Tregs markedly increased at 72 h after reperfusion.

3.4. Correlation of $CD4^+CD25^+Foxp3^+$ Tregs and $CXCR3^+CD4^+CD25^+Foxp3^+$ Tregs with Kidney Injury in the IRI Group. Numbers of $CD4^+CD25^+Foxp3^+$ Tregs in the kidney from the IRI group were negatively correlated with BUN ($r = -0.71$, $P < 0.05$) and Scr ($r = -0.70$, $P < 0.05$), while the relationship with tubular necrosis score was not clear ($r = -0.48$, $P > 0.05$) (Figures 4(a), 4(b), and 4(c)).

Numbers of $CXCR3^+CD4^+CD25^+Foxp3^+$ Tregs in the kidney from the IRI group were negatively correlated with BUN ($r = -0.79$, $P < 0.05$), Scr ($r = -0.78$, $P < 0.05$), and

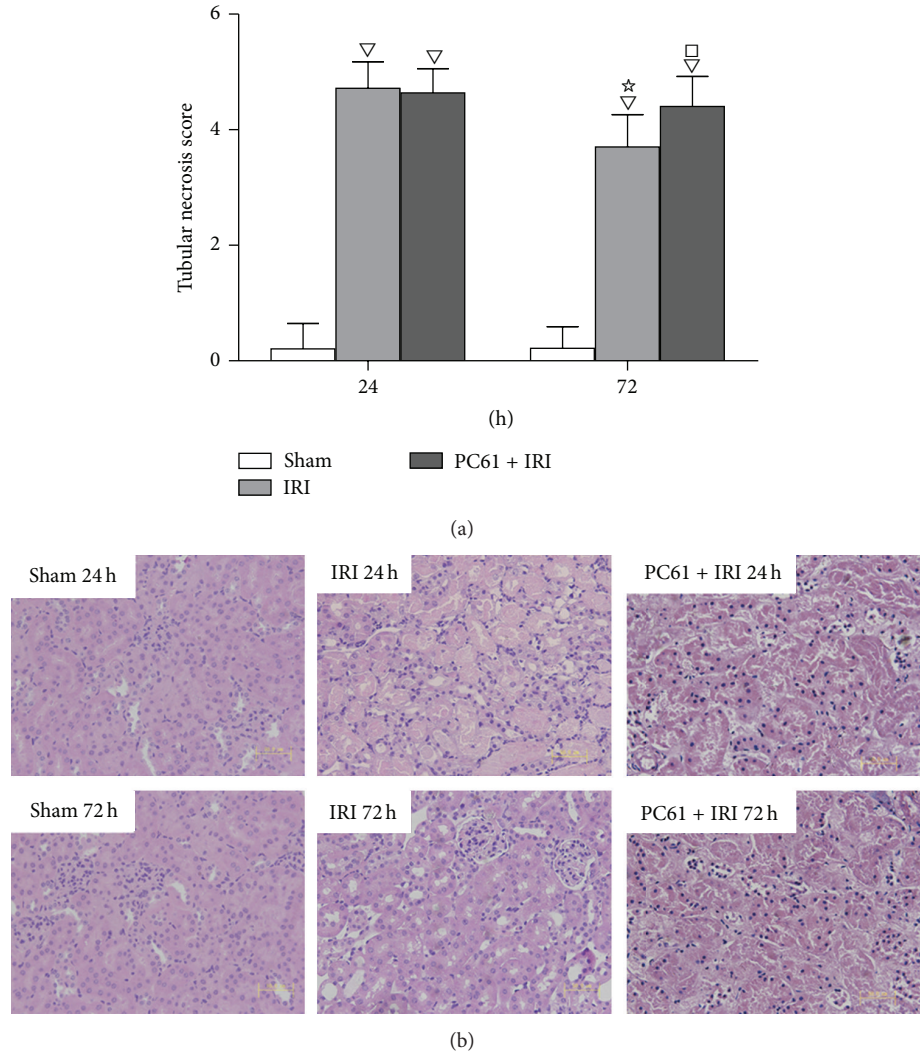

Figure 2: Renal histology at 24 h and 72 h after reperfusion. (a) Tubular necrosis scores in each group. Values of the bar graphs represent the mean ± SD ($n = 8$ per group). Compared with the Sham group, $^{\triangledown}P < 0.05$; compared with the IRI group at 24 h after reperfusion, $^{\star}P < 0.05$; compared with the IRI group at 72 h after reperfusion, $^{\square}P < 0.05$. (b) Representative histology images of H&E stained renal sections at 24 h and 72 h after reperfusion (original magnification: ×400, scale bar: 50 μm). After IRI, a large number of tubular epithelial cells swelled with vacuolar degeneration, parts of the cells shrunk and had dark nuclei, parts of the cells lost intracellular structure due to cellular necrosis and abscission, and cellular debris and casts were seen in the enlarged lumen.

tubular necrosis score ($r = -0.69$, $P < 0.05$) (Figures 4(d), 4(e), and 4(f)).

4. Discussion

In the present study, we observed the protective effect and migratory phenomenon of Tregs in the kidney after IRI. BUN, Scr levels, and tubular necrosis scores, all potential measures of kidney injury, were greater in the IRI group than in the Sham group. Numbers of Tregs were increased at 72 h after reperfusion in the kidney. PC61 mAb preconditioning decreased the numbers of Tregs and aggravated kidney injury. There were no $CXCR3^+$ Tregs in normal kidneys, while this population expanded at 72 h after reperfusion and was inversely correlated with BUN, Scr, and kidney histology score.

Tregs are a subset of helper T cells and have potent immunosuppressive effects. CD25 expression on T lymphocytes is upregulated by antigenic or mitogenic stimulation [18–20]. Soluble CD25/IL-2Rα is produced as a consequence of lymphocyte stimulation and is found in biological fluids following inflammatory responses. As nuclear transcription factor Foxp3 has been shown not only to represent a specific marker for $CD4^+CD25^+$Tregs but also to regulate their development and function [21, 22], it is currently the most accepted marker for identification of Tregs. Thus, $CD4^+CD25^+Foxp3^+$ T cells were defined as Tregs in our study.

Few Tregs were observed in kidneys from normal mice or mice in the IRI group at 24 h after reperfusion, while their numbers significantly increased at 72 h after reperfusion. The BUN and Scr levels as well as the tubular necrosis score reflected kidney damage after IRI. These results showed that

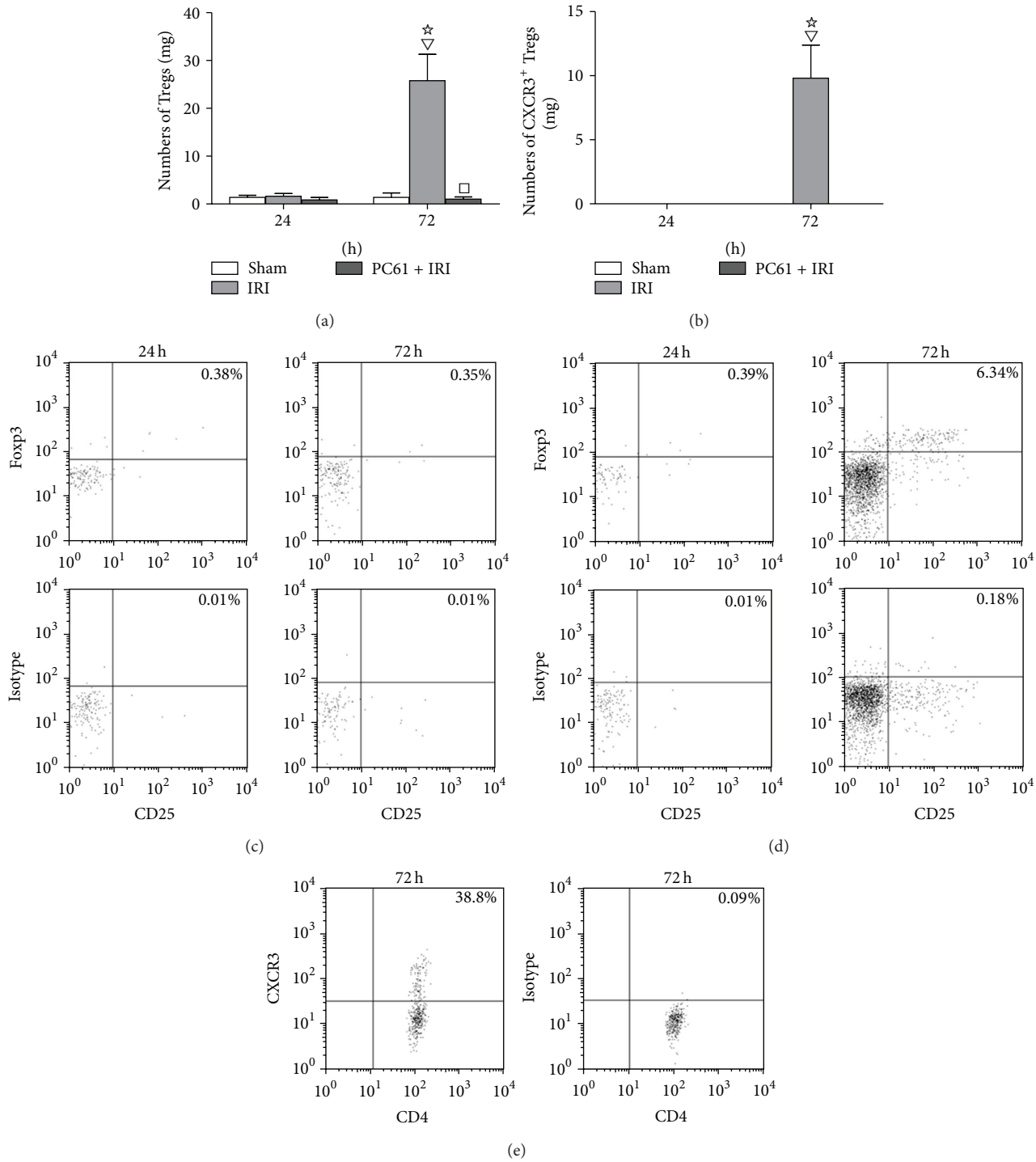

FIGURE 3: Numbers of Tregs and CXCR3$^+$ Tregs in kidney at 24 h and 72 h after reperfusion measured by flow cytometry analysis. (a) Numbers of CD4$^+$CD25$^+$Foxp3$^+$ Tregs in kidney at 24 h and 72 h after reperfusion. (b) Numbers of CXCR3$^+$CD4$^+$CD25$^+$Foxp3$^+$ Tregs in kidney at 24 h and 72 h after reperfusion. Values of the bar graphs represent the mean ± SD (n = 8 per group). Compared with the Sham group, $^{\triangledown}P < 0.05$; compared with the IRI group at 24 h after reperfusion, $^{\star}P < 0.05$; compared with the IRI group at 24 h or 72 h after reperfusion, $^{\square}P < 0.05$. (c) Representative dot plots of Tregs in kidney from Sham group at 24 h and 72 h after reperfusion. (d) Representative dot plots of Tregs in kidney from IRI group at 24 h and 72 h after reperfusion. The CD4$^+$ T cells were initially gated from the lymphocyte area by forward scatter (FSC) *versus* side scatter (SSC), and then the expression of CD25 and Foxp3 was analyzed in this population. The percentage of CD4$^+$CD25$^+$Foxp3$^+$ Tregs in CD4$^+$ cells was obtained in the upper right quadrant. (e) Representative dot plots of CXCR3$^+$ Tregs from the IRI group. Because there were no CXCR3$^+$ Tregs detected in the kidney from the Sham or IRI group at 24 h after IRI, only dot plots from the IRI group at 72 h after reperfusion were shown. The percentage of CXCR3 in the CD4$^+$CD25$^+$Foxp3$^+$ population was shown in the upper right quadrant.

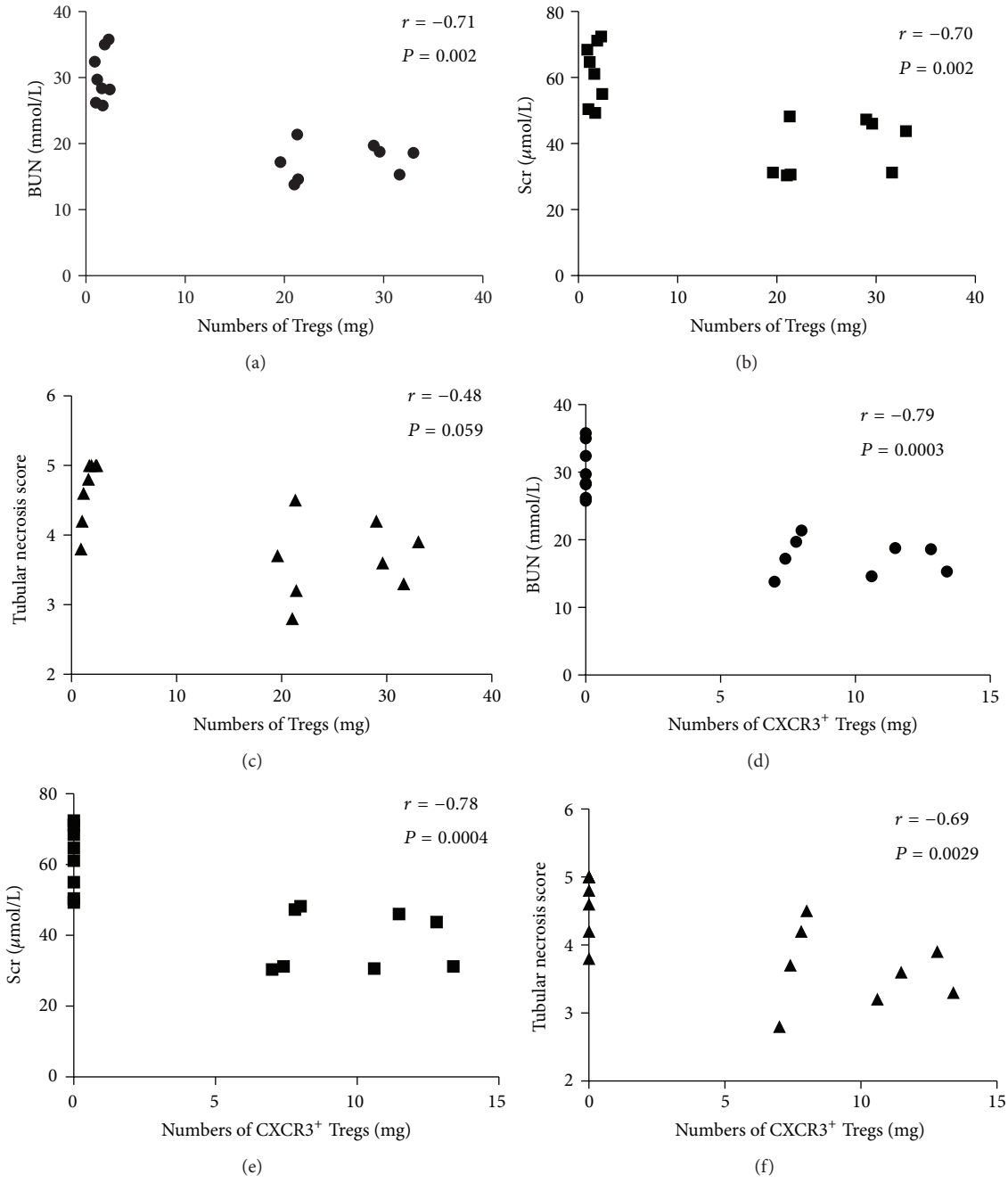

Figure 4: Correlation of $CD4^+CD25^+Foxp3^+$ Tregs and $CXCR3^+CD4^+CD25^+Foxp3^+$ Tregs with BUN, Scr, and tubular necrosis score in the IRI group. The numbers of $CD4^+CD25^+Foxp3^+$ Tregs in the kidney were negatively correlated with BUN (a) and Scr (b) but not tubular necrosis score (c). The numbers of $CXCR3^+CD4^+CD25^+Foxp3^+$ Tregs in the kidney were negatively correlated with BUN (d), Scr (e), and tubular necrosis score (f). Each symbol represents a single individual ($n = 16$).

significant renal injury occurred at 24 h after reperfusion and that there was gradual recovery at 72 h. It is reasonable to conclude that the increasing numbers of Tregs had an effect on improvement of renal function after reperfusion. To validate this hypothesis, we used PC61 to investigate this protective effect.

A rat IgG1 anti-mouse-CD25 (IL-2Rα) mAb called PC61 has been shown to selectively deplete $CD4^+CD25^+$ T cells *in vivo*, and this depletion was reversible within a few days [23, 24]. In a preliminary study, we tested the effect of the PC61 mAb and found that it depleted almost all Tregs in both Sham and IRI mice by intraperitoneal injection. Hence, the PC61 mAb was used to abolish the effect of Tregs and investigate its function in IRI. We found that depletion of Tregs with an anti-CD25 mAb potentiated kidney damage at 72 h after reperfusion. These results proved Tregs had protective effects

on the kidneys after IRI. Using a murine model of ischemic acute kidney injury, Gandolfo et al. [25] found that there was significant trafficking of Tregs into the kidneys from 3 to 10 days after reperfusion. The infusion of Tregs after IRI had minimal effects on neutrophil and macrophage infiltration but had a late beneficial effect on kidney repair, likely through the modulation of proinflammatory cytokine production of other T-cell subsets. This result showed the important role of Tregs in the repair of ischemic acute kidney injury. Key issues to address include understanding why there are almost no Tregs in normal kidneys and when and how did these cells appear in the inflammatory tissue.

CXCR3 is an important chemokine receptor activated by three interferon-inducible ligands CXCL9, CXCL10, and CXCL11. Early studies demonstrated a role for CXCR3 in the trafficking of Th1 and CD8 T cells to peripheral sites of Th1-type inflammation and the establishment on Th1 amplification loop mediated by IFNγ and the IFNγ-inducible CXCR3 ligands. More recent studies have also suggested that CXCR3 plays a role in the migration of T cells in the microenvironment of the peripheral tissue and lymphoid compartment, facilitating the interaction of T cells with antigen presenting cells leading to the generation of effector and memory cells [26]. It has been reported [13] that Tregs accumulated in areas of inflammation in the liver of patients who had chronic hepatitis. These Treg cells expressed high levels of the chemokine receptor CXCR3. In a murine model of autoimmune hepatic inflammation [27], the $CD4^+CD25^+$Treg cells accumulated in the inflamed liver and this phenomenon was associated with the upregulation of CXCR3. These results provided strong evidence that CXCR3 is an important chemokine receptor that guides Treg cells into inflamed tissues and mediates local immune responses. However, whether CXCR3 is also important to the migratory function of Tregs in renal IRI remains unclear.

In our study, no $CXCR3^+$ Tregs were detected in in the kidneys of normal mice. The subset significantly expanded in the IRI group at 72 h but not at 24 h after reperfusion. This observation demonstrated that $CXCR3^+$ Tregs were not a resident population in normal kidney but accumulated in kidney after IRI. In addition, the inverse correlation of $CXCR3^+$ Tregs with BUN and Scr levels as well as the tubular necrosis score in IRI mice was observed. This indicated that the increase in the number of $CXCR3^+$ Tregs was associated with the recovery from kidney injury.

In the present study, we did not directly block CXCR3 to inhibit the migratory function. CXCR3 is expressed not only on helper T cells, but also on effector T cells and dendritic cells. The inflammatory CXCR3-chemokine dependent amplification loop also exits in hypoxia-reperfusion injury [28, 29]. Blocking CXCR3 would also inhibit the migratory function of inflammatory cells into the kidney and influence the process of IRI.

On the other hand, it should be noted that only 40% of Tregs in the kidney expressed CXCR3 after reperfusion in the present study. There might be other chemokines that also had the effect of recruiting Tregs into inflammatory tissue. Hoerning et al. [30] found not only CXCR3 but also CCR5 was related to the trafficking function of Tregs in renal transplantation in mice. Although further investigation is needed, our results still support CXCR3 as an important chemokine for the migratory function of Tregs in renal IRI.

5. Conclusions

In summary, the expanded Tregs participated in the repair of the early phase of renal IRI. CXCR3 might be an important chemokine receptor involved in the migration of Tregs into kidney tissue to serve an immunosuppressive function. These data revealed new insights into the pathogenesis of ischemic acute renal failure and suggest potential novel therapeutic approaches.

Conflict of Interests

There was no conflict of interests regarding this study. The paper has been seen and approved by all authors and it is not under consideration for publication elsewhere in a similar form, in any language, except in abstract form.

Authors' Contribution

Cao Jun contributed to the design of the experiments. Li Qingshu contributed to sample preparation for pathology measurements, the test for tubular necrosis scores, the histology evaluation of kidney injury, and data analysis. Wei Ke participated in establishment of the animal model and prepared the paper. Li Ping contributed to the design of the experimental protocol and data collection. Cao Jun and Dong Jun finished the flow cytometry measurements and data interpretation. Luo Jie helped organize the experiments, animal studies, antibodies, and equipment. Min Su approved the final paper.

Acknowledgments

The authors thank the staff of the Animal Center of Chongqing Medical University for their support during surgeries and their excellent animal care. This study was supported by funds from the National Key Clinical Specialist of the Ministry of Public Health, the Medical Key Subjects in Chongqing province, and the Chongqing Medical Science Research Project (2013-2-021).

References

[1] O. Liangos, R. Wald, J. W. O'Bell, L. Price, B. J. Pereira, and B. L. Jaber, "Epidemiology and outcomes of acute renal failure in hospitalized patients: a national survey," *Clinical Journal of the American Society of Nephrology*, vol. 1, no. 1, pp. 43–51, 2006.

[2] R. Munshi, C. Hsu, and J. Himmelfarb, "Advances in understanding ischemic acute kidney injury," *BMC Medicine*, vol. 9, article 11, 2011.

[3] J. J. Friedewald and H. Rabb, "Inflammatory cells in ischemic acute renal failure," *Kidney International*, vol. 66, no. 2, pp. 486–491, 2004.

[4] N. E. Kieran and H. Rabb, "Immune responses in kidney preservation and reperfusion injury," *Journal of Investigative Medicine*, vol. 52, no. 5, pp. 310–314, 2004.

[5] D. K. Ysebaert, K. E. de Greef, S. R. Vercauteren et al., "Identification and kinetics of leukocytes after severe ischaemia/reperfusion renal injury," *Nephrology Dialysis Transplantation*, vol. 15, no. 10, pp. 1562–1574, 2000.

[6] M. J. Burne, F. Daniels, A. El Ghandour et al., "Identification of the $CD4^+$ T cell as a major pathogenic factor in ischemic acute renal failure," *The Journal of Clinical Investigation*, vol. 108, no. 9, pp. 1283–1290, 2001.

[7] M. J. Burne-Taney, D. B. Ascon, F. Daniels, L. Racusen, W. Baldwin, and H. Rabb, "B cell deficiency confers protection from renal ischemia reperfusion injury," *The Journal of Immunology*, vol. 171, no. 6, pp. 3210–3215, 2003.

[8] Y.-J. Day, L. Huang, H. Ye, L. Li, J. Linden, and M. D. Okusa, "Renal ischemia-reperfusion injury and adenosine 2A receptor-mediated tissue protection: the role of $CD4^+$ T cells and IFN-γ," *The Journal of Immunology*, vol. 176, no. 5, pp. 3108–3114, 2006.

[9] J. D. Fontenot and A. Y. Rudensky, "A well adapted regulatory contrivance: regulatory T cell development and the forkhead family transcription factor Foxp3," *Nature Immunology*, vol. 6, no. 4, pp. 331–337, 2005.

[10] D. A. A. Vignali, "How many mechanisms do regulatory T cells need?" *European Journal of Immunology*, vol. 38, no. 4, pp. 908–911, 2008.

[11] J. Huehn and A. Hamann, "Homing to suppress: address codes for Treg migration," *Trends in Immunology*, vol. 26, no. 12, pp. 632–636, 2005.

[12] H. Hasegawa, A. Inoue, M. Kohno et al., "Therapeutic effect of CXCR3-expressing regulatory T cells on liver, lung and intestinal damages in a murine acute GVHD model," *Gene Therapy*, vol. 15, no. 3, pp. 171–182, 2008.

[13] Y. H. Oo, C. J. Weston, P. F. Lalor et al., "Distinct roles for CCR4 and CXCR3 in the recruitment and positioning of regulatory T cells in the inflamed human liver," *The Journal of Immunology*, vol. 184, no. 6, pp. 2886–2898, 2010.

[14] G. R. Kinsey, R. Sharma, L. Huang et al., "Regulatory T cells suppress innate immunity in kidney ischemia-reperfusion injury," *Journal of the American Society of Nephrology*, vol. 20, no. 8, pp. 1744–1753, 2009.

[15] J. W. Lowenthal, P. Corthesy, C. Tougne, R. Lees, H. R. MacDonald, and M. Nabholz, "High and low affinity IL 2 receptors: analysis by IL 2 dissociation rate and reactivity with monoclonal anti-receptor antibody PC61," *Journal of Immunology*, vol. 135, no. 6, pp. 3988–3994, 1985.

[16] H. Rabb, C. C. Mendiola, J. Dietz et al., "Role of CD11a and CD11b in ischemic acute renal failure in rats," *American Journal of Physiology: Renal Fluid and Electrolyte Physiology*, vol. 267, no. 6, pp. F1052–F1058, 1994.

[17] H. Rabb, G. Ramirez, S. R. Saba et al., "Renal ischemic-reperfusion injury in L-selectin-deficient mice," *The American Journal of Physiology*, vol. 271, no. 2, pp. F408–F413, 1996.

[18] W. Kasinrerk, O. Majdic, K. Praputpittaya, and N. Sittisombut, "Enhancement of human lymphocyte proliferative response to purified protein derivative by an anti-interleukin-2 receptor α chain antibody (CD25)," *Immunology*, vol. 83, no. 1, pp. 33–37, 1994.

[19] T. Mutis, T. Aarts-Riemens, and L. F. Verdonck, "The association of CD25 expression on donor $CD8^+$ and $CD4^+$ T cells with graft-versus-host disease after donor lymphocyte infusions," *Haematologica*, vol. 90, no. 10, pp. 1389–1395, 2005.

[20] T. M. Brusko, C. H. Wasserfall, M. A. Hulme, R. Cabrera, D. Schatz, and M. A. Atkinson, "Influence of membrane CD25 stability on T lymphocyte activity: implications for immunoregulation," *PLoS ONE*, vol. 4, no. 11, Article ID e7980, 2009.

[21] S. Hori, T. Nomura, and S. Sakaguchi, "Control of regulatory T cell development by the transcription factor Foxp3," *Science*, vol. 299, no. 5609, pp. 1057–1061, 2003.

[22] Y. M. Kerdiles, E. L. Stone, D. L. Beisner et al., "Foxo transcription factors control regulatory T cell development and function," *Immunity*, vol. 33, no. 6, pp. 890–904, 2010.

[23] J. Shimizu, S. Yamazaki, and S. Sakaguchi, "Induction of tumor immunity by removing $CD25^+CD4^+$ T cells: a common basis between tumor immunity and autoimmunity," *Journal of Immunology*, vol. 163, no. 10, pp. 5211–5218, 1999.

[24] S. Onizuka, I. Tawara, J. Shimizu, S. Sakaguchi, T. Fujita, and E. Nakayama, "Tumor rejection by in vivo administration of anti-CD25 (interleukin-2 receptor α) monoclonal antibody," *Cancer Research*, vol. 59, no. 13, pp. 3128–3133, 1999.

[25] M. T. Gandolfo, H. R. Jang, S. M. Bagnasco et al., "$Foxp3^+$ regulatory T cells participate in repair of ischemic acute kidney injury," *Kidney International*, vol. 76, no. 7, pp. 717–729, 2009.

[26] J. R. Groom and A. D. Luster, "CXCR3 in T cell function," *Experimental Cell Research*, vol. 317, no. 5, pp. 620–631, 2011.

[27] C. Saeki, M. Nakano, H. Takahashi et al., "Accumulation of functional regulatory T cells in actively inflamed liver in mouse dendritic cell-based autoimmune hepatic inflammation," *Clinical Immunology*, vol. 135, no. 1, pp. 156–166, 2010.

[28] B. D. Medoff, J. C. Wain, E. Seung et al., "CXCR3 and its ligands in a murine model of obliterative bronchiolitis: regulation and function," *The Journal of Immunology*, vol. 176, no. 11, pp. 7087–7095, 2006.

[29] W. W. Hancock, W. Gao, V. Csizmadia, K. L. Faia, N. Shemmeri, and A. D. Luster, "Donor-derived IP-10 initiates development of acute allograft rejection," *Journal of Experimental Medicine*, vol. 193, no. 8, pp. 975–980, 2001.

[30] A. Hoerning, S. Köhler, C. Jun et al., "Peripherally Circulating $CD4^+$ $FOXP3^+$ $CXCR3^+$ T Regulatory Cells Correlate with Renal Allograft Function," *Scandinavian Journal of Immunology*, vol. 76, no. 3, pp. 320–328, 2012.

Hindawi Publishing Corporation
Mediators of Inflammation
Volume 2015, Article ID 819232, 12 pages
http://dx.doi.org/10.1155/2015/819232

Research Article

Captopril Pretreatment Produces an Additive Cardioprotection to Isoflurane Preconditioning in Attenuating Myocardial Ischemia Reperfusion Injury in Rabbits and in Humans

Yi Tian,[1] Haobo Li,[2] Peiyu Liu,[3] Jun-mei Xu,[4] Michael G. Irwin,[2] Zhengyuan Xia,[2,5] and Guogang Tian[1]

[1]*Department of Anesthesiology, Haikou Municipal Hospital, Affiliated Haikou Hospital Xiangya School of Medicine, Central South University, Haikou 570208, China*
[2]*Department of Anesthesiology, The University of Hong Kong, Hong Kong*
[3]*Department of Anesthesiology, Hainan Municipal Corps Hospital, Chinese People's Armed Police Force, Haikou 570203, China*
[4]*Department of Anesthesiology, The Second Xiangya Hospital, Central South University, Changsha, Hunan 410011, China*
[5]*Department of Anesthesiology, Affiliated Hospital of Guangdong Medical College, Zhanjiang 524023, China*

Correspondence should be addressed to Zhengyuan Xia; zhengyuan_xia@yahoo.com and Guogang Tian; dr_tgg@126.com

Received 23 November 2014; Accepted 27 December 2014

Academic Editor: Huang-Ping Yu

Background. Pretreatment with the angiotensin-converting inhibitor captopril or volatile anesthetic isoflurane has, respectively, been shown to attenuate myocardial ischemia reperfusion (MI/R) injury in rodents and in patients. It is unknown whether or not captopril pretreatment and isoflurane preconditioning (Iso) may additively or synergistically attenuate MI/R injury. *Methods and Results.* Patients selected for heart valve replacement surgery were randomly assigned to five groups: untreated control (Control), captopril pretreatment for 3 days (Cap3d), or single dose captopril (Cap1hr, 1 hour) before surgery with or without Iso (Cap3d+Iso and Cap1hr+Iso). Rabbit MI/R model was induced by occluding coronary artery for 30 min followed by 2-hour reperfusion. Rabbits were randomized to receive sham operation (Sham), MI/R (I/R), captopril (Cap, 24 hours before MI/R), Iso, or the combination of captopril and Iso (Iso+Cap). In patients, Cap3d+Iso but not Cap1hr+Iso additively reduced postischemic myocardial injury and attenuated postischemic myocardial inflammation. In rabbits, Cap or Iso significantly reduced postischemic myocardial infarction. Iso+Cap additively reduced cellular injury that was associated with improved postischemic myocardial functional recovery and reduced myocardial apoptosis and attenuated oxidative stress. *Conclusion.* A joint use of 3-day captopril treatment and isoflurane preconditioning additively attenuated MI/R by reducing oxidative stress and inflammation.

1. Introduction

Myocardial ischemia reperfusion (MI/R) injury is a major perioperative complication that is associated with significant morbidity and mortality in coronary artery bypass graft (CABG) surgery [1, 2] and in patients undergoing heart valve replacement surgery [3] using cardiopulmonary bypass (CPB), especially in patients with comorbidities (e.g., age [4] and diabetes [5]). Volatile anesthetic preconditioning (e.g., isoflurane preconditioning, Iso) provides cardioprotective effects during CABG [6, 7]. Given that the isoflurane preconditioning cardioprotection is optimal or effective only when duration of the index ischemia is limited within 25–40 minutes [8] while the typical period of cardiac ischemia during CABG surgery is usually longer than 60 minutes, the cardioprotective potential of Iso in the clinical settings is limited. Moreover, in aging [9] and diabetes [10], in which myocardial oxidative stress and inflammation are increased

concomitant with reduced endogenous antioxidant capacity, cardioprotection of Iso is diminished or abolished.

Increased systemic oxidative stress induced by robust production of reactive oxygen species (ROS) has been suggested as the main cause which adversely affects postoperative cardiac functional recovery in patients undergoing CABG surgery using CPB [11]. ROS not only increases oxidative stress by increasing lipid peroxidation but also reduces myocardial antioxidant capacity by diminishing endogenous antioxidant enzymes activities (e.g., superoxide dismutase) [12, 13]. In addition, proinflammatory cytokines release (e.g., tumor necrosis factor- (TNF-) α) is also enhanced after CPB [14], which may further increase ROS production and exacerbate myocardial function [15]. Experimental studies show that Iso confers cardioprotection against myocardial IRI by stimulating the generation of small amount of ROS which triggers cardiac protective signaling pathways [16, 17]. On the other hand, experimental studies showed that volatile anesthetic preconditioning exert cardioprotective effects against myocardial ischemic reperfusion injury through reducing nuclear factor- (NF-) kB-dependent inflammatory gene expression and decreasing TNF-α production [18, 19].

Captopril, an angiotensin-converting enzyme (ACE) inhibitor, has been shown to be cardioprotective in the prevention and regression of left ventricular hypertrophy or attenuation of MI/R injury in both clinical [20] and experimental settings [21]. Captopril pretreatment exerts cardioprotective effects by increasing tissue antioxidant activity, scavenging different types of ROS, and thus prevents lipid peroxidation [22, 23]. Captopril by inhibiting angiotensin-converting enzyme activity reduced the degradation of bradykinin, resulting in enhanced formation of prostacyclin and nitric oxide, and in turn increases myocardial antioxidant and anti-inflammatory properties [20, 24] and confers cardioprotective effects [25]. Therefore, the mechanism of captopril cardioprotection is totally different from that of isoflurane preconditioning. Thus, it is plausible that captopril in combination with isoflurane preconditioning may synergistically or additively attenuate MI/R in clinical settings. Therefore, we hypothesized that alternative use of captopril pretreatment and isoflurane preconditioning may confer superior protection against MI/R injury to either isoflurane or captopril regimen alone and that the mechanism of the additive/synergistic effect is related to reducing cardiomyocytes apoptosis and myocardial oxidative stress.

2. Methods

2.1. Patient Population and Study Design. The clinical trial was carried out in accordance with the Declaration of Helsinki (2000) of the World Medical Association. The study protocol was approved by the institutional ethics committee. All subjects gave written informed consent after having been given full explanation of the purpose, nature, and risk of all procedures used.

After obtaining written informed consent, 100 ASA (American Association of Anesthesiologists) class II to III patients, aged 38–55 years, presenting for scheduling for heart mitral valve replacement surgery were assigned according to a computer-generated random code to one of the five groups: a control group receiving midazolam and fentanyl (group control; $n = 20$); captopril pretreatment for 1 hour (Cap1hr, 12.5 mg, oral administration) or 3 days (Cap3d, 12.5 mg, 3 times per day, oral administration) before surgery groups ($n = 20$ per group); and a combination of isoflurane preconditioning (Iso) and captopril pretreatment (1 hour or 3 days before surgery) (group Cap1hr+Iso or Cap3d+Iso; $n = 20$ per group). Subjects were assigned treatment numbers in ascending chronological order of admission in the study. The surgeons, research assistants, and medical and nursing staff in the operation room were blinded to the group assignments, facilitated by covering the drug infusion pump and lines and shielding the isoflurane vaporizer from view.

The exclusion criteria were (a) cardiogenic shock, (b) left main coronary artery occlusion or severe stenosis, (c) blood flow in the infarct-related artery > thrombolysis in myocardial infarction grade 1, (d) treatment with glycoprotein IIb/IIIa receptor antagonists before the procedure, and (e) infection or surgery within 2 weeks [6, 26].

2.2. Anesthetic Protocols and Surgery. All patients received standard premedication of scopolamine at 0.006 mg/kg of body weight and morphine at 0.1 mg/kg of body weight intramuscularly 60 min before surgery. In all groups, anaesthesia was induced with etomidate at 0.3 mg/kg of body weight, fentanyl at 8 μg/kg of body weight, and pancuronium bromide at 0.1 mg/kg of body weight given intravenously. After induction, all patients received continuous infusions of fentanyl at 0.6 $\mu g \cdot kg^{-1}$ of body weight$\cdot min^{-1}$ and pancuronium bromide at 15 $\mu g \cdot kg^{-1}$ of body weight$\cdot min^{-1}$ during surgery. The anaesthesia protocol in various groups is as follows (see Figure 1): anaesthesia was maintained either with fentanyl and midazolam (group control, Cap1hr, and Cap3d) or with isoflurane 1.1 MAC (minimum alveolar anesthetic concentration) end tidal before surgery (group Cap1hr+Iso or Cap3d+Iso). During anaesthesia, patients were monitored with five-lead ECG, pulse oximetry, capnography, invasive arterial pressure, and pulmonary artery pressure during the operation.

Central venous blood samples were obtained prior to CPB (Baseline), 20 min after CPB induction, 30 min, 4 h, and 24 h after aortic declamping for the measurements of plasma levels of cTnI (cardiac troponin I) and CK-MB (creatine kinase MB), TNF- (tumor necrosis factor-) α, IL- (interleukin-) 6, and ICAM (intercellular adhesion molecule). Samples were immediately cooled to 4°C and centrifuged at 1000 g for 10 min at 4°C. Plasma was collected and stored at −70°C until analyzed.

2.3. Animal Study Experimental Protocol. The study was approved by the institutional ethic committee and conforms with U.S. National Institutes of Health guidelines. Adult New Zealand white rabbits (1.8 kg) were anaesthetized with sodium pentobarbital (30 mg/kg, Alfasan, Holland). The rabbits were ventilated with 100% oxygen and end tidal PCO_2 were maintained between 35 and 45 mmHg. Myocardial ischemia reperfusion (I/R) was produced by exteriorizing the heart through a left thoracic incision and occluding the

Group control		Fentanyl + midazolam	Surgery
Group Cap1hr	Captopril, 12.5 mg, 1 hour before surgery	Fentanyl + midazolam	Surgery
Group Cap3d	Captopril, 12.5 mg, 3 times per day for 3 days	Fentanyl + midazolam	Surgery
Group Cap1hr+Iso	Captopril, 12.5 mg, 1 hour before surgery	Isoflurane, 1.1 MAC for 30 min	Surgery
Group Cap3d+Iso	Captopril, 12.5 mg, 3 times per day for 3 days	Isoflurane, 1.1 MAC for 30 min	Surgery

Figure 1: Protocol used in experimental groups. Patients were pretreated without or with captopril for 1 hour (Cap1hr, 12.5 mg, oral administration) or 3 days (Cap3d, 12.5 mg, 3 times per day, oral administration) before surgery. After induction, all patients received continuous infusions of fentanyl at 0.6 $\mu g \cdot kg^{-1}$ of body weight$\cdot min^{-1}$ and pancuronium bromide at 15 $\mu g \cdot kg^{-1}$ of body weight$\cdot min^{-1}$ during surgery. The anaesthesia protocol in various groups is as follows: anaesthesia was maintained either with fentanyl and midazolam (group control, Cap1hr, and Cap3d) or with isoflurane 1.1 MAC (minimum alveolar anesthetic concentration) end tidal before surgery (group Cap1hr+Iso or Cap3d+Iso).

LAD (left anterior descending artery) with a silk slipknot. After 40 min of ischemia, the slipknot was released and the myocardium was reperfused for 4 hrs. Sham (sham operated control rabbits) underwent the same surgical procedures except that the LAD was not occluded.

Rabbits were randomized to receive one of the following treatments ($n = 8$ each): Sham, rabbits receiving vehicle (0.9% NaCl) without being subjected to I/R; I/R, rabbits receiving vehicle during reperfusion; IPC, rabbits receiving IPC (3 cycles of 10 s of coronary artery reocclusion and reperfusion) before ischemia; Iso, rabbits receiving isoflurane (15 min 1.1% end tidal isoflurane followed by a 15 min washout period) before inducing ischemia; Cap, rabbits receiving captopril (25 mg/kg, oral administration) 24 hours before inducing ischemia; Iso+Cap, rabbits receiving isoflurane in combination with captopril before inducing ischemia.

2.4. Determination of Myocardial Functional Recovery in Rabbits. In the rabbits, LV function was continuously monitored during the entire MI/R period via a Millar Mikro-Tip catheter pressure transducer inserted into the LV via left carotid artery as we have described previously. HR (heart rate), MAP, and RPP were derived by computer algorithms (Chengdu Instrument).

2.5. Determination of Postischemic Myocardial Infarct Size in Rabbits and Cellular Injury. The infarct size was measured with a double-staining technique using Evans Blue-TTC (Triphenyltetrazolium Chloride) staining and a digital imaging system, as described previously (additional $n = 8$ rabbits per group were used for infarct size determination). Blood samples were drawn before ligation and at the end of reperfusion. Plasma cTnI (cardiac-specific troponin I) from rabbits and patients were measured spectrophotometrically (Backman DU 640 instrument) with commercially available assay kits (Nanjing Jiancheng). The plasma samples were coded, and the levels of cTnI (cardiac specific troponin I) were assayed in duplicate by an investigator initially blinded to the research groups. Plasma IL-6, ICAM, TNF-α, and CK-MB were measured using ELISA kits (R&D Systems). Plasma samples used for biochemical assays were coded, and the laboratory investigator was blinded in regard to treatment regimen. All haemodynamic data were collected by trained observers who did not take an authorship in this study and who were blinded to the methods regarding anaesthetic and captopril usage.

2.6. Assessment of Rabbit Myocardial Apoptosis by Flow Cytometry Analysis. At the end of reperfusion, hearts were removed and washed twice with ice-cold phosphate-buffered saline; cell suspensions were prepared using the Medimachine System (Becton-Dickinson). Cardiomyocyte cells were collected by flow cytometry with the use of an antibody to a-sarcomeric actin. The cells were resuspended in binding buffer, after adding FITC-Annexin V and propidium iodide, the mixture was incubated for 10 minutes in the dark at 4°C, and then cellular fluorescence was measured with a fluorescence activated cell sorter scan flow cytometer (Becton, Dickinson and Company, Franklin Lakes, NJ) as described [27].

2.7. Determination of MDA (Malondialdehyde) and SOD (Superoxide Dismutase) in Rabbit. MDA is end product of the ROS- (reactive oxygen species-) mediated lipid peroxidation cascade. Rabbit blood samples were collected, and the MDA levels were measured with a commercial kit (Baster Biological Tech), expressed as nmol/mL. SOD activity was detected in cardiac tissue homogenates using commercially available kit (Cayman Chemical) as described previously, expressed as U/mL.

2.8. Western Blot Analysis. Equal amount of proteins from rabbit heart homogenate was resolved by 7.5–15% sodium dodecyl sulfate polyacrylamide gel electrophoresis and transferred to nitrocellulose membranes and processed as described. The primary antibodies against BCL-2, Bax, and GAPDH were purchased from Cell Signaling Technology (Beverly, MA). Immunoreactive bands were visualized by enzymatic chemiluminescence method and quantified with Quantity One image software.

2.9. Sample Size Estimation. Group sample size was estimated based on differences in cTnI concentration measured at 4 h after CPB in a pilot study of patients who received isoflurane (1–1.5 minimum alveolar concentration throughout the surgery) anaesthesia. The formula $n = 15.7/ES^2 + 1$, where ES = effect size = (difference between groups)/(mean of the S.D. between groups), with $\alpha = 0.05$ and power = 0.8, was used to determine that the study would be adequately powered with $n = 20$ per group.

2.10. Statistical Analysis. All continuous data are expressed as means ± SD. Statistical evaluation of patients' file and perioperative data was performed by unpaired Student's t-test or χ^2 test when appropriate. Between-groups and within-group differences of bioassay data were analyzed using two-way ANOVA with repeated measures and Bonferroni's corrections (Graphpad Prism). Values were considered statistically significant when $P < 0.05$.

3. Results

3.1. Human Study Data

3.1.1. Preoperative and Intraoperative Data in Patients. As shown in Table 1. The patients' baseline demographics, clinical measures of cardiac function, and medications (digoxin and diuretic) did not differ among groups. As shown in Table 2, the operation time, aortic clamping time, and bypass time did not differ among groups. Automatic rebeating rate in groups Cap3d+Iso and Cap1hr+Iso was significantly higher than that in control group, while no significant difference was observed in groups Cap3d and Cap1hr as compared to control group. Arrhythmia incidence was significantly higher in control group than that in all treatment groups (Cap3d+Iso, Cap1hr+Iso, Cap3d, and Cap1hr) and there is no difference among all treatment groups. Similarly, dopamine usage was significantly reduced in all treatment groups compared with the control groups and there was no difference among all treatment groups. Sodium nitroprusside usage was significantly reduced in all treatment groups compared with the control groups and sodium nitroprusside usage was significantly reduced in group Cap3d+Iso relative to other groups.

3.1.2. Postoperative Outcome Data in Patients. As shown in Table 2, durations of postoperative ICU stay in all treatment groups were shorter than that in the control group, and durations of postoperative ICU stay in groups Cap3d+Iso and Cap1hr+Iso were significantly shorter than that in groups Cap3d and Cap1hr. The duration of hospital stay in group Cap3d+Iso, but not groups Cap3d or Cap1hr, was shorter than that in Cap1hr+Iso and the duration of hospital stay in all treatment was significantly reduced compared with control group. All patients were discharged from hospital uneventfully.

3.1.3. Isoflurane and Captopril Attenuated Postischemic Myocardial Cellular Injury and Reduced Proinflammatory Cytokines TNF-α, IL-6, and ICAM in Patients. Baseline plasma levels of cTnI, CK-MB, TNF-α, IL-6, and ICAM did not differ among groups, but all significantly increased in control group both during CPB and during reperfusion at 30 minutes and 4 hours after CPB (Figures 2(a)–2(e)), while post-CPB plasma levels of CK-MB, TNF-α, IL-6, and ICAM did not differ from that in baseline (Figures 2(b)–2(e)). During CPB and during reperfusion at 30 minutes, 4 hours, and 24 hours after CPB, plasma levels of cTnI, CK-MB, TNF-α, IL-6, and ICAM in Cap3d+Iso, Cap1hr+Iso, and Cap3d, but not in Cap1hr, were significantly lower than that in the control groups, and those in group Cap3d+Iso and Cap1hr+Iso were significantly lower than that in other groups (Figures 2(a)–2(e)). Plasma levels of cTnI during CPB and during reperfusion at 30 minutes, 4 hours, and 24 hours after CPB in group Cap3d+Iso were significantly lower than that in Cap1hr+Iso (Figure 2(a)).

3.2. Animal Study Data

3.2.1. Isoflurane and Captopril Reduced Postischemic Myocardial Injury, Ameliorated Myocardial Inflammation, and Attenuated Cardiac Ultrastructural Alterations in Rabbits. As shown in Figure 2, the myocardial area at risk did not differ among groups (Figure 3(a)). I/R resulted in significantly increased myocardial IS in I/R group. IPC, Iso, or Cap alone significantly reduced IS, while Cap in combination with Iso (Cap+Iso group) yielded an additive effect in that they further decreased IS as compared with either Iso or Cap alone (Figure 3(b)). Biopsies taken from sham operated control rabbit heart showed basically normal ultrastructure, with regular intercalated disks, sarcomere preservation, and normal mitochondrial morphology, although mild cytosolic, intermyofibrillar edema, and nuclear chromatin margination could occasionally be seen. In contrast, biopsies taken after postischemic reperfusion from rabbit heart showed signs of injury; in particular, cytosolic and intermyofibrillar edema was moderate to marked, and mitochondria showed more extensive damage compared with that in sham operated group. Biopsies taken from IPC, Cap, Iso, and Cap+Iso groups showed normal myofibrillar ultrastructure and mild separation of the mitochondrial cristae without swelling and vacuolation (Figure 3(c)).

3.2.2. Isoflurane and Captopril Improved Postischemic Myocardial Function Recovery in Rabbits. As shown in Figure 3, heart rate in groups Iso and Cap+Iso was significantly higher than that in other groups at baseline, and during ischemia, and during reperfusion at reperfusion 30 minutes, respectively, while no significant difference was observed among groups during reperfusion at reperfusion 60 minutes

Table 1: Baseline characteristics of the study population.

Item	Control	Cap1hr	Cap3d	Cap1hr+Iso	Cap3d+Iso
Gender (male/female)	14/6	14/6	15/5	13/7	14/6
Age (years)	46.2 ± 5.9	46.8 ± 7.5	44.5 ± 6.9	43.2 ± 7.2	45.3 ± 6.1
Body weight (Kg)	58.2 ± 7.2	61.7 ± 8.1	62.1 ± 9.0	61.2 ± 7.9	59.7 ± 8.3
LVEF (%)	55.2 ± 6.9	55.3 ± 6.9	53.1 ± 7.8	54.2 ± 7.4	56.6 ± 6.3
Premedication					
Digoxin (*n*)	6	6	7	5	6
Diuretic (*n*)	8	7	6	7	8

Control: untreated control; Cap1hr: captopril treatment for 1 h before surgery (12.5 mg, p.o., 1 h before surgery); Cap3d: captopril treatment for 3 days (12.5 mg, p.o., 3 times a day) before surgery; Cap1hr+Iso: captopril treatment for 1 h in combination with inhalational isoflurane (Iso) at 1.1% end tidal concentration administrated for 30 min before CPB; Cap3d+Iso: captopril treatment for 3 days in combination with Iso before CPB. Values are means ± S.D. or the number of patients. No significant differences were observed among groups; LVEF: left ventricular ejection fraction.

Table 2: Intraoperative and postoperative procedure characteristics of the patients.

Item	Control	Cap1hr	Cap3d	Cap1hr+Iso	Cap3d+Iso
Operation time (min)	147 ± 43	147 ± 45	142 ± 41	144 ± 45	148 ± 42
Aortic clamping time (min)	46 ± 18	46 ± 17	45 ± 19	47 ± 16	43 ± 18
Bypass time (min)	65 ± 19	67 ± 19	68 ± 20	67 ± 22	68 ± 21
Automatic rebeating rate (%)	40	$50^{\#}$	$50^{\#}$	70^{*}	80^{*}
Arrhythmia incidence (%)	45	35^{*}	35^{*}	30^{*}	20^{*}
Dopamine (mg)	687 ± 63	$513 \pm 71^{*\#}$	$478 \pm 67^{*\#}$	$317 \pm 46^{*}$	$243 \pm 54^{*\#}$
Sodium nitroprusside (mg)	813 ± 64	$796 \pm 66^{\#}$	$749 \pm 81^{\#}$	$706 \pm 83^{*}$	$641 \pm 83^{*\#}$
ICU stay (h)	68.6 ± 9.1	$62.0 \pm 8.9^{*\#}$	$59.1 \pm 8.8^{*\#}$	$54.5 \pm 8.9^{*}$	$43.1 \pm 9.3^{*}$
Hospital stay (d)	16.2 ± 2.5	$14.69 \pm 2.9^{*\#}$	$13.2 \pm 2.8^{*}$	$12.8 \pm 2.1^{*}$	$10.3 \pm 1.6^{*\#}$
Death in hospital (*n*)	0	0	0	0	0

Control: untreated control; Cap1hr: captopril treatment for 1 h before surgery (12.5 mg, p.o., 1 h before surgery); Cap3d: captopril treatment for 3 days (12.5 mg, p.o., 3 times a day) before surgery; Cap1hr+Iso: captopril treatment for 1 h in combination with inhalational isoflurane (Iso) at 1.1% end tidal concentration administrated for 30 min before CPB; Cap3d+Iso: captopril treatment for 3 days in combination with Iso before CPB. Values are means ± S.D. or the number of patients. $^{*}P < 0.05$ versus Control, $^{\#}P < 0.05$ versus Cap1hr+Iso.

and 120 minutes (Figure 4(a)). Mean arterial pressure (MAP) in groups Iso and Cap+Iso was significantly lower than that in other groups and did not differ between groups in baseline, ischemia for 30 minutes, reperfusion for 30 minutes, and reperfusion for 60 minutes, and no significant differences of MAP were observed among groups (Figure 4(b)). Rate pressure product (RPP) in groups Iso and Iso+Cap was significantly lower than that in other groups at baseline, during I/R, and reperfusion, while there was no difference between Iso and Iso+Cap groups (Figure 4(c)).

3.2.3. Isoflurane and Captopril Attenuated Postischemic Myocardial Apoptosis in Rabbits. Bcl-2, an antiapoptotic protein, was moderately increased in I/R groups but was significantly increased in IPC, Iso, Cap, and Iso+Cap groups, and Bcl-2 in IPC and Iso+Cap groups were significantly higher than that in Iso or Cap groups (Figure 5(a)). Proapoptotic protein Bax was significantly increased in I/R and significantly reduced in IPC, Iso, Cap, and Iso+Cap groups, and there was no significant difference among IPC, Iso, Cap, and Iso+Cap groups (Figure 5(b)). Bcl-2/Bax ratio was significantly reduced in I/R group compared with Sham group. Bcl-2/Bax ratio was enhanced by IPC, Iso, Cap, and Iso+Cap as compared to control, and IPC and Iso+Cap significantly further increased Bcl-2/Bax ratio compared with Iso or Cap alone (Figure 5(c)); the respective protein expressions were further confirmed by flow cytometry (Figures 5(d) and 5(e)).

3.2.4. Isoflurane and Captopril Ameliorated Postischemic Myocardial Oxidative Stress in Rabbits. MDA, an index of lipid peroxidation, was significantly increased in I/R and was moderately reduced in IPC, Iso, Cap, and Iso+Cap groups relative to I/R groups (Figure 6(a)). Plasma SOD in I/R group was significantly lower as compared to sham operative group, and IPC, Iso, Cap, and Iso+Cap slightly increased SOD as compared to I/R but the difference did not reach statistical difference (Figure 6(b)).

4. Discussion

The novel finding of the present clinical and animal studies is that the application of 3-day captopril treatment, but not 1-hour captopril treatment, in combination with isoflurane preconditioning before prolonged index ischemia was superior to either captopril treatment (3 days or 1 hour) or isoflurane alone in reducing postischemic myocardial oxidative stress,

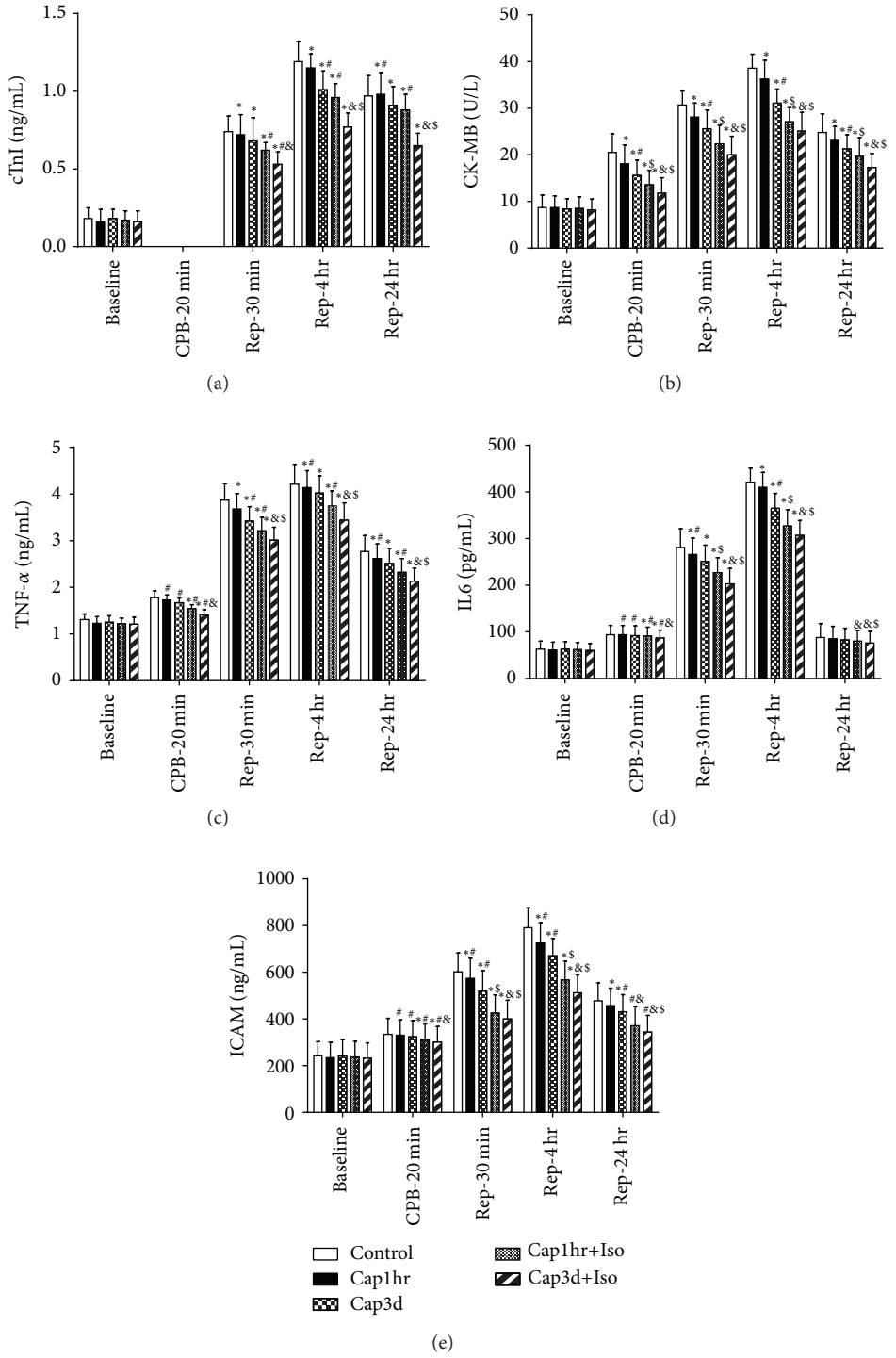

Figure 2: Isoflurane (Iso) and captopril (Cap) attenuated postischemic myocardial cellular injury and reduced proinflammatory cytokines release in patients. (a) Plasma cardiac troponin I (cTnI), (b) plasma creatine kinase- (CK-) MB, (c) plasma tumor necrosis factor- (TNF-) α, (d) plasma interleukin- (IL-) 6, and (e) plasma intercellular adhesion molecule (ICAM). Control: untreated control; Cap1hr: captopril treatment for 1 h before surgery (12.5 mg, p.o., 1 h before surgery); Cap3d: captopril treatment for 3 days (12.5 mg, p.o., 3 times a day) before surgery; Cap1hr+Iso: captopril treatment for 1 h in combination with inhalational isoflurane (Iso) at 1.1% end tidal concentration administrated for 30 min before CPB; Cap3d+Iso: captopril treatment for 3 days in combination with Iso before CPB. Data are shown as means ± SD, with $n = 20$ per group. $^{\#}P < 0.05$ versus Baseline, $^{*}P < 0.05$ and $^{\$}P < 0.01$ versus Control, and $^{\&}P < 0.05$ versus Cap1hr+Iso.

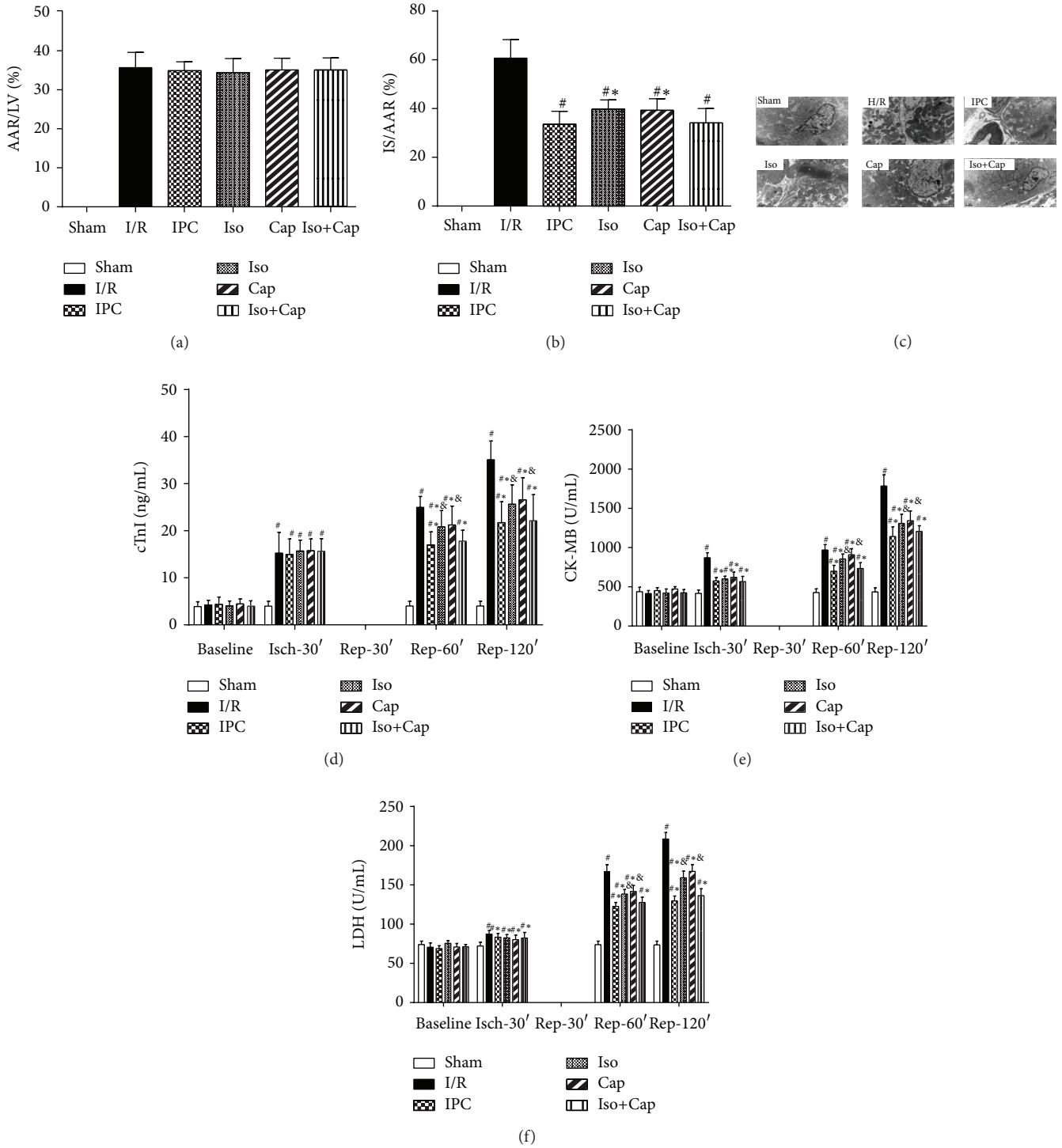

FIGURE 3: Isoflurane (Iso) and captopril (Cap) reduced postischemic myocardial injury, ameliorated myocardial inflammation, and attenuated cardiac ultrastructural alterations in rabbits. (a) Ratio of area at risk (AAR) to left ventricular (LV), (b) percentage of infarct size (IS) expressed as a percentage of AAR, (c) representative images of electron micrograph of rabbit hearts, (d) plasma cTnI, (e) plasma CK-MB, and (f) lactate dehydrogenase (LDH). Sham: sham operated control; I/R: rabbits subjected to myocardial ischemia reperfusion (MI/R); Cap: rabbits treated with captopril (25 mg/kg given intravenously 24 h) prior to inducing MI/R; Iso: rabbits received isoflurane preconditioning (15 min 1.1% end tidal isoflurane followed by a 15 min washout period before inducing MI/R); Iso+Cap: rabbits received captopril in combination with Iso. Data are shown as means ± SD, with $n = 8$ animals per group. $^{\#}P < 0.05$ or $P < 0.01$ versus I/R, $^{*}P < 0.05$ versus IPC, and $^{\&}P < 0.05$ versus Baseline.

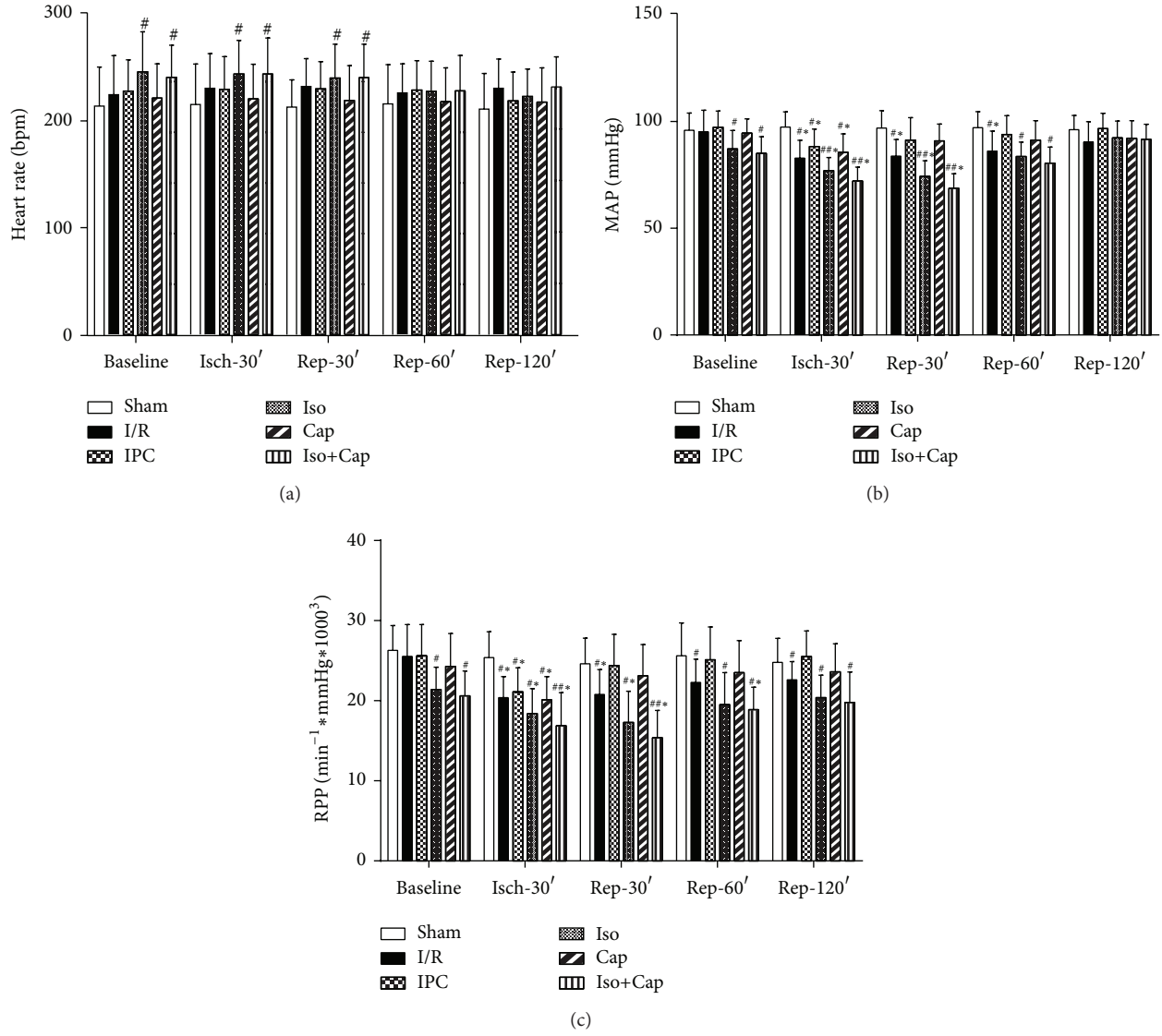

Figure 4: Isoflurane (Iso) and captopril (Cap) improved postischemic myocardial function recovery in rabbits. (a) Heart rate, (b) mean arterial pressure (MAP), and (c) rate pressure product (RPP) at baseline and during ischemia and reperfusion. Sham: sham operated control; I/R: rabbits subjected to myocardial ischemia reperfusion (MI/R); Cap: rabbits treated with captopril (25 mg/kg given intravenously 24 h) prior to inducing MI/R; Iso: rabbits received isoflurane preconditioning (15 min 1.1% end tidal isoflurane followed by a 15 min washout period before inducing MI/R); Iso+Cap: rabbits received captopril in combination with Iso. Data are shown as means ± SD, with $n = 8$ animals per group. $^{\#}P < 0.05$ or $P < 0.01$ versus Sham, $^{*}P < 0.05$ versus Baseline.

proinflammatory cytokines release, and myocardial injury. Combinational use of captopril as well as isoflurane preconditioning confers antioxidative stress and anti-inflammatory effects not only during ischemia but also during reperfusion stage in patients undergoing CPB. To our knowledge, this is the first study to demonstrate that captopril and isoflurane preconditioning can additively attenuate myocardial ischemia reperfusion (MI/R) injury.

When ischemia occurs, the oxygen and nutrient supply to the myocardium is reduced due to the decrease of blood flow. This deprivation of oxygen as well as nutrient supply results in the accumulation of sodium, hydrogen, and calcium ions, culminating in tissue acidosis, which leads to mitochondrial membrane depolarization, ATP depletion, and inhibition of myocardial contractile function [28]. Reperfusion, in turn, elicits rapid alterations in ion flux, stimulates a robust formation of ROS [29], and promotes the proinflammatory cytokines release [30], which eventually results in or exacerbates MI/R injury [31, 32]. Modulation of the early events induced by ischemia is of particular importance in combating MI/R. In the present study, in patients with CPB, a joint use of captopril and isoflurane preconditioning significantly reduced MI/R-induced proinflammatory cytokines (TNF-α, IL-6, and ICAM-1) release during CPB, which was associated with reduced myocardial injury during CPB and after CPB (reperfusion), and this protective effect of

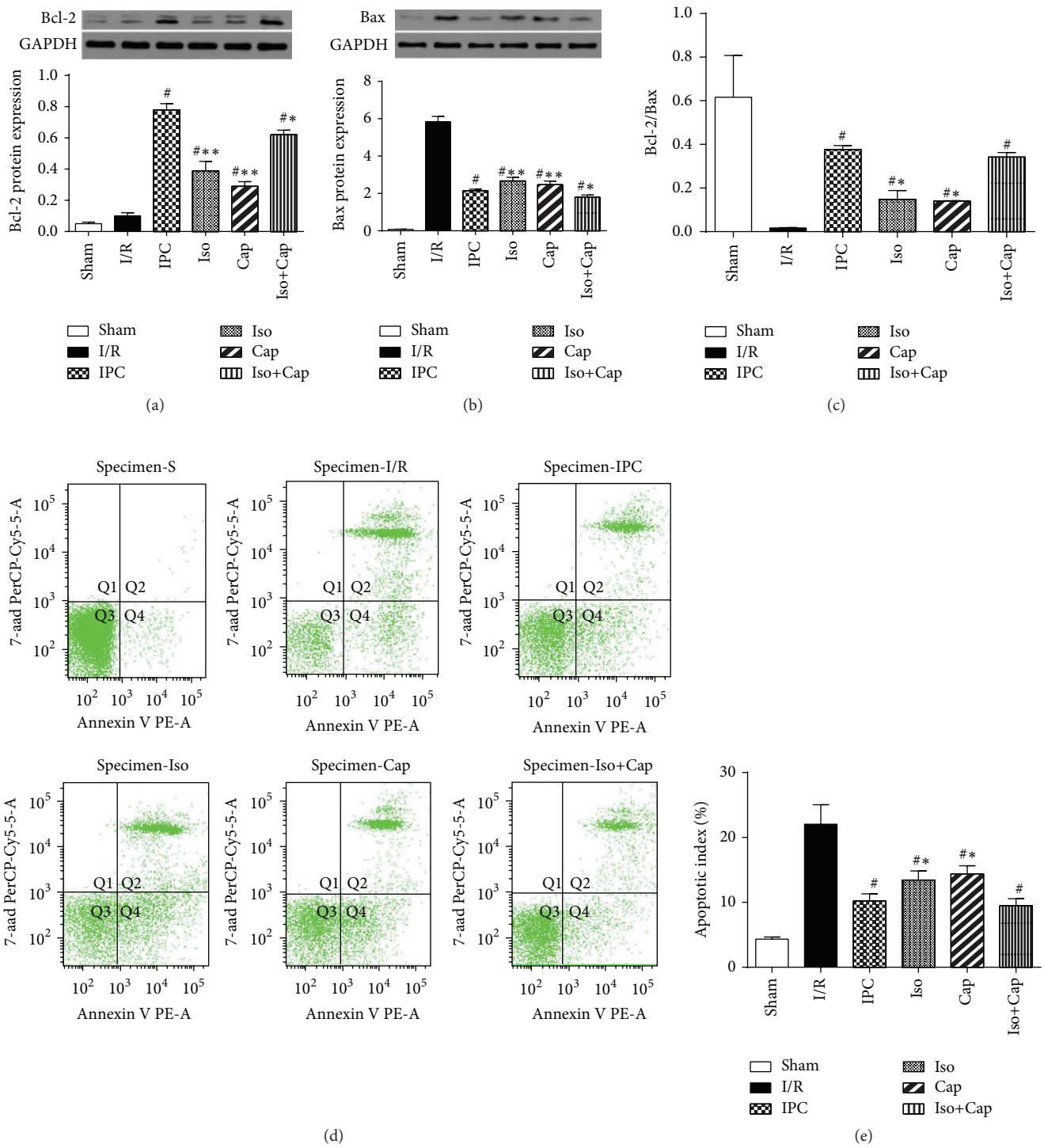

Figure 5: Isoflurane (Iso) and captopril (Cap) attenuated postischemic myocardial apoptosis in rabbits. (a) Protein expression of cardiac Bcl-2, (b) protein expression of cardiac Bax, (c) ratio of Bcl-2 to Bax, (d) representative graphs showing the proportion of apoptotic myocytes, and (e) quantitation of apoptotic myocytes. Sham: sham operated control; I/R: rabbits subjected to myocardial ischemia reperfusion (MI/R); Cap: rabbits treated with captopril (25 mg/kg given intravenously 24 h) prior to inducing MI/R; Iso: rabbits received isoflurane preconditioning (15 min 1.1% end tidal isoflurane followed by a 15 min washout period before inducing MI/R); Iso+Cap: rabbits received captopril in combination with Iso. Data are shown as means ± SD, with $n = 8$ animals per group. $^{\#}P < 0.05$ versus I/R, $^{*}P < 0.05$ versus IPC.

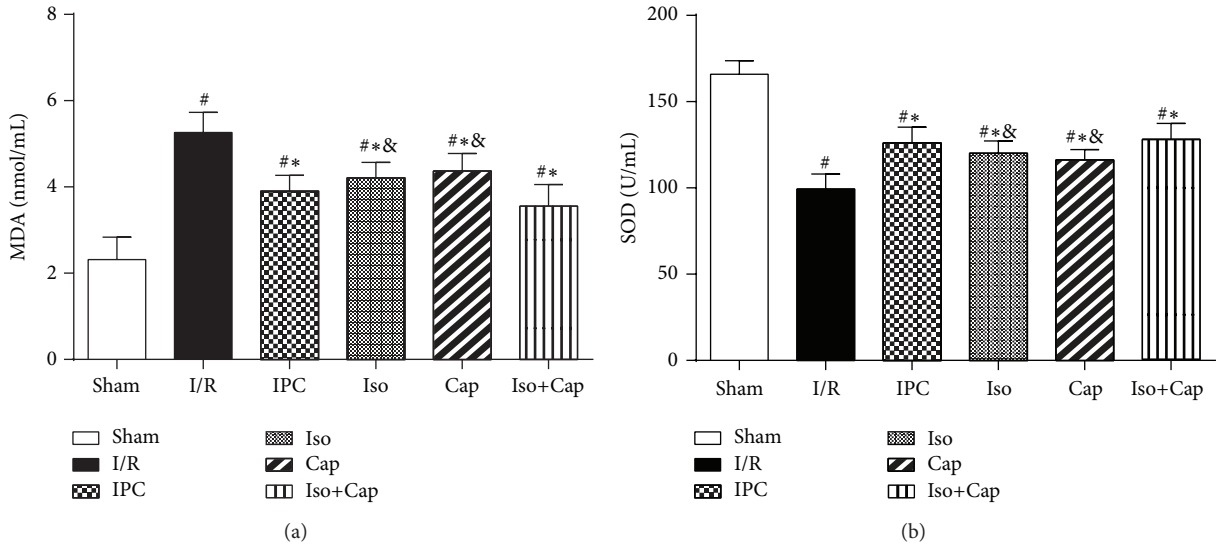

Figure 6: Isoflurane (Iso) and captopril (Cap) ameliorated postischemic myocardial oxidative stress in rabbits. (a) Cardiac malondialdehyde (MDA) content, (b) plasma superoxide dismutases (SOD) levels. Sham: sham operated control; I/R: rabbits subjected to myocardial ischemia reperfusion (MI/R); Cap: rabbits treated with captopril (25 mg/kg given intravenously 24 h) prior to inducing MI/R; Iso: rabbits received isoflurane preconditioning (15 min 1.1% end tidal isoflurane followed by a 15 min washout period before inducing MI/R); Iso+Cap: rabbits received captopril in combination with Iso. Data are shown as means ± SD, with $n = 8$ animals per group. $^{\#}P < 0.05$ versus Sham, $^{*}P < 0.05$ versus I/R, and $^{\&}P < 0.05$ versus IPC.

captopril in combination of isoflurane preconditioning is superior to captopril treatment for 3 days or 1 hour alone. Solenkova et al. reported that, in isolated rabbit heart model, cardioprotection of ischemic preconditioning is dependent on activation of adenosine receptors during the first minutes of reperfusion following termination of the index ischemia [33]. Similarly, Kin et al. showed that the first minute of the onset of reperfusion is critical to the cardioprotective effects of ischemic postconditioning, which protects the heart against MI/R injury by inhibiting oxidant generation and oxidant mediated injury in rats [34]. These together with the results from our present study jointly support the notion that inhibition of myocardial oxidative stress and inflammation occurred during ischemia or in the early minutes at the onset of reperfusion is important for developing cardioprotective strategies against MI/R. Results from our present study provide a clue that inhibition of myocardial oxidative stress and inflammation as early as during ischemia plays a pivotal role in ameliorating myocardial injury in MI/R. Of note, in animal study, captopril, isoflurane, and their combination all mimic the protective effects of IPC in reducing myocardial injury during ischemia, while there is no significant difference observed among all treatment groups (IPC, Cap, Iso, and Iso+Cap). This is not consistent with the results seen in our human study which showed that additive effects of captopril and isoflurane preconditioning exist as early as ischemia induction (CPB). One possible explanation is that the severity of MI/R injury is different between patients with CPB and animals received MI/R in the current study and that captopril treatment for 24 hours in animals may not precisely mimic that in our human study (3 days or 1 hour before CPB).

Increased oxidative stress and evaluated inflammation have been suggested as the main cause of MI/R injury. We previously showed that antioxidant N-acetylcysteine and allopurinol confer cardioprotective effects in rat subjected to MI/R [29, 35] and isoflurane preconditioning and propofol postconditioning synergistically reduced MI/R injury in patients undergoing CPB by upregulating endothelial nitric oxide synthase protein expression and reducing oxidative stress and proinflammatory cytokines release [6]. Similarly, in the present study, in animal model of MI/R, captopril, isoflurane preconditioning, and their combination all reduced MDA (marker of lipid peroxidation) and increased SOD activity, which were accompanied with decreased myocyte apoptosis and reduced myocardial injury and inflammation. Captopril in combination with isoflurane preconditioning confers superior protection to either captopril or isoflurane alone in rabbits subjected to MI/R. However, in patients with CPB, captopril (3 days or 1 hour) in combination with isoflurane preconditioning and captopril treatment alone, for 3 days but not 1 hour, reduced MI/R injury and mycocardial inflammation. This inconsistence suggests that captopril cardioprotective effects maybe depend on the duration of the treatment. van den Heuvel et al. demonstrated that captopril treatment for 3 months reduces the incidence of ischemia-related events after myocardial infarction, but a high incidence of clinical events occurred with withdrawal from captopril after 3-month treatment relative to 1-year captopril treatment [36]. This is consistent with our present finding that no cardioprotective effect was observed in patients treated with captopril 1 hour before CPB, while 3-day captopril treatment exerted profound protection. It is of

notice that, although captopril treatment for 1 hour alone did not show a protective effect in patients underwent CPB in the current study, captopril treatment for 1 hour in combination of isoflurane preconditioning conferred cardioprotective effects, indicating that captopril treatment may facilitate isoflurane preconditioning to confer protection. Captopril by inhibiting angiotensin-converting enzyme activity reduces the degradation of bradykinin, resulting in enhanced formation of prostacyclin and nitric oxide (NO), consequently exerting its antioxidant and anti-inflammatory properties [20, 24] and conferring cardioprotective effects [25]. NO has been proven as a trigger and mediator of isoflurane preconditioning cardioprotection. Isoflurane preconditioning by increasing endothelial nitric oxide synthase (NOS), but not inducible or neuronal NOS, enhances NO production and confers cardioprotection in a rabbit MI/R model [37]. These together suggest that captopril and isoflurane preconditioning can confer additive/synergistic effects in combating MI/R. This is confirmed in our present clinical study and animal study. However, further study is needed to elucidate the specific molecular mechanism governing the synergy of captopril and isoflurane preconditioning in the setting of MI/R.

5. Conclusions

In summary, we demonstrated that isoflurane preconditioning, combined with captopril treatment (3 days but not 1 hour), acts additively in attenuating postischemic myocardial reperfusion injury as determined by the surrogate markers of myocardial injury and function. Further large-scale and long-term studies are required to confirm the clinical benefit of this novel pharmacologic regimen, which may offer a promising therapeutic approach to cardioprotection patients undergoing cardiac surgery.

Conflict of Interests

No competing interests are declared.

Authors' Contribution

Zhengyuan Xia and Guogang Tian designed the study. Yi Tian, Haobo Li, and Peiyu Liu performed experiments and analyzed data; Yi Tian, Haobo Li, Peiyu Liu, Michael G. Irwin, and Jun-mei Xu interpreted results of experiments; Yi Tian and Haobo Li drafted paper; Zhengyuan Xia and Guogang Tian edited and revised paper; Zhengyuan Xia and Guogang Tian approved final version of paper. Zhengyuan Xia and Guogang Tian have full access to all the data in the study and take responsibility for the integrity of the data and the accuracy of the data analysis. Yi Tian, Haobo Li, and Peiyu Liu contributed equally to this study.

Acknowledgments

This work was supported, in part, by grants from the Natural Science Foundation of Hainan Province, China (808242), and Scientific Research Foundation of Department of Health of Hainan Province, China (2010-77).

References

[1] A. L. Hawkes, M. Nowak, B. Bidstrup, and R. Speare, "Outcomes of coronary artery bypass graft surgery," *Vascular Health and Risk Management*, vol. 2, no. 4, pp. 477–484, 2006.

[2] Y. Cao, T. Yang, S. Yu, G. Sun, C. Gu, and D. Yi, "Relationships of adiponectin with markers of systemic inflammation and insulin resistance in infants undergoing open cardiac surgery," *Mediators of Inflammation*, vol. 2013, Article ID 187940, 6 pages, 2013.

[3] P. Genereux, D. J. Cohen, M. Mack et al., "Incidence, predictors, and prognostic impact of late bleeding complications after transcatheter aortic valve replacement," *Journal of the American College of Cardiology*, vol. 64, no. 24, pp. 2605–2615, 2014.

[4] A. P. Furnary, G. Gao, G. L. Grunkemeier et al., "Continuous insulin infusion reduces mortality in patients with diabetes undergoing coronary artery bypass grafting," *Journal of Thoracic and Cardiovascular Surgery*, vol. 125, no. 5, pp. 1007–1021, 2003.

[5] S. Yusuf, D. Zucker, P. Peduzzi et al., "Effect of coronary artery bypass graft surgery on survival: overview of 10-year results from randomised trials by the Coronary Artery Bypass Graft Surgery Trialists Collaboration," *The Lancet*, vol. 344, no. 8922, pp. 563–570, 1994.

[6] Z. Huang, X. Zhong, M. G. Irwin et al., "Synergy of isoflurane preconditioning and propofol postconditioning reduces myocardial reperfusion injury in patients," *Clinical Science*, vol. 121, no. 2, pp. 57–69, 2011.

[7] D. Belhomme, J. Peynet, M. Louzy, J.-M. Launay, M. Kitakaze, and P. Menasché, "Evidence for preconditioning by isoflurane in coronary artery bypass graft surgery," *Circulation*, vol. 100, no. 19, supplement, pp. II340–II344, 1999.

[8] L. G. Kevin, P. Katz, A. K. S. Camara, E. Novalija, M. L. Riess, and D. F. Stowe, "Anesthetic preconditioning: effects on latency to ischemic injury in isolated hearts," *Anesthesiology*, vol. 99, no. 2, pp. 385–391, 2003.

[9] Y. Mio, M. W. Bienengraeber, J. Marinovic et al., "Age-related attenuation of isoflurane preconditioning in human atrial cardiomyocytes: roles for mitochondrial respiration and sarcolemmal adenosine triphosphate-sensitive potassium channel activity," *Anesthesiology*, vol. 108, no. 4, pp. 612–620, 2008.

[10] K. Tanaka, F. Kehl, W. Gu et al., "Isoflurane-induced preconditioning is attenuated by diabetes," *The American Journal of Physiology—Heart and Circulatory Physiology*, vol. 282, no. 6, pp. H2018–H2023, 2002.

[11] G. Clermont, C. Vergely, S. Jazayeri et al., "Systemic free radical activation is a major event involved in myocardial oxidative stress related to cardiopulmonary bypass," *Anesthesiology*, vol. 96, no. 1, pp. 80–87, 2002.

[12] P. A. Checchia, R. A. Bronicki, J. T. Muenzer et al., "Nitric oxide delivery during cardiopulmonary bypass reduces postoperative morbidity in children—a randomized trial," *Journal of Thoracic and Cardiovascular Surgery*, vol. 146, no. 3, pp. 530–536, 2013.

[13] L. Millucci, L. Ghezzi, E. Paccagnini et al., "Amyloidosis, inflammation, and oxidative stress in the heart of an alkaptonuric patient," *Mediators of Inflammation*, vol. 2014, Article ID 258471, 12 pages, 2014.

[14] J. Börgermann, I. Friedrich, S. Flohé et al., "Tumor necrosis factor-α production in whole blood after cardiopulmonary bypass: downregulation caused by circulating cytokine-inhibitory activities," *Journal of Thoracic and Cardiovascular Surgery*, vol. 124, no. 3, pp. 608–617, 2002.

[15] R. Khosravi, K. Ka, T. Huang et al., "Tumor necrosis factor-α and interleukin-6: potential interorgan inflammatory mediators contributing to destructive periodontal disease in obesity or metabolic syndrome," *Mediators of Inflammation*, vol. 2013, Article ID 728987, 6 pages, 2013.

[16] P. H. Lou, E. Lucchinetti, L. Zhang et al., "Loss of Intralipid but not sevoflurane-mediated cardioprotection in early type-2 diabetic hearts of fructose-fed rats: importance of ROS signaling," *PLoS ONE*, vol. 9, no. 8, Article ID e104971, 2014.

[17] H. Wang, L. Wang, N. Li et al., "Subanesthetic isoflurane reduces zymosan-induced inflammation in murine Kupffer cells by inhibiting ROS-activated p38 MAPK/NF-κB signaling," *Oxidative Medicine and Cellular Longevity*, vol. 2014, Article ID 851692, 13 pages, 2014.

[18] F. Kehl, P. S. Pagel, J. G. Krolikowski et al., "Isoflurane does not produce a second window of preconditioning against myocardial infarction in vivo," *Anesthesia and Analgesia*, vol. 95, no. 5, pp. 1162–1168, 2002.

[19] M. Wakeno-Takahashi, H. Otani, S. Nakao, H. Imamura, and K. Shingu, "Isoflurane induces second window of preconditioning through upregulation of inducible nitric oxide synthase in rat heart," *American Journal of Physiology—Heart and Circulatory Physiology*, vol. 289, no. 6, pp. H2585–H2591, 2005.

[20] P. Sogaard, C. O. Gotzsche, J. Ravkilde, and K. Thygesen, "Effects of captopril on ischemia and dysfunction of the left ventricle after myocardial infarction," *Circulation*, vol. 87, no. 4, pp. 1093–1099, 1993.

[21] J. Gurevitch, D. Pevni, I. Frolkis et al., "Captopril in cardioplegia and reperfusion: protective effects on the ischemic heart," *The Annals of Thoracic Surgery*, vol. 63, no. 3, pp. 627–633, 1997.

[22] A. W. Scribner, J. Loscalzo, and C. Napoli, "The effect of angiotensin-converting enzyme inhibition on endothelial function and oxidant stress," *European Journal of Pharmacology*, vol. 482, no. 1-3, pp. 95–99, 2003.

[23] Y.-H. Liu, Y. You, T. Song, S.-J. Wu, and L.-Y. Liu, "Impairment of endothelium-dependent relaxation of rat aortas by homocysteine thiolactone and attenuation by captopril," *Journal of Cardiovascular Pharmacology*, vol. 50, no. 2, pp. 155–161, 2007.

[24] F. M. B. de Gusmão, C. Becker, M. H. C. Carvalho, and L. F. M. Barros, "Angiotensin II inhibition during myocardial ischemia-reperfusion in dogs: effects on leukocyte infiltration, nitric oxide synthase isoenzymes activity and left ventricular ejection fraction," *International Journal of Cardiology*, vol. 100, no. 3, pp. 363–370, 2005.

[25] W. Linz, G. Wiemer, and B. A. Scholkens, "ACE-inhibition induces NO-formation in cultured bovine endothelial cells and protects isolated ischemic rat hearts," *Journal of Molecular and Cellular Cardiology*, vol. 24, no. 8, pp. 909–919, 1992.

[26] Q. Fan, X.-C. Yang, Y. Liu et al., "Postconditioning attenuates myocardial injury by reducing nitro-oxidative stress in vivo in rats and in humans," *Clinical Science*, vol. 120, no. 6, pp. 251–261, 2011.

[27] J. Xu, H. Li, M. G. Irwin et al., "Propofol ameliorates hyperglycemia-induced cardiac hypertrophy and dysfunction via heme oxygenase-1/signal transducer and activator of transcription 3 signaling pathway in rats," *Critical Care Medicine*, vol. 42, no. 8, pp. e583–e594, 2014.

[28] D. J. Hausenloy and D. M. Yellon, "Myocardial ischemia-reperfusion injury: a neglected therapeutic target," *The Journal of Clinical Investigation*, vol. 123, no. 1, pp. 92–100, 2013.

[29] T. Wang, X. Mao, H. Li et al., "*N*-Acetylcysteine and allopurinol up-regulated the Jak/STAT3 and PI3K/Akt pathways via adiponectin and attenuated myocardial postischemic injury in diabetes," *Free Radical Biology and Medicine*, vol. 63, pp. 291–303, 2013.

[30] J. Vinten-Johansen, R. Jiang, J. G. Reeves, J. Mykytenko, J. Deneve, and L. J. Jobe, "Inflammation, proinflammatory mediators and myocardial ischemia-reperfusion injury," *Hematology/Oncology Clinics of North America*, vol. 21, no. 1, pp. 123–145, 2007.

[31] D. M. Yellon and D. J. Hausenloy, "Myocardial reperfusion injury," *The New England Journal of Medicine*, vol. 357, no. 11, pp. 1074–1135, 2007.

[32] G. M. Fröhlich, P. Meier, S. K. White, D. M. Yellon, and D. J. Hausenloy, "Myocardial reperfusion injury: looking beyond primary PCI," *European Heart Journal*, vol. 34, no. 23, pp. 1714–1724, 2013.

[33] N. V. Solenkova, V. Solodushko, M. V. Cohen, and J. M. Downey, "Endogenous adenosine protects preconditioned heart during early minutes of reperfusion by activating Akt," *American Journal of Physiology—Heart and Circulatory Physiology*, vol. 290, no. 1, pp. H441–H449, 2006.

[34] H. Kin, Z.-Q. Zhao, H.-Y. Sun et al., "Postconditioning attenuates myocardial ischemia-reperfusion injury by inhibiting events in the early minutes of reperfusion," *Cardiovascular Research*, vol. 62, no. 1, pp. 74–85, 2004.

[35] X. Mao, T. Wang, Y. Liu et al., "N-acetylcysteine and allopurinol confer synergy in attenuating myocardial ischemia injury via restoring HIF-1α/HO-1 signaling in diabetic rats," *PLoS ONE*, vol. 8, no. 7, Article ID e68949, 2013.

[36] A. F. van den Heuvel, W. H. van Gilst, D. J. van Veldhuisen, R. J. de Vries, P. H. Dunselman, and J. H. Kingma, "Long-term anti-ischemic effects of angiotensin-converting enzyme inhibition in patients after myocardial infarction. The Captopril and Thrombolysis Study (CATS) Investigators," *Journal of the American College of Cardiology*, vol. 30, no. 2, pp. 400–405, 1997.

[37] P. C. Chiari, M. W. Bienengraeber, D. Weihrauch et al., "Role of endothelial nitric oxide synthase as a trigger and mediator of isoflurane-induced delayed preconditioning in rabbit myocardium," *Anesthesiology*, vol. 103, no. 1, pp. 74–83, 2005.

Hindawi Publishing Corporation
Mediators of Inflammation
Volume 2015, Article ID 726243, 9 pages
http://dx.doi.org/10.1155/2015/726243

Research Article

In Vivo Evaluation of the Ameliorating Effects of Small-Volume Resuscitation with Four Different Fluids on Endotoxemia-Induced Kidney Injury

Yan-ling Wang,[1] Jing-hui Chen,[2] Qiong-fang Zhu,[3] Gao-feng Yu,[2] Chen-fang Luo,[1] Gang-jian Luo,[1] Shang-rong Li,[1] and Zi-qing Hei[1]

[1]*Department of Anesthesiology, The Third Affiliated Hospital of Sun Yat-sen University, No. 600 Tianhe Road, Tianhe District, Guangzhou 510630, China*
[2]*Department of Anesthesiology, Guangzhou Women and Children's Medical Center, No. 9 Jinsui Road, Guangzhou 510623, China*
[3]*Department of Anesthesiology, The First Affiliated Hospital of Sun Yat-sen University, No. 58 Zhongshan Road II, Guangzhou 510080, China*

Correspondence should be addressed to Zi-qing Hei; heiziqing@sina.com

Received 15 October 2014; Accepted 10 December 2014

Academic Editor: Huang-Ping Yu

Acute kidney injury associated with renal hypoperfusion is a frequent and severe complication during sepsis. Fluid resuscitation is the main therapy. However, heart failure is usually lethal for those patients receiving large volumes of fluids. We compared the effects of small-volume resuscitation using four different treatment regimens, involving saline, hypertonic saline (HTS), hydroxyethyl starch (HES), or hypertonic saline hydroxyethyl starch (HSH), on the kidneys of rats treated with lipopolysaccharide (LPS) to induce endotoxemia. LPS injection caused reduced and progressively deteriorated systemic (arterial blood pressure) and renal hemodynamics (renal blood flow and renal vascular resistance index) over time. This deterioration was accompanied by marked renal functional and pathological injury, as well as an oxidative and inflammatory response, manifesting as increased levels of tumor necrosis factor-α, nitric oxide, and malondialdehyde and decreased activity of superoxide dismutase. Small-volume perfusion with saline failed to improve renal and systemic circulation. However, small-volume perfusion with HES and HSH greatly improved the above parameters, while HTS only transiently improved systemic and renal hemodynamics with obvious renal injury. Therefore, single small-volume resuscitation with HES and HSH could be valid therapeutic approaches to ameliorate kidney injury induced by endotoxemia, while HTS transiently delays injury and saline shows no protective effects.

1. Introduction

Endotoxemia frequently occurs during critical phases of clinical diseases, including trauma and infectious diseases, and inevitably causes shock and organ damage contributing to poor survival rate [1, 2]. Acute kidney injury (AKI) is a common complication following endotoxic shock and is associated with a high morbidity rate of up to 64% [3]. Despite significant advances in control of endotoxemia, there remains an urgent need to promptly prevent the occurrence of AKI or restore impaired renal function associated with sepsis [4].

In sepsis, renal blood flow is frequently reduced with progressive development of renal inflammation and oxidative stress, thereby contributing to the genesis of AKI [5, 6]. Early resuscitation using crystal or colloid fluids to improve tissue perfusion and inhibit oxidative and inflammatory response may provide a meaningful degree of renal protection [7, 8]. However, infusion of large-volume fluids is always limited to critically ill patients, although caution must be exercised in patients with heart dysfunction, in whom small-volume resuscitation is typically used [9]. The potential protective effects of small-volume fluid resuscitation on kidney injury induced by endotoxemia are currently unknown.

Fortunately, small-volume resuscitation with hypertonic solutions has been successfully applied in clinical rescue of hemorrhagic and septic shock [10–12]. However, the debate

persists regarding which solution (crystalloids or colloids) is most beneficial [13, 14]. For instance, it is reported that appropriate administration of colloids seemed to be associated with reduced mortality, while others consider that resuscitation with balanced crystalloids was associated with a lower risk of in-hospital mortality [15, 16]. In the present study, we compared the effects of small-volume resuscitation with saline, 7.5% hypertonic saline (HTS), hydroxyethyl starch 130/0.4 (HES), and hypertonic saline hydroxyethyl starch 40 (HSH) at a dose of 4 mL/kg on acute kidney injury induced by endotoxemia. The potential mechanism of the hypothesized protection was further explored, focusing on renal perfusion and variations of oxidative and inflammatory mediators.

2. Methods

2.1. Animal Procedures. The study was reviewed and approved by the Research Ethics Committee of The Third Affiliated Hospital of Sun Yat-sen University, Guangzhou, China. Thirty adult male Sprague-Dawley (SD) rats (180–250 g body weight) were provided by the Experimental Animal Center of Sun Yat-sen Medical School and were treated in accordance with both international and institutional guidelines.

Experimental procedures on rats were performed as previously described [10]. Briefly, after anesthesia, animals were ventilated with 40–50% oxygen (Rodent Ventilator 638, Harvard Apparatus, Boston, MA, USA), with proper tidal volume (7 mL/kg) and respiratory rate (approximately 30 breaths/min). The left carotid artery was catheterized for continuous monitoring of arterial pressure. A phased-array, low-frequency probe (frequency 2.0–5.0 MHz) was placed in the left renal door cross-sectional level for kidney color velocity imaging (CVI) detection. All animals were given intravenous administration of 1 mg LPS/kg through the right internal jugular vein to establish the endotoxemia model.

2.2. Drug and Fluids. Sodium pentobarbital in saline was obtained from Sigma Chemical Co. (St. Louis, MO, USA). LPS was isolated from *E. coli* 0111:B4 and purchased from Sigma Chemical Co. The experimental solutions were 0.9% saline (Zhejiang Chimin Pharmaceutical Co., Ltd., Taizhou, China), 7.5% hypertonic saline (HTS, The Third Affiliated Hospital of Sun Yat-Sen University, Guangdong, China), hydroxyethyl starch (HES, Fresenius Kabi Pharmaceutical Co., Ltd., Bad Homburg, Germany), and hypertonic saline hydroxyethyl starch (HSH, Shanghai Huayuan Chang Fu Co., Ltd., Shanghai, China).

2.3. Experimental Groups. Rats were randomized into five groups, including control and four resuscitation groups (n = 6 per group). The groups were designated as follows: (1) group C (control group): 4 mL 0.9% saline/kg; (2) group S (saline group): LPS 1 mg/kg + 4 mL 0.9% saline/kg; (3) group HTS: LPS 1 mg/kg + 4 mL 7.5% HTS/kg; (4) group HES: LPS 1 mg/kg + 4 mL HES/kg; and (5) group HSH: LPS 1 mg/kg + 4 mL HSH/kg. Four kinds of resuscitation solutions at a dose of 4 mL/kg were administered at 30 min after intravenous injection of LPS. And fluids were administered within 5 min according to [17]. After performing systemic hemodynamic and renal blood flow measurements, rats were euthanized, blood was collected by cardiac puncture, and the kidneys were harvested.

2.4. Systemic Hemodynamic and Renal Microcirculatory Measurements. Systolic arterial pressure (SAP) was monitored from catheterized internal carotid arteries with a Hewlett-Packard monitor. Renal flow indices were measured by Doppler ultrasound using a Technos MPx DU8 instrument (Esaote Biomedica, Genoa, Italy). Image-Pro Plus Image Analysis software was used to calculate the ratio of renal blood signal and the peak renal cross-section area. SAP and renal microcirculation indices (renal blood flow signals (CVI), peak-systolic velocity (V_{max}), and end-diastolic velocity (V_{min})) were recorded before LPS administration (T_0, baseline), 30 min after LPS administration (T_1), and 10 min (T_2), 30 min (T_3), and 60 min (T_4) after small-volume resuscitation.

Renal vascular resistance index (RVRI) was calculated by the formula

$$\text{RVRI} = \frac{V_{max} - V_{min}}{V_{max}}. \quad (1)$$

2.5. Renal Function Parameters. Blood samples were obtained from the abdominal aorta 60 min after small-volume resuscitation. Renal function was determined by assaying serum for serum creatinine (Scr) and blood urea nitrogen (BUN) using the AV800 Chemistry Analyzer (Hitachi, Hitachi City, Japan).

2.6. Renal Histopathology Images Obtained by Light and Electron Microscopy. Renal tissues were taken 60 min after small-volume resuscitation and fixed in 10% formaldehyde. After being processed in an Autotechnicon, tissues were embedded in paraffin for light microscopy. Sections of 5 μm thickness were cut with a microtome and stained with hematoxylin-eosin (H&E). The degree of each abnormality was graded numerically by the Paller score according to [18].

Separated tissue samples were fixed in 2% paraformaldehyde and 2.5% glutaraldehyde in 0.1 M PBS (pH 7.4) at 4°C for 1 day for electron microscopy. After being postfixed with 2% osmium tetroxide, tissues were dehydrated in graded ethanol and embedded into araldite. The stained sections were examined using a Leo 906E electron microscope.

2.7. Detection of Renal Cortical TNF-α and NO Levels. Because the renal cortex is highly sensitive to LPS challenge, renal cortical tissue was separated from the rest of the kidney for analyses [19]. Levels of TNF-α and NO were quantified with specific ELISA and NO kits (Boster Company, Wuhan, China, and Nanjing Jiancheng Bioengineering Institute, Nanjing, China, resp.).

2.8. Detection of Renal Cortical MDA Level and SOD Activity. Renal cortex was homogenized for assessment of MDA level and SOD activity with kits based on the thiobarbituric acid

reactive substance assay and xanthine oxidase method, respectively (both by Jiancheng Bioengineering Institute, Nanjing, China).

2.9. Data Exclusion and Statistical Analyses. Data were expressed as means ± SEM. Statistical analysis of data was performed by using one-way analysis of variance (ANOVA), while repeated measurements of ANOVA were used for CVI analyses. Tukey's HSD test was used for intragroup comparisons. Pathology scores were analyzed by a nonparametric t-test. Differences were considered to be statistically significant if $P < 0.05$.

3. Results

3.1. Renal Function and Pathology Changes. Small-volume resuscitation with HES and HSH markedly decreased the augmented Scr and BUN levels ($P = 0.028$ versus group S) due to LPS exposure, while HTS resuscitation was less effective (Figures 1(a) and 1(b)).

LPS caused severe renal tubular injury, manifested as significant tubular degeneration, disintegration, edema, necrosis, and abscission of renal tubular epithelium, as well as cellular debris obstructing the collecting tubules and basal membrane fracture (Figures 1(d) and 1(e)). Small-volume resuscitation with colloid and hyperoncotic solutions markedly ameliorated the renal injury, showing that local epithelial and mitochondrial edema, cellular necrosis, and abscission were seen in the HTS group, while kidneys in the HES and HSH groups appeared with only slight edema with occasional cellular necrosis and abscission. These changes were correlated with the Paller histology grading of LPS-mediated kidney damage at 60 min after resuscitation (Figure 1(c)).

3.2. Effects of Small-Volume Resuscitation on Systemic Circulation and Renal Perfusion. SAP was measured to evaluate the systemic circulatory state and renal perfusion was detected through Doppler ultrasound by simultaneously monitoring renal blood flow signals (CVI), V_{max}, V_{min}, and the calculated RVRI [20]. Based on the measurement of these parameters, the LPS-induced deterioration of systemic and renal hemodynamics was assessed by comparisons among the five groups at the T_0 time point, while improvement after small-volume resuscitation was evaluated by comparisons among the five groups at the T_1 time point.

Doppler ultrasound showed that renal blood flow signal (CVI) was strongly and uniformly distributed with adequate cortex perfusion before LPS administration and then dramatically decreased with discrepant distribution and weak renal perfusion (CVI) under LPS challenge. Small-volume resuscitation with HES and HSH markedly improved CVI, while saline and HTS showed only slight improvement on renal blood flow (Figure 2).

The time courses for measurements of SAP, V_{max}, V_{min}, RVRI, and CVI throughout the five sequential study time points are presented in Figures 2 and 3. LPS caused marked decreases in SAP, V_{max}, and V_{min}, and increased RVRI ($P = 0.012$ versus T_0); effects of LPS continuously worsened over time in group S ($P = 0.028$ versus T_0 and T_1). Although resuscitation with HES and HSH failed to completely restore systemic and renal hemodynamics to baseline ($P = 0.017$, versus T_0), the detected associated parameters were immediately and persistently improved ($P = 0.027$, versus T_1), while HTS only temporarily ameliorated these indices ($P = 0.039$; T_2 versus T_1). Figures 3(c) and 3(d) (line graph) illustrate date shown in Figures 3(a) and 3(b) (histogram) in a different manner.

3.3. Effects of Small-Volume Resuscitation on Renal Cortical TNF-α and NO Levels. Production of TNF-α and production of NO, two important inflammatory mediators, were both promoted by the LPS treatment, demonstrating generation of an inflammatory response. In this study, the levels of renal cortical TNF-α and NO markedly increased after LPS challenge ($P = 0.001$; all versus group C) and were influenced to different degrees by the four types of fluid resuscitation. In the HES and HSH groups, TNF-α levels decreased ($P = 0.013$ versus group S) (Figure 4(a)) and NO levels did not change, while in the HTS group both TNF-α and NO were maintained at high levels (Figure 4(b)).

3.4. Effects of Small-Volume Resuscitation on Renal Cortical MDA Level and SOD Activity. MDA, a by-product of lipid peroxidation, reflects the extent of oxidative damage, while the activity of SOD, a critical antioxidant, can be used to represent the antioxidative capacity. LPS challenge increased renal cortical levels of MDA and inhibited activity of SOD ($P = 0.002$; all versus group C). Small-volume resuscitation improved the renal oxidative stress state, with resuscitation with HES and HSH decreasing the augmented MDA level and enhancing the SOD activity ($P = 0.036$, versus group S or HTS) (Figures 4(c) and 4(d)).

4. Discussion

Severe infection causes endotoxemia and the kidney is one of the first organ systems affected by LPS [21]. Reports indicate that endotoxemia-induced renal hypoperfusion contributes to an ischemia-reperfusion insult that potentially leads to the activation of renal inflammation and oxidative stress [10]. Fluid resuscitation has always been recognized as the primary resuscitation strategy for patients with AKI after endotoxemia [7, 11, 12, 20]. Although large amounts of fluid infusion could quickly improve renal perfusion, it is strictly limited to use in some critically ill patients suffering from endotoxemia and is contraindicated in patients with heart dysfunctions [22].

Small-volume resuscitation with hypertonic fluids has been regarded as an effective strategy for hemorrhagic shock, but it is unclear how different kinds of fluids affect kidney injury induced by LPS. Hence, our purpose here was to investigate the varying ameliorating effects of small-volume resuscitation with saline, 7.5% hypertonic saline, hydroxyethyl starch 130/0.4, and hypertonic saline hydroxyethyl starch 40 on LPS-induced AKI. Based on the available reports [23], we used the intravenous resuscitation dose of 4 mL/kg as an effective and safe dose. To this end, we conducted assessments of pathology images, systemic blood pressure, and renal

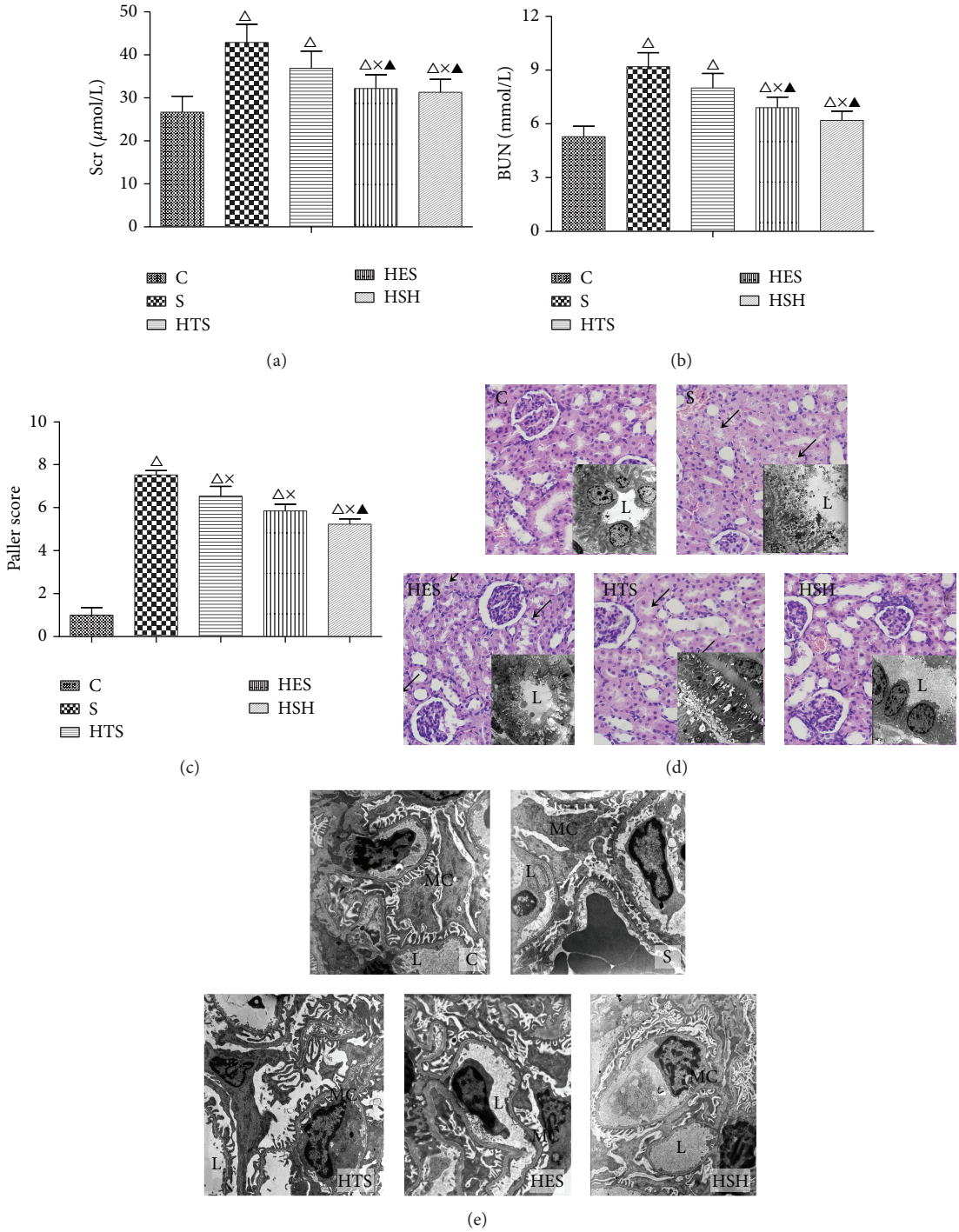

Figure 1: Small-volume resuscitation alleviated the severity of renal injury in rats with LPS-induced endotoxemia. (a) and (b) show alterations in renal function parameters in response to small-volume resuscitation with different solutions after LPS administration. (c) shows Paller scores in different groups. (d) Renal pathology changes under light (stained with HE, ×400) and electron microscopy (for tubular ultrastructure, ×2950). Photomicrograph shows an intact epithelial system with normal renal tubules and glomeruli in group C, while the renal tubule exhibited serious degeneration, disintegration, and edema in epithelial cells as well as cellular debris obstructing the collecting tubules in group S (as shown by ↙); HTS-treated group showed only local epithelial and mitochondrial edema with less necrosis and abscission, while the HES- and HSH-treated groups only showed occasional injury. Ultrastructure (L: lumen, EC: epithelial cells). (e) Ultrastructure of glomerulus under an electron microscope (×5200). Photomicrograph shows normal glomerular structure in group C, while the number of foot processes in podocytes decreased and these foot processes were locally confluent with small amounts of dense deposits inside the basement membrane in group S. However, the podocytes were restored to a normal state with no dense deposits in photomicrographs from the HTS-, HES-, and HSH-treated groups. (L: lumen; MC: mesangial cell; RC: red cell; WC: white cell). $^{\triangle}P \leq 0.05$ compared to group C; $^{\times}P \leq 0.05$ compared to group S; $^{\blacktriangle}P \leq 0.05$ compared to the HTS group.

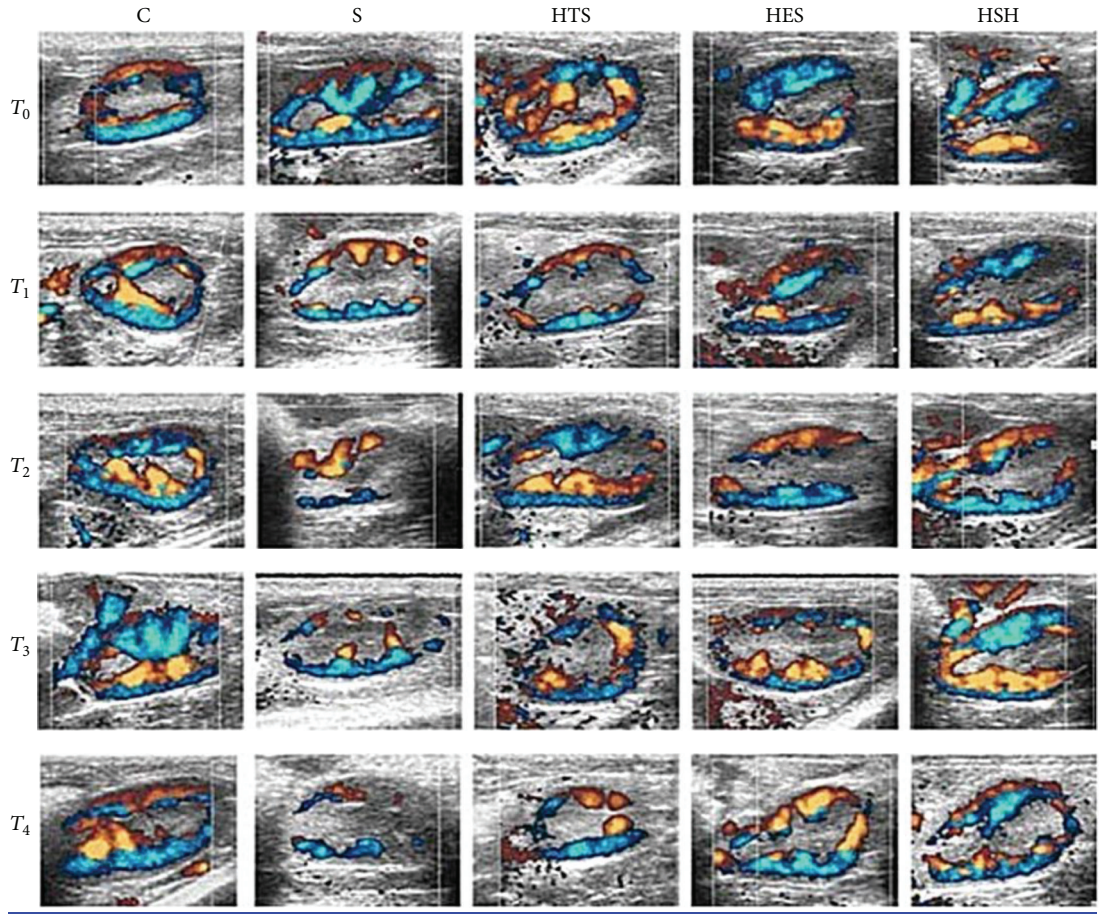

Figure 2: Color velocity imaging (CVI) of kidney at left renal door cross-sectional level. In group C and other groups at the T_0 time point, renal blood flow signals were strongly and uniformly distributed with adequate cortical perfusion, while it decreased dramatically with discrepant distribution and weak cortical perfusion at T_1 in the four experimental groups, among which there existed some degree of improvement with time in the HTS, HES, and HSH groups.

perfusion, as well as renal levels of TNF-α, NO, and MDA and activity of SOD. Our results showed that, as compared with saline, small-volume hydroxyethyl starch 130/0.4 and hypertonic saline hydroxyethyl starch 40 could rapidly ameliorate the severity or postpone the development of renal tubular injury in the rat model of endotoxemia. At the same time, hydroxyethyl starch 130/0.4 and hypertonic saline hydroxyethyl starch 40 immediately restored systemic and renal blood flow and even reduced the renal inflammatory response and oxidative stress. In contrast, 7.5% hypertonic saline only temporarily improved systemic circulation and renal blood flow without having effects on cytokine release.

Endotoxemia has been proven to be associated with progressive renal dysfunction, even in the presence of normal or elevated blood pressure and cardiac output [13, 14]. Insight into renal microcirculation should provide more meaningful information about the underlying mechanisms of renal dysfunction. Doppler ultrasound is a precise method to evaluate renal blood flow [24]. In the present study, we applied Doppler ultrasound and showed that small-volume resuscitation with HES and HSH immediately and permanently improved the deceased renal blood flow that resulted from LPS challenge, while HTS showed only slight and temporary effects compared to those elicited by saline. Meanwhile, parameters for systemic blood pressure evolved in coincidence with the trend of renal blood flow and pathological damage. These results suggest that the choice of different fluids is closely related to the improvement by small-volume resuscitation of renal perfusion. Accordingly, we conclude that infusion of colloids is better for clinical small-volume resuscitation for endotoxemia patients having complications with heart dysfunction. Furthermore, because the small-volume resuscitation could not completely restore systemic circulation and renal blood flow, other strategies should be adopted to improve the protective effect, including resuscitation in combination with vasoactive or organ-protective drugs.

Normal saline, an isotonic solution, is rapidly distributed around vessels, while hypertonic saline can transfer interstitial fluids into vessels to improve circulation based on its hypertonicity. However, it has a short duration of action because of the rapid reestablishment of osmotic balance between intra- and extracellular fluids. HES and HSH can elevate colloid osmotic pressure and stay longer in vessels

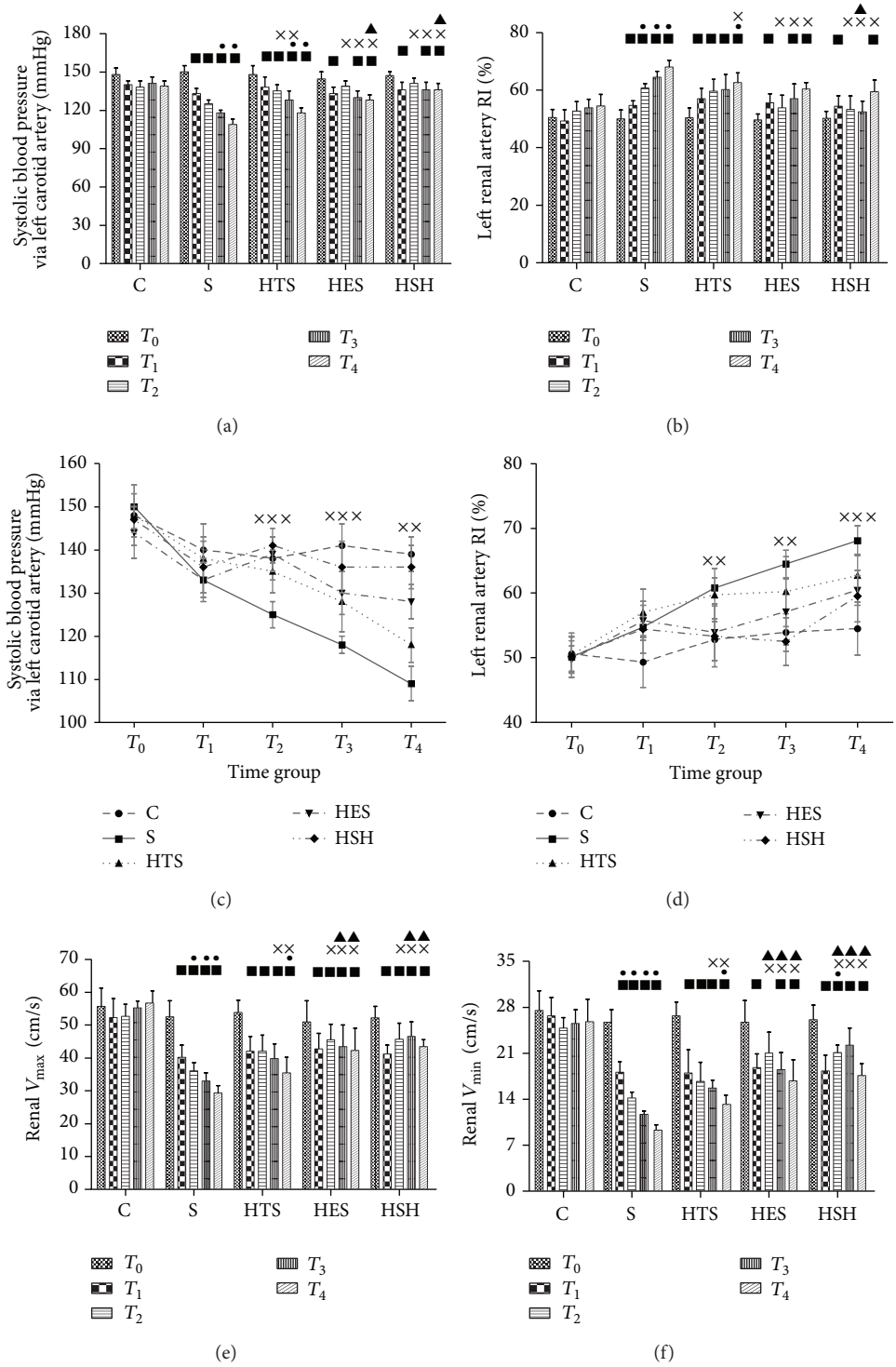

Figure 3: Small-volume resuscitation improved systemic and renal hemodynamics (mean ± SEM, $n = 6$). (a), (b), (e), and (f) show the early stage alterations to SAP, RVRI, V_{max}, and V_{min} in different groups over time. $^{\blacksquare}P \leq 0.05$ versus T_0; $^{\bullet}P \leq 0.05$ versus T_1; $^{\times}P \leq 0.05$ versus group S; $^{\blacktriangle}P \leq 0.05$ versus group HTS. (c) and (d) are the line charts for mean arterial blood pressure (MAP) expressed in mmHg throughout the experimental procedure and left renal artery RI (RARI) expressed as $(V_{max} - V_{min})/V_{max}$. $^{\times\times\times}P \leq 0.05$, S versus HTS, HES, and HSH; $^{\times\times}P \leq 0.05$, S versus HES and HSH.

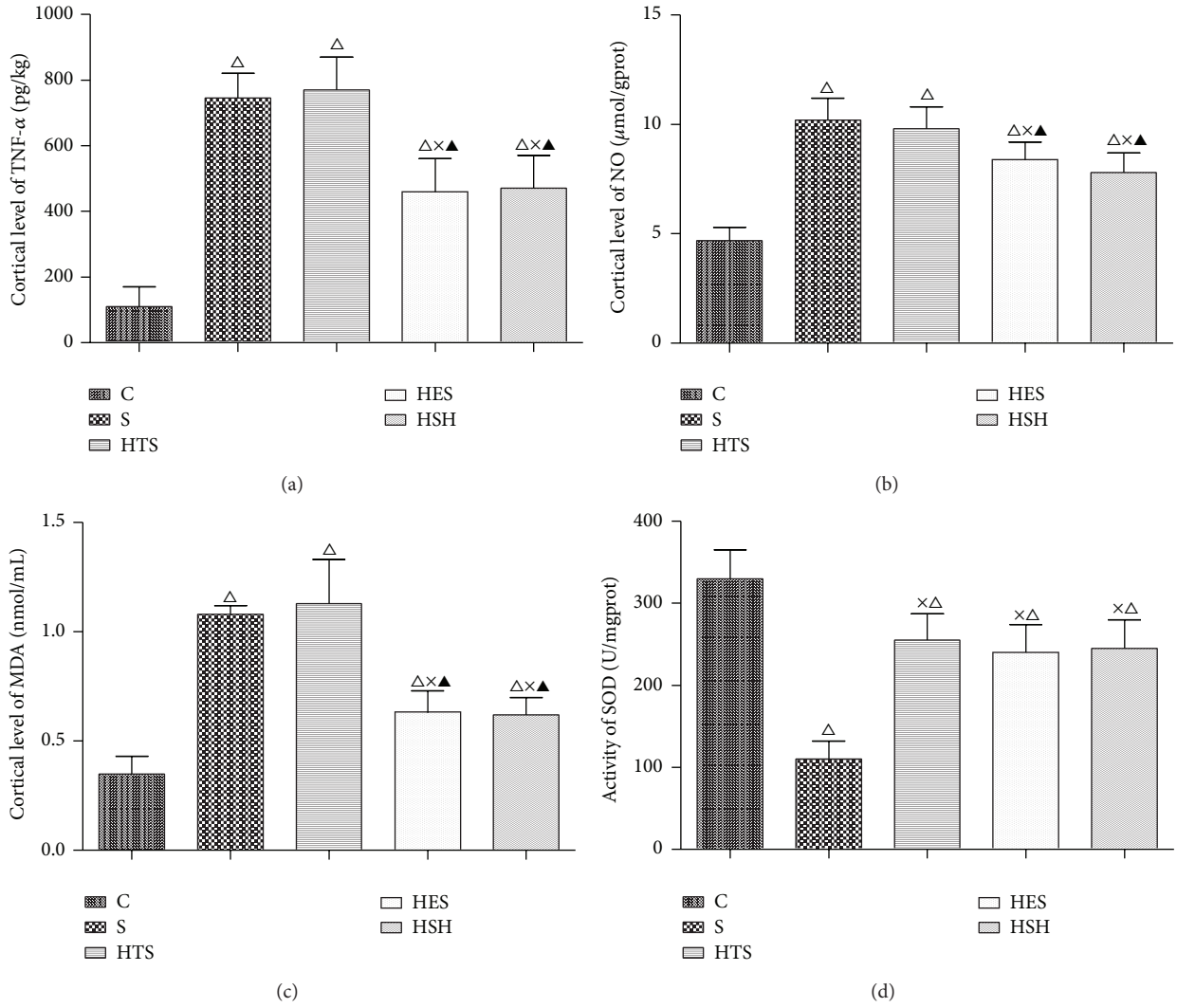

Figure 4: Variations in biochemical indexes in the different treatment groups. $^{\triangle}P \leq 0.0$, compared to group C; $^{\times}P \leq 0.05$ compared to group S; $^{\blacktriangle}P \leq 0.05$ compared to the HTS group.

to effectively maintain intravascular volume [25]. This may be the main reason why small-volume resuscitation with HES and HSH alleviates kidney injury by improving renal hemodynamics and microperfusion.

During the initial period of endotoxemia, it is the severity of the inflammatory response and oxidative stress that trigger microvascular dysfunction and early organ failure, and treatment during the first six to twenty-four hours is critical for patient outcome and survival [26–28]. In addition to cytokine storms (e.g., TNF-α, IFN-γ, and IL), NO has been increasingly recognized as a biological mediator that plays an important role in the damage process [29]. As to sepsis, both experimental and clinical investigations have revealed enhanced NO in the plasma, which correlates inversely with arterial BP [30]. Here, we analyzed alterations to the levels of TNF-α, NO, and MDA, as well as SOD activity, and found that small-volume resuscitation with HSH and HES reduced renal cortical inflammatory response and oxidative stress, while HTS did not. Several studies of fluid resuscitation have also verified that renal perfusion is closely related to local renal oxidative and inflammatory response in endotoxic and hemorrhagic shock models [31]. Based on the previous and these current results, we conclude that HSH and HES were more effective in improving renal blood flow. This was associated with decreases in renal inflammatory response and oxidative stress.

Considerable controversy exists, however, about the safety and effectiveness of using colloid solutions in critical care units. Of note, one clinical trial indicated that application of HES is associated with increased rates of renal-replacement therapy [32]. Indeed, patients in this trial repeatedly or predominantly received infusion with HES, resulting in collagen deposition in the perinephric space, contributing to the main cause of HES-associated renal injury. Similarly, another randomized controlled study found that HES provided significantly better lactate clearance and less renal injury than saline [2]. The authors concluded that resuscitation with hydroxyethyl starch improves renal function and lactate clearance in

penetrating trauma [33]. In the present study, we showed that early single resuscitation with small-volume colloids or hyperoncotic solutions could effectively alleviate renal injury and was better than the use of crystalloids. Therefore, our results provide a rationale and valuable strategy for ameliorating renal injury in the early stage of endotoxemia using resuscitation with a single small volume of colloids or hyperoncotic solutions, especially for patients complicated with heart dysfunction.

Indeed, we have several limitations in this study. The first is that we did not assess the long-term outcome of rats, including survival rate and mortality rate observation. Secondly, albumin is another kind of colloids being considered to infuse during the early resuscitation of patients with severe sepsis. In the future study, we will replenish the detected parameters and added group albumin to make the investigation more integrated.

In conclusion, our study provides the important finding that early small-volume resuscitation with single small volumes of hydroxyethyl starch 130/0.4 and hypertonic saline hydroxyethyl starch 40 leads to renal-protective effects from the damage due to LPS exposure.

Disclosure

Yan-ling Wang and Jing-hui Chen are co-first authors.

Conflict of Interests

The authors declare that there is no conflict of interests regarding the publication of this paper.

Acknowledgments

The authors thank Professor Jinghua Ou (Department of Pharmacology, Zhongshan College of Medicine, Sun Yat-sen University, Guangzhou, China) for the professional artwork and technical assistance on septic shock kidney research. This study was supported by Grants from Natural Science Foundation of China in 2011 (no. 81170449) and Guangdong Medical Research Foundation in 2014 (B2014151).

References

[1] S. Uchino, J. A. Kellum, R. Bellomo et al., "Acute renal failure in critically ill patients: a multinational, multicenter study," *The Journal of the American Medical Association*, vol. 294, no. 7, pp. 813–818, 2005.

[2] S. M. Bagshaw, S. Lapinsky, S. Dial et al., "Acute kidney injury in septic shock: clinical outcomes and impact of duration of hypotension prior to initiation of antimicrobial therapy," *Intensive Care Medicine*, vol. 35, no. 5, pp. 871–881, 2009.

[3] M. Plataki, K. Kashani, J. Cabello-Garza et al., "Predictors of Acute kidney injury in septic shock patients: an observational cohort study," *Clinical Journal of the American Society of Nephrology*, vol. 6, no. 7, pp. 1744–1751, 2011.

[4] R. W. Schrier and W. Wang, "Acute renal failure and sepsis," *The New England Journal of Medicine*, vol. 351, no. 2, pp. 159–169, 2004.

[5] J. C. Alves-Filho, B. M. Tavares-Murta, C. Barja-Fidalgo et al., "Neutrophil function in the severe sepsis," *Endocrine, Metabolic and Immune Disorders—Drug Targets*, vol. 6, no. 2, pp. 151–158, 2006.

[6] N. Li, H. Xie, L. Li et al., "Effects of honokiol on sepsis-induced acute kidney injury in an experimental model of sepsis in rats," *Inflammation*, vol. 37, no. 4, pp. 1191–1199, 2014.

[7] U. Aksu, R. Bezemer, C. Demirci, and C. Ince, "Acute effects of balanced versus unbalanced colloid resuscitation on renal macrocirculatory and microcirculatory perfusion during endotoxemic shock," *Shock*, vol. 37, no. 2, pp. 205–209, 2012.

[8] C. A. Hickey, T. J. Beattie, J. Cowieson et al., "Early volume expansion during diarrhea and relative nephroprotection during subsequent hemolytic uremic syndrome," *Archives of Pediatrics and Adolescent Medicine*, vol. 165, no. 10, pp. 884–889, 2011.

[9] G. Yu, X. Chi, Z. Hei et al., "Small volume resuscitation with 7.5% hypertonic saline, hydroxyethyl starch 130/0.4 solution and hypertonic sodium chloride hydroxyethyl starch 40 injection reduced lung injury in endotoxin shock rats: comparison with saline," *Pulmonary Pharmacology & Therapeutics*, vol. 25, no. 1, pp. 27–32, 2012.

[10] M. Albert, M.-R. Losser, D. Hayon, V. Faivre, and D. Payen, "Systemic and renal macro- and microcirculatory responses to arginine vasopressin in endotoxic rabbits," *Critical Care Medicine*, vol. 32, no. 9, pp. 1891–1898, 2004.

[11] S. Finfer, B. Liu, C. Taylor et al., "Resuscitation fluid use in critically ill adults: an international cross-sectional study in 391 intensive care units," *Critical Care*, vol. 14, no. 5, article R185, 2010.

[12] R. P. Dellinger, M. M. Levy, A. Rhodes et al., "Surviving sepsis campaign: international guidelines for management of severe sepsis and septic shock: 2012," *Critical Care Medicine*, vol. 39, no. 2, pp. 165–228, 2013.

[13] A. Dyson, R. Bezemer, M. Legrand, G. Balestra, M. Singer, and C. Ince, "Microvascular and interstitial oxygen tension in the renal cortex and medulla studied in A 4-H rat model of LPS-induced endotoxemia," *Shock*, vol. 36, no. 1, pp. 83–89, 2011.

[14] J. Pottecher, S. Deruddre, J.-L. Teboul et al., "Both passive leg raising and intravascular volume expansion improve sublingual microcirculatory perfusion in severe sepsis and septic shock patients," *Intensive Care Medicine*, vol. 36, no. 11, pp. 1867–1874, 2010.

[15] B. Rochwerg, W. Alhazzani, A. Sindi et al., "Fluid resuscitation in sepsis: a systematic review and network meta-analysis," *Annals of Internal Medicine*, vol. 161, no. 5, pp. 347–355, 2014.

[16] K. Raghunathan, A. Shaw, B. Nathanson et al., "Association between the choice of IV crystalloid and in-hospital mortality among critically ill adults with sepsis," *Critical Care Medicine*, vol. 42, no. 7, pp. 1585–1591, 2014.

[17] A. D. P. G. Garrido, R. J. Cruz Junior, L. F. Poli de Figueiredo, and M. Rocha e Silva, "Small volume of hypertonic saline as the initial fluid replacement in experimental hypodynamic sepsis," *Critical Care*, vol. 10, no. 2, p. R62, 2006.

[18] M. S. Paller, T. V. Neumann, E. Knobloch, and M. Patten, "Reactive oxygen species and rat renal epithelial cells during hypoxia and reoxygenation," *Kidney International*, vol. 40, no. 6, pp. 1041–1049, 1991.

[19] C. G. M. Millar and C. Thiemermann, "Intrarenal haemodynamics and renal dysfunction in endotoxaemia: effects of nitric oxide synthase inhibition," *British Journal of Pharmacology*, vol. 121, no. 8, pp. 1824–1830, 1997.

[20] E. Rivers, B. Nguyen, S. Havstad et al., "Early goal-directed therapy in the treatment of severe sepsis and septic shock," *The New England Journal of Medicine*, vol. 345, no. 19, pp. 1368–1377, 2001.

[21] T. Stiehl, K. Thamm, J. Kaufmann et al., "Lung-targeted RNA interference against angiopoietin-2 ameliorates multiple organ dysfunction and death in sepsis," *Critical Care Medicine*, vol. 42, no. 10, pp. e654–e662, 2014.

[22] S. Goldstein, S. Bagshaw, M. Cecconi et al., "Pharmacological management of fluid overload," *British Journal of Anaesthesia*, vol. 113, no. 5, pp. 756–763, 2014.

[23] A. Granfeldt, H. L. Letson, J. A. Hyldebrandt et al., "Small-volume 7.5% NaCl adenosine, lidocaine, and Mg^{2+} has multiple benefits during hypotensive and blood resuscitation in the pig following severe blood loss: rat to pig translation," *Critical Care Medicine*, vol. 42, no. 5, pp. e329–e344, 2014.

[24] L. Wan, N. Yang, C.-Y. Hiew et al., "An assessment of the accuracy of renal blood flow estimation by Doppler ultrasound," *Intensive Care Medicine*, vol. 34, no. 8, pp. 1503–1510, 2008.

[25] T. Haas, D. Fries, C. Holz et al., "Less impairment of hemostasis and reduced blood loss in pigs after resuscitation from hemorrhagic shock using the small-volume concept with hypertonic saline/hydroxyethyl starch as compared to administration of 4% gelatin or 6% hydroxyethyl starch solution," *Anesthesia and Analgesia*, vol. 106, no. 4, pp. 1078–1086, 2008.

[26] C. Quoilin, A. Mouithys-Mickalad, S. Lécart, M.-P. Fontaine-Aupart, and M. Hoebeke, "Evidence of oxidative stress and mitochondrial respiratory chain dysfunction in an in vitro model of sepsis-induced kidney injury," *Biochimica et Biophysica Acta*, vol. 1837, no. 10, pp. 1790–1800, 2014.

[27] E. Liverani, M. C. Rico, L. Yaratha, A. Y. Tsygankov, L. E. Kilpatrick, and S. P. Kunapuli, "LPS-induced systemic inflammation is more severe in P2Y12 null mice," *Journal of Leukocyte Biology*, vol. 95, no. 2, pp. 313–323, 2014.

[28] M. M. Levy, W. L. Macias, J.-L. Vincent et al., "Early changes in organ function predict eventual survival in severe sepsis," *Critical Care Medicine*, vol. 33, no. 10, pp. 2194–2202, 2005.

[29] O. McCook, P. Radermacher, C. Volani et al., "H_2S during circulatory shock: some unresolved questions," *Nitric Oxide: Biology and Chemistry*, vol. 41, pp. 48–61, 2014.

[30] C. Banuls, M. Rocha, S. Rovira-Llopis et al., "The pivotal role of nitric oxide: effects on the nervous and immune systems," *Current Pharmaceutical Design*, vol. 20, no. 29, pp. 4679–4689, 2014.

[31] U. Aksu, R. Bezemer, B. Yavuz, A. Kandil, C. Demirci, and C. Ince, "Balanced *vs* unbalanced crystalloid resuscitation in a near-fatal model of hemorrhagic shock and the effects on renal oxygenation, oxidative stress, and inflammation," *Resuscitation*, vol. 83, no. 6, pp. 767–773, 2012.

[32] A. Perner, N. Haase, A. B. Guttormsen et al., "Hydroxyethyl starch 130/0.42 versus Ringer's acetate in severe sepsis," *The New England Journal of Medicine*, vol. 367, no. 2, pp. 124–134, 2012.

[33] M. F. M. James, W. L. Michell, I. A. Joubert, A. J. Nicol, P. H. Navsaria, and R. S. Gillespie, "Resuscitation with hydroxyethyl starch improves renal function and lactate clearance in penetrating trauma in a randomized controlled study: the FIRST trial (Fluids in Resuscitation of Severe Trauma)," *British Journal of Anaesthesia*, vol. 107, no. 5, pp. 693–702, 2011.

Hindawi Publishing Corporation
Mediators of Inflammation
Volume 2015, Article ID 896576, 10 pages
http://dx.doi.org/10.1155/2015/896576

Research Article

Bone Components Downregulate Expression of Toll-Like Receptor 4 on the Surface of Human Monocytic U937 Cells: A Cell Model for Postfracture Immune Dysfunction

Jui-An Lin,[1,2,3] Feng-Yen Lin,[1,4] and Ta-Liang Chen[1,2,3]

[1]*Graduate Institute of Clinical Medicine, College of Medicine, Taipei Medical University, Taipei 11031, Taiwan*
[2]*Department of Anesthesiology, School of Medicine, College of Medicine, Taipei Medical University, Taipei 11031, Taiwan*
[3]*Department of Anesthesiology, Taipei Medical University Hospital, Taipei 11031, Taiwan*
[4]*Department of Internal Medicine, School of Medicine, College of Medicine, Taipei Medical University, Taipei 11031, Taiwan*

Correspondence should be addressed to Feng-Yen Lin; g870905@tmu.edu.tw and Ta-Liang Chen; tlc@tmu.edu.tw

Received 6 January 2015; Revised 17 March 2015; Accepted 2 April 2015

Academic Editor: Mashkoor A. Choudhry

To mimic the immune status of monocyte in the localized fracture region, toll-like receptor 4 (TLR4) surface expression in human monocytic U937 cells was used as the main target to assess immune dysfunction following bone component exposure. We first identified the effects of bone components (including the marrow content) on TLR4 surface expression and then examined the mechanisms underlying the changes. The level of microRNA-146a expression, an indicator of endotoxin tolerance, was also assayed. Bone component exposure downregulated TLR4 surface expression at 24 h by flow cytometry analysis, compatible with the result obtained from the membranous portion of TLR4 by western blot analysis. The cytoplasmic portion of TLR4 paradoxically increased after bone component exposure. Impaired TLR4 trafficking from the cytoplasm to the membrane was related to gp96 downregulation, as observed by western blot analysis, and this was further evidenced by gp96-TLR4 colocalization under confocal microscopy. TaqMan analysis revealed that the expression of microRNA-146a was also upregulated. This cell model demonstrated that bone component exposure downregulated TLR4 surface expression in a gp96-related manner in human monocytic U937 cells, an indicator of immunosuppression at 24 h. Immune dysfunction was further evidenced by upregulation of microRNA-146a expression at the same time point.

1. Introduction

Based on projections of economic and social development, it is estimated that, by 2030, trauma will account for one of the major disease burdens worldwide, possibly even ahead of ischemic heart disease [1]. Trauma is the leading cause of death among people aged 15 through 44 years [2, 3]. Sepsis after trauma increases the rate of organ failure and in-hospital mortality. Despite advances in trauma care and research, the incidence of posttraumatic sepsis still remained as high as 10% over the last decade [4]. The general lack of effective therapeutic options for trauma patients is mainly due to the complexity of interacting inflammatory and physiological components at multiple levels [5, 6]. Therefore, focusing on the impact of individual components helps to evaluate trauma conditions in depth.

Approximately 90% of multiple trauma patients show long-bone fractures [7] and patients dying from sepsis after trauma frequently have orthopedic injuries [8]; thus, orthopedic trauma is a major specialty in the field of trauma research. Multiple superimposed insults contribute to a complicated postfracture immune alteration, including the fracture itself and related surgery/anesthesia; soft tissue trauma and accompanying ischemia reperfusion injury; and hemorrhage and ensuing blood transfusion [9]. Besides, trauma alone accounts for a substantial proportion of genetic changes and the addition of hemorrhagic shock only increases the magnitude of the expression with relatively few extra genes

recruited [5]. Evidence shows that the fracture itself depresses both the innate and adaptive immune functions [10, 11]. As a result, a localized immune microenvironment is created [12] and the overspill of local trauma mediators may be responsible for the systemic alteration of trauma-specific cytokines [13]. An earlier study also demonstrated that the wound fluid might be the source of posttraumatic immunosuppression, which is related to mortality [14]. Monocytes predominate within the hematoma at the fracture site, and suppression of their antigen-presenting capacity is also found to be greater than that in the peripheral blood [12], indicating that monocytes might play a key role in posttraumatic immunosuppression. Furthermore, damage-associated molecular patterns, such as pathogen-recognition molecular patterns and alarmins, activate the innate immune response after trauma primarily through toll-like receptors (TLR) [15]. More than any one of the other TLR family members, TLR4 sits at the interface of microbial and sterile (such as trauma) inflammation [16] and variation within TLR4 gene is associated with severity of posttraumatic sepsis [17]. As described above, TLR4 expression of monocytes at the localized fracture site might direct the immune status in trauma patients.

A pseudofracture model developed by bone component injection into thighs has been used to help recovery of rodents from trauma for longer-term studies [18–20]. However, no specific cell model is available for in-depth investigations of related mechanisms and possible gene manipulation. We aimed to use TLR4 surface expression on bone component-treated monocytes as the target to mimic the localized post-fracture immune condition.

2. Materials and Methods

2.1. Extraction of Bone Components. The procedure for preparing bone components was modified from the pseudofracture model [18–20]. C57BL/6 male mice were sacrificed and 2 femurs and 2 tibias from the lower extremities were harvested under sterile conditions. The bones were crushed using a triturator and suspended in 2 mL of PBS. This suspension was then homogenized and also flushed through a 70 μm cell strainer (BD Biosciences, San Jose, CA, USA). The concentration of bone components was assayed using the Bradford Protein Assay Kit (Bio-Rad, Hercules, CA, USA) and stored at −80°C.

2.2. Cell Culture. U937 cells (human monocytic cell line) were obtained from the American Type Culture Collection (ATCC, Manassas, VA, USA) and grown in RPMI 1640 medium with 4.5 g/L glucose, 10 mmol/L HEPES, and 1.0 mmol/L sodium pyruvate, supplemented with 10% fetal bovine serum, 2 mM L-glutamine, and 1% antibiotic-antimycotic mixture. Cell density was maintained between 5×10^4 and 8×10^5 viable cells/mL, and the medium was replaced every 2 or 3 days.

2.3. Flow Cytometry Analysis. To examine membrane TLR4 expression on U937 cells, 1×10^5 cells were incubated with a phycoerythrin-conjugated mouse anti-human TLR4 antibody (BioLegend, San Diego, CA, USA). After the cells were washed with staining buffer (PBS containing 0.1% bovine serum albumin and 0.1% sodium azide), TLR4 expression was analyzed on a fluorescence-activated cell sorting Calibur flow cytometer (Becton Dickinson, San Jose, CA, USA).

Table 1

TLR4	Forward primer: 5′-AAGCCGAAAGGTGATTGTTG-3′
	Reverse primer: 5′-CTGTCCTCCCACTCCAGGTA-3′
GAPDH	Forward primer: 5′-TGCCCCCTCTGCTGATGCC-3′
	Reverse primer: 5′-CCTCCGACGCCTGCTTCACCAC-3′

2.4. Quantitative Real-Time Polymerase Chain Reaction. Total RNA was isolated using the TRIzol Reagent (Invitrogen, Carlsbad, CA, USA), and cDNA was synthesized according to the manufacturer's instructions. The cross-point values were calculated in the quantitative real-time polymerase chain reaction (qPCR) to detect the presence of TLR4 mRNA against glyceraldehyde-3-phosphate dehydrogenase (GAPDH) as an internal control. The PCR primers used for the amplification of TLR4 and GAPDH were as in Table 1.

2.5. Actinomycin D Chase Experiment. Actinomycin D (10 μg/mL) was added to the cells for 30 min following treatment under various experimental conditions. Total RNA was extracted at 30–360 min time points after the addition of actinomycin D, and qPCR was performed.

2.6. Western Blot Analysis. Total cell lysates were extracted from U937 cells. Proteins were separated by SDS-PAGE and transferred to a PVDF membrane. The membranes were probed with mouse anti-TLR4 (Abcam, Cambridge, MA, USA), mouse anti-β-actin (Labvision/NeoMarkers, Kalamazoo, MI, USA), goat anti-Gαs (Santa Cruz, Dallas, TX, USA), mouse anti-protein associated with toll-like receptor 4 (PRAT4A) (Abcam), or chicken antiglycoprotein 96 (gp96) (GeneTex, Irvine, CA, USA) antibodies. The proteins were visualized with an enhanced chemiluminescence detection kit (Amersham Biosciences, Pittsburgh, PA, USA). Mouse anti-β-actin (Labvision/NeoMarkers) antibody was used as a loading control. Membrane and cytosolic fractions were separated according to the protocols described previously [21] with the extract lysed in the membrane protein lysis buffer (20 mM Tris-HCl, pH 8.0, 137 mM NaCl, 10% glycerol, 1% NP-40, 2 mM EDTA, and 1 mM phenylmethylsulfonyl fluoride (PMSF)). For the membrane fraction, rabbit anti-Gαs (Abcam) antibody was used as the internal control.

2.7. Immunofluorescent Staining. Cells were fixed with 4% paraformaldehyde and quickly plated onto coverslips using a Shandon CytoSpin III Cytocentrifuge (GMI, Ramsey, MN, USA). Cell membranes were fenestrated with 0.4% Triton X-100-PBS, and nonspecific binding sites were blocked with 2% BSA-PBS-Tween 20 (0.1% v/v). Samples were stained with mouse anti-TLR4 (Abcam), mouse anti-PRAT4A (Abcam),

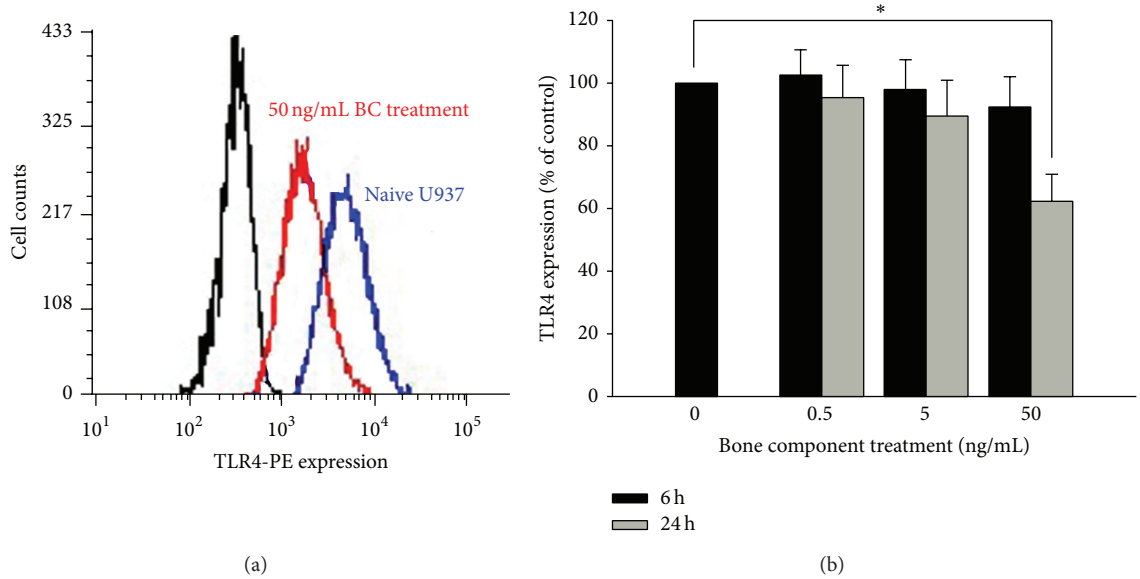

FIGURE 1: Downregulation of TLR4 surface expression by bone component (BC) exposure in U937 cells. (a) U937 cells were treated with (red graph) or without (blue graph) 50 ng/mL BC for 24 h. The TLR4 membranous portion was stained with a phycoerythrin-conjugated anti-TLR4 antibody and analyzed using flow cytometry. Negative control analyses were performed in the absence of the specific phycoerythrin-conjugated anti-TLR4 antibody (black graph). (b) U937 cells were treated with 0.5–50 ng/mL BC for 6 or 24 hrs. TLR4 levels in U937 cells were examined using flow cytometry, and the results are presented as percentages of the control. Data are presented as mean ± SEM ($n = 3$); $^*P < 0.05$ compared with the control group.

or chicken anti-gp96 (GeneTex) antibodies and were incubated with Alexa-conjugated secondary antibodies. 4′,6-Diamidino-2-phenylindole stain was used to identify the cell nuclei. All slides were examined by confocal microscopy (LSM510, ZEISS Inc., Germany).

2.8. MicroRNA Expression Analysis. The mirVana miRNA Isolation Kit (Applied Biosystems, Grand Island, NY, USA) was used to extract the small RNA; the TaqMan microRNA Reverse Transcription Kit and TaqMan MicroRNA Assay Kit (Applied Biosystems) were used to analyze the expression of microRNA-146a (miRNA-146a).

2.9. Statistical Analysis. The values are expressed as the mean ± SEM. Data were analyzed using Student's t-test. Probability values (P) < 0.05 were considered to be significant.

3. Results

To test the effect of bone component treatment on monocytic TLR4 expression, we first examined the amount of functional TLR4, that is, cell surface expression. As shown in Figure 1, bone components did not alter TLR4 surface expression until 24 h exposure, and only the higher concentration of the bone component (50 ng/mL) induced downregulation of TLR4 expression.

Downregulation of TLR4 expression may be either globally or regionally regulated. TLR4 mRNA (transcriptional level) and mRNA stability (posttranscriptional level) were not altered during the 24 h bone component exposure (Figure 2). Furthermore, total TLR4 protein expression was not affected by bone component exposure (Figure 3), thus validating the fact that regional changes in TLR4 could account for the downregulation of its surface expression. The subcellular distribution was further accessed by TLR4 protein amount. The expression of the membranous portion of the TLR4 protein decreased in cells treated with a moderately high concentration (50 ng/mL) of bone components, which was consistent with the flow cytometry result. However, the expression of the cytoplasmic portion of the TLR4 protein increased with bone component exposure as compared to the control (Figure 3), suggesting that TLR4 protein accumulation within the cytoplasm is a possible cause of decreased membranous expression. According to recent comprehensive reviews regarding the mechanisms of TLR4 localization [22, 23], trafficking from the endoplasmic reticulum to the membrane and lysosome-mediated TLR4 degradation are 2 major ways of controlling TLR4 surface expression. Figure 4(a) showed that pretreatment with high-dose lysosomal inhibitor, chloroquine, did not alter the downregulation of membranous TLR4 expression after 50 ng/mL bone component exposure, thus ruling out a protein-degradation pathway and favoring a protein-accumulation mechanism (in combination with Figure 3) to explain the bone component-mediated TLR4 downregulation. Chaperones currently known to regulate TLR4 localization and surface expression, for example, gp96 and PRAT4A [23], were examined to determine if their expressions changed with bone component exposure. We found that, unlike PRAT4A expression, gp96 expression decreased at a moderately high concentration (50 ng/mL) of bone components (Figure 4(b)). Localization of TLR4, gp96, and PRAT4A was also detected by immunofluorescence and

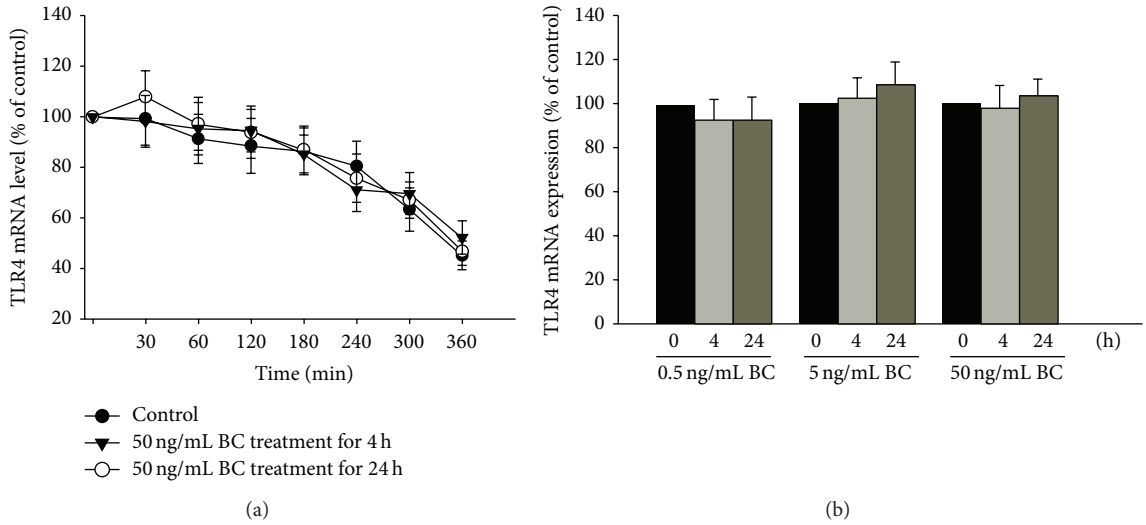

Figure 2: Regulation of TLR4 expression by bone component (BC) exposure in U937 cells not mediated by transcriptional and posttranscriptional modifications. (a) Actinomycin D chase experiment to evaluate the stability of TLR4 mRNA in 50 ng/mL BC-treated U937 cells. (b) U937 cells were treated with 0.5–50 ng/mL BC for the indicated time (4 or 24 h). TLR4 mRNA levels were analyzed by quantitative real-time PCR after normalization to GAPDH mRNA. Data are presented as mean ± SEM ($n = 3$).

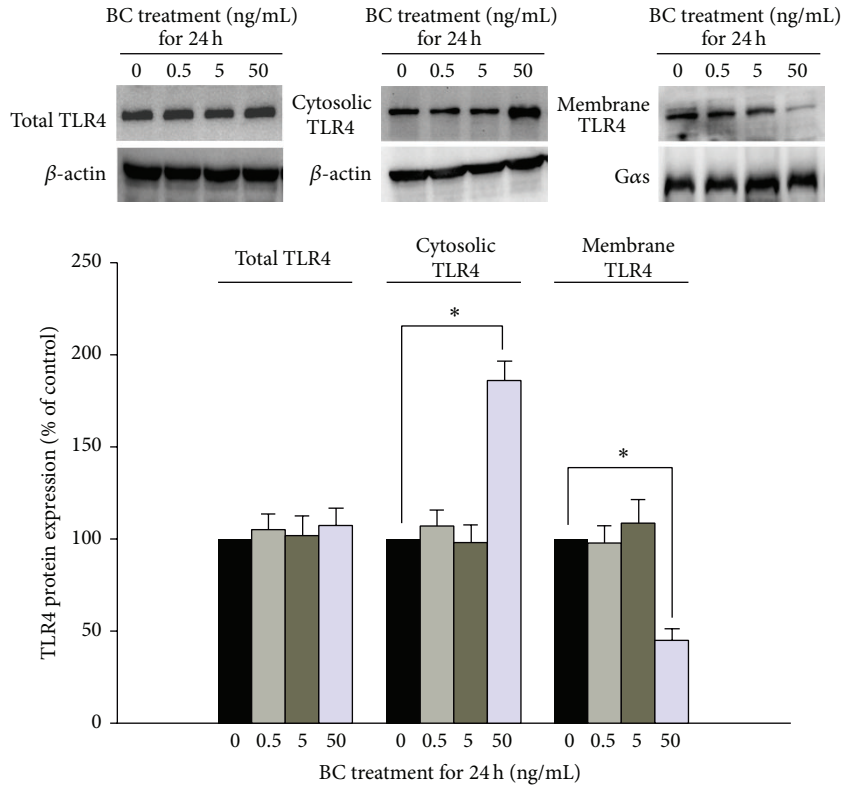

Figure 3: Alteration of subcellular distribution of TLR4 protein by bone component (BC) exposure in U937 cells. U937 cells were treated with 0.5–50 ng/mL BC for 24 hr. Total protein, cytoplasmic portion, and membranous portion of TLR4 in U937 cells were detected using western blot analysis. The β-actin and Gαs were used as an internal control. The bar diagram represents quantification of TLR4 expression in U937 cells. Data represent the results of 3 independent experiments (mean ± SEM; $^{*}P < 0.05$ between groups).

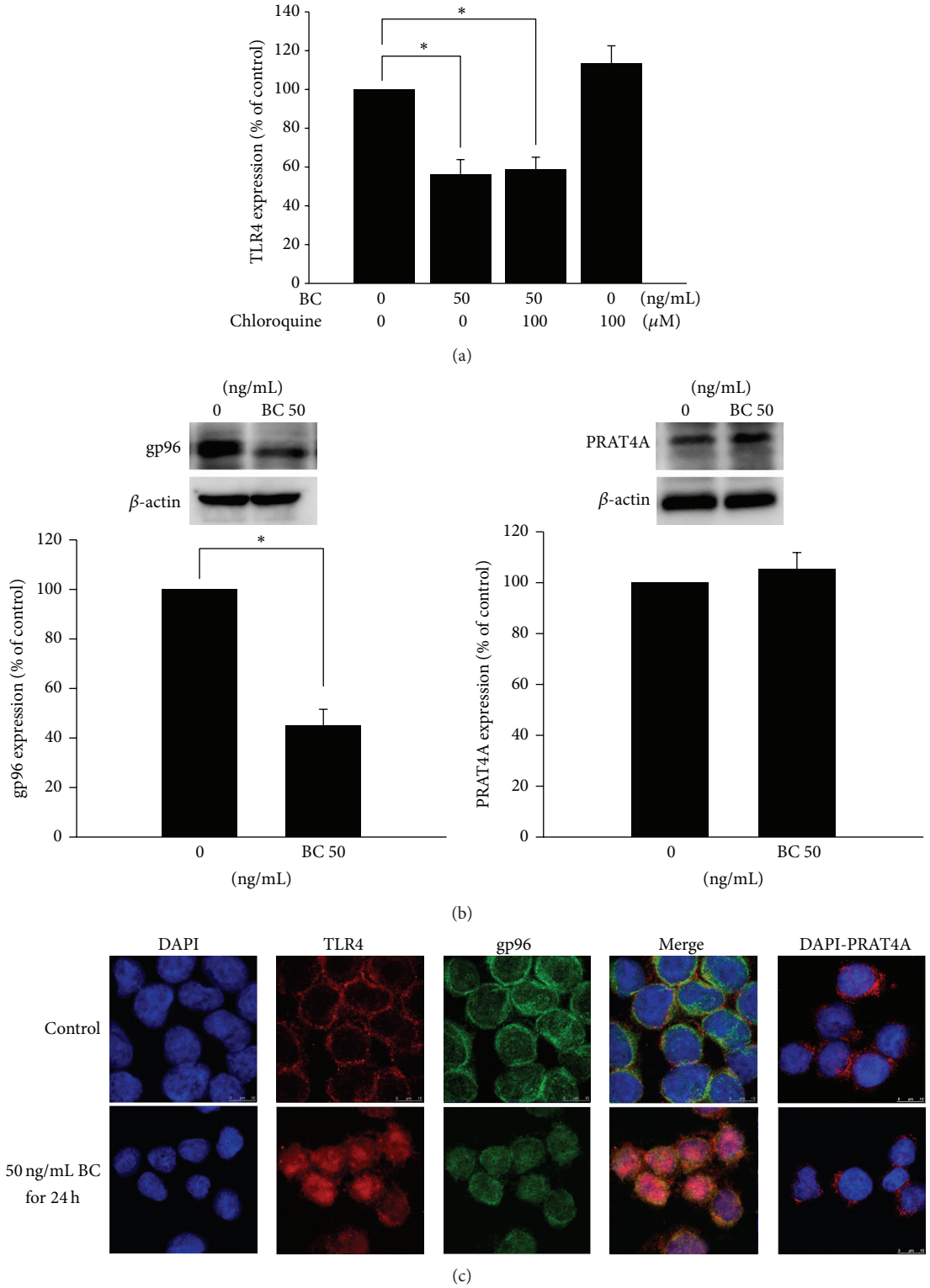

Figure 4: Involvement of glycoprotein 96 (gp96) but not protein associated with toll-like receptor 4 (PRAT4A) in the downregulation of TLR4 surface expression in U937 cells after bone component (BC) exposure. (a) U937 cells were pretreated with 100 μM chloroquine for 2 h before 50 ng/mL BC treatment for 24 h. Membranous portion of TLR4 in U937 cells was examined using flow cytometry, and results are presented as percentages of the control. Data are presented as mean ± SEM ($n = 3$); $^*P < 0.05$ compared with the control group. (b) U937 cells were treated with 50 ng/mL BC for 24 h. Cellular gp96 and PRAT4A in U937 cells were detected using western blot analysis. β-actin was used as an internal control. Data represent the results of 3 independent experiments (mean ± SEM; $^*P < 0.05$ was considered significant). (c) U937 cells were stimulated with 50 ng/mL BC for 24 h. The gp96, PRAT4A, and TLR4 proteins were identified with specific antibodies by immunofluorescence. 4′,6-Diamidino-2-phenylindole was used to characterize the nucleus. The slides were observed by confocal microscopy.

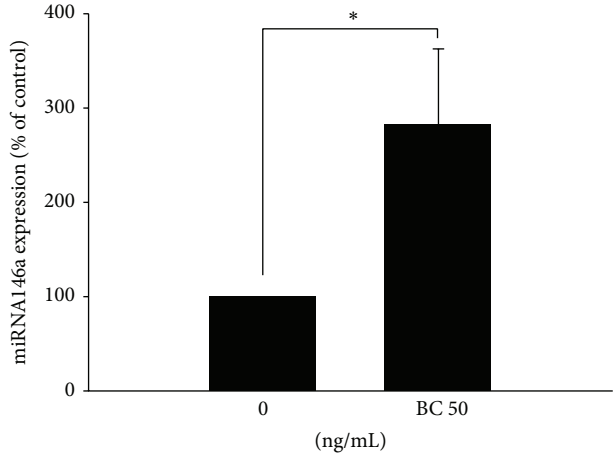

Figure 5: Upregulation of miRNA-146a expression in U937 cells after bone component (BC) exposure. U937 cells were treated with 50 ng/mL BC for 24 h. The levels of miRNA-146a in U937 cells were analyzed by quantitative real-time PCR after normalization to U6 small nuclear RNA. Data are presented as means ± SEM ($n = 4$); $^{*}P < 0.05$ compared with the control group.

observed by confocal microscopy. Impaired TLR4 trafficking from the cytoplasm to the membrane and colocalization of TLR4 with cytoplasmic gp96 were found after bone component exposure (Figure 4(c)).

After elucidating the mechanism underlying the downregulation of TLR4 surface expression, we further determined if miR-146a, the major contributing factor to endotoxin tolerance [24], was also involved in the immunosuppressive consequence in this postfracture cell model. After exposure to a moderately high concentration (50 ng/mL) of bone components, upregulation of miR-146a expression was found (Figure 5) to support the existence of endotoxin tolerance at this time point in the cell model.

4. Discussion

We successfully developed a cell model assessing the impact of bone components on the immune status of monocytes. TLR4 surface expression on human monocytes was downregulated after exposure to bone components for 24 h. After excluding the possibilities of altered transcription, posttranscriptional modification, and degradation, we found that membranous TLR4 downregulation resulted from impaired translocation from the cytoplasm to the membrane in a gp96-related manner. A negative regulator of TLR4 signaling, miR-146a, was also found to be upregulated following exposure to bone components.

As the maxim states, "to every action there is always opposed an equal reaction." A complicated manifestation of this general physics principle is found in the human body, which can mount an overreacted, an underreacted, or a balanced reaction to trauma [25]. Compensatory anti-inflammatory response syndrome is postulated to occur either in a 2-wave process after or concomitantly with systemic inflammatory response syndrome [26]. As the compensatory anti-inflammatory response syndrome predominates, trauma results in immunosuppression and increases the susceptibility to sepsis [25].

A genome-wide expression analysis regarding trauma-induced multiorgan dysfunction syndrome reveals that molecular interactions exist between monocytes and T cells, including increased expression of inhibitory costimulation receptor/ligand combinations and decreased expression of stimulatory receptor/ligand combinations between monocytes and T cells [27]. Among the various interactions, prolonged monocyte dysfunction has been proposed to initiate a cascade of septic complications [28]. A retrospective analysis carried out in trauma patients with human immunodeficiency virus infection shows that posttraumatic bacterial infection correlates only with the injury severity, not the progression severity of human immunodeficiency virus [29]. This indicates that mechanisms other than those involving $CD4^{+}$ T lymphocytes, such as the monocyte being the research target in our model, may be the leading mechanisms in posttraumatic immunosuppression. As for the choice of functional indicators in the trauma monocyte model, human leukocyte antigen- (HLA-) DR expression used to be one of them to examine the decrease of antigen-presenting capacity in the trauma setting [28]. However, conflicting results exist regarding the correlation between monocyte HLA-DR expression and trauma outcome, and *ex vivo* lipopolysaccharide- (LPS-) induced cytokine release seems to be an earlier and better predictor of patient survival than HLA-DR expression in "traumatized" monocytes [30]. Among the receptors necessary for LPS signaling of patient's monocytes, that is, TLR4 and TLR2, only TLR4 expression is selectively impaired by trauma [9]. TLR4 is also the key to sterile inflammation and remote organ dysfunction (such as postfracture acute lung injury) [19] and both immunosuppression and hyperinflammation contribute to immune dysfunction. Therefore, TLR4 is obviously the most suitable indicator of postfracture immune dysfunction. Furthermore, HLA-DR expression is deficient due to DNA hypermethylation in human monocytic U937 cells [31], which we chose as the cell to be studied in the model. As for the TLR4-mediated immune response, a cross-talk between HLA-DR and TLR4 has been reported [32]. Therefore, U937 cell may provide a naturally HLA-DR-deficient model to more specifically evaluate the effect of bone components on monocytic TLR4 surface expression. As shown in our result, bone components downregulated TLR4 expression as the concentration increased to 50 ng/mL. Both fracture-induced vessel tears and/or bone marrow leakage contribute to the fracture site hematoma, where monocytes, either from peripheral blood or bone marrow, may expose themselves to the bone components. Our results implicated that the nearer the bone components (thus the higher exposed concentration), the higher the possibility of TLR4 downregulation on the surface of monocytes. In patients with major trauma (injury severity score of 25 or more), expression of TLR4 on the surface of monocytes is more profoundly decreased (about 40% of healthy control) [9] than shown in our result. The clinical implications are twofold. First, our result demonstrated bone component

exposure alone altered TLR4 expression in the same direction as clinical setting (downregulation). Second, the extent of TLR4 downregulation might be accentuated by other factors in addition to bone component exposure because an additive or synergistic effect on immune-suppression has been proven among fracture itself, soft tissue injury, and hemorrhage [10, 11].

The timing of the investigation for posttraumatic monocyte dysfunction is a critical issue. Although, in a rabbit model, a considerable rate of apoptosis of blood monocytes and lymphocytes occurs as early as 2 h after femur fracture, apoptotic cells disappear from systemic circulation within 24 h [33]. This means that early apoptosis of monocytes might be responsible only for initiation but not for the maintenance of postfracture immunoparalysis. In the clinical scenario, the differential blood count of patients shows unchanged relative frequencies of monocytes at 6–72 h after trauma [34]. The functional state, rather than the total number of monocytes, is responsible for traumatic paralysis of the mononuclear phagocyte system and T cell commitment [35]. Immunosuppression usually occurs at 24–48 h after trauma [20, 36]. The capacity of circulating monocytes to produce intracellular cytokines *de novo* reaches a nadir at 24 h following trauma [34]. This probably addresses the precise timing of the occurrence of immunoparalysis. Functional disturbance of circulating monocytes is alleviated at 72 h following trauma [34] due to influx of newly derived monocytes [34, 37]. Furthermore, monocyte function within 24 h of hospital admission has been incorporated into formulating the outcome predictive score [38]. Therefore, "24 h" seemed to be an appropriate time point for the study of functional disturbances of the "traumatized" monocyte. Why the LPS reactivity of monocytes reaches a nadir at 24 h after trauma remains unknown [34]. None of the following immunosuppressors, including IL-10, transforming growth factor-β, β2-agonist, catecholamine and prostaglandin E2, could fully explain the specific impairment in certain monocyte responses to LPS [39]. Most studies failed to find a correlation between plasma cytokine levels and the development of organ dysfunction because of short half-lives of cytokines or their assessment in mixed blood cell cultures. Although intracellular cytokine analysis can overcome these biological drawbacks, it has not found great clinical acceptance over the years owing to its complicated work-flow [34]. Besides, impaired LPS signaling through the CD14 coreceptor cannot account for monocyte hyporesponsiveness to LPS after trauma. Altered TLR status has been proposed as an important contributor to the decreased cytokine responses observed in trauma patients [35]. Our results validated that bone component exposure for 24 h downregulated TLR4 protein expression on the surface of monocyte in a gp96-related manner. TLR4 cycles between the Golgi and the plasma membrane of human monocytes in the resting state [22]. An inverse relationship between the cytoplasmic and membranous portions of TLR4 shown by our data suggested that the bone component caused TLR4 to accumulate during transportation and fail to express normally on the cell surface. Our results demonstrated that the expression of gp96 but not PRAT4A is reduced by bone component exposure, suggesting that TLR4-MD-2 complex formation [40] rather than TLR4 glycosylation [41] might be impaired during the insult. In addition to TLR4, gp96 can also chaperone several other TLRs, including TLR2, 5, 7, and 9 [42], on which the effect of bone component exposure has not yet been examined to evidence cross-tolerance induced by bone component exposure.

In multiple trauma patients, microorganisms can enter the circulation via alterations in the gastrointestinal mucosal barrier. Of all cases of sepsis, approximately 60% are caused by gram-negative bacteria, suggesting a critical role of bacterial LPS, endotoxin, in traumatic insults [43]. *Pseudomonas aeruginosa* has been reported to be the translocating species accompanying early apoptosis of monocytes after multiple trauma [33]. Endotoxin tolerance can be induced by a wide variety of stimuli, in addition to endotoxin. Injuries, particularly multiple trauma, may also induce a state of endotoxin tolerance [44], which correlates well with trauma severity according to the monocytic response to endotoxin [43]. Our result evidenced that stimulation exclusively by the bone component itself suffices to upregulate the expression of miR-146a, a critical indicator of endotoxin tolerance [24], and the importance of bone component stimulation for the development of endotoxin tolerance in case of multiple trauma. Although endotoxin tolerance was initially thought to be a beneficial adaptive negative feedback, it may be a component of immune dysfunction complicating sepsis management. Moreover, high levels of endotoxin tolerance render them susceptible to further lethal infection [45]. It is interesting that posttraumatic immunosuppression and endotoxin tolerance share something in common. The concept of selective reprogramming rather than generalized functional suppression could be applied both in endotoxin tolerance [44] and in posttraumatic immunosuppression [9]. Both endotoxin tolerance [46] and posttraumatic immune responses [47, 48] have been shown to be independent of the TLR4 coreceptor CD14, although the TLR4 signaling pathway is altered [9, 44]. A recent review concluded that miR-146a is a negative regulator of TLR4 signaling *in vivo* and miR-146a expression parallels the level of endotoxin tolerance by regulating TLR4 downstream effectors [45]. Although there is a possibility of interaction between miR-146a and the TLR4 3′ untranslated region through cross-matching in multiple databases, our results show that bone components did not alter TLR4 mRNA stability, thus excluding the possibility of a direct action by miR-146a on the posttranscriptional modification of TLR4 mRNA expression.

Several limitations exist. Bone components were harvested from mice, not humans. Although monocytes treated with samples from human long-bone fracture sites best simulate human conditions, our model was developed according to the recently validated pseudofracture animal model [18–20], which facilitates laboratory research and animal model translation at the cellular level. Bone component solutions provided in our model were not separated into 3 parts (bone marrow cells, bone marrow supernatant, and bone suspension), because each part has been shown to cause a significant systemic inflammatory response after injection into rodent thighs [19]. In clinical situations, all 3 parts would be exposed to the injured site. The pseudofracture animal model was

also developed based on the mixed bone component solution, instead of the individual component, to more adequately mimic the true fracture condition [20]. Current knowledge about the mixed bone component solution did not provide enough evidence for us to find out the key factor. Despite subdividing the mixed bone component solution into individual bone component for the study, the authors who invented the bone component solution ended up concluding that multiple cell types and ligands account for TLR4-related immune responses because of the diverse composition of the exposed bone components [19]. They also suggested that the better way to maintain homeostasis is to target it at the level of TLR4 receptor [19]. Therefore, in the present study, we used TLR4 expression as the target to evaluate the effect of mixed bone component solution on its alteration mechanisms, including transcription, posttranscriptional modification, and protein degradation as well as protein trafficking and found that gp96 took part in the mechanism regarding bone component-interfered TLR4 trafficking.

In conclusion, our cell model provides solid evidence of monocyte dysfunction by downregulation of TLR4 surface expression and upregulation of miR-146a following bone component exposure. Several applications and clinical implications exist. Firstly, manipulation of TLR4 trafficking by chaperones has been proposed as a possible medical treatment for septic shock [23], such as gp96 in the case of long-bone fracture. To further identify the gp96-related pathway mediating bone component-induced TLR4 distribution, TLR4-MD-2 association assay should be examined in this model. Secondly, *in vivo* regulation of miR-146a expression is currently possible [49, 50] and future therapeutic strategies could be aimed at fine-tuning miR-146a expression during a high-tolerance state to avoid an overwhelming secondary infection [45]. Cause-effect relationship between TLR4 downregulation and miR-146a upregulation can be further elucidated by gene manipulation. Moreover, based on our model, direction of monocyte differentiation as well as monocyte-T cell interaction following bone component exposure could also be examined to delineate the complicated trauma cascade step by step. This cell model could be reasonably utilized to bridge the pseudofracture animal model because bone components are prepared in the same way from the same source.

Conflict of Interests

The authors declare no conflict of interests.

Acknowledgments

This work was supported by the Grant from Taipei Medical University Hospital (99TMU-TMUH-09) and Ministry of Science and Technology, Taiwan (MOST 103-2314-B-038-036-).

References

[1] C. D. Mathers and D. Loncar, "Projections of global mortality and burden of disease from 2002 to 2030," *PLoS Medicine*, vol. 3, no. 11, article e442, 2006.

[2] E. G. Krug, G. K. Sharma, and R. Lozano, "The global burden of injuries," *American Journal of Public Health*, vol. 90, no. 4, pp. 523–526, 2000.

[3] World Health Organization, *Injury: A Leading Cause of the Global Burden of Disease*, World Health Organization, Geneva, Switzerland, 2000, http://whqlibdoc.who.int/publications/2002/9241562323.pdf.

[4] A. Wafaisade, R. Lefering, B. Bouillon et al., "Epidemiology and risk factors of sepsis after multiple trauma: an analysis of 29,829 patients from the Trauma Registry of the German Society for Trauma Surgery," *Critical Care Medicine*, vol. 39, no. 4, pp. 621–628, 2011.

[5] C. E. Lagoa, J. Bartels, A. Baratt et al., "The role of initial trauma in the host's response to injury and hemorrhage: insights from a correlation of mathematical simulations and hepatic transcriptomic analysis," *Shock*, vol. 26, no. 6, pp. 592–600, 2006.

[6] A. J. E. Seely and N. V. Christou, "Multiple organ dysfunction syndrome: exploring the paradigm of complex nonlinear systems," *Critical Care Medicine*, vol. 28, no. 7, pp. 2193–2200, 2000.

[7] E. Faist, A. E. Baue, H. Dittmer, and G. Heberer, "Multiple organ failure in polytrauma patients," *The Journal of Trauma*, vol. 23, no. 9, pp. 775–787, 1983.

[8] C. C. Baker, L. Oppenheimer, B. Stephens, F. R. Lewis, and D. D. Trunkey, "Epidemiology of trauma deaths," *The American Journal of Surgery*, vol. 140, no. 1, pp. 144–150, 1980.

[9] M. Adib-Conquy, P. Moine, K. Asehnoune et al., "Toll-like receptor-mediated tumor necrosis factor and interleukin-10 production differ during systemic inflammation," *American Journal of Respiratory and Critical Care Medicine*, vol. 168, no. 2, pp. 158–164, 2003.

[10] M. W. Wichmann, R. Zellweger, C. M. DeMaso, A. Ayala, C. Williams, and I. H. Chaudry, "Immune function is more compromised after closed bone fracture and hemorrhagic shock than hemorrhage alone," *Archives of Surgery*, vol. 131, no. 9, pp. 995–1000, 1996.

[11] M. W. Wichmann, A. Ayala, and I. H. Chaudry, "Severe depression of host immune functions following closed-bone fracture, soft-tissue trauma, and hemorrhagic shock," *Critical Care Medicine*, vol. 26, no. 8, pp. 1372–1378, 1998.

[12] C. J. Hauser, X. Zhou, P. Joshi et al., "The immune microenvironment of human fracture/soft-tissue hematomas and its relationship to systemic immunity," *The Journal of Trauma—Injury, Infection and Critical Care*, vol. 42, no. 5, pp. 895–904, 1997.

[13] M. Perl, F. Gebhard, M. W. Knöferl et al., "The pattern of preformed cytokines in tissues frequently affected by blunt trauma," *Shock*, vol. 19, no. 4, pp. 299–304, 2003.

[14] S. A. Lazarou, A. Barbul, H. L. Wasserkrug, and G. Efron, "The wound is a possible source of posttraumatic immunosuppression," *Archives of Surgery*, vol. 124, no. 12, pp. 1429–1431, 1989.

[15] P. F. Stahel, W. R. Smith, and E. E. Moore, "Role of biological modifiers regulating the immune response after trauma," *Injury*, vol. 38, no. 12, pp. 1409–1422, 2007.

[16] K. P. Mollen, R. J. Anand, A. Tsung, J. M. Prince, R. M. Levy, and T. R. Billiar, "Emerging paradigm: toll-like receptor 4—sentinel for the detection of tissue damage," *Shock*, vol. 26, no. 5, pp. 430–437, 2006.

[17] S. Shalhub, C. E. Junker, S. D. Imahara, M. N. Mindrinos, S. Dissanaike, and G. E. O'Keefe, "Variation in the TLR4 gene influences the risk of organ failure and shock posttrauma: a cohort

study," *The Journal of Trauma—Injury, Infection, and Critical Care*, vol. 66, no. 1, pp. 115–123, 2009.

[18] S. S. Darwiche, P. Kobbe, R. Pfeifer, L. Kohut, H.-C. Pape, and T. Billiar, "Pseudofracture: an acute peripheral tissue trauma model," *Journal of Visualized Experiments*, no. 50, Article ID e2074, 2011.

[19] P. Kobbe, D. J. Kaczorowski, Y. Vodovotz et al., "Local exposure of bone components to injured soft tissue induces Toll-like receptor 4-dependent systemic inflammation with acute lung injury," *Shock*, vol. 30, no. 6, pp. 686–691, 2008.

[20] C. L. Menzel, R. Pfeifer, S. S. Darwiche et al., "Models of lower extremity damage in mice: time course of organ damage and immune response," *The Journal of Surgical Research*, vol. 166, no. 2, pp. e149–e156, 2011.

[21] K. R. Smith, L. R. Klei, and A. Barchowsky, "Arsenite stimulates plasma membrane NADPH oxidase in vascular endothelial cells," *American Journal of Physiology—Lung Cellular and Molecular Physiology*, vol. 280, no. 3, pp. L442–L449, 2001.

[22] A. F. McGettrick and L. A. O'Neill, "Localisation and trafficking of Toll-like receptors: an important mode of regulation," *Current Opinion in Immunology*, vol. 22, no. 1, pp. 20–27, 2010.

[23] S.-I. Saitoh, "Chaperones and transport proteins regulate TLR4 trafficking and activation," *Immunobiology*, vol. 214, no. 7, pp. 594–600, 2009.

[24] M. A. Nahid, K. M. Pauley, M. Satoh, and E. K. L. Chan, "miR-146a is critical for endotoxin-induced tolerance: implication in innate immunity," *The Journal of Biological Chemistry*, vol. 284, no. 50, pp. 34590–34599, 2009.

[25] R. C. Bone, "Sir Isaac Newton, sepsis, SIRS, and CARS," *Critical Care Medicine*, vol. 24, no. 7, pp. 1125–1128, 1996.

[26] M. Adib-Conquy and J.-M. Cavaillon, "Compensatory anti-inflammatory response syndrome," *Thrombosis and Haemostasis*, vol. 101, no. 1, pp. 36–47, 2009.

[27] K. Laudanski, C. Miller-Graziano, W. Xiao et al., "Cell-specific expression and pathway analyses reveal alterations in trauma-related human T cell and monocyte pathways," *Proceedings of the National Academy of Sciences of the United States of America*, vol. 103, no. 42, pp. 15564–15569, 2006.

[28] S. K. Tschoeke and W. Ertel, "Immunoparalysis after multiple trauma," *Injury*, vol. 38, no. 12, pp. 1346–1357, 2007.

[29] A. A. Guth, S. R. Hofstetter, and H. L. Pachter, "Human immunodeficiency virus and the trauma patient: factors influencing postoperative infectious complications," *The Journal of Trauma—Injury, Infection and Critical Care*, vol. 41, no. 2, pp. 251–256, 1996.

[30] M. Ploder, L. Pelinka, C. Schmuckenschlager et al., "Lipopolysaccharide-induced tumor necrosis factor α production and not monocyte human leukocyte antigen-DR expression is correlated with survival in septic trauma patients," *Shock*, vol. 25, no. 2, pp. 129–134, 2006.

[31] B. M. Peterlin, T. A. Gonwa, and J. D. Stobo, "Expression of HLA-DR by a human monocyte cell line is under transcriptional control," *The Journal of Molecular and Cellular Immunology*, vol. 1, no. 3, pp. 191–200, 1984.

[32] X. Liu, Z. Zhan, D. Li et al., "Intracellular MHC class II molecules promote TLR-triggered innate immune responses by maintaining activation of the kinase Btk," *Nature Immunology*, vol. 12, no. 5, pp. 416–424, 2011.

[33] N. Efstathopoulos, T. Tsaganos, E. J. Giamarellos-Bourboulis et al., "Early apoptosis of monocytes contributes to the pathogenesis of systemic inflammatory response and of bacterial translocation in an experimental model of multiple trauma," *Clinical and Experimental Immunology*, vol. 145, no. 1, pp. 139–146, 2006.

[34] C. Kirchhoff, P. Biberthaler, W. E. Mutschler, E. Faist, M. Jochum, and S. Zedler, "Early down-regulation of the pro-inflammatory potential of monocytes is correlated to organ dysfunction in patients after severe multiple injury: a cohort study," *Critical Care*, vol. 13, no. 3, article R88, 2009.

[35] Z. Spolarics, M. Siddiqi, J. H. Siegel et al., "Depressed interleukin-12-producing activity by monocytes correlates with adverse clinical course and a shift toward Th2-type lymphocyte pattern in severely injured male trauma patients," *Critical Care Medicine*, vol. 31, no. 6, pp. 1722–1729, 2003.

[36] M. J. Cohen, K. Brohi, C. S. Calfee et al., "Early release of high mobility group box nuclear protein 1 after severe trauma in humans: role of injury severity and tissue hypoperfusion," *Critical Care*, vol. 13, no. 6, article R174, 2009.

[37] R. B. Johnston Jr., "Current concepts: immunology. Monocytes and macrophages," *The New England Journal of Medicine*, vol. 318, no. 12, pp. 747–752, 1988.

[38] W. G. Cheadle, M. Mercer-Jones, M. Heinzelmann, and H. C. Polk Jr., "Sepsis and septic complications in the surgical patient: Who is at risk?" *Shock*, vol. 6, supplement 1, pp. S6–S9, 1996.

[39] J. E. Wang, M. K. Dahle, and A. O. Aasen, "Impaired monocyte Toll-like receptor-4 signaling in trauma and sepsis: is SIGIRR the answer?" *Critical Care Medicine*, vol. 34, no. 9, pp. 2498–2500, 2006.

[40] F. Randow and B. Seed, "Endoplasmic reticulum chaperone gp96 is required for innate immunity but not cell viability," *Nature Cell Biology*, vol. 3, no. 10, pp. 891–896, 2001.

[41] K. Takahashi, T. Shibata, S. Akashi-Takamura et al., "A protein associated with Toll-like receptor (TLR) 4 (PRAT4A) is required for TLR-dependent immune responses," *The Journal of Experimental Medicine*, vol. 204, no. 12, pp. 2963–2976, 2007.

[42] Y. Yang, B. Liu, J. Dai et al., "Heat shock protein gp96 is a master chaperone for toll-like receptors and is important in the innate function of macrophages," *Immunity*, vol. 26, no. 2, pp. 215–226, 2007.

[43] S. Wutzler, M. Maier, M. Lehnert et al., "Suppression and recovery of LPS-stimulated monocyte activity after trauma is correlated with increasing injury severity: a prospective clinical study," *The Journal of Trauma—Injury, Infection, and Critical Care*, vol. 66, no. 5, pp. 1273–1280, 2009.

[44] M. A. West and W. Heagy, "Endotoxin tolerance: a review," *Critical Care Medicine*, vol. 30, no. 1, pp. S64–S73, 2002.

[45] E. M. Quinn, J. H. Wang, and H. P. Redmond, "The emerging role of microRNA in regulation of endotoxin tolerance," *Journal of Leukocyte Biology*, vol. 91, no. 5, pp. 721–727, 2012.

[46] W. Heagy, C. Hansen, K. Nieman, and M. A. West, "Evidence for a CD14- and serum-independent pathway in the induction of endotoxin-tolerance in human monocytes and THP-1 monocytic cells," *Shock*, vol. 19, no. 4, pp. 321–327, 2003.

[47] J. M. Prince, R. M. Levy, R. Yang et al., "Toll-Like receptor-4 signaling mediates hepatic injury and systemic inflammation in hemorrhagic shock," *Journal of the American College of Surgeons*, vol. 202, no. 3, pp. 407–417, 2006.

[48] R. M. Levy, J. M. Prince, R. Yang et al., "Systemic inflammation and remote organ damage following bilateral femur fracture requires Toll-like receptor 4," *American Journal of Physiology-Regulatory Integrative and Comparative Physiology*, vol. 291, no. 4, pp. R970–R976, 2006.

[49] J. Krützfeldt, N. Rajewsky, R. Braich et al., "Silencing of microRNAs in vivo with 'antagomirs'," *Nature*, vol. 438, no. 7068, pp. 685–689, 2005.

[50] C. Schmelzer, M. Kitano, G. Rimbach et al., "Effects of ubiquinol-10 on microRNA-146a expression in vitro and in vivo," *Mediators of Inflammation*, vol. 2009, Article ID 415437, 7 pages, 2009.

Hindawi Publishing Corporation
Mediators of Inflammation
Volume 2015, Article ID 614518, 9 pages
http://dx.doi.org/10.1155/2015/614518

Research Article

Origin of Circulating Free DNA in Sepsis: Analysis of the CLP Mouse Model

Shigeto Hamaguchi,[1,2] Yukihiro Akeda,[2] Norihisa Yamamoto,[1,2] Masafumi Seki,[1] Kouji Yamamoto,[3] Kazunori Oishi,[2,4] and Kazunori Tomono[1]

[1] *Division of Infection Control and Prevention, Osaka University Graduate School of Medicine, Osaka 565-0871, Japan*
[2] *International Research Center for Infectious Diseases, Research Institute for Microbial Diseases, Osaka University, Osaka 565-0871, Japan*
[3] *Department of Clinical Epidemiology and Biostatistics, Osaka University Graduate School of Medicine, Osaka 565-0871, Japan*
[4] *Infectious Disease Surveillance Center, National Institute of Infectious Diseases, Tokyo 162-8640, Japan*

Correspondence should be addressed to Kazunori Tomono; tomono@hp-infect.med.osaka-u.ac.jp

Received 25 September 2014; Revised 2 January 2015; Accepted 20 January 2015

Academic Editor: Mashkoor A. Choudhry

Recently, it has been reported that circulating free DNA (cf-DNA) in the blood is increased in various infectious diseases, including sepsis. Moreover, a relationship between cf-DNA and neutrophil extracellular traps (NETs) has been suggested. However, it is still unclear what the source and physiological role of cf-DNA in sepsis are. In this study, we examined the source of cf-DNA by detecting citrullinated histone H3, a characteristic feature of NET formation, in cecal ligation and puncture- (CLP-)operated mice. In addition, neutrophil depletion using anti-Ly6G antibodies was performed to assess the association between neutrophils and cf-DNA. Increased cf-DNA levels were observed only in CLP mice and not in the control groups; the qPCR findings revealed that the cf-DNA was mainly host-derived, even in bacteremic conditions. Citrullinated histone H3 was not increased in the neutrophils upon CLP, and the depletion of neutrophils showed limited effects on decreasing the amount of cf-DNA. Taken together, these results suggested that elevated cf-DNA levels during early-phase sepsis may represent a candidate biomarker for the severity of sepsis and that, contrary to previous findings, cf-DNA is not derived from neutrophils or NETs.

1. Introduction

Sepsis is an emergency condition associated with significant mortality and excessive inflammation [1–5]. Sepsis caused by bacteremia arises from the host response to infection. Currently, the diagnosis of sepsis caused by bacteremia relies on culture-based pathogen detection and physiological criteria, including changes in the body temperature and heart/respiration rates. While these clinical diagnostic criteria are simple and clear, novel sepsis biomarkers that can lead to a more reliable early diagnosis and therapeutic decision-making are urgently needed. Until now, a number of molecules have been proposed as candidate sepsis biomarkers; however, there are currently few useful predictive biomarkers for the severity and prognosis of sepsis available in clinical practice [6].

Recently, it was reported that the circulating free DNA (cf-DNA) levels in the blood are increased in various infectious diseases, including sepsis [7, 8]. Accordingly, cf-DNA has been suggested as a potential predictive biomarker for several different conditions, including cancer and injury [9, 10]; moreover, one study of sepsis patients reported that greatly elevated plasma DNA and nucleosome levels (>800 ng/mL) were associated with a poorer outcome [7].

Furthermore, recent studies have reported that cf-DNA is associated with neutrophil extracellular traps (NETs) [7, 8, 10]. NETs were first reported as a novel innate immune mechanism of neutrophils in 2004 [11]. These are fibrous mesh-like structures that can rapidly trap and kill microbial pathogens [12]. In activated neutrophils, a mixture of chromosomal DNA and intracellular contents is extruded to the extracellular space as a fibrous structure upon a variety

of proinflammatory stimuli [13–15]. Moreover, citrullinated histone H3 has been reported as a characteristic molecule involved in NET formation *in vitro*, with citrullination of histone H3 by peptidylarginine deiminase 4 playing a pivotal role in chromatin decondensation during "NETosis" [15, 16]. In terms of the contribution of NETs to the host defense, it has been reported that depletion of NETs can lead to hypersusceptibility to polymicrobial sepsis in mice [17]. Taken together, these previous findings suggest a potential relationship between cf-DNA and NETs in various aspects. However, it should be noted that most of the previous studies on cf-DNA were conducted using only human samples, and whether cf-DNA is indeed derived from NETs remains unclear.

In this study, using a mouse cecal ligation and puncture (CLP) sepsis model, we confirmed the elevation of the cf-DNA levels during sepsis and investigated whether the source of this cf-DNA was neutrophils, with particular focus on the NETs, or not.

2. Materials and Methods

2.1. Cecal Ligation and Puncture (CLP) Mouse Model. The CLP model for polymicrobial sepsis developed by Chaudry et al. [18] was established as previously described [19], with some modifications. In brief, 7-8-week-old C57BL/6J mice were used for the CLP operation; these were housed under specific pathogen-free conditions with free access to standard rodent food and water. We used five C57BL/6J mice per group for each experiment, except for the experiment shown in Figure 2(a), for which 13 mice in each group were used. Under general anesthesia, midline laparotomy was performed and the cecum was exposed and ligated distal to the ileocecal valve to prevent bowel obstruction, and the distal part of the cecum was punctured with a 22-gauge needle. A small amount of cecal content was manually extruded from the punctured cecum into the abdominal cavity. In all studies, after returning the cecum into the abdomen, 1 mL of phosphate-buffered saline (PBS) for fluid resuscitation was administered to create a more clinically relevant sepsis model as the standard care for human operations. The abdomen was closed using a single-layer technique. The sham mice were treated identically as the operated mice with the exception of the ligation and puncture of the gut. Under these conditions, all CLP mice showed signs of severe illness within 24 hours after the operation and high lethality after 48 hours. Further, treatment-naïve mice were included as additional controls for some experiments. All animal experiments were conducted in accordance with the Institutional Animal Care and Use Committee Guidelines of Osaka University.

2.2. Measurement of Plasma cf-DNA Amount. Whole blood was collected from each mouse by cardiac puncture under anesthesia and transferred into ethylenediaminetetraacetic acid-2Na tubes. The plasma was separated by centrifugation at 800 g for 10 minutes and immediately frozen at −80°C.

In order to explore the dynamics of cf-DNA under septic conditions, plasma was collected at 6 and 24 hours after the CLP operation from all mice, and the amount of cf-DNA in the plasma at each time point was quantified directly using the Quant-iT PicoGreen dsDNA Quantification Reagent Kit (Molecular Probes, Leiden, The Netherlands) and a fluorescence microplate reader (SH-9000 Lab, Hitachi High-Technologies, Tokyo, Japan) according to the manufacturers' instructions. PicoGreen specifically binds dsDNA, and after excitation at 485 nm, the dsDNA/PicoGreen fluorescence complex can be detected at 538 nm [20].

2.3. Measurement of Plasma Interleukin-6 (IL-6). The plasma IL-6 levels were measured by enzyme-linked immunosorbent assay (Quantikine mouse IL-6 immunoassay kit; R&D Systems, Wiesbaden, Germany) according to the manufacturer's instructions.

2.4. Counting the Numbers of Bacteria. Bacteremia in the CLP mouse model was confirmed through analysis of whole blood immediately obtained by cardiac puncture. The local bacterial load in the CLP mice was determined by 10-fold serial dilution to a maximum of 10^8. All samples were plated on sheep blood agar plates and incubated overnight at 37°C under aerobic conditions. The numbers of bacteria were determined by manual counting of the colonies on the plates.

2.5. Measurement of Bacterial/Host-Derived DNA. DNA was purified from the mouse plasma using the QIAamp Blood DNA Midi Kit (Qiagen, Venlo, The Netherlands) in accordance with the manufacturer's instructions. To quantify the estimated amount of DNA in the plasma, 16S rDNA and mouse β-2-microglobulin (B2M) were selected as representative targets of bacterial DNA and mouse-derived DNA, respectively, and TaqMan quantitative polymerase chain reaction (qPCR) assay of the purified DNA was subsequently performed using an ABI 7900HT real-time PCR machine (Applied Biosystems, Foster City, CA, USA). Amplification of each target was performed using the KAPA SYBR fast qPCR kit (Kapa Biosystems, Inc., Woburn, MA, USA) with the following primers: 16S-forward primer (1055f: 5′-ATGGCTGTCGTCAGCT-3′), 16S-reverse primer (1392r: 5′-ACGGGCGGTGTGTAC-3′), B2M-forward primer (B2M exon4-F; 5′-CTTTTGGTAAAGCAAAGAGGCC-3′), and B2M-reverse primer (B2M exon4-R; 5′-TTGGGGGTGAGAATTGCTAAG-3′) [21]. The reaction mixture (8 μL) contained 5 μL of KAPA SYBR qPCR Master Mix, 0.2 μL of distilled water, 0.4 μL of each 5 μM primer, and 2 μL of sample DNA. PCR was performed at 95°C for 60 seconds, followed by 40 cycles of 95°C for 15 seconds, 60°C for 60 seconds, and final extension at 72°C for 15 seconds. The results were analyzed using SDS 2.3 software (Applied Biosystems). A standard curve was determined based on the concentration gradient of the purified DNA from mouse whole blood for mice B2M and the purified DNA from *Streptococcus pneumoniae* for 16S rDNA.

2.6. Blood Cell Counting and Isolation of Neutrophils from Mice. For each mouse, 20 μL of blood was analyzed to count the number of white blood cells (WBCs) using the Celltac hematology analyzer (MEK-6308; Nihon Kohden, Tokyo, Japan).

For neutrophil isolation, blood was collected from each mouse followed by separation with centrifugation for 20 minutes at 800 g using Histopaque-1119 (Sigma-Aldrich, St. Louis, MO, USA). The neutrophil-rich phase was collected, washed in PBS, and separated by discontinuous density-gradient centrifugation in Percoll (GE Healthcare, Buckinghamshire, UK), as previously described [22]. Subsequently, the neutrophils were collected from the 70–75% layer of the Percoll gradient and washed with PBS; after hypotonic lysis with 0.2% and 1.6% NaCl solutions to remove residual erythrocytes, the cells were resuspended in RPMI-1640 (Invitrogen, Waltham, MA, USA). Purity and viability were routinely assessed using Diff-Quik stain (Sysmex, Kobe, Japan) and trypan blue stain (Wako Pure Chemical Industries, Osaka, Japan), respectively, under a microscope.

2.7. Detection of Citrullinated Histone H3 as a NET Marker. For flow cytometric analyses, isolated neutrophils were fixed in 2% paraformaldehyde for 5 minutes and washed three times in PBS with 3% fetal bovine serum (FBS). Intracellular citrullinated histone H3 staining was carried out as follows: fixed neutrophils were incubated (10^6 cells/mL) in RPMI-1640 (Sigma-Aldrich) with 1% FBS for 30 minutes in the presence of 0.5% saponin. After washing with PBS, the cells were incubated with Alexa488-conjugated rabbit citrullinated histone H3 antibody (ab5103; Abcam, Cambridge, UK) using the Alexa Fluor 488 Monoclonal Antibody Labeling Kit (Invitrogen) or isotype control antibody (sc-45068; Santa Cruz Biotechnology Inc., Santa Cruz, CA, USA) for 20 minutes and then washed in PBS with 3% FBS. The cells were analyzed using fluorescence-activated cell sorting (FACS) Calibur with CellQuest software (BD Biosciences, San Jose, CA, USA).

For western blotting, cell lysates of Percoll gradient-purified neutrophils were subjected to SDS-PAGE and transferred to a PVDF membrane blocked with Can Get Signal blocking buffer (TOYOBO, Osaka, Japan) and incubated with goat polyclonal anti-histone H3 antibody (ab5103, Abcam; 1 : 1000 in tris-buffered saline-Tween 20 [TBST]) or rabbit polyclonal anti-citrullinated histone H3 antibody (ab12079; Abcam; 1 : 1000 in TBST) for 1 hour at room temperature. The proteins were detected upon incubation with horseradish peroxidase-conjugated anti-goat or anti-rabbit IgG (1 : 10,000) for 15 minutes using ECL Western Blotting Reagent (GE Healthcare).

2.8. Neutrophil Depletion In Vivo. Ly6G-specific monoclonal antibody was used to specifically deplete neutrophils in the mice [23]. The mice were intraperitoneally injected with 1 mg of isotype control rat IgG or rat monoclonal anti-Ly6G antibody (1A8; BioXCell, Lebanon, NH, USA) 2 days before and on the day of CLP operation. After neutrophil depletion, the mice were operated for CLP or sham operation. Subsequently, the mice were sacrificed and the whole blood and intraperitoneal wash from each mouse were subjected to cell counting at 6 and 24 hours after the operation. Neutrophil depletion was confirmed by morphology using Diff-Quik stain and by cell counts using the Celltac hematology analyzer.

2.9. Statistical Analysis. Statistical analyses were performed using GraphPad Prism (version 5.02; GraphPad Software, San Diego, CA, USA). All data are presented as mean ± standard deviation. Data obtained from multiple groups were tested using the nonparametric Kruskal-Wallis test followed by post hoc Dunn's multiple comparison tests. Data were considered to be statistically significant at $P < 0.05$. In the Figures 1, 2, and 4, statistical significance is indicated by asterisks.

3. Results

3.1. Establishment of Septic Condition in CLP Mice. For each experiment, CLP or sham operation was performed in five C57BL/6J mice each, and blood samples were collected at 6 and 24 hours after the operation. In the CLP mice, the plasma IL-6 levels were found to be increased 6 and 24 hours after CLP. In contrast, plasma obtained from the sham-operated mice and naïve mice contained extremely low levels of IL-6 (Figure 1(a)). Likewise, no local bacterial load was detected from any of the blood cultures from these mice. On the other hand, for the CLP mice, 2 out of 5 blood cultures were positive at 6 hours, and these contained approximately 1×10^2 CFU/mL; at 24 hours, all samples (5/5) were positive for bacterial growth (approximately 1×10^5 CFU/mL; Figure 1(b)). These results confirmed that CLP mice at 6 and 24 hours after CLP operation are under septic conditions [17] and can be used as a septic model for further analyses.

3.2. Dynamics of cf-DNA under Septic Conditions in CLP Mice. The amount of cf-DNA gradually increased at 6 hours after the CLP operation and peaked at 24 hours. In contrast, the cf-DNA levels were not elevated in the sham-operated mice and naïve mice (Figure 2(a)). Significant differences between the CLP and sham groups were observed at each time point. As the elevation of the cf-DNA amount may have been caused by bacteremia, the origin of the cf-DNA was determined by qPCR of the plasma cf-DNA using organism-specific primers (mouse B2M and bacterial 16S rDNA) [24]. The amount of 16S rDNA was slightly increased in the plasma from the CLP group at 6 hours after CLP (Figure 2(b)), whereas the amount of B2M was significantly increased in the plasma from the CLP group at 6 and 24 hours after CLP (Figure 2(c)). Similar increments in the amount of B2M were observed in each CLP group, with the amount of 16S rDNA being only approximately 1% of that of mouse B2M at each time point. These results suggested that, even under septic conditions, the cf-DNA was mainly derived from the host cells.

3.3. Association between Neutrophils and Serum cf-DNA Elevation under Septic Conditions. It has been proposed that neutrophils contribute to the elevation of cf-DNA in the blood; however, it has not been demonstrated whether neutrophils, or more precisely NETs, correlate with increased cf-DNA levels under septic conditions. Recently, it was reported that citrullinated histone H3 represents a likely hallmark of NET formation via peptidylarginine deiminase 4. To test this hypothesis, whole blood was collected from the CLP mice, and the neutrophils were isolated and subjected to western blotting and FACS analysis using anti-citrullinated histone

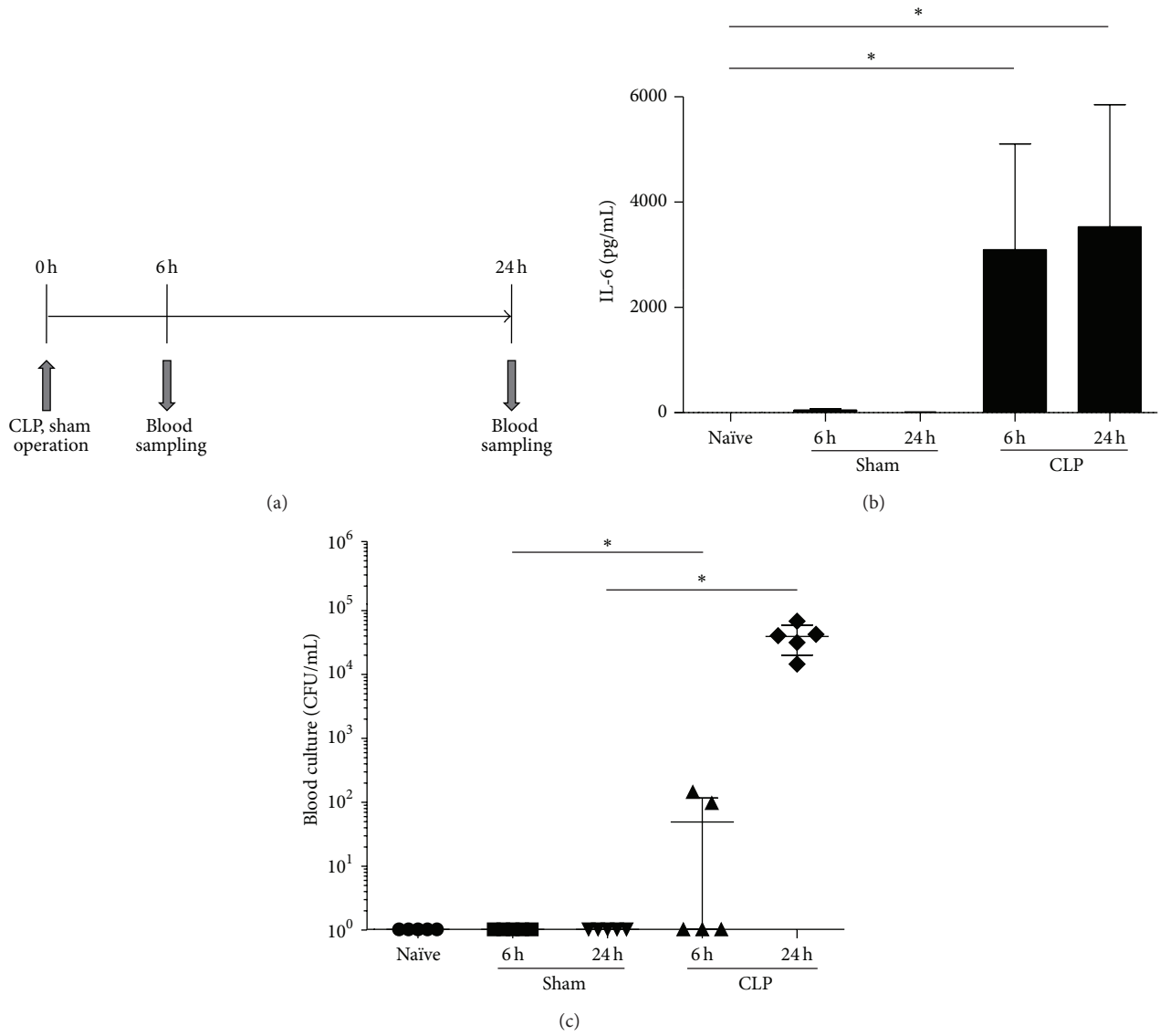

Figure 1: Establishment of sepsis in the cecal ligation and puncture (CLP) mice. (a) Plasma levels of interleukin-6 (IL-6) at 6 and 24 hours after CLP or sham operation. (b) Bacterial counts of the blood culture at 6 and 24 hours after CLP or sham operation. Five mice from each group were used for each experiment. The error bars represent the mean ± standard deviation; $^*P < 0.05$.

H3 as a NET marker. Compared with the neutrophils of naïve mice, minimal differences in terms of the size of the anti-citrullinated histone H3 antibody bands were observed upon western blotting (Figure 3(a)). Similarly, FACS analysis also revealed no shifts of the fluorescent peaks of citrullinated histone H3 between sham-operated and CLP mice as compared with naïve mice (Figure 3(b)).

3.4. Dynamics of cf-DNA in Neutrophil-Depleted Mice. To assess the involvement of neutrophils, the neutrophils were depleted by injection of anti-Ly6G antibodies [23]. When the anti-Ly6G antibody was injected to the sham-operated group, their WBC numbers in the blood decreased, with less than 2% neutrophils observed in the WBC at 6 and 24 hours by Diff-Quik stain of the blood smear, confirming successful depletion of neutrophils. Using the same protocol of neutrophil depletion, the neutrophil-depleted CLP-operated mice showed significantly lower numbers of WBCs in the blood than those of the sham-operated mice. However, the CLP-operated group treated with the control antibody showed similar low numbers of WBCs in the blood, which may have resulted from the consumption of the WBCs in the circulation at inflammation sites under septic condition (Figure 4(a)). On the other hand, the WBC counts in the ascites from the CLP-operated group with neutrophil depletion showed lower cell counts than those of the CLP-operated group treated with the control antibody (Figure 4(b)). Along with the WBC counts, the bacterial load was also examined and indicated that neutrophil depletion had no effect on the bacterial load in the blood and ascites with versus without

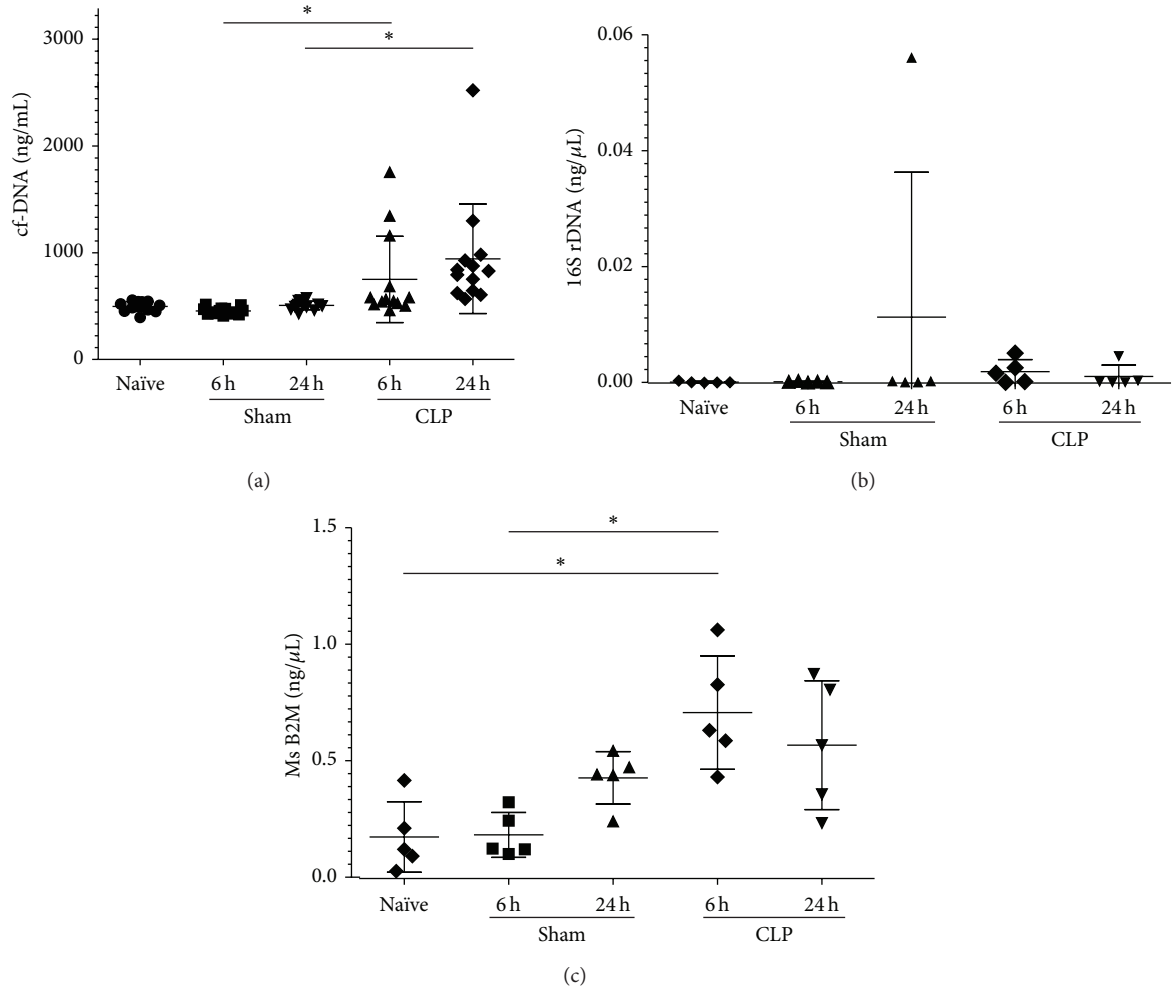

Figure 2: Dynamics of circulating free (cf) DNA and quantification of host-derived and bacteria-derived cf-DNA. (a) Amount of cf-DNA in the plasma at 6 and 24 hours after cecal ligation and puncture (CLP) or sham operation (n = 13 mice per group). (b) Amount of bacteria-derived DNA, quantified based on 16s rDNA by quantitative real-time polymerase chain reaction (PCR) (n = 5 mice per group). (c) Amount of host-derived DNA, quantified based on mouse beta-2-microgloblin by quantitative real-time PCR (n = 5 mice per group).

neutrophils (Figures 4(c) and 4(d)). Finally, the amount of cf-DNA in each group was measured and revealed that the neutrophil depletion did not affect the amount of cf-DNA in the blood under septic conditions (Figure 4(e)). Taken together, these results suggested that the increasing levels of cf-DNA in the blood under septic conditions were derived from host cells other than neutrophils, which have been reported as a likely source of cf-DNA by NET formation.

4. Discussion

The presence of abnormally high levels of cf-DNA in the plasma of patients with malignant diseases was first described in the 1970s [18]. However, it is only recently that cf-DNA has attracted attention in terms of its potential use as a diagnostic or prognostic marker [6, 9].

In this study, *in vivo* experiments using a CLP mouse model of sepsis showed that the cf-DNA levels increased in a time-dependent manner after the onset of sepsis (Figure 2(a)). This finding confirmed the conclusion of previous clinical studies reporting that cf-DNA correlated with the severity of the clinical outcome of sepsis [7, 8]. cf-DNA is found in many pathophysiological conditions, including infection and cancer [7, 9, 25–27]. These conditions generally involve apoptosis and/or necrosis; therefore, it is reasonable to consider apoptosis and necrosis as sources for the presence of cf-DNA [28]. To date, cf-DNA has been evaluated primarily as a biomarker of septic condition, whereas the potential function of cf-DNA has not been investigated in detail. Our results indicate that the sepsis model used in this study, the CLP mouse model, is sufficient as an evaluation model for cf-DNA.

As another important result, we found that the increase in cf-DNA in CLP mice contained mostly host cf-DNA and only negligibly amounts of bacterial DNA. This finding suggests that the cf-DNA was mainly derived from the host

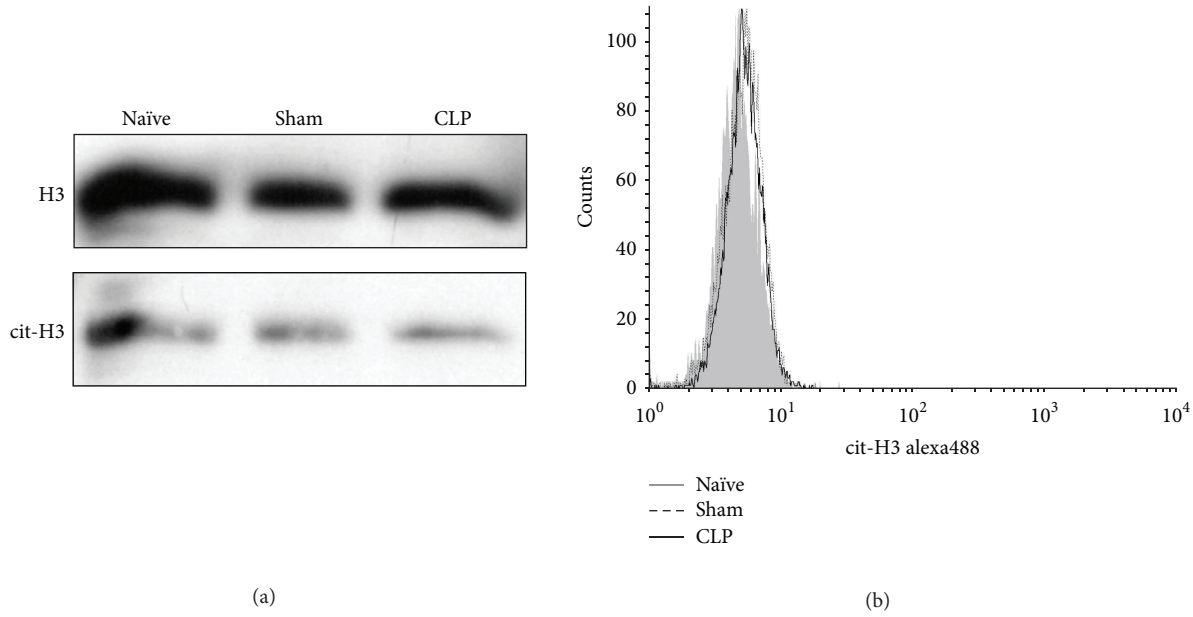

Figure 3: Involvement of citrullinated histone H3 in sepsis. (a) Western blot analysis of histone H3 and citrullinated histone H3 after cecal ligation and puncture (CLP) or sham operation. (b) Flow cytometric analysis of citrullinated histone H3 after CLP or sham operation. The samples were collected from a single mouse from each group, and the experiments were repeated at least three times.

cells even under septic/bacteremic conditions. Further, our study investigated whether NET formation occurred during sepsis in our model, using citrullination of histone H3, a known NET marker. Interestingly, two independent experiments (western blotting and FACS analysis) showed that citrullinated histone H3 was barely increased under septic conditions. As mentioned, citrullinated histone H3 has been reported as a characteristic feature of NET formation and has been specifically implicated in the decondensation of the nucleus [16, 29]. Therefore, our results suggested that, under septic conditions, the increase of cf-DNA might not be derived from the NETs produced by neutrophils, but rather from other types of host cells. Although the relationship between citrullinated histone H3 and NET formation was recently demonstrated *in vitro*, it has been suggested that the presence of citrullinated histone H3 is not an ultimate prerequisite for the formation of NETs within individual neutrophils and the absence of an increase in the amount of citrullinated histone H3 in neutrophils observed in the present study implies a lack of involvement of NETs in cf-DNA production under *in vivo* septic conditions. Although we originally hypothesized that neutrophils were the main source of cf-DNA, as the citrullination of histone did not increase even under septic conditions, this hypothesis was refuted. Additionally, our hypothesis was also refuted by the results of the neutrophil depletion. Previously, our group observed the presence of NETs in circulating blood under systemic inflammatory response syndrome conditions, including sepsis, using fluorescent immunohistochemical analysis of blood smears [30], and several other studies have reported similar findings, hence suggesting a potential relationship between NETs and cf-DNA [7, 8, 10, 17]. Therefore, the results acquired in the present study were surprising for us, as we expected that the cf-DNA would comprise mainly NET-derived DNA. The exact mechanism of cf-DNA production in the blood is still not understood; although our experiments did not reveal the cells of cf-DNA origin, our findings do indicate that NETs do not participate in the production of cf-DNA, at least not under severe bacteremic conditions. This discrepancy in terms of the source of cf-DNA will need to be examined and confirmed by further experiments in the future.

Nonetheless, we speculate that a potential source of cf-DNA might be necrotic tissue or apoptotic cells at the infection site, or, more specifically, endothelial cells. In fact, a relationship between cf-DNA and plasma levels of typical cellular apoptotic markers has been described in lung cancer patients [31]. Moreover, an association between NET-related endothelial damage and platelets has also been described [32].

To study the innate immune mechanisms, host-derived and bacterial DNA must be distinguished. In addition to citrullinated histone H3 used in this study, other mechanisms to accurately recognize host DNA, including NETs, such as detection of specific proteins like Toll-like receptor-9 or detection of ds-DNA or the CpG motif, may prove useful in future experiments. In innate immune mechanism, it is strictly controlled to distinguish between host-derived DNA and bacterial DNA. It would be possible to find out another unknown mechanism to recognize host DNA including NETs by specific protein such as cit-H3, besides Toll-like receptor-9 to detect ds-DNA of CpG motif.

From our results and those of the previous reports on the topic, we believe that cf-DNA shows potential as a noninvasive, useful biomarker of sepsis and bacteremia.

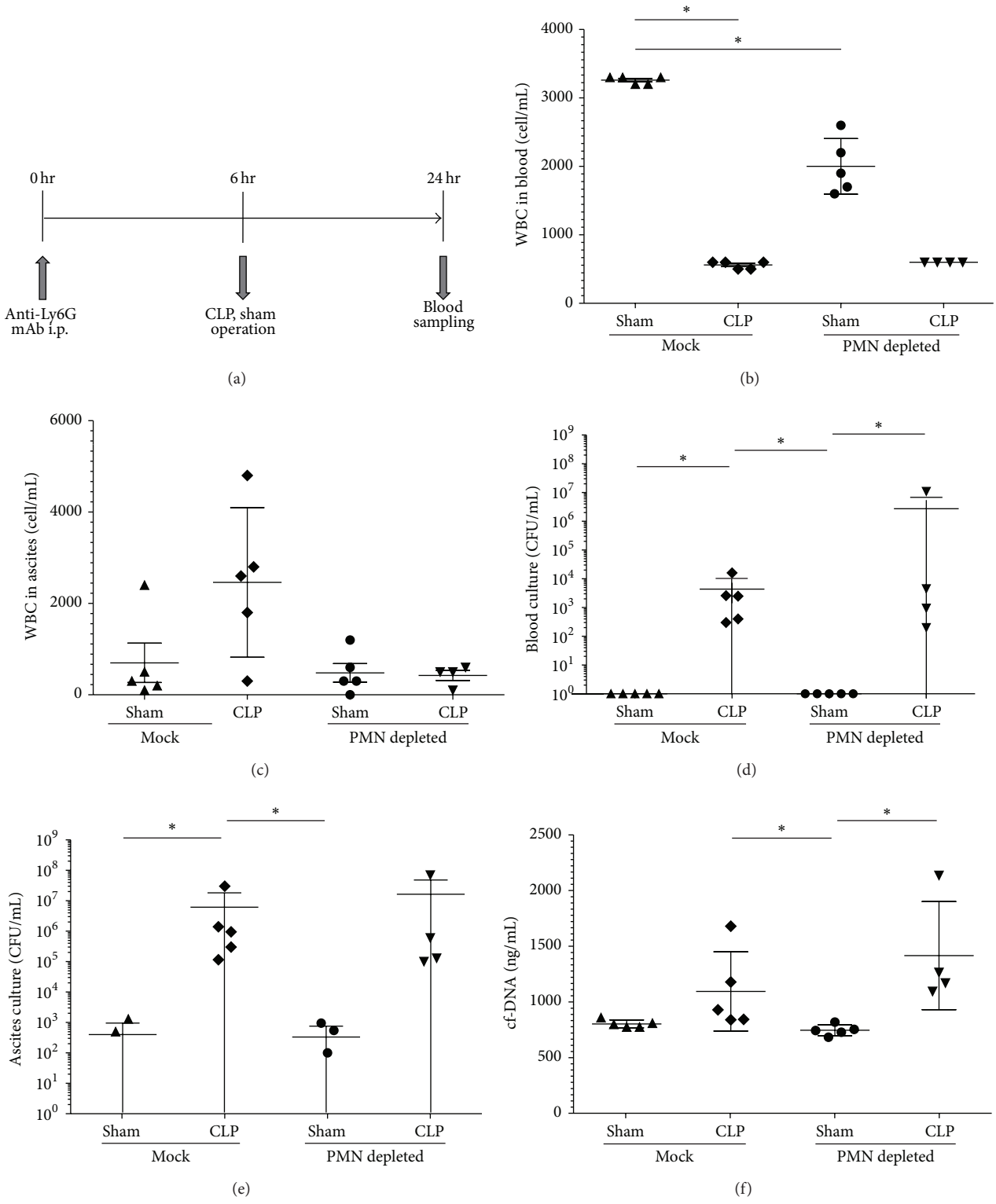

Figure 4: Effect of neutrophil depletion on circulating free (cf) DNA. (a), (b) White blood cell number in (a) the blood and (b) ascites at 24 hours after the operation, with or without neutrophil depletion. (c), (d) Bacterial count of (c) the blood and (d) ascites cultures at 24 hours after the operation, with or without neutrophil depletion. (e) Amount of cf-DNA in the plasma at 24 hours after cecal ligation and puncture (CLP) or sham operation, with or without neutrophil depletion. Five mice from each group were used for each experiment.

However, the significance of cf-DNA under sepsis has not yet been fully investigated. Our experiments indicated that the CLP mouse model is a promising model for studying the significance of cf-DNA. In the future, using this model along with different animal models of sepsis, the mechanism of cf-DNA production should be clarified to confirm the utility of cf-DNA as a biomarker for sepsis, and clinical research on the relationship between cf-DNA and clinical manifestations should be performed.

5. Conclusion

In conclusion, our study using CLP mice revealed that the cf-DNA levels were elevated in the early phase of septic condition, implying a potential of cf-DNA to reflect the severity of sepsis and indicating its usefulness as a biomarker for the early detection of septic conditions. Unexpectedly, under septic conditions, it was moreover observed that cf-DNA was not derived from NETs produced by neutrophils, but mainly from host cells other than neutrophils. We hypothesize that the main source of cf-DNA might be dead tissue particles, such as necrotic cells. This may change the pathophysiological concept of cf-DNA formation during sepsis, at least in part, and further studies are needed to confirm this hypothesis.

Conflict of Interests

The authors declare that they have no financial or nonfinancial competing interests.

References

[1] M. M. Levy, A. Artigas, G. S. Phillips et al., "Outcomes of the Surviving Sepsis Campaign in intensive care units in the USA and Europe: a prospective cohort study," *The Lancet Infectious Diseases*, vol. 12, no. 12, pp. 919–924, 2012.

[2] B. D. Winters, M. Eberlein, J. Leung, D. M. Needham, P. J. Pronovost, and J. E. Sevransky, "Long-term mortality and quality of life in sepsis: a systematic review," *Critical Care Medicine*, vol. 38, no. 5, pp. 1276–1283, 2010.

[3] T. M. Perl, L. Dvorak, T. Hwang, and R. P. Wenzel, "Long-term survival and function after suspected gram-negative sepsis," *Journal of the American Medical Association*, vol. 274, no. 4, pp. 338–345, 1995.

[4] R. P. Dellinger, M. M. Levy, J. M. Carlet et al., "Surviving sepsis campaign: international guidelines for management of severe sepsis and septic shock: 2008," *Critical Care Medicine*, vol. 36, no. 1, pp. 296–327, 2008.

[5] T. van der Poll and S. M. Opal, "Host-pathogen interactions in sepsis," *The Lancet Infectious Diseases*, vol. 8, no. 1, pp. 32–43, 2008.

[6] K. Reinhart, M. Bauer, N. C. Riedemann, and C. S. Hartog, "New approaches to sepsis: molecular diagnostics and biomarkers," *Clinical Microbiology Reviews*, vol. 25, no. 4, pp. 609–634, 2012.

[7] S. Margraf, T. Lögters, J. Reipen, J. Altrichter, M. Scholz, and J. Windolf, "Neutrophil-derived circulating free DNA (CF-DNA/NETs): a potential prognostic marker for posttraumatic development of inflammatory second hit and sepsis," *Shock*, vol. 30, no. 4, pp. 352–358, 2008.

[8] T. Lögters, A. Paunel-Görgülü, C. Zilkens et al., "Diagnostic accuracy of neutrophil-derived circulating free DNA (cf-DNA/NETs) for septic arthritis," *Journal of Orthopaedic Research*, vol. 27, no. 11, pp. 1401–1407, 2009.

[9] V. Swarup and M. R. Rajeswari, "Circulating (cell-free) nucleic acids—a promising, non-invasive tool for early detection of several human diseases," *FEBS Letters*, vol. 581, no. 5, pp. 795–799, 2007.

[10] J. Altrichter, S. Zedler, R. Kraft et al., "Neutrophil-derived circulating free DNA (cf-DNA/NETs), a potential prognostic marker for mortality in patients with severe burn injury," *European Journal of Trauma and Emergency Surgery*, vol. 36, no. 6, pp. 551–557, 2010.

[11] V. Brinkmann, U. Reichard, C. Goosmann et al., "Neutrophil extracellular traps kill bacteria," *Science*, vol. 303, no. 5663, pp. 1532–1535, 2004.

[12] T. Lögters, S. Margraf, J. Altrichter et al., "The clinical value of neutrophil extracellular traps," *Medical Microbiology and Immunology*, vol. 198, no. 4, pp. 211–219, 2009.

[13] C. F. Urban, U. Reichard, V. Brinkmann, and A. Zychlinsky, "Neutrophil extracellular traps capture and kill *Candida albicans* and hyphal forms," *Cellular Microbiology*, vol. 8, no. 4, pp. 668–676, 2006.

[14] T. A. Fuchs, U. Abed, C. Goosmann et al., "Novel cell death program leads to neutrophil extracellular traps," *Journal of Cell Biology*, vol. 176, no. 2, pp. 231–241, 2007.

[15] Q. Remijsen, T. W. Kuijpers, E. Wirawan, S. Lippens, P. Vandenabeele, and T. V. Berghe, "Dying for a cause: NETosis, mechanisms behind an antimicrobial cell death modality," *Cell Death and Differentiation*, vol. 18, no. 4, pp. 581–588, 2011.

[16] I. Neeli, S. N. Khan, and M. Radic, "Histone deimination as a response to inflammatory stimuli in neutrophils," *The Journal of Immunology*, vol. 180, no. 3, pp. 1895–1902, 2008.

[17] W. Meng, A. Paunel-Görgülü, S. Flohé et al., "Depletion of neutrophil extracellular traps in vivo results in hypersusceptibility to polymicrobial sepsis in mice," *Critical Care*, vol. 16, no. 4, article R137, 2012.

[18] I. H. Chaudry, K. A. Wichterman, and A. E. Baue, "Effect of sepsis on tissue adenine nucleotide levels," *Surgery*, vol. 85, no. 2, pp. 205–211, 1979.

[19] J. T. Muenzer, C. G. Davis, B. S. Dunne, J. Unsinger, W. M. Dunne, and R. S. Hotchkiss, "Pneumonia after cecal ligation and puncture: a clinically relevant 'two-hit' model of sepsis," *Shock*, vol. 26, no. 6, pp. 565–570, 2006.

[20] X. Y. Xue, M. D. Teare, I. Holen, Y. M. Zhu, and P. J. Woll, "Optimizing the yield and utility of circulating cell-free DNA from plasma and serum," *Clinica Chimica Acta*, vol. 404, no. 2, pp. 100–104, 2009.

[21] G. Harms, A. C. Layton, H. M. Dionisi et al., "Real-time PCR quantification of nitrifying bacteria in a municipal wastewater treatment plant," *Environmental Science and Technology*, vol. 37, no. 2, pp. 343–351, 2003.

[22] V. Brinkmann, B. Laube, U. Abu Abed, C. Goosmann, and A. Zychlinsky, "Neutrophil extracellular traps: how to generate and visualize them," *Journal of Visualized Experiments*, no. 36, Article ID e1724, 2010.

[23] J. M. Daley, A. A. Thomay, M. D. Connolly, J. S. Reichner, and J. E. Albina, "Use of Ly6G-specific monoclonal antibody to deplete neutrophils in mice," *Journal of Leukocyte Biology*, vol. 83, no. 1, pp. 64–70, 2008.

[24] P. C. Y. Woo, S. K. P. Lau, J. L. L. Teng, H. Tse, and K.-Y. Yuen, "Then and now: use of 16S rDNA gene sequencing for bacterial identification and discovery of novel bacteria in clinical microbiology laboratories," *Clinical Microbiology and Infection*, vol. 14, no. 10, pp. 908–934, 2008.

[25] G. Sozzi, D. Conte, M. Leon et al., "Quantification of free circulating DNA as a diagnostic marker in lung cancer," *Journal of Clinical Oncology*, vol. 21, no. 21, pp. 3902–3908, 2003.

[26] A. A. Kamat, F. Z. Bischoff, D. Dang et al., "Circulating cell-free DNA: a novel biomarker for response to therapy in ovarian carcinoma," *Cancer Biology & Therapy*, vol. 5, no. 10, pp. 1369–1374, 2006.

[27] S. Breitbach, S. Tug, and P. Simon, "Circulating cell-free DNA: an up-coming molecular marker in exercise physiology," *Sports Medicine*, vol. 42, no. 7, pp. 565–586, 2012.

[28] K. Jung, M. Fleischhacker, and A. Rabien, "Cell-free DNA in the blood as a solid tumor biomarker—a critical appraisal of the literature," *Clinica Chimica Acta*, vol. 411, no. 21-22, pp. 1611–1624, 2010.

[29] Y. Wang, M. Li, S. Stadler et al., "Histone hypercitrullination mediates chromatin decondensation and neutrophil extracellular trap formation," *Journal of Cell Biology*, vol. 184, no. 2, pp. 205–213, 2009.

[30] S. Hamaguchi, T. Hirose, Y. Akeda et al., "Identification of neutrophil extracellular traps in the blood of patients with systemic inflammatory response syndrome," *Journal of International Medical Research*, vol. 41, no. 1, pp. 162–168, 2013.

[31] G. J. Fournié, J.-P. Courtin, F. Laval et al., "Plasma DNA as a marker of cancerous cell death. Investigations in patients suffering from lung cancer and in nude mice bearing human tumours," *Cancer Letters*, vol. 91, no. 2, pp. 221–227, 1995.

[32] S. R. Clark, A. C. Ma, S. A. Tavener et al., "Platelet TLR4 activates neutrophil extracellular traps to ensnare bacteria in septic blood," *Nature Medicine*, vol. 13, no. 4, pp. 463–469, 2007.

Hindawi Publishing Corporation
Mediators of Inflammation
Volume 2015, Article ID 918361, 9 pages
http://dx.doi.org/10.1155/2015/918361

Research Article

Dexmedetomidine Ameliorate CLP-Induced Rat Intestinal Injury via Inhibition of Inflammation

Yanqing Chen, Liyan Miao, Yusheng Yao, Weilan Wu, Xiaodan Wu, Cansheng Gong, Liangcheng Qiu, and Jianping Chen

Department of Anesthesiology, Fujian Provincial Hospital and The Shengli Medical Clinical College of Fujian Medical University, Fuzhou 350001, China

Correspondence should be addressed to Yanqing Chen; fjslyys@gmail.com

Received 7 January 2015; Accepted 28 February 2015

Academic Editor: Huang-Ping Yu

The aim was to verify that dexmedetomidine (DEX) can attenuate CLP-induced intestinal injury via inhibition of inflammation. Male Sprague-Dawley (SD) rats were randomly allocated into Sham group and the other three CLP model groups, in terms of different treatments: placebo, DEX, and yohimbine plus DEX (DEX + YOH) groups. Pathology examination was conducted with HE stain. To identify differences among groups, the levels of DAO, and D-lactate in serum were measured by spectrophotometry, and the levels of TNF-α, IL-1β, and IL-6 in serum and organ were measured by ELISA. The expressions of occludin and TLR4 in tissue were detected by Western blot. The survival rate of an additional group of animals within 7 d was recorded. In DEX group, mortality was lower, histology change was minor, DAO, and D-lactate levels were reduced, and occludin expression was increased; the expressions of TNF-α, IL-1β, IL-6, and TLR4 were also decreased in DEX group. These results indicated that acute intestinal injury induced by CLP was mitigated by DEX treatment. However, these effects of DEX were significantly attenuated by yohimbine in DEX + YOH group. Our study indicated the protective effects of DEX on CLP-induced injury, which may be associated with the inhibition of inflammation via modulating TLR4 pathway and can be blocked by yohimbine.

1. Introduction

Sepsis, characterized by hyperinflammatory state, was complex and devastating, which can lead to catastrophic effects. Despite the fact that progressions were made in diagnosis and treatment of these patients, the morbidity and mortality of rates of sepsis remained constantly high, up to 50% [1–3]. Excessive synthesis of proinflammatory cytokine induced by severe sepsis causes damage to vital organs, including intestine [4, 5].

Among the immune system in human body, intestinal mucosa served as key protective barrier, of which the dysfunction with accompanying bacterial translocation can be fatal to sepsis patients for the associated systemic inflammatory response and consequent impairments of the end-organ function [6, 7]. Such sequential reactions were considered to be crucial in etiology of sepsis induced multiorgan dysfunction syndrome (MODS) [8–10]. Since intestine plays a key role in the pathogenesis of sepsis, the method for the treatment of intestinal damage emerged endlessly, including reasonable use of antibiotics [11] or low-dose corticosteroids [12], nutritional support therapy [13], and regulation of intestinal flora [14].

Dexmedetomidine (DEX) has been regarded as a highly selective α_2-adrenoceptor agonist, which mostly applied to different clinical settings for sedative or analgesic requirements [15]. Its attenuation of inflammation by activation on the α_2-adrenoceptors was confirmed by several investigations [16, 17]. Clinical evidence suggested that DEX sedated with DEX will suppress the inflammatory response mediated by TNF-α, IL-1β, IL-6, and so on, for septic patients [18]. Animal studies also revealed that the inhibitory efficacy of DEX on released cytokine in inflammatory responses and subsequently decreased in mortality [19, 20]. The anti-inflammatory properties of DEX by exerting protective effects on different organs and tissues have been noted by several experiments [21–23]. However, whether the administration of DEX can affect the sepsis induced intestinal injury remains

unclear. On the basis of the characteristics of DEX from previous studies, we designed this research to verify the hypothesis that DEX can ameliorate CLP-induced intestinal injury via inhibition of inflammation.

2. Materials and Methods

2.1. Animals. Adult male Sprague-Dawley (SD) rats (220~270 g) were obtained from Laboratorial Animal Center of Fujian Medical University. All animals were kept in standard environment with temperature and humidity control under a 12 h day/night cycle and free access to food and drink condition. The study protocols were approved by the institutional review board (IRB) and conducted in compliance with the institutional criteria for the practical care and use of laboratory animals in biomedical research.

2.2. CLP Model [24]. All rats were anesthetized with intraperitoneal injection of 10% chloral hydrate (0.3 mL/100 g) before surgical procedures, while their body temperatures were maintained at 36~38°C by a heating pad. An intravenous 24-gauge catheter was installed in tail vein for drug and saline administration. Next, after skin shaving and the preparation of abdominal wall with 10% povidone-iodine solution, a 2 cm incision was then performed through midline. The cecum was carefully isolated and ligated at distal to the ileocecal valve with a 4-0 silk suture to avoid intestinal obstruction and then punctured twice with a sterile 20-gauge needle and gently squeezed to extrude a small amount of feces from the perforation sites. We tried to guarantee the quantity of extruded feces was consistent in all rats. The quantity of extruded feces were limited (small droplet, about 1 mm in diameter) and consistent in all rats. Then placed back the cecum, the abdominal cavity was closed in two layers with continuous suture of 3-0 silk. The group Sham was treated in an identical manner, but no cecal ligation or puncture was performed. Each rat received a subcutaneous injection of 1 ml normal saline for fluid resuscitation after surgery. All animals were well tolerated throughout the procedures without further sedatives to maintain immobility, and no antibiotics were administrated during then.

2.3. Experimental Protocol and Drug Administration. A total of 64 rats were randomly assigned into four groups (n = 16 per group): the Sham group, cecum ligation and puncture (CLP) group, CLP plus intravenous injection of DEX (5 $\mu g \cdot kg^{-1} \cdot h^{-1}$, Hengrui Medicine, Jiangsu, China) 30 minutes after CLP for 1 h (DEX) group, and combination of α_2-adrenergic antagonist yohimbine (1.0 mg/kg, injection process lasting no less than 15 min, Sigma Chemical Co., St. Louis, MO, USA) prior to DEX treatment (DEX + YOH) group. The infusion rate was fixed at 5 $mL \cdot kg^{-1} \cdot h^{-1}$ [25] to eliminate the influences of fluid load; therefore the concentrations of drugs were different individually. The rats in Sham and CLP groups received normal saline over the same period. The doses of DEX and yohimbine used in the present study were according to the previous research [20, 26, 27].

2.4. Mortality Rate Observation. The survival studies were conducted on 10 animals from each group as the above. The mortality and 7-day survival rate after surgery were investigated through close follow-up; the estimated probability was analyzed by Kaplan-Meier survival curve.

2.5. Serum and Intestinal Tissues Collection. At 12 h and 24 h after CLP, blood samples were harvested from the inferior vena cava (3 mL of each); the serum was separated by centrifugation at 3000 rpm for 15 min at 4°C and then stored at −80°C for ELISA and spectrophotometry analysis. Then the rats were sacrificed for a 0.5~1.0 cm segment of the terminal ileum 5 cm proximal to the ileocecal valve, fixed in 4% formaldehyde for pathological examination. Two segments of intestine (300 mg) from 10 cm to ileocecal valve were obtained and immediately frozen in liquid nitrogen; then the intestinal tissues were homogenized and centrifuged at 12,000 rpm at 4°C for 15 minutes; the supernatant was collected for Western blot and ELISA.

2.6. Pathological Examination of Intestine. The tissues of intestine were embedded in paraffin wax and sectioned at 5 μm and then stained with hematoxylin and eosin (HE) and examined under a microscope (Nikon, Tokyo, Japan). The Pathological changes were evaluated by the same pathologist, who was blinded to the experimental protocols.

2.7. Determination of the Levels of Diamine Oxidase (DAO) and D-Lactate by Spectrophotometric Assay and TNF-α, IL-1β, and IL-6 by ELISA. The levels of DAO and D-lactate in serum were measured using spectrophotometry [28] and enzyme-linked ultraviolet spectrophotometry [29], respectively (Sigma Chemical Co., St. Louis, MO, USA). TNF-α, L-1β, and IL-6 in serum and intestine were measured by commercial ELISA kits (Bio Swamp Life Science Inc., Wuhan, China) in accordance with the manufacturers' instructions.

2.8. Determination the Expressions of TLR4 and Occludin by Western Blot. The protein concentration in the supernatant fluid was measured by BCA protein assay. Equal amounts of protein were subjected to SDS-PAGE and transferred to PVDF membranes. The transferred proteins were blocked with 5% skim milk and then incubated overnight with anti-TLR4, anti-occludin, and anti-β-actin primary antibodies (Cell Signaling Technology Inc., NY, USA), respectively. Immunoreactivity was detected with horseradish peroxidase conjugated secondary antibodies (Sigma Chemical Co., St. Louis, MO, USA) and visualized by enhanced chemiluminescence detection film.

2.9. Statistical Analysis. The normality of distribution was assessed with the Kolmogorov–Smirnov test. Parametric data were reported as mean (standard deviation (SD)) and nonparametric data were reported as median and interquartile range (IQR). SPSS 20.0 software was used for experimental results analysis. DAO, D-lactate, TNF-α, IL-1β, IL-6, and TLR4 among groups were analyzed using one-way analysis of variance (ANOVA). Post hoc comparisons were made with

least significant difference (LSD) test. Intergroup differences between two time points were analyzed with the unpaired Student's t-test. The survival analyses among groups were compared using Kaplan–Meier and the Mantel–Cox methods. Statistical significance was defined as $P < 0.05$.

3. Results

3.1. Mortality Rate. As shown in Figure 1, the mortality rates within 7 d in Sham, CLP, DEX, and DEX + YOH groups were 0%, 80%, 30%, 70%, respectively. Most of the deaths occur within the first 3 days. The mortality rate was higher in CLP group and DEX + YOH group than in Sham group ($P < 0.05$) but lower in DEX group than in CLP and DEX + YOH group (all $P < 0.05$). No significant diffidence was found between CLP and DEX + YOH groups ($P > 0.05$).

3.2. DEX Alleviated Morphology of Intestine Injury Induced by Sepsis. The pathological analysis showed integrated intestinal mucosa and compactly arrayed epithelium in the rats of Sham group (Figure 2). However, glands of the intestines were significantly damaged; severe edema of mucosal villi and neutrophil infiltration were observed in the rats of CLP and DEX + YOH groups at 12 h and 24 h after the induction of sepsis. By contrast, DEX ameliorated the pathological injury of the ileum with improved villi height and reduced neutrophil infiltration compared with sepsis group.

3.3. Detection of the Levels of DAO and D-Lactate in Serum and the Expression of Occludin in Intestine. Pathological examination is relatively crude to evaluate organ injury. Therefore, biochemical tests were performed to evaluate intestine damage. A similar pattern of changes was noted in intestinal barrier function (Figure 3). The serum DAO was significantly increased at 12 h and 24 h in CLP group compared with Sham group ($P < 0.05$) and more so in 24 h than 12 h following the operation. Treatment with DEX 5 $\mu g \cdot kg^{-1} \cdot h^{-1}$ resulted in lower DAO levels at 12 h and 24 h, respectively, compared to CLP group ($P < 0.05$). A more specific marker of intestinal barrier function, D-lactate, was also measured at 12 h and 24 h after CLP. The D-lactate levels were consistent with the DAO levels and showed a similar trend among the groups indicating that DEX can alleviate intestinal permeability in the CLP model. Occludin plays a key role in maintaining the integrity of intestinal barrier. Our results show that the level of the occludin was reduced in intestine of CLP rats compared with Sham controls ($P < 0.05$) and was more serious in 24 h. Taken together, the data presented in Figure 3 indicate that obvious intestinal injury occurred in septic mice. In contrast, DEX restored the inhibition of occludin expression ($P < 0.05$). The effects of DEX were partially inhibited by yohimbine ($P < 0.05$) relative to CLP rats.

3.4. Effect of DEX on the Levels of TNF-α, IL-1β, and IL-6 in Serum and Intestine. As shown in Figure 4, the levels of TNF-α, IL-1β, and IL-6 in serum were significantly higher in the CLP group than in the Sham group (all $P < 0.05$).

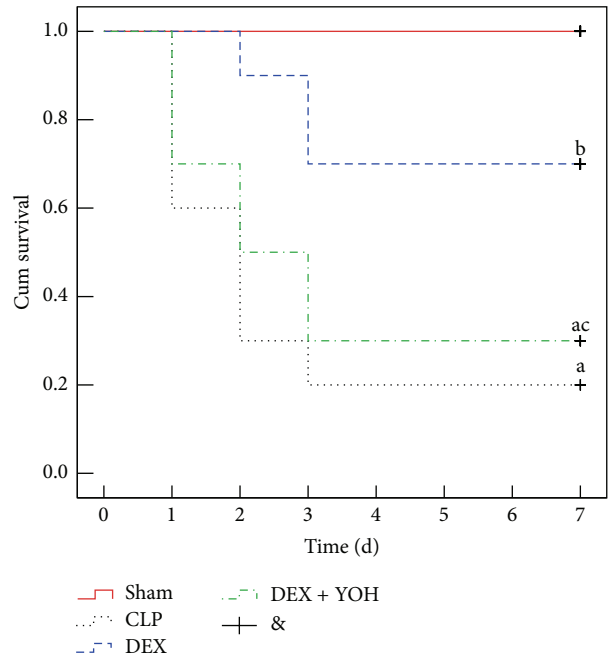

Figure 1: DEX treatment improved the survival of CLP-induced septic rats. Kaplan–Meier survival curves for four groups of rats 7 d ($n = 10$). [a]$P < 0.05$, versus Sham group; [b]$P < 0.05$, versus CLP group; [c]$P < 0.05$, versus DEX group.

In addition to activity of inflammatory factors in serum, expressions of TNF-α, IL-1β, and IL-6 in intestine were also all increased in CLP group compared to Sham group. The levels of inflammatory factors were significantly decreased at 24 h but were still higher than normal. DEX significantly inhibited the rise of TNF-α, IL-1β, and IL-6 (all $P < 0.05$) compared to CLP rats, which were effectively reversed by cotreatment with yohimbine ($P < 0.05$, versus DEX group), respectively. There was no significant difference between CLP group and DEX + YOH group in terms of intestinal TNF-α at 12 h and IL-1β at 24 h ($P > 0.05$).

3.5. Effect of DEX on the Expression of TLR4 in Intestine. To investigate the molecular mechanisms of DEX induced anti-inflammatory effect, we assessed TLR4 expression in intestine using Western blotting (Figure 5) in 12 h and 24 h. There was a weak expression of TLR4 in the Sham group. However, untreated septic rats significantly increased the expression of TLR4 compared with Sham group ($P < 0.05$). The higher levels of TLR4 in septic rats were observed at 12 h. In contrast, septic rats treated with DEX exhibited a decrease in the expression of TLR4 compared with untreated septic rats ($P < 0.05$). Yohimbine reduced but could not completely abolish the effect of DEX, suggesting that anti-inflammatory effect may be partially dependent on α_2-adrenoceptors.

4. Discussion

Experimental sepsis in our study was induced with the cecal ligation and puncture (CLP) technique to establish standard

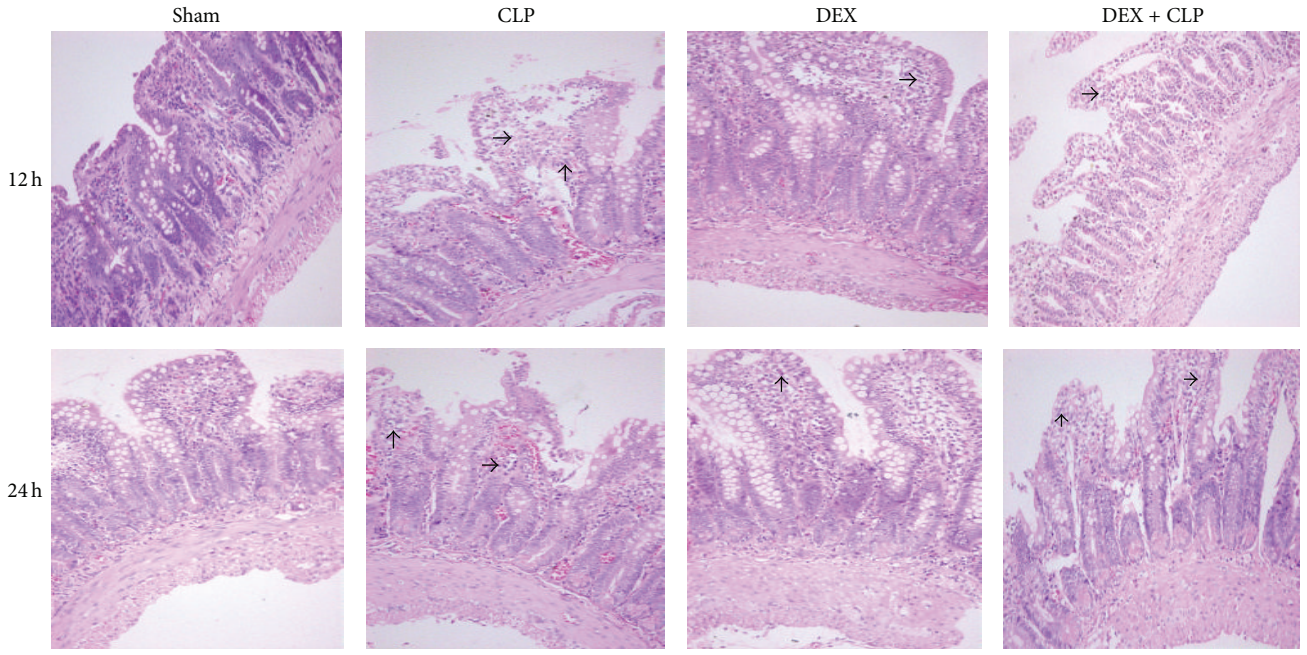

Figure 2: DEX treatment alleviated intestinal injury induced by CLP. Microscopic findings of the intestines stained with HE at 12 h and 24 h in Sham, CLP, DEX, and DEX + YOH groups (×200).

animal model of sepsis in mice [30]. Considering the high mortality rate in rats and the elevated concentrations of inflammatory factors in serum, it was indicated that the model used in our study was successful. In this present study, the application of DEX alleviated the pathological damage in intestine tissue, significantly attenuated in concentrations of DAO and D-lactate, and increased the expression of occludin. Besides, DEX also decreased the expression levels of TNF-α, IL-1β, IL-6, and TLR4 in intestine. These results indicated that DEX can ameliorate damage to intestine tissue by modulating inflammatory responses, which could be associated with the inhibition of TLR4 receptor in CLP-induced sepsis.

Investigations on the influence of gastrointestinal barrier injury in severe sepsis and subsequent MODS have increased over time [10]. Changes of histology and permeability in intestinal mucosa correlated with the cytokines and intestinal bacteria-endotoxin translocation [31]. The pathogenesis has not yet been fully understood; however, prompt and effective treatment with antibiotics affects the prognosis in clinical settings. Substantial evidences provided by previous studies prove that DEX has beneficial effects in sepsis condition. Lai et al. demonstrated that DEX suppressed the overexpression of inflammatory mediators in LPS activated murine macrophages [32]. Sezer et al. found that DEX may have protective effect on liver pathological changes in sepsis [33]. Shi et al. showed that DEX can protect against the lung tissue injury of LPS-induced sepsis in rats [34]. These evidences suggested that DEX can alleviate acute organ injuries during sepsis, which is consistent with our study that DEX can greatly impact the CLP-induced sepsis that resulted in a significant decrease in mortality.

As a functional intestinal marker enzyme, concentrations of DAO in plasma increased with the intestine inflammation, integrity of intestine mucosal, or permeability of the intestinal barrier [35]. D-lactate is one of the metabolites of luminal microbiota, whose level indicated the severity of intestine injury and also consistently changed with the epithelium function of the intestinal barrier [36]. In our study, septic rats revealed serious pathological damage including the destruction of intestinal mucosa and inflammatory cell infiltration. Elevated DAO and D-lactate in serum indicated that intestinal mucosal mechanical barrier was severely damaged in CLP model. The present results demonstrated that administration of DEX had beneficial effects on maintaining the integrity of intestinal mucosa barrier, as indicated by the reduction of DAO and D-lactate. In addition, DEX suppressed the reduction of tight junction protein occludin, which is the structural basis of mechanical barrier [37]. The decrease in occludin directly reflected the damage of intestinal mucosa induced by CLP. DEX also improved the intestines histological examination. The levels of DAO and D-lactate among the groups were consistent with the pathological evaluation. Therefore, these results indicate that DEX may avoid intestinal injury during sepsis.

It was known that an increase in the levels of inflammatory cytokines, including TNF-α, IL-1β, and IL-6, plays important role in the process of intestinal injury [4]. TNF-α is widely accepted as the initial mediators in the pathogenesis of sepsis; it plays a key role in endogenous inflammation to induce IL-1β and IL-6 production during the early phase of CLP. In the current study, DEX reduced TNF-α, IL-1β, and IL-6 production in serum and intestine, which was partially in accordance with previous study of the inhibitory effects of DEX on cytokines [38].

A growing body of evidence demonstrates that Toll-like receptors (TLRs) are highly conserved protein

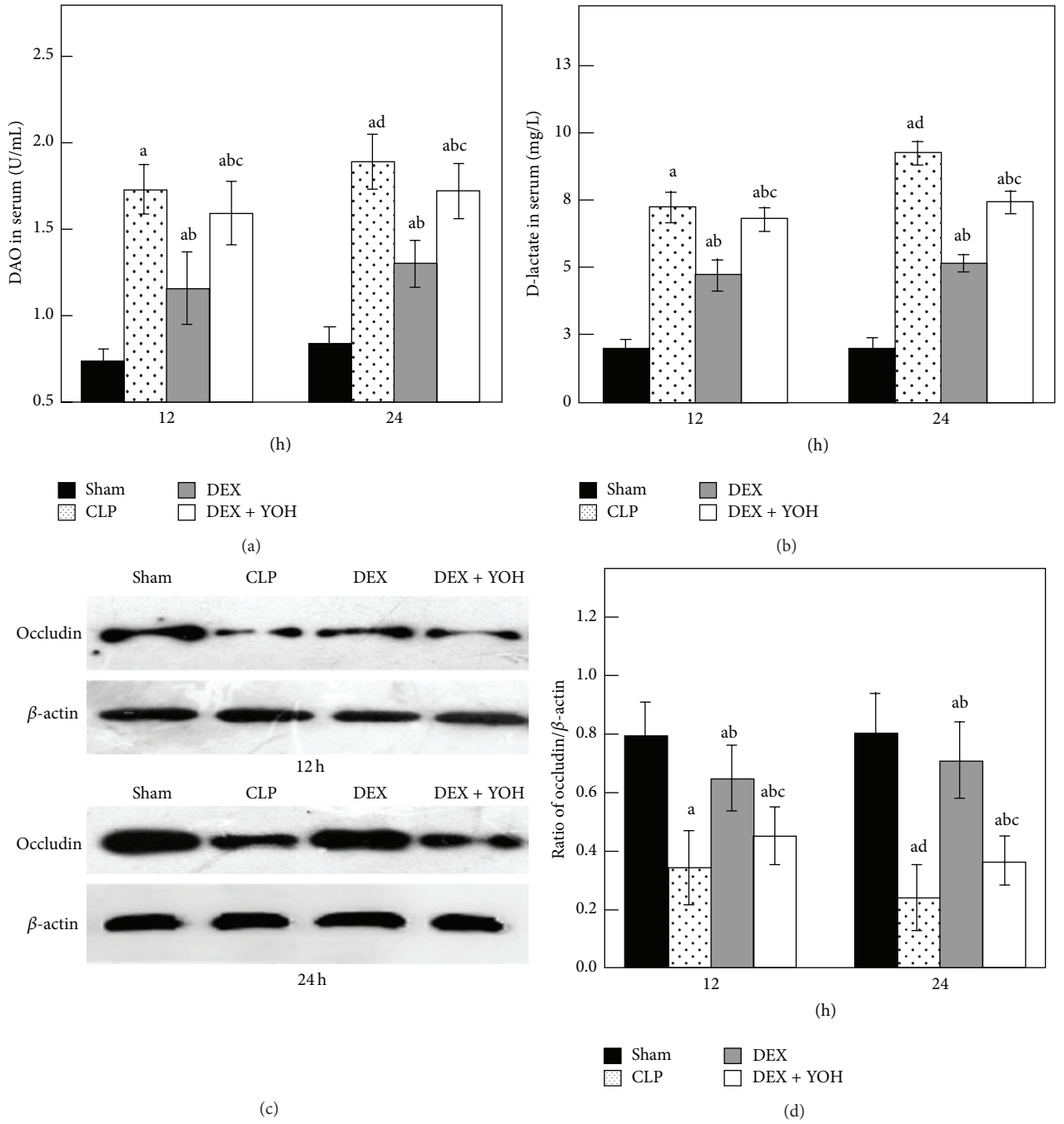

Figure 3: DAO and D-lactate in serum and occludin in intestine in experiment rats among four groups at 12 h and 24 h ($n = 8$). Data are expressed as mean ± SD. [a]$P < 0.05$, versus Sham group; [b]$P < 0.05$, versus CLP group; [c]$P < 0.05$, versus DEX group; [d]$P < 0.05$, versus CLP group 12 h.

receptors involved in the pathogenesis of critical illnesses, including sepsis. TLR4, together with CD14 and MD2 adapter molecule, has gained the most attention and was reported playing a pivotal role in the initiation and development of immune responses to microbial pathogens [39, 40]. It has been shown to be triggered by damage-associated molecular patterns (DAMPs). DAMPs bind to TLR4 leading to the activation of downstream signaling molecules including NF-κB and MAPKs. These could augment the production of proinflammatory cytokines (TNF-α, IL-1β, IL-6, etc.) and eventually lead to robust inflammatory response [41]. LPS, TNF-α, or IL-1β can also trigger the generation of TLR4, which means that TLR4 may participate in "cross talk" for the amplification of inflammatory responses [42]. To further explore the mechanism of DEX protective effect on intestine, TLR4 was examined. Our data are consistent with the hypothesis that level of TLR4 was elevated in septic rats but

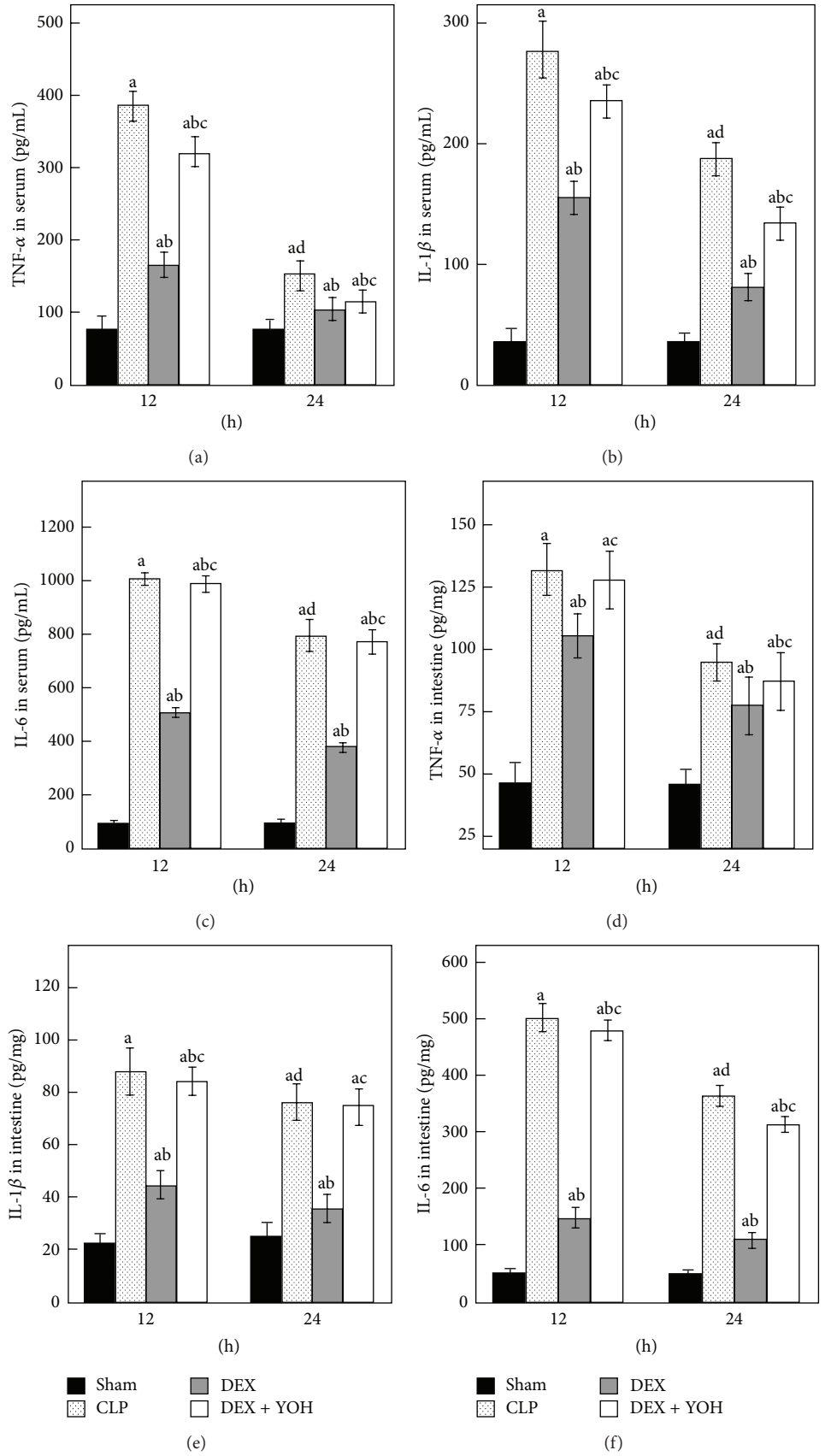

FIGURE 4: TNF-α, IL-1β, and IL-6 in experiment rats among four groups ($n = 8$). Data are expressed as mean ± SD. [a] $P < 0.05$, versus Sham group; [b] $P < 0.05$, versus CLP group; [c] $P < 0.05$, versus DEX group; [d] $P < 0.05$, versus CLP group 12 h.

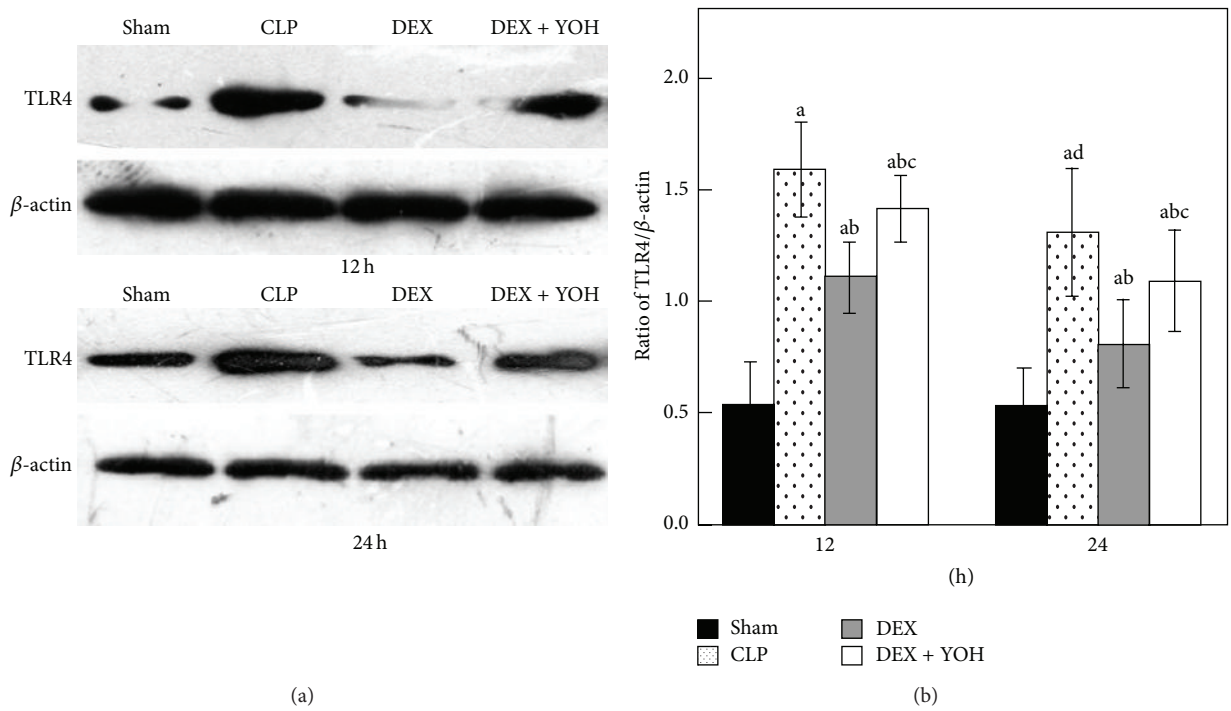

Figure 5: Expression of TLR4 in intestine by Western blotting in experiment rats among four groups ($n = 8$). Data are expressed as mean ± SD. [a]$P < 0.05$, versus Sham group; [b]$P < 0.05$, versus CLP group; [c]$P < 0.05$, versus DEX group; [d]$P < 0.05$, versus CLP group 12 h.

was significantly attenuated by DEX. These data provide strong evidence that inhibition of the TLR4 may contribute to anti-inflammatory effect in sepsis.

Collectively, these results indicated that the protective effects of DEX on septic intestinal injury might be partially achieved by altering the expressions of TLR4. In fact, our results are partly consistent with a previous study which demonstrated that DEX suppressed the TLR4 mediated inflammatory circuitry [32, 43].

In addition, yohimbine, a nonspecific α_2-adrenoceptor antagonist, was applied in the current study to further explore whether α_2-adrenoceptors are involved in the protective effect of DEX. It is believed that DEX provided its effect via α_2-adrenoceptors, since yohimbine partly reversed the protective effect of DEX because of the disappearance of its anti-inflammatory function. It has been previously reported that yohimbine itself does not suppress inflammation [27, 44]. Besides that, based on the result of previous research [7], we concluded that yohimbine abolished the intestinal protective effect of dexmedetomidine but it had no effect on intestinal injury during intestinal ischemia-reperfusion in rats. The results indicated that the therapeutic effects of DEX might be mediated, at least in part, by α_2-adrenoceptors during sepsis. Nevertheless, dexmedetomidine can also activate I_1-type imidazoline receptors [45]; previous studies indicated that imidazoline receptors possess significant anti-inflammatory capacity [46, 47]. So it is possible that the aforementioned effect of DEX is related to its effects on imidazoline receptor.

Our current research chose a single dose of DEX ($5\,\mu g{\cdot}kg^{-1}{\cdot}h^{-1}$), which was based on previous findings. It seems to be relatively high compared with the clinical doses used to produce anesthesia in humans. The recommended safe and effective clinical dosage range of DEX is only 0.5–1 μg/kg [48]. However, recent papers indicate that some patients might need higher doses of DEX (maybe 2–5 times higher than the usual clinical dose) to achieve adequate sedation [49]. Simultaneously, there may be differences in the doses of DEX between different species. Further investigation is needed on this point.

Several possible limitations of the present study should be noted. First, we demonstrated the inhibition effect of DEX on proinflammatory mediators, but it still is unclear whether DEX has any effect on the production of anti-inflammatory cytokines such as IL-10. Second, we did not maintain plasma levels of DEX, but intravenous injection usually results in good plasma levels. We do not monitor the hemodynamics in rats, so it is difficult to distinguish whether the protective effect is affected by hemodynamics fluctuations. Finally, we only studied short-time effects of DEX on CLP induced injury in intestine but more doses and long-term effect of DEX also need to be clarified.

5. Conclusion

In conclusion, our study indicated that DEX could exert protective role against sepsis-induced intestinal barrier dysfunction via attenuating intestinal inflammatory responses and then effectively prevent the development of sepsis. Thus, our results provide a new insight for the clinical use of DEX and suggest that DEX sedation may have a therapeutic potential in reducing intestinal injury associated with sepsis.

Conflict of Interests

The authors declare that there is no conflict of interests.

Authors' Contribution

Yanqing Chen and Liyan Miao are equal first authors.

Acknowledgment

This study was supported by Social Development of Key Projects in Fujian Province (2012Y0012).

References

[1] J.-L. Vincent, J. Rello, J. Marshall et al., "International study of the prevalence and outcomes of infection in intensive care units," *The Journal of the American Medical Association*, vol. 302, no. 21, pp. 2323–2329, 2009.

[2] D. C. Angus, W. T. Linde-Zwirble, J. Lidicker, G. Clermont, J. Carcillo, and M. R. Pinsky, "Epidemiology of severe sepsis in the United States: analysis of incidence, outcome, and associated costs of care," *Critical Care Medicine*, vol. 29, no. 7, pp. 1303–1310, 2001.

[3] E. B. Milbrandt, A. Kersten, M. T. Rahim et al., "Growth of intensive care unit resource use and its estimated cost in Medicare," *Critical Care Medicine*, vol. 36, no. 9, pp. 2504–2510, 2008.

[4] F. Tamion, V. Richard, Y. Lacoume, and C. Thuillez, "Intestinal preconditioning prevents systemic inflammatory response in hemorrhagic shock. Role of HO-1," *The American Journal of Physiology—Gastrointestinal and Liver Physiology*, vol. 283, no. 2, pp. G408–G414, 2002.

[5] R. S. Hotchkiss and I. E. Karl, "The pathophysiology and treatment of sepsis," *The New England Journal of Medicine*, vol. 348, no. 2, pp. 138–150, 2003.

[6] P. Yu and C. M. Martin, "Increased gut permeability and bacterial translocation in Pseudomonas pneumonia-induced sepsis," *Critical Care Medicine*, vol. 28, no. 7, pp. 2573–2577, 2000.

[7] X.-Y. Zhang, Z.-M. Liu, S.-H. Wen et al., "Dexmedetomidine administration before, but not after, ischemia attenuates intestinal injury induced by intestinal ischemia-reperfusion in rats," *Anesthesiology*, vol. 116, no. 5, pp. 1035–1046, 2012.

[8] Y.-Z. Cao, Y.-Y. Tu, X. Chen, B.-L. Wang, Y.-X. Zhong, and M.-H. Liu, "Protective effect of Ulinastatin against murine models of sepsis: inhibition of TNF-alpha and IL-6 and augmentation of IL-10 and IL-13," *Experimental and Toxicologic Pathology*, vol. 64, no. 6, pp. 543–547, 2012.

[9] H. T. Hassoun, B. C. Kone, D. W. Mercer, F. G. Moody, N. W. Weisbrodt, and F. A. Moore, "Post-injury multiple organ failure: the role of the gut," *Shock*, vol. 15, no. 1, pp. 1–10, 2001.

[10] J. A. Clark and C. M. Coopersmith, "Intestinal crosstalk: a new paradigm for understanding the gut as the 'motor' of critical illness," *Shock*, vol. 28, no. 4, pp. 384–393, 2007.

[11] R. P. Dellinger, J. M. Carlet, H. Masur et al., "Surviving Sepsis Campaign guidelines for management of severe sepsis and septic shock," *Critical Care Medicine*, vol. 32, no. 3, pp. 858–873, 2004.

[12] D. Annane, E. Bellissant, P.-E. Bollaert et al., "Corticosteroids in the treatment of severe sepsis and septic shock in adults: a systematic review," *Journal of the American Medical Association*, vol. 301, no. 22, pp. 2362–2375, 2009.

[13] H. Azuma, S. Mishima, J. Oda et al., "Enteral supplementation enriched with glutamine, fiber, and oligosaccharide prevents gut translocation in a bacterial overgrowth model," *The Journal of Trauma—Injury, Infection and Critical Care*, vol. 66, no. 1, pp. 110–114, 2009.

[14] C. Alberda, L. Gramlich, J. Meddings et al., "Effects of probiotic therapy in critically ill patients: a randomized, double-blind, placebo-controlled trial," *The American Journal of Clinical Nutrition*, vol. 85, no. 3, pp. 816–823, 2007.

[15] J. Mantz, J. Josserand, and S. Hamada, "Dexmedetomidine: new insights," *European Journal of Anaesthesiology*, vol. 28, no. 1, pp. 3–6, 2011.

[16] J. Gu, J. Chen, P. Xia, G. Tao, H. Zhao, and D. Ma, "Dexmedetomidine attenuates remote lung injury induced by renal ischemia-reperfusion in mice," *Acta Anaesthesiologica Scandinavica*, vol. 55, no. 10, pp. 1272–1278, 2011.

[17] H. Ayoglu, S. Gul, V. Hanci et al., "The effects of dexmedetomidine dosage on cerebral vasospasm in a rat subarachnoid haemorrhage model," *Journal of Clinical Neuroscience*, vol. 17, no. 6, pp. 770–773, 2010.

[18] D. Memiş, S. Hekimoğlu, I. Vatan, T. Yandim, M. Yüksel, and N. Süt, "Effects of midazolam and dexmedetomidine on inflammatory responses and gastric intramucosal pH to sepsis, in critically ill patients," *British Journal of Anaesthesia*, vol. 98, no. 4, pp. 550–552, 2007.

[19] T. Taniguchi, Y. Kidani, H. Kanakura, Y. Takemoto, and K. Yamamoto, "Effects of dexmedetomidine on mortality rate and inflammatory responses to endotoxin-induced shock in rats," *Critical Care Medicine*, vol. 32, no. 6, pp. 1322–1326, 2004.

[20] T. Taniguchi, A. Kurita, K. Kobayashi, K. Yamamoto, and H. Inaba, "Dose- and time-related effects of dexmedetomidine on mortality and inflammatory responses to endotoxin-induced shock in rats," *Journal of Anesthesia*, vol. 22, no. 3, pp. 221–228, 2008.

[21] R. M. Venn, A. Bryant, G. M. Hall, and R. M. Grounds, "Effects of dexmedetomidine on adrenocortical function, and the cardiovascular, endocrine and inflammatory responses in postoperative patients needing sedation in the intensive care unit," *British Journal of Anaesthesia*, vol. 86, no. 5, pp. 650–656, 2001.

[22] K. Engelhard, C. Werner, S. Kaspar et al., "Effect of the α 2-agonist dexmedetomidine on cerebral neurotransmitter concentrations during cerebral ischemia in rats," *Anesthesiology*, vol. 96, no. 2, pp. 450–457, 2002.

[23] U. Koca, Ç. G. Olguner, B. U. Ergür et al., "The effects of dexmedetomidine on secondary acute lung and kidney injuries in the rat model of intra-abdominal sepsis," *The Scientific World Journal*, vol. 2013, Article ID 292687, 11 pages, 2013.

[24] E. Otero-Antón, A. González-Quintela, A. López-Soto, S. López-Ben, J. Llovo, and L. F. Pérez, "Cecal ligation and puncture as a model of sepsis in the rat: Influence of the puncture size on mortality, bacteremia, endotoxemia and tumor necrosis factor alpha levels," *European Surgical Research*, vol. 33, no. 2, pp. 77–79, 2001.

[25] X. Wu, X. Song, N. Li, L. Zhan, Q. Meng, and Z. Xia, "Protective effects of dexmedetomidine on blunt chest trauma-induced pulmonary contusion in rats," *The Journal of Trauma and Acute Care Surgery*, vol. 74, no. 2, pp. 524–530, 2013.

[26] C.-L. Yang, P.-S. Tsai, and C.-J. Huang, "Effects of dexmedetomidine on regulating pulmonary inflammation in a rat model of ventilator-induced lung injury," *Acta Anaesthesiologica Taiwanica*, vol. 46, no. 4, pp. 151–159, 2008.

[27] J. Shen, G. Fu, L. Jiang, J. Xu, L. Li, and G. Fu, "Effect of dexmedetomidine pretreatment on lung injury following intestinal ischemia-reperfusion," *Experimental and Therapeutic Medicine*, vol. 6, no. 6, pp. 1359–1364, 2013.

[28] J.-Y. Li, D. Sun, Y. Lu et al., "Change in intestinal function in sepsis in rat," *Chinese Critical Care Medicine*, vol. 16, no. 6, pp. 352–354, 2004.

[29] R. B. Brandt, S. A. Siegel, M. G. Waters, and M. H. Bloch, "Spectrophotometric assay for D-(−)-lactate in plasma," *Analytical Biochemistry*, vol. 102, no. 1, pp. 39–46, 1980.

[30] J. G. Heuer, D. L. Bailey, G. R. Sharma et al., "Cecal ligation and puncture with total parenteral nutrition: a clinically relevant model of the metabolic, hormonal, and inflammatory dysfunction associated with critical illness," *The Journal of Surgical Research*, vol. 121, no. 2, pp. 178–186, 2004.

[31] D. A. De-Souza and L. J. Greene, "Intestinal permeability and systemic infections in critically ill patients: effect of glutamine," *Critical Care Medicine*, vol. 33, no. 5, pp. 1125–1135, 2005.

[32] Y.-C. Lai, P.-S. Tsai, and C.-J. Huang, "Effects of dexmedetomidine on regulating endotoxin-induced up-regulation of inflammatory molecules in murine macrophages," *The Journal of Surgical Research*, vol. 154, no. 2, pp. 212–219, 2009.

[33] A. Sezer, D. Memiş, U. Usta, and N. Süt, "The effect of dexmedetomidine on liver histopathology in a rat sepsis model: an experimental pilot study," *Turkish Journal of Trauma & Emergency Surgery*, vol. 16, no. 2, pp. 108–112, 2010.

[34] Q. Q. Shi, H. Wang, and H. Fang, "Dose-response and mechanism of protective functions of selective alpha-2 agonist dexmedetomidine on acute lung injury in rats," *Saudi Medical Journal*, vol. 33, no. 4, pp. 375–381, 2012.

[35] C. Cai, W. Li, J. Chen, X. Li, and S. Chen, "Diamine oxidase as a marker for diagnosis of superior mesenteric arterial occlusion," *Hepato-Gastroenterology*, vol. 59, no. 113, pp. 155–158, 2012.

[36] I. Lorenz and S. Vogt, "Investigations on the association of D-lactate blood concentrations with the outcome of therapy of acidosis, and with posture and demeanour in young calves with diarrhoea," *Journal of Veterinary Medicine Series A: Physiology Pathology Clinical Medicine*, vol. 53, no. 9, pp. 490–494, 2006.

[37] V. Braniste, A. Jouault, E. Gaultier et al., "Impact of oral bisphenol a at reference doses on intestinal barrier function and sex differences after perinatal exposure in rats," *Proceedings of the National Academy of Sciences of the United States of America*, vol. 107, no. 1, pp. 448–453, 2010.

[38] L. Xu, H. Bao, Y. Si, and X. Wang, "Effects of dexmedetomidine on early and late cytokines during polymicrobial sepsis in mice," *Inflammation Research*, vol. 62, no. 5, pp. 507–514, 2013.

[39] S. Akira and K. Takeda, "Toll-like receptor signalling," *Nature Reviews Immunology*, vol. 4, no. 7, pp. 499–511, 2004.

[40] J. Krishnan, K. Selvarajoo, M. Tsuchiya, G. Lee, and S. Choi, "Toll-like receptor signal transduction," *Experimental and Molecular Medicine*, vol. 39, no. 4, pp. 421–438, 2007.

[41] L. A. J. O'Neill and A. G. Bowie, "The family of five: TIR-domain-containing adaptors in Toll-like receptor signalling," *Nature Reviews Immunology*, vol. 7, no. 5, pp. 353–364, 2007.

[42] U. Andersson, H. Wang, K. Palmblad et al., "High mobility group 1 protein (HMG-1) stimulates proinflammatory cytokine synthesis in human monocytes," *The Journal of Experimental Medicine*, vol. 192, no. 4, pp. 565–570, 2000.

[43] J. Gu, P. Sun, H. Zhao et al., "Dexmedetomidine provides renoprotection against ischemia-reperfusion injury in mice," *Critical Care*, vol. 15, no. 3, article R153, 2011.

[44] L. Jiang, L. Li, J. Shen, Z. Qi, and L. Guo, "Effect of dexmedetomidine on lung ischemia-reperfusion injury," *Molecular Medicine Reports*, vol. 9, no. 2, pp. 419–426, 2014.

[45] P. Bousquet, "Imidazoline receptors," *Neurochemistry International*, vol. 30, no. 1, pp. 3–7, 1997.

[46] D. L. Feinstein, D. J. Reis, and S. Regunathan, "Inhibition of astroglial nitric oxide synthase type 2 expression by idazoxan," *Molecular Pharmacology*, vol. 55, no. 2, pp. 304–308, 1999.

[47] M. Fornai, C. Blandizzi, R. Colucci et al., "Role of cyclooxygenases 1 and 2 in the modulation of neuromuscular functions in the distal colon of humans and mice," *Gut*, vol. 54, no. 5, pp. 608–616, 2005.

[48] K. P. Mason, D. Zurakowski, S. E. Zgleszewski et al., "High dose dexmedetomidine as the sole sedative for pediatric MRI," *Paediatric Anaesthesia*, vol. 18, no. 5, pp. 403–411, 2008.

[49] P. P. Pandharipande, B. T. Pun, D. L. Herr et al., "Effect of sedation with dexmedetomidine vs lorazepam on acute brain dysfunction in mechanically ventilated patients: the MENDS randomized controlled trial," *The Journal of the American Medical Association*, vol. 298, no. 22, pp. 2644–2653, 2007.

Hindawi Publishing Corporation
Mediators of Inflammation
Volume 2015, Article ID 643763, 9 pages
http://dx.doi.org/10.1155/2015/643763

Review Article

Anti-Inflammatory and Organ-Protective Effects of Resveratrol in Trauma-Hemorrhagic Injury

Fu-Chao Liu,[1,2,3] Yung-Fong Tsai,[1,2,3] Hsin-I Tsai,[1,2,3] and Huang-Ping Yu[1,2]

[1]*Department of Anesthesiology, Chang Gung Memorial Hospital, Taoyuan City 333, Taiwan*
[2]*College of Medicine, Chang Gung University, Taoyuan City 333, Taiwan*
[3]*Graduate Institute of Clinical Medical Sciences, Chang Gung University, Taoyuan City 333, Taiwan*

Correspondence should be addressed to Huang-Ping Yu; yuhp2001@adm.cgmh.org.tw

Received 3 October 2014; Accepted 4 December 2014

Academic Editor: Zhengyuan Xia

Resveratrol, a natural polyphenolic compound of grape and red wine, owns potential anti-inflammatory effects, which results in the reduction of cytokines overproduction, the inhibition of neutrophil activity, and the alteration of adhesion molecules expression. Resveratrol also possesses antioxidant, anti-coagulation and anti-aging properties, and it may control of cell cycle and apoptosis. Resveratrol has been shown to reduce organ damage following traumatic and shock-like states. Such protective phenomenon is reported to be implicated in a variety of intracellular signaling pathways including the activation of estrogen receptor, the regulation of the sirtuin 1/nuclear factor-kappa B and mitogen-activated protein kinases/hemeoxygenase-1 pathway, and the mediation of proinflammatory cytokines and reactive oxygen species formation and reaction. In the recent studies, resveratrol attenuates hepatocyte injury and improves cardiac contractility due to reduction of proinflammatory mediator expression and ameliorates hypoxia-induced liver and kidney mitochondrial dysfunction following trauma and hemorrhagic injuries. Moreover, through anti-inflammatory effects and antioxidant properties, the resveratrol is believed to protect organ function in trauma-hemorrhagic injury. In this review, the organ-protective and anti-inflammatory effects of resveratrol in trauma-hemorrhagic injury will be discussed.

1. Introduction

Resveratrol is a naturally occurring plant antibiotic known as phytoalexins, found in various plants and fruits, especially abundant in grapes and red wine [1, 2]. Previous reports have demonstrated the protective effects of resveratrol in different pathological conditions and experimental models [3–7]. Many clinical studies also indicated the beneficial effects of resveratrol in human diseases [8–13]. A growing body of evidence showed that resveratrol might play potential therapeutic roles in human health by its anti-inflammatory, antioxidant, antiaging, antidiabetic, anticoagulative, and apoptotic properties [1, 7, 14, 15]. Resveratrol attenuates organ injury in trauma-hemorrhagic (T-H) injury through multiple pathways, in which a number of the molecular targets and protective effects of resveratrol have been identified, including the estrogen receptors (ER) [16, 17], the protein kinase B (Akt), the AMP-activated protein kinase (AMPK) [18, 19], the hemeoxygenase-1 (HO-1) [20–22], the histone/protein deacetylase sirtuin 1 (SIRT1) [23, 24], and nuclear factor-kappa B (NF-κB) [25, 26] (Figure 1).

A variety of laboratory and clinical researches also show that resveratrol may lead to tissue- and organ-protective effects against various injuries [27–33]. Traumatic injury is recognized to induce the excessive production of oxidants and proinflammatory mediators and subsequent development of multiple organ dysfunctions [34–37] and resveratrol has been suggested to have organ-protective effect on trauma and hemorrhagic injuries due to its antioxidative activities and anti-inflammatory effects [18, 20, 38–42]. Trauma-hemorrhagic injury causes excessive production of proinflammatory mediators, cytokines, and chemokines. The enhanced secretion of proinflammatory cytokines is a critical factor in the initiation and perpetuation of organ injury [39, 43, 44]. These cytokines recruit other immune cells including neutrophils, thereby increasing leukocyte activation and

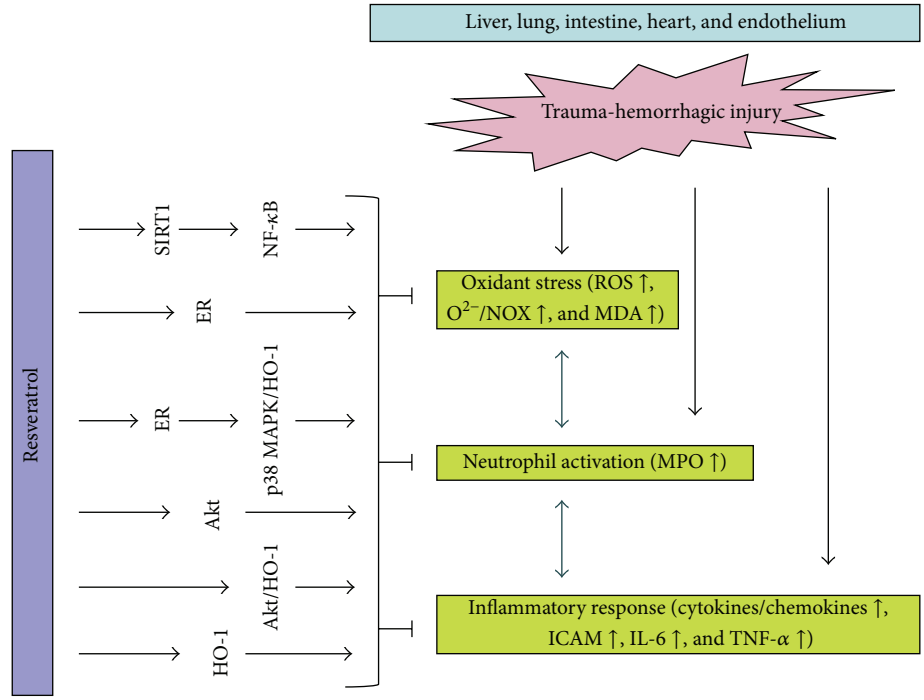

Figure 1: The anti-inflammatory and protective pathways of resveratrol in trauma-hemorrhagic injury. ER: estrogen receptor; SIRT1: sirtuin 1; HO-1: hemeoxygenase-1; p38 MAPK: p38 mitogen-activated protein kinase; NF-κB: nuclear factor-kappa B; ROS: reactive oxygen species; MDA: malondialdehyde; NOX: NADPH oxidase; MPO: myeloperoxidase; ICAM: intercellular adhesion molecule; IL-6: interleukin 6.

trafficking result in organ injury [45–47]. In this review, we summarize the protective effects and possible mechanisms of resveratrol on the preservation of organ function in T-H injury (Table 1).

2. The Pulmonary Protective Effect of Resveratrol in T-H Injury

The activation of neutrophils in T-H injury [39, 47–49] and pulmonary injury is associated with an increased neutrophil accumulation [40, 42]. Neutrophils leave the microcirculation and migrate to matrix proteins or other cells and release mediators, which diffuse across the endothelium and hurt parenchymal cells [46, 47]. The intercellular adhesion molecule 1 (ICAM-1), constitutively present on the surface of endothelial cells, enhances firm adhesion of neutrophils to the vascular endothelium and is markedly upregulated following T-H injury [40, 47, 50]. For example, pulmonary ICAM-1 expression is increased in the lung in T-H shock [40, 47, 51]. The activated neutrophils appear to infiltrate the injured lung in parallel with increased expression of adhesion molecules on endothelial cells and also lead to the elevation of local chemokines/cytokines [40, 47, 51]. Chemotaxis has an important functional response to chemokines and is a key event in the recruitment of neutrophils in inflammation. Cytokine-induced neutrophil chemoattractant 1 (CINC-1) and CINC-3 are members of the IL-8 family and are potent chemoattractants for neutrophils [39, 42]. Moreover, the levels of the CINC-1 and CINC-3 are elevated in T-H injury. Furthermore, convincing evidence has shown that interleukin 6 (IL-6) plays an important role in organ injuries and is required for the expression of adhesion molecules and release of chemokines [52–54]. IL-6-deficient mice show less neutrophils infiltration and organ damage as compared with wild-type mice under hemorrhagic shock [54]. IL-6 could be released from macrophages and lymphocytes and appears to be an essential component of the inflammatory cascade that is associated with organ damage in T-H injury [51, 55].

Resveratrol has a protective role in organ damage following T-H injury via the reduction of neutrophil accumulation [46, 47, 49]. The role of resveratrol in the attenuation of lung injury is likely due to the reduction of chemokines in T-H injury [40, 42, 51]. IL-6, a critical early mediator in the lung during T-H injury, is inhibited by resveratrol treatment [42, 51]. The ability of resveratrol to modulate the expression of inflammatory cytokines, adhesion molecules, and chemokines suggests a role for resveratrol in the regulation of lung inflammation.

3. The Liver Protective Effect of Resveratrol in T-H Injury

The liver is considered to be a critical organ in the development of delayed organ dysfunction in patients having traumatic injuries and hemorrhagic shock [37, 39, 45, 56]. T-H injury results in massive production of proinflammatory mediators (IL-6, ICAM-1, CINC-1, and CINC-3) and the subsequent accumulation of neutrophils in the injured liver [39, 41, 47, 48]. Resveratrol reduces cytokine production and

Table 1: The organ-protective effects and mechanisms of resveratrol in trauma-hemorrhagic injury.

Species	Target organ	Effective dose	Effects and mechanisms	Ref.
Sprague-Dawley rat	Liver	30 mg/kg/BW	Estrogen receptor-dependent HO-1 expression↑	[20]
Sprague-Dawley rat	Liver	30 mg/kg/BW	Reduction of T-H-induced proinflammatory parameters (CINC-1↓, CINC-3↓, ICAM-1, MPO↓, and IL-6↓); Akt-dependent HO-1 expression↑	[39]
Sprague-Dawley rat	Liver	30 mg/kg/BW	Reduction of T-H-induced proinflammatory parameters (CINC-1↓, CINC-3↓, ICAM-1, MPO↓, and IL-6↓); estrogen receptor-mediated pathway	[41]
Sprague-Dawley rat	Liver	30 mg/kg/BW	Reduction of T-H-induced mitochondria damage and hepatocyte injury; increase in SIRT1 expression; and decrease in p53 and NF-κB activity; IL-6↓, MDA↓	[73]
Sprague-Dawley rat	Lung	30 mg/kg/BW	Reduction of T-H-induced proinflammatory parameters (CINC-1↓, CINC-3↓, ICAM-1, MPO↓, and IL-6↓)	[40]
Sprague-Dawley rat	Lung	30 mg/kg/BW	Estrogen receptor-dependent HO-1 expression↑	[20]
Sprague-Dawley rat	Intestine	30 mg/kg/BW	Reduction of T-H-induced proinflammatory parameters (CINC-1↓, CINC-3↓, ICAM-1, MPO↓, IL-6↓, and TNF-α↓); estrogen receptor-dependent P38/HO-1 expression↑	[18]
Sprague-Dawley rat	Heart	8 mg/kg/BW	Reduction of T-H-induced left ventricular contractility impairment through elevated SIRT1 expression; cardiac ATP↓, cytosolic cytochrome C↓, and plasma TNF-α↓	[86]
Sprague-Dawley rat	Heart	Not available	Reduction of T-H-induced mitochondria damage and improving left ventricular function through restored SIRT1 activity and PDK1 expression	[94]
Sprague-Dawley rat	Heart	30 mg/kg/BW	Reduction of T-H-induced proinflammatory parameters (ICAM-1↓, MPO↓, and IL-6↓); reduction of T-H-induced cardiac injury through elevated p-Akt activity	[38]
Sprague-Dawley rat	Endothelium	30 mg/kg/BW	Acetylcholine-induced endothelium-dependent relaxation↓ through estrogen receptor-dependent pathway; ROS radical/NADPH oxidase expression↓	[20]
Sprague-Dawley rat	Aorta	30 mg/kg/BW	NADPH-stimulated ROS↓; aortic p22phox, p47phox, gp91phox, NOX1, and NOX4 mRNA levels↓	[20]

Note: the species (Sprague-Dawley rat) are all the same in Table 1.
BW: body weight; ER: estrogen receptor; HO-1: hemeoxygenase-1; SIRT1: sirtuin 1; NF-κB: nuclear factor-kappa B; MDA: malondialdehyde; TNF-α: tumor necrosis factor-alpha; CINC-1: cytokine-induced neutrophil chemoattractant 1; ICAM-1: intercellular adhesion molecule 1; MPO: myeloperoxidase; IL-6: interleukin 6; ROS: reactive oxygen species; NOX: NADPH oxidase; PDK1: pyruvate dehydrogenase kinase 1.

neutrophil accumulation in a rodent model of LPS-induced hepatic oxidative stress and inflammation [57].

Resveratrol binds to ER-α and ER-β and therefore alters the transcriptional activity of estrogen-responsive target genes [17, 19, 58, 59]. Resveratrol could modulate TNF-α genes expression and suppress IL-6 transcription via an ER-α signal integration [16]. Other studies demonstrated the role of sexual dimorphism in response to injury and showed the importance of sex steroids on the maintenance of organ function in T-H injury [45, 47, 60, 61]. The administration of

resveratrol in combination with an ER antagonist ICI 182,780 blocks the hepatoprotective effect and such ER pathway is critical in hepatoprotection in T-H injury [41]. Building on these findings, ER pathways may be potentially useful therapies in the treatment of trauma patients [41, 62, 63]. In addition, estrogen treatment upregulates phosphatidylinositol 3-kinase (PI3K)/Akt expression via an estrogen receptor following T-H injury [64].

HO-1, a stress-inducible heme-degrading enzyme, provides cytoprotection against oxidative stress and inflammatory reaction [65, 66]. HO-1 expression is upregulated during T-H injury, and its induction appears to play a central role in the preservation of organ microcirculation under such conditions [67, 68]. A growing body of evidence demonstrates that Akt activation induces HO-1, which is known to have a protective effect in many organs under various deleterious conditions, including T-H injury [39, 42, 68, 69]. The upregulation of HO-1 causes a reduction of chemokines, cytokines, and adhesion molecules. It also decreases neutrophil accumulation and ameliorates organ injury in trauma-related shock status [39, 42, 70]. The administration of 17β-estradiol or flutamide (an antiandrogen drug) in T-H injury increases HO-1 expression, which attenuates the organs' dysfunction and injury [67–69]. The PI3K/Akt is an important signaling pathway controlling endogenous negative feedback or compensatory mechanism, in which proinflammation and chemotactic events are limited in response to injury [37, 39, 64]. Activation of PI3K/Akt signaling cascade by resveratrol has been observed in different tissues [38, 39, 71, 72]. Resveratrol-mediated increase in HO-1 is found to be Akt-dependent. When resveratrol is coadministered with PI3K/Akt antagonist, it abolishes the resveratrol-mediated HO-1 increase and hepatic protective effects in T-H injury [39, 70]. These results indicate that resveratrol attenuated liver damage and decreased proinflammatory mediator expression in T-H injury, likely through Akt-dependent HO-1 pathway [39, 70].

In addition, Powell et al. demonstrated that resveratrol could reduce T-H injury-induced mitochondria damage and hepatocyte injury. Resveratrol illustrates a protective effect through an increase in SIRT1 expression and a decrease in p53 and NF-κB activity. It also inhibits proinflammatory mediator IL-6 and lipoperoxidation MDA expression [73].

4. The Intestinal Protective Effect of Resveratrol in T-H Injury

Intestinal tract is highly sensitive to injury. T-H injury could induce oxidants release, leading to microvascular permeability change, interstitial edema, mucosal barrier dysfunction, and inflammatory cell infiltration. ER also plays a pivotal role in intestinal injury after T-H shock. Previous reports showed that ER leads to the induction of p38 MAPK [18, 47, 74, 75], which contributes to the protection of cell/tissue in response to a variety of stimuli [76–78]. Estrogen-mediated anti-inflammatory and organ-protective effects are abolished by the administration of a p38 MAPK inhibitor SB-203580 following T-H injury [18, 75].

P38 MAPK activation regulates mucosal recovery in ischemic-injured porcine ileum [79] and protects glomerular epithelial cells against complement-mediated cell injury [80]. The p38 MAPK phosphorylation contributes to intestine-protection in T-H injury after ischemic preconditioning or T-H [18, 47, 74, 75]. Resveratrol also reduces chronic colonic inflammation [81] and protects H_2O_2-treated embryonic rat heart H9c2 cells via the p38 MAPK pathway [82].

The upregulation of HO-1 is known for its protective role in cellular stress during inflammation, ischemia, and radiation, as well as the anti-inflammatory and antiapoptotic effects. Resveratrol protects the intestinal epithelial barrier function against TNF-α and oxidative stress through upregulation of HO-1 expression in intestinal ischemia/reperfusion injury [83]. p38 MAPK activation induces HO-1 expression and maintains organ function under various stresses and injuries. Recent studies indicate that the treatment of animals with SB-203580, which blocks p38 MAPK, abolishes resveratrol-induced upregulation of HO-1 after T-H [18, 75]. These findings indicate that the salutary effects of resveratrol-mediated attenuation of intestinal injury in T-H are mediated, at least in part, through ER-dependent p38 MAPK/HO-1 upregulation.

5. The Cardioprotective Effect of Resveratrol in T-H Injury

Resveratrol has been shown to possess cardioprotective effects during ischemia-reperfusion injury [84, 85] and decreases organ injury in T-H injury [38, 86]. Cardiac injury is associated with increased neutrophil accumulation [38, 47] and such in small intestine is correlated with the attenuation of trauma-hemorrhage-induced cardiac dysfunction [18].

Activation of the PI3K pathway protects cells or organs against hypoxia and ischemia-reperfusion injury via inhibition of the apoptosis machinery [87, 88]. Modulation of the PI3K/Akt pathway with the PI3K inhibitor wortmannin suppresses coagulation and inflammation and decreases the survival of mice subjected to sepsis [89]. PI3K/Akt pathway also mediates neutrophils activation and regulates leukocyte signaling and function, to undergo chemotaxis [90]. Resveratrol decreases the production of proinflammatory mediators and ameliorates cardiac injury in T-H injury [38]. Blockade of Akt activation abolishes the salutary effects of resveratrol in the heart following T-H [38]. Altogether, resveratrol-related cardioprotective effect is likely mediated through an Akt-dependent pathway in T-H injury [38].

SIRT1 has been shown to regulate the mammalian genes transcription and silence the tumor suppressor genes [91, 92]. The SIRT1 transcription-modulating proteins demonstrate a fine balance in response to intracellular stimulus, such as hypoxia or stress signals. The beneficial effects of resveratrol mediated by SIRT1 activation can be contributed by different organs [24, 86, 93, 94]. Resveratrol improves heart function following T-H injury by downregulating SIRT1 expression [86]. The protective effect of resveratrol on left ventricular contractility and systemic TNF-α levels is abolished by sirtinol (a SIRT1 inhibitor) [86]. In addition, Jian et al.

indicated that SIRT1 enzyme activity is decreased following T-H injury [94]. SIRT1 modulates left ventricular function in T-H injury through regulation of cellular energetic. The results suggest that the reduced SIRT1 levels in T-H injury may be related to declining mitochondrial function [94].

6. The Endothelial Protective Effect of Resveratrol in T-H Injury

Oxidative stress and superoxide radical generation are believed to contribute to the pathogenesis of endothelial dysfunction in low-flow states [95–97], resulting in inadequate tissue perfusion [96, 97].

Endothelial nicotinamide adenine dinucleotide phosphate-oxidase (NOX) is an important source of reactive oxygen species (ROS) of the vasculature, and, under various stressful conditions, a significant increase in NOX-generated ROS by the endothelium has been observed [95, 98]. Elevated ROS is a critical contributing factor to endothelial dysfunction, and antioxidants have been demonstrated to reduce ROS-induced injuries [95, 98]. Resveratrol has broad antioxidant and anti-inflammatory activities in a number of biological reactions [15, 99, 100], for instance, cardiovascular beneficial effects on atherosclerosis, ventricular arrhythmia, and myocardial ischemia-reperfusion I/R injury [101, 102]. Resveratrol's cardioprotective effects in I/R injury are achieved through its ROS-scavenging activity [77, 103]. However, the cardiovascular benefit of resveratrol may not simply be attributable to its antioxidant effect. Recent findings show that resveratrol reduces NOX activity in rat aortic endothelial cells and macrophages [20, 104, 105]. Resveratrol prevents T-H injury-induced oxidative stress and protects endothelium from subsequent oxidative functional damages [20]. The beneficial effects include inhibition of the NOX activity and direct scavenging of ROS. The protective effects of resveratrol are likely through suppression of the NOX enzyme complex activity in the cell membrane and the cytosol, including decreased membrane-bound proteins p22phox and gp91phox and cytosolic protein p47phox [20].

HO-1 appears to act as a protective agent in many organs against insults, such as trauma, ischemia, and oxidative stress [67, 106, 107]. Estrogen or flutamide enhances HO-1 expression, and resveratrol can modulate HO-1 induction via ER-related pathway [18, 20]. The upregulation in HO-1 is associated with the prevention of endothelial dysfunction and the salutary effects of resveratrol on endothelial function are mediated in part by upregulation of the HO-1-related pathway via ER [20].

7. Conclusions

Resveratrol has been shown to possess the beneficial effects in various studies and experimental conditions. There is increasing evidence that resveratrol maintains organ function after trauma or shock-like states. Resveratrol can attenuate organs injury in T-H injury through multiple pathways. However, the protective benefits of resveratrol may not simply be attributed to its anti-inflammatory or antioxidant effect. It is implicated that resveratrol is also mediated in part via a variety of intracellular signaling pathways, including the regulation of the HO-1/MAPK, PI3K/Akt, ER, and SIRT1. This complex network needs additional elucidation in future experimental studies and clinical trials.

Abbreviations

T-H:	Trauma-hemorrhage
ER:	Estrogen receptor
SIRT1:	Sirtuin 1
HO-1:	Hemeoxygenase-1
p38 MAPK:	p38 mitogen-activated protein kinase
PI3K:	Phosphatidylinositol 3-kinase
Akt:	Protein kinase B
NF-κB:	Nuclear factor-kappa B
ROS:	Reactive oxygen species
MDA:	Malondialdehyde
NOX:	NADPH oxidase
MPO:	Myeloperoxidase
CINC-1:	Cytokine-induced neutrophil chemoattractant 1
ICAM-1:	Intercellular adhesion molecule 1
IL-6:	Interleukin 6
TNF-α:	Tumor necrosis factor-alpha
PDK1:	Pyruvate dehydrogenase kinase 1.

Conflict of Interests

The authors declare that there is no conflict of interests regarding the publication of this paper.

Acknowledgments

This work was partially supported by grants from the National Science Council (NSC102-2314-B-182A-051-MY3) and Chang Gung Memorial Hospital (CMRPG3B1052 and CMRPG3B1053) to Huang-Ping Yu. Support was also provided by the National Science Council (NSC103-2314-B-182-046-MY2) and Chang Gung Memorial Hospital (CMRPG3B1623) to Fu-Chao Liu.

References

[1] W. Yu, Y. C. Fu, and W. Wang, "Cellular and molecular effects of resveratrol in health and disease," *Journal of Cellular Biochemistry*, vol. 113, no. 3, pp. 752–759, 2012.

[2] L. M. Chu, A. D. Lassaletta, M. P. Robich, and F. W. Sellke, "Resveratrol in the prevention and treatment of coronary artery disease," *Current Atherosclerosis Reports*, vol. 13, no. 6, pp. 439–446, 2011.

[3] S. M. Hamza and J. R. B. Dyck, "Systemic and renal oxidative stress in the pathogenesis of hypertension: modulation of long-term control of arterial blood pressure by resveratrol," *Frontiers in Physiology*, vol. 5, article 292, 2014.

[4] L. Song, L. Chen, X. Zhang, J. Li, and W. Le, "Resveratrol ameliorates motor neuron degeneration and improves survival in $SOD1^{G93A}$ mouse model of amyotrophic lateral sclerosis,"

BioMed Research International, vol. 2014, Article ID 483501, 10 pages, 201.

[5] S. Yavuz, N. E. Aydin, O. Celik, E. Yilmaz, E. Ozerol, and K. Tanbek, "Resveratrol successfully treats experimental endometriosis through modulation of oxidative stress and lipid peroxidation," *Journal of Cancer Research and Therapeutics*, vol. 10, no. 2, pp. 324–329, 2014.

[6] J. M. O. Andrade, A. F. Paraíso, M. V. M. de Oliveira et al., "Resveratrol attenuates hepatic steatosis in high-fat fed mice by decreasing lipogenesis and inflammation," *Nutrition*, vol. 30, no. 7-8, pp. 915–919, 2014.

[7] M. Azachi, R. Yatuv, A. Katz, Y. Hagay, and A. Danon, "A novel red grape cells complex: health effects and bioavailability of natural resveratrol," *International Journal of Food Sciences and Nutrition*, vol. 65, no. 7, pp. 848–855, 2014.

[8] S. Heebøll, K. L. Thomsen, S. B. Pedersen, H. Vilstrup, J. George, and H. Grønbæk, "Effects of resveratrol in experimental and clinical non-alcoholic fatty liver disease," *World Journal of Hepatology*, vol. 6, no. 4, pp. 188–198, 2014.

[9] J. Tian and J. W. Chen, "The application of resveratrol in treating rheumatic disease: a review," *Zhongguo Zhong Xi Yi Jie He Za Zhi*, vol. 32, no. 12, pp. 1710–1713, 2012.

[10] K. Legg, "Metabolic disease: identifying novel targets of resveratrol," *Nature Reviews Drug Discovery*, vol. 11, no. 4, p. 273, 2012.

[11] K. Magyar, R. Halmosi, A. Palfi et al., "Cardioprotection by resveratrol: a human clinical trial in patients with stable coronary artery disease," *Clinical Hemorheology and Microcirculation*, vol. 50, no. 3, pp. 179–187, 2012.

[12] F. Li, Q. Gong, H. Dong, and J. Shi, "Resveratrol, a neuroprotective supplement for Alzheimer's disease," *Current Pharmaceutical Design*, vol. 18, no. 1, pp. 27–33, 2012.

[13] L. G. Wood, P. A. B. Wark, and M. L. Garg, "Antioxidant and anti-inflammatory effects of resveratrol in airway disease," *Antioxidants and Redox Signaling*, vol. 13, no. 10, pp. 1535–1548, 2010.

[14] A. Csiszar, "Anti-inflammatory effects of resveratrol: possible role in prevention of age-related cardiovascular disease," *Annals of the New York Academy of Sciences*, vol. 1215, no. 1, pp. 117–122, 2011.

[15] W. Wang, L. Sun, P. Zhang, J. Song, and W. Liu, "An anti-inflammatory cell-free collagen/resveratrol scaffold for repairing osteochondral defects in rabbits," *Acta Biomaterialia*, vol. 10, no. 12, pp. 4983–4995, 2014.

[16] J. C. Nwachukwu, S. Srinivasan, N. E. Bruno et al., "Resveratrol modulates the inflammatory response via an estrogen receptor-signal integration network," *eLife*, vol. 3, p. e02057, 2014.

[17] M. C. Saleh, B. J. Connell, and T. M. Saleh, "Resveratrol induced neuroprotection is mediated via both estrogen receptor subtypes, ER_{α} and ER_{β}," *Neuroscience Letters*, vol. 548, pp. 217–221, 2013.

[18] H.-P. Yu, T.-L. Hwang, P.-W. Hsieh, and Y.-T. Lau, "Role of estrogen receptor-dependent upregulation of P38 MAPK/heme oxygenase 1 in resveratrol-mediated attenuation of intestinal injury after trauma-hemorrhage," *Shock*, vol. 35, no. 5, pp. 517–523, 2011.

[19] C. M. Klinge, K. A. Blankenship, K. E. Risinger et al., "Resveratrol and estradiol rapidly activate MAPK signaling through estrogen receptors alpha and beta in endothelial cells," *The Journal of Biological Chemistry*, vol. 280, no. 9, pp. 7460–7468, 2005.

[20] H.-P. Yu, T.-L. Hwang, T.-L. Hwang, C.-H. Yen, and Y.-T. Lau, "Resveratrol prevents endothelial dysfunction and aortic superoxide production after trauma hemorrhage through estrogen receptor-dependent hemeoxygenase-1 pathway," *Critical Care Medicine*, vol. 38, no. 4, pp. 1147–1154, 2010.

[21] J. Ren, C. Fan, N. Chen, J. Huang, and Q. Yang, "Resveratrol pretreatment attenuates cerebral ischemic injury by upregulating expression of transcription factor Nrf2 and HO-1 in Rats," *Neurochemical Research*, vol. 36, no. 12, pp. 2352–2362, 2011.

[22] Y. Zheng, Y. Liu, J. Ge et al., "Resveratrol protects human lens epithelial cells against H_2O_2- induced oxidative stress by increasing catalase, SOD-1, and HO-1 expression," *Molecular Vision*, vol. 16, pp. 1467–1474, 2010.

[23] N. Tamaki, R. C. Orihuela-Campos, Y. Inagaki, M. Fukui, T. Nagata, and H.-O. Ito, "Resveratrol improves oxidative stress and prevents the progression of periodontitis via the activation of the Sirt1/AMPK and the Nrf2/antioxidant defense pathways in a rat periodontitis model," *Free Radical Biology and Medicine*, vol. 75, pp. 222–229, 2014.

[24] J. Li, L. Feng, Y. Xing et al., "Radioprotective and antioxidant effect of resveratrol in hippocampus by activating Sirt1," *International Journal of Molecular Sciences*, vol. 15, no. 4, pp. 5928–5939, 2014.

[25] Z. Ren, L. Wang, J. Cui et al., "Resveratrol inhibits NF-κB signaling through suppression of p65 and IkappaB kinase activities," *Pharmazie*, vol. 68, no. 8, pp. 689–694, 2013.

[26] J. Zhang, J. Chen, J. Yang et al., "Resveratrol attenuates oxidative stress induced by balloon injury in the rat carotid artery through actions on the ERK1/2 and NF-kappa B pathway," *Cellular Physiology and Biochemistry*, vol. 31, no. 2-3, pp. 230–241, 2013.

[27] M. Mokni, S. Hamlaoui, I. Karkouch et al., "Resveratrol provides cardioprotection after ischemia/reperfusion injury via modulation of antioxidant enzyme activities," *Iranian Journal of Pharmaceutical Research*, vol. 12, no. 4, pp. 867–875, 2013.

[28] H. A. Bagriyanik, N. Ersoy, C. Cetinkaya et al., "The effects of resveratrol on chronic constriction injury of sciatic nerve in rats," *Neuroscience Letters*, vol. 561, pp. 123–127, 2014.

[29] J. Zhang, N. Tong, Y. Chen, P. Li, S. Yang, and X. Zhao, "Resveratrol protects against vinorelbine-induced vascular endothelial cell injury," *Toxicology Mechanisms and Methods*, vol. 23, no. 9, pp. 665–671, 2013.

[30] H. X. Zhang, G. L. Duan, C. N. Wang, Y. Q. Zhang, X. Y. Zhu, and Y. J. Liu, "Protective effect of resveratrol against endotoxemia-induced lung injury involves the reduction of oxidative/nitrative stress," *Pulmonary Pharmacology & Therapeutics*, vol. 27, no. 2, pp. 150–155, 2014.

[31] A. P. Vin, H. Hu, Y. Zhai et al., "Neuroprotective effect of resveratrol prophylaxis on experimental retinal ischemic injury," *Experimental Eye Research*, vol. 108, pp. 72–75, 2013.

[32] T. Tunali-Akbay, O. Sehirli, F. Ercan, and G. Sener, "Resveratrol protects against methotrexate-induced hepatic injury in rats," *Journal of Pharmacy and Pharmaceutical Sciences*, vol. 13, no. 2, pp. 303–310, 2010.

[33] T. de Jesus Soares, R. A. Volpini, H. D. C. Francescato, R. S. Costa, C. G. A. da Silva, and T. M. Coimbra, "Effects of resveratrol on glycerol-induced renal injury," *Life Sciences*, vol. 81, no. 8, pp. 647–656, 2007.

[34] J. W. Gatson, M. M. Liu, K. Abdelfattah et al., "Resveratrol decreases inflammation in the brain of mice with mild traumatic brain injury," *Journal of Trauma and Acute Care Surgery*, vol. 74, no. 2, pp. 470–475, 2013.

[35] L. J. McGhan and D. E. Jaroszewski, "The role of toll-like receptor-4 in the development of multi-organ failure following traumatic haemorrhagic shock and resuscitation," *Injury*, vol. 43, no. 2, pp. 129–136, 2012.

[36] D. M. Stein, J. Menaker, K. McQuillan, C. Handley, B. Aarabi, and T. M. Scalea, "Risk factors for organ dysfunction and failure in patients with acute traumatic cervical spinal cord injury," *Neurocritical Care*, vol. 13, no. 1, pp. 29–39, 2010.

[37] F.-C. Liu, Y.-F. Tsai, and H.-P. Yu, "Sirtinol attenuates trauma hemorrhage-induced hepatic injury through Akt-dependent pathway in rats," *Journal of Trauma and Acute Care Surgery*, vol. 74, no. 4, pp. 1027–1032, 2013.

[38] Y.-F. Tsai, F.-C. Liu, Y.-T. Lau, and H.-P. Yu, "Role of Akt-dependent pathway in resveratrol-mediated cardioprotection after trauma-hemorrhage," *Journal of Surgical Research*, vol. 176, no. 1, pp. 171–177, 2012.

[39] H.-P. Yu, S.-C. Yang, Y.-T. Lau, and T.-L. Hwang, "Role of Akt-dependent up-regulation of hemeoxygenase-1 in resveratrol-mediated attenuation of hepatic injury after trauma hemorrhage," *Surgery*, vol. 148, no. 1, pp. 103–109, 2010.

[40] C.-T. Wu, H.-P. Yu, C.-Y. Chung, Y.-T. Lau, and S.-K. Liao, "Attenuation of lung inflammation and pro-inflammatory cytokine production by resveratrol following trauma-hemorrhage," *The Chinese Journal of Physiology*, vol. 51, no. 6, pp. 363–368, 2008.

[41] H.-P. Yu, J.-C. Hsu, T.-L. Hwang, C.-H. Yen, and Y.-T. Lau, "Resveratrol attenuates hepatic injury after trauma-hemorrhage via estrogen receptor-related pathway," *Shock*, vol. 30, no. 3, pp. 324–328, 2008.

[42] F.-C. Liu, Y.-J. Day, C.-H. Liao, J.-T. Liou, C.-C. Mao, and H.-P. Yu, "Hemeoxygenase-1 upregulation is critical for sirtinol-mediated attenuation of lung injury after trauma-hemorrhage in a rodent model," *Anesthesia & Analgesia*, vol. 108, no. 6, pp. 1855–1861, 2009.

[43] H.-P. Yu, M. A. Choudhry, T. Shimizu et al., "Mechanism of the salutary effects of flutamide on intestinal myeloperoxidase activity following trauma-hemorrhage: up-regulation of estrogen receptor-β-dependent HO-1," *Journal of Leukocyte Biology*, vol. 79, no. 2, pp. 277–284, 2006.

[44] D. I. Sonnier, A. T. Makley, L. A. W. Friend, S. R. Bailey, A. B. Lentsch, and T. A. Pritts, "Hemorrhagic shock induces a proinflammatory milieu in the gut lumen," *Journal of Surgical Research*, vol. 170, no. 2, pp. 272–279, 2011.

[45] T. Shimizu, H.-P. Yu, Y.-C. Hsieh et al., "Flutamide attenuates pro-inflammatory cytokine production and hepatic injury following trauma-hemorrhage via estrogen receptor-related pathway," *Annals of Surgery*, vol. 245, no. 2, pp. 297–304, 2007.

[46] T. Suzuki, T. Shimizu, H.-P. Yu et al., "Tissue compartment-specific role of estrogen receptor subtypes in immune cell cytokine production following trauma-hemorrhage," *Journal of Applied Physiology*, vol. 102, no. 1, pp. 163–168, 2007.

[47] H.-P. Yu, T. Shimizu, Y.-C. Hsieh et al., "Tissue-specific expression of estrogen receptors and their role in the regulation of neutrophil infiltration in various organs following trauma-hemorrhage," *Journal of Leukocyte Biology*, vol. 79, no. 5, pp. 963–970, 2006.

[48] F.-C. Liu, H.-P. Yu, T.-L. Hwang, and Y.-F. Tsai, "Protective effect of tropisetron on rodent hepatic injury after trauma-hemorrhagic shock through P38 MAPK-dependent hemeoxygenase-1 expression," *PLoS ONE*, vol. 7, no. 12, Article ID e53203, 2012.

[49] F.-C. Liu, Y.-J. Day, J.-T. Liou, Y.-T. Lau, and H.-P. Yu, "Sirtinol attenuates hepatic injury and pro-inflammatory cytokine production following trauma-hemorrhage in male Sprague-Dawley rats," *Acta Anaesthesiologica Scandinavica*, vol. 52, no. 5, pp. 635–640, 2008.

[50] H.-P. Yu, P.-W. Hsieh, Y.-J. Chang, P.-J. Chung, L.-M. Kuo, and T.-L. Hwang, "DSM-RX78, a new phosphodiesterase inhibitor, suppresses superoxide anion production in activated human neutrophils and attenuates hemorrhagic shock-induced lung injury in rats," *Biochemical Pharmacology*, vol. 78, no. 8, pp. 983–992, 2009.

[51] H.-P. Yu, S. Yang, Y.-C. Hsieh, M. A. Choudhry, K. I. Bland, and I. H. Chaudry, "Maintenance of lung myeloperoxidase activity in proestrus females after trauma-hemorrhage: upregulation of heme oxygenase-1," *The American Journal of Physiology—Lung Cellular and Molecular Physiology*, vol. 291, no. 3, pp. L400–L406, 2006.

[52] S. D. Dayal, G. Haskó, Q. Lu et al., "Trauma/hemorrhagic shock mesenteric lymph upregulates adhesion molecule expression and IL-6 production in human umbilical vein endothelial cells," *Shock*, vol. 17, no. 6, pp. 491–495, 2002.

[53] R. Yang, X. Han, T. Uchiyama et al., "IL-6 is essential for development of gut barrier dysfunction after hemorrhagic shock and resuscitation in mice," *The American Journal of Physiology: Gastrointestinal and Liver Physiology*, vol. 285, no. 3, pp. G621–G629, 2003.

[54] Z. H. Meng, K. Dyer, T. R. Billiar, and D. J. Tweardy, "Essential role for IL-6 in postresuscitation inflammation in hemorrhagic shock," *American Journal of Physiology—Cell Physiology*, vol. 280, no. 2, pp. C343–C351, 2001.

[55] T. Suzuki, T. Shimizu, H.-P. Yu et al., "Estrogen receptor-alpha predominantly mediates the salutary effects of 17beta-estradiol on splenic macrophages following trauma-hemorrhage," *The American Journal of Physiology: Cell Physiology*, vol. 293, no. 3, pp. C978–C984, 2007.

[56] H.-P. Yu, S.-T. Pang, and I. H. Chaudry, "Hepatic gene expression patterns following trauma-hemorrhage: effect of posttreatment with estrogen," *Shock*, vol. 39, no. 1, pp. 77–82, 2013.

[57] H. Sebai, M. Sani, M. T. Yacoubi, E. Aouani, N. Ghanem-Boughanmi, and M. Ben-Attia, "Resveratrol, a red wine polyphenol, attenuates lipopolysaccharide-induced oxidative stress in rat liver," *Ecotoxicology and Environmental Safety*, vol. 73, no. 5, pp. 1078–1083, 2010.

[58] M. A. Choudhry, K. I. Bland, and I. H. Chaudry, "Trauma and immune response—effect of gender differences," *Injury*, vol. 38, no. 12, pp. 1382–1391, 2007.

[59] M. A. Choudhry, M. G. Schwacha, W. J. Hubbard et al., "Gender differences in acute response to trauma-hemorrhage," *Shock*, vol. 24, no. 1, pp. 101–106, 2005.

[60] T. Shimizu, H.-P. Yu, T. Suzuki et al., "The role of estrogen receptor subtypes in ameliorating hepatic injury following trauma-hemorrhage," *Journal of Hepatology*, vol. 46, no. 6, pp. 1047–1054, 2007.

[61] T. Suzuki, T. Shimizu, H.-P. Yu, Y.-C. Hsieh, M. A. Choudhry, and I. H. Chaudry, "Salutary effects of 17beta-estradiol on T-cell signaling and cytokine production after trauma-hemorrhage are mediated primarily via estrogen receptor-alpha," *The American Journal of Physiology: Cell Physiology*, vol. 292, no. 6, pp. C2103–C2111, 2007.

[62] H.-P. Yu and I. H. Chaudry, "The role of estrogen and receptor agonists in maintaining organ function after trauma-hemorrhage," *Shock*, vol. 31, no. 3, pp. 227–237, 2009.

[63] H. P. Yu, Y. C. Hsieh, T. Suzuki et al., "Salutary effects of estrogen receptor-β agonist on lung injury after trauma-hemorrhage," *The American Journal of Physiology—Lung Cellular and Molecular Physiology*, vol. 290, no. 5, pp. L1004–L1009, 2006.

[64] H. P. Yu, Y. C. Hsieh, T. Suzuki et al., "The PI3K/Akt pathway mediates the nongenomic cardioprotective effects of estrogen following trauma-hemorrhage," *Annals of Surgery*, vol. 245, no. 5, pp. 971–977, 2007.

[65] A. A. Elmarakby, J. Faulkner, B. Baban, and J. C. Sullivan, "Induction of hemeoxygenase-1 reduces renal oxidative stress and inflammation in diabetic spontaneously hypertensive rats," *International Journal of Hypertension*, vol. 2012, Article ID 957235, 11 pages, 2012.

[66] A. A. Elmarakby, J. Faulkner, S. P. Posey, and J. C. Sullivan, "Induction of hemeoxygenase-1 attenuates the hypertension and renal inflammation in spontaneously hypertensive rats," *Pharmacological Research*, vol. 62, no. 5, pp. 400–407, 2010.

[67] J.-T. Hsu, W.-H. Kan, C.-H. Hsieh, M. A. Choudhry, K. I. Bland, and I. H. Chaudry, "Mechanism of salutary effects of estrogen on cardiac function following trauma-hemorrhage: akt-dependent HO-1 up-regulation," *Critical Care Medicine*, vol. 37, no. 8, pp. 2338–2344, 2009.

[68] J.-T. Hsu, W. H. Kan, C.-H. Hsieh et al., "Mechanism of estrogen-mediated attenuation of hepatic injury following trauma-hemorrhage: Akt-dependent HO-1 up-regulation," *Journal of Leukocyte Biology*, vol. 82, no. 4, pp. 1019–1026, 2007.

[69] J.-T. Hsu, H.-C. Yeh, T.-H. Chen et al., "Role of Akt/HO-1 pathway in estrogen-mediated attenuation of trauma-hemorrhage-induced lung injury," *Journal of Surgical Research*, vol. 182, no. 2, pp. 319–325, 2013.

[70] F.-C. Liu, T.-L. Hwang, Y.-T. Lau, and H.-P. Yu, "Mechanism of salutary effects of astringinin on rodent hepatic injury following trauma-hemorrhage: Akt-dependent hemeoxygenase-1 signaling pathways," *PLoS ONE*, vol. 6, no. 10, Article ID e25907, 2011.

[71] B. Chen, J. Xue, X. Meng, J. L. Slutzky, A. E. Calvert, and L. G. Chicoine, "Resveratrol prevents hypoxia-induced arginase II expression and proliferation of human pulmonary artery smooth muscle cells via Akt-dependent signaling," *The American Journal of Physiology—Lung Cellular and Molecular Physiology*, vol. 307, no. 4, pp. L317–L325, 2014.

[72] F. Simão, A. Matté, A. S. Pagnussat, C. A. Netto, and C. G. Salbego, "Resveratrol prevents CA1 neurons against ischemic injury by parallel modulation of both GSK-3beta and CREB through PI3-K/Akt pathways," *European Journal of Neuroscience*, vol. 36, no. 7, pp. 2899–2905, 2012.

[73] R. D. Powell, J. H. Swet, K. L. Kennedy, T. T. Huynh, I. H. McKillop, and S. L. Evans, "Resveratrol attenuates hypoxic injury in a primary hepatocyte model of hemorrhagic shock and resuscitation," *Journal of Trauma and Acute Care Surgery*, vol. 76, no. 2, pp. 409–417, 2014.

[74] F.-C. Liu, F.-W. Liu, and H.-P. Yu, "Ondansetron attenuates hepatic injury via p38 MAPK-dependent pathway in a rat haemorrhagic shock model," *Resuscitation*, vol. 82, no. 3, pp. 335–340, 2011.

[75] J.-T. Hsu, W.-H. Kan, C.-H. Hsieh et al., "Mechanism of estrogen-mediated intestinal protection following trauma-hemorrhage: p38 MAPK-dependent upregulation of HO-1," *The American Journal of Physiology—Regulatory Integrative and Comparative Physiology*, vol. 294, no. 6, pp. R1825–R1831, 2008.

[76] X. W. Liu, E. F. Ji, P. He, R. X. Xing, B. X. Tian, and X. D. Li, "Protective effects of the p38 MAPK inhibitor SB203580 on NMDA-induced injury in primary cerebral cortical neurons," *Molecular Medicine Reports*, vol. 10, no. 4, pp. 1942–1948, 2014.

[77] S. Wang, Q. Huang, J. Guo et al., "Local thermal injury induces general endothelial cell contraction through p38 MAP kinase activation," *Acta Pathologica, Microbiologica et Immunologica Scandinavica*, vol. 122, no. 9, pp. 832–841, 2014.

[78] J. Ma, Y.-Q. Fang, A.-M. Gu, F.-F. Wang, S. Zhang, and K.-C. Li, "P38 activation is more important than ERK activation in lung injury induced by prolonged hyperbaric oxygen," *Undersea and Hyperbaric Medicine*, vol. 40, no. 4, pp. 313–318, 2013.

[79] D. E. Shifflett, S. L. Jones, A. J. Moeser, and A. T. Blikslager, "Mitogen-activated protein kinases regulate COX-2 and mucosal recovery in ischemic-injured porcine ileum," *The American Journal of Physiology: Gastrointestinal and Liver Physiology*, vol. 286, no. 6, pp. G906–G913, 2004.

[80] L. Aoudjit, M. Stanciu, H. Li, S. Lemay, and T. Takano, "p38 mitogen-activated protein kinase protects glomerular epithelial cells from complement-mediated cell injury," *The American Journal of Physiology—Renal Physiology*, vol. 285, no. 4, pp. F765–F774, 2003.

[81] S. Sánchez-Fidalgo, A. Cárdeno, I. Villegas, E. Talero, and C. A. de la Lastra, "Dietary supplementation of resveratrol attenuates chronic colonic inflammation in mice," *European Journal of Pharmacology*, vol. 633, no. 1–3, pp. 78–84, 2010.

[82] X. C. Lv and H. Y. Zhou, "Resveratrol protects H9c2 embryonic rat heart derived cells from oxidative stress by inducing autophagy: role of p38 mitogen-activated protein kinase," *Canadian Journal of Physiology and Pharmacology*, vol. 90, no. 5, pp. 655–662, 2012.

[83] D. Babu, S. J. Soenen, K. Raemdonck et al., "TNF-α/cycloheximide-induced oxidative stress and apoptosis in murine intestinal epithelial MODE-K cells," *Current Pharmaceutical Design*, vol. 18, no. 28, pp. 4414–4425, 2012.

[84] M. Mokni, F. Limam, S. Elkahoui, M. Amri, and E. Aouani, "Strong cardioprotective effect of resveratrol, a red wine polyphenol, on isolated rat hearts after ischemia/reperfusion injury," *Archives of Biochemistry and Biophysics*, vol. 457, no. 1, pp. 1–6, 2007.

[85] L.-M. Hung, M.-J. Su, and J.-K. Chen, "Resveratrol protects myocardial ischemia-reperfusion injury through both NO-dependent and NO-independent mechanisms," *Free Radical Biology and Medicine*, vol. 36, no. 6, pp. 774–781, 2004.

[86] B. Jian, S. Yang, I. H. Chaudry, and R. Raju, "Resveratrol improves cardiac contractility following trauma-hemorrhage by modulating Sirt1," *Molecular Medicine*, vol. 18, no. 2, pp. 209–214, 2012.

[87] X. Jiang, C. Ai, E. Shi, Y. Nakajima, and H. Ma, "Neuroprotection against spinal cord ischemia-reperfusion injury induced by different ischemic postconditioning methods: roles of phosphatidylinositol 3-kinase-akt and extracellular signal-regulated kinase," *Anesthesiology*, vol. 111, no. 6, pp. 1197–1205, 2009.

[88] L. Lv, Q. Meng, J. Xu, J. Gong, Y. Cheng, and S. Jiang, "Ligustrazine attenuates myocardial ischemia reperfusion injury in rats by activating the phosphatidylinositol 3-kinase/Akt pathway," *Annals of Clinical and Laboratory Science*, vol. 42, no. 2, pp. 198–202, 2012.

[89] G. Schabbauer, M. Tencati, B. Pedersen, R. Pawlinski, and N. Mackman, "PI3K-Akt pathway suppresses coagulation and inflammation in endotoxemic mice," *Arteriosclerosis, Thrombosis, and Vascular Biology*, vol. 24, no. 10, pp. 1963–1969, 2004.

[90] W.-P. Fung-Leung, "Phosphoinositide 3-kinase delta (PI3Kδ) in leukocyte signaling and function," *Cellular Signalling*, vol. 23, no. 4, pp. 603–608, 2011.

[91] H. He, F. X. Yu, C. Sun, and Y. Luo, "CBP/p300 and SIRT1 are involved in transcriptional regulation of S-phase specific histone genes," *PLoS ONE*, vol. 6, no. 7, Article ID e22088, 2011.

[92] K. Pruitt, R. L. Zinn, J. E. Ohm et al., "Inhibition of SIRT1 reactivates silenced cancer genes without loss of promoter DNA hypermethylation," *PLoS Genetics*, vol. 2, no. 3, article e40, 2006.

[93] Y.-G. Li, W. Zhu, J.-P. Tao et al., "Resveratrol protects cardiomyocytes from oxidative stress through SIRT1 and mitochondrial biogenesis signaling pathways," *Biochemical and Biophysical Research Communications*, vol. 438, no. 2, pp. 270–276, 2013.

[94] B. Jian, S. Yang, I. H. Chaudry, and R. Raju, "Resveratrol restores sirtuin 1 (SIRT1) activity and pyruvate dehydrogenase kinase 1 (PDK1) expression after hemorrhagic injury in a rat model," *Molecular Medicine*, vol. 20, no. 1, pp. 10–16, 2014.

[95] H.-P. Yu, P.-W. Lui, T.-L. Hwang, C.-H. Yen, and Y.-T. Lau, "Propofol improves endothelial dysfunction and attenuates vascular superoxide production in septic rats," *Critical Care Medicine*, vol. 34, no. 2, pp. 453–460, 2006.

[96] Z. F. Ba, J. F. Kuebler, L. W. Rue III, K. I. Bland, P. Wang, and I. H. Chaudry, "Gender dimorphic tissue perfusion response after acute hemorrhage and resuscitation: role of vascular endothelial cell function," *American Journal of Physiology: Heart and Circulatory Physiology*, vol. 284, no. 6, pp. H2162–H2169, 2003.

[97] P. Wang, Z. F. Ba, and I. H. Chaudry, "Endothelial cell dysfunction occurs very early following trauma- hemorrhage and persists despite fluid resuscitation," *The American Journal of Physiology: Heart and Circulatory Physiology*, vol. 265, no. 3, part 2, pp. H973–H979, 1993.

[98] A. C. Montezano and R. M. Touyz, "Reactive oxygen species and endothelial function—role of nitric oxide synthase uncoupling and nox family nicotinamide adenine dinucleotide phosphate oxidases," *Basic & Clinical Pharmacology and Toxicology*, vol. 110, no. 1, pp. 87–94, 2012.

[99] P. Orsu, B. V. S. N. Murthy, and A. Akula, "Cerebroprotective potential of resveratrol through anti-oxidant and anti-inflammatory mechanisms in rats," *Journal of Neural Transmission*, vol. 120, no. 8, pp. 1217–1223, 2013.

[100] S. Bo, G. Ciccone, A. Castiglione et al., "Anti-inflammatory and antioxidant effects of resveratrol in healthy smokers a randomized, double-blind, placebo-controlled, cross-over trial," *Current Medicinal Chemistry*, vol. 20, no. 10, pp. 1323–1331, 2013.

[101] G. Petrovski, N. Gurusamy, and D. K. Das, "Resveratrol in cardiovascular health and disease," *Annals of the New York Academy of Sciences*, vol. 1215, no. 1, pp. 22–33, 2011.

[102] H. Z. Toklu, Ö. Şehirli, M. Erşahin et al., "Resveratrol improves cardiovascular function and reduces oxidative organ damage in the renal, cardiovascular and cerebral tissues of two-kidney, one-clip hypertensive rats," *Journal of Pharmacy and Pharmacology*, vol. 62, no. 12, pp. 1784–1793, 2010.

[103] X. Cong, Y. Li, N. Lu et al., "Resveratrol attenuates the inflammatory reaction induced by ischemia/reperfusion in the rat heart," *Molecular Medicine Reports*, vol. 9, no. 6, pp. 2528–2532, 2014.

[104] Y. Tang, J. Xu, W. Qu et al., "Resveratrol reduces vascular cell senescence through attenuation of oxidative stress by SIRT1/NADPH oxidase-dependent mechanisms," *The Journal of Nutritional Biochemistry*, vol. 23, no. 11, pp. 1410–1416, 2012.

[105] S.-E. Chow, Y.-C. Hshu, J.-S. Wang, and J.-K. Chen, "Resveratrol attenuates oxLDL-stimulated NADPH oxidase activity and protects endothelial cells from oxidative functional damages," *Journal of Applied Physiology*, vol. 102, no. 4, pp. 1520–1527, 2007.

[106] J. Wang, X. Hu, and H. Jiang, "Nrf-2-HO-1-HMGB1 axis: an important therapeutic approach for protection against myocardial ischemia and reperfusion injury," *International Journal of Cardiology*, vol. 172, no. 1, pp. 223–224, 2014.

[107] S. Tsuchihashi, Y. Zhai, C. Fondevila, R. W. Busuttil, and J. W. Kupiec-Weglinski, "HO-1 upregulation suppresses type 1 IFN pathway in hepatic ischemia/reperfusion injury," *Transplantation Proceedings*, vol. 37, no. 4, pp. 1677–1678, 2005.

Hindawi Publishing Corporation
Mediators of Inflammation
Volume 2015, Article ID 965925, 12 pages
http://dx.doi.org/10.1155/2015/965925

Clinical Study

I-gel Laryngeal Mask Airway Combined with Tracheal Intubation Attenuate Systemic Stress Response in Patients Undergoing Posterior Fossa Surgery

Chaoliang Tang, Xiaoqing Chai, Fang Kang, Xiang Huang, Tao Hou, Fei Tang, and Juan Li

Department of Anesthesiology, Anhui Provincial Hospital, Anhui Medical University, No.1 Swan Lake Road, Hefei 230036, China

Correspondence should be addressed to Juan Li; huamuzi1999@126.com

Received 9 January 2015; Accepted 13 February 2015

Academic Editor: Huang-Ping Yu

Background. The adverse events induced by intubation and extubation may cause intracranial hemorrhage and increase of intracranial pressure, especially in posterior fossa surgery patients. In this study, we proposed that I-gel combined with tracheal intubation could reduce the stress response of posterior fossa surgery patients. *Methods*. Sixty-six posterior fossa surgery patients were randomly allocated to receive either tracheal tube intubation (Group TT) or I-gel facilitated endotracheal tube intubation (Group TI). Hemodynamic and respiratory variables, stress and inflammatory response, oxidative stress, anesthesia recovery parameters, and adverse events during emergence were compared. *Results*. Mean arterial pressure and heart rate were lower in Group TI during intubation and extubation ($P < 0.05$ versus Group TT). Respiratory variables including peak airway pressure and end-tidal carbon dioxide tension were similar intraoperative, while plasma β-endorphin, cortisol, interleukin-6, tumor necrosis factor-alpha, malondialdehyde concentrations, and blood glucose were significantly lower in Group TI during emergence relative to Group TT. Postoperative bucking and serious hypertensions were seen in Group TT but not in Group TI. *Conclusion*. Utilization of I-gel combined with endotracheal tube in posterior fossa surgery patients is safe which can yield more stable hemodynamic profile during intubation and emergence and lower inflammatory and oxidative response, leading to uneventful recovery.

1. Introduction

Systemic and cerebral hemodynamic changes caused by extubation and emergence from anesthesia may endanger neurosurgical patients and increase the risk of postoperative intracranial hemorrhage and cerebral edema and may even result in the requirement of reoperation [1].

Orotracheal intubation has been proven to be a reliable method for securing the airway and is considered to be the standard technique for intraoperative management of the airway during neurosurgery. During the procedure, the patient's head is covered and hidden under the surgical field and held in a position that is not convenient to control the airway. Therefore, intubation that can ensure adequate ventilation for long period may be the best choice. However, endotracheal intubation induces more intense hemodynamic effects and physical stress than those caused by the use of a laryngeal mask airway (LMA). During emergence from anesthesia and extubation, these differences are even more intense that can lead to increases in cerebral blood flow, intracranial pressure, and regional brain oxygen saturation (rSO_2) [2].

Generally, stress is defined as the hormonal and metabolic changes that follow any injury to the biological system. Such stress response is characterized by the systemic reaction to injury which encompasses a wide range of endocrinological, immunologic, and hematological effects [3]. The severity of stress response during surgery affects not only patient outcomes but also health care system. The plasma concentrations of β-endorphin (β-EP), cortisol (Cor), and blood glucose level (BG) are a reflection of stress sensitive indicators during anesthesia and surgery, and significant fluctuations in serum glucose levels accompany the stress response of surgery. In the recent decade, the brain has been regarded as an organ, which is susceptible to inflammation or immune activation, and also thought to be largely affected by systemic inflammatory and

immune responses and oxidative stress [4, 5]. Pathological inflammatory states can have far ranging clinical effects and negatively influence a patient's neurological outcome [6–8]. Cytokines regulate the acute phase response. Several cytokines are released during periods of stress, including interleukin-6 (IL-6), interleukin-8 (IL-8), and tumor necrosis factor-alpha (TNF-α) [9]. Studies have shown that surgical and anesthesia manipulation-induced sympathetic activation and oxidative stress may be the main factors that lead to hypertension, which could trigger the sympathetic nervous system and seems to be injurious to the patients, especially for neurosurgical patients [10]. Modification of the circulating hormone Cor, β-EP, BG level, inflammatory cytokine, and oxidative stress may be necessary to improve the surgical outcome [11].

In recent years, LMA is widely used in clinical practice due to its simple operation, low stimulation, and light stress reaction [12–14]. I-gel without sac is made of special medical grade thermoplastic elastomer and does not need to be inflated. It has a unique baffle that prevents the epiglottis folding and airway obstruction to reduce the likelihood of airway obstruction [15, 16]. I-gel without sac can be inserted into the stomach tube to prevent regurgitation and aspiration, and its massive air duct may help with the endotracheal tube placement. Due to the special position of posterior fossa surgery, simply placing a LMA is not conducive to ensure adequate ventilation that may lead to the accumulation of carbon dioxide and increases of intracranial pressure. I-gel combined with bronchial occlude for thoracic surgery has been reported [17]. However, the clinical use of I-gel combined with endotracheal tube for posterior fossa surgery has not been explored.

We compared the safety characteristics, systemic hemodynamic variables, the stress and inflammatory response, oxidative stress, and cough incidence during the induction and emergence of posterior fossa surgery patients receiving general anesthesia either used this new I-gel combined with endotracheal tube technique or used a traditional endotracheal tube airway technique in a prospective randomized clinical trial. Primary outcome measures were ease of perioperative stress and inflammatory response, and oxidative stress, airway management, and incidence of coughing.

2. Material and Methods

This prospective, randomized, clinical trial was approved by the Ethics Committee of Anhui Provincial Hospital, Anhui Medical University (file number 2011/07), and registered at Chinese Clinical Trial Registry (ChiCTR) with registration number ChiCTR-OOC-14005623.

2.1. Patients. Informed consent was obtained from all the patients. Sixty-six patients of either sex with the American Society Anesthesiologists physical status I-II, aged between 18 and 60 years, undergoing posterior fossa surgery under general anesthesia from the neurosurgery department of our center were recruited. Types of surgery included 12 cases of cerebellar hemisphere tumors, 6 cases of cerebellar vermis tumor, 12 cases of cerebellopontine angle tumors, 6 cases of fourth ventricle tumor, 25 cases of acoustic neuroma, and 5 cases of slope tumor. All patients were informed of the experimental protocol and purpose of the study.

Exclusion criteria included heart diseases, endocrine system diseases, and uncontrolled high blood pressure detected during preoperative assessment; predicted difficult airway, risk of bronchial aspiration (e.g., gastroesophageal reflux disease or lower cranial nerve palsy) and patients who need respirator for assisted ventilation after operation; obesity (BMI $> 30\,kg/m^2$); I-gel inserted unsuccessfully more than twice, patients with contraindications for early emergence based on anesthetic or surgical criteria or as a result of complications developing during surgery was also withdrawn from our study.

2.2. Study Design and Anesthesia Procedure. Four senior anesthetists and three high qualification residencies performed all the operations. The patients were randomized to the two study groups by random number table method, which was prepared by an unwitting statistician, tracheal tube intubation (Group TT) and I-gel facilitated endotracheal tube intubation (Group TI) ($n = 33$).

Patients took omeprazole (20 mg) on the ward the night before surgery. In the operating room, patients were premeditated with penehyclidine hydrochloride (0.5 to 1 mg, *i.m.*). Standard monitoring consisted of five-lead electrocardiography (ECG), oxygen saturation (SpO_2), mean arterial pressure (MAP), arterial and central venous pressures, and depth of anesthesia as assessed by BIS. Then all patients received hydroxyethyl starch 130/0.4 (Voluven) 8~10 mL/kg and were supplemented with oxygen (4 liter/min) via an O_2 nasal cannula. Dexmedetomidine was given at 0.6 μg/kg and then changed into 0.4 μg/kg/h for maintenance after 15 min. Before the start of anesthesia induction, an arterial line was inserted under local anesthesia and located the transducer probe at the level of the foramen of Monro; the line remained in place till the patient shifted to the surgical ward. 100% oxygen was pre-oxygenated before induction, which was delivered through a facial mask for no less than 3 minutes. General anesthesia was provided in the supine position with intravenous propofol (Cp 3.0–4.0 μg/mL) and remifentanil (Cp 3.0–4.0 ng/mL) delivered through a target controlled infusion system (ALARIS MK III, CareFusion, Switzerland) and rocuronium bromide (0.6–0.8 mg/kg). Manual facemask ventilation was continued for no less than 4 minutes until the jaw was relaxed and the BIS was less than 50. The endotracheal tube was inserted with the help of direct laryngoscope in Group TT (using ID 7.5 or 8 mm, for women or men, resp.). For patients in Group TI, the I-gel was inserted according to the manufacturer's instruction (using size 3 or 4, for 30~60 kg or 50–90 kg, resp.). Then the endotracheal tube was inserted through the I-gel's air duc under the guidance of the 2.8-mm Flexible Intubation Videoscope (TIC-SD-II; UESCOPE, China) (using ID 6.0 or 6.5 mm, for size 3 I-gel or 4 I-gel, resp.). The successful placement criteria of I-gel were confirmed by sides of the thoracic move ups and downs properly and lung respiratory sound was auscultated symmetrically, no sound was detected

when airway pressure > 20 cmH_2O, $ETCO_2$ waveform was normal, and the insertion of stomach tube was easy.

A ventilator (S/5; Datex Ohmeda, Helsinki, Finland) was connected immediately afterwards. Respiratory parameters were set at: VT 10 mL/kg, RR 12 times/min, and FiO_2 60% to maintain $ETCO_2$ in the normal range. 1% sevoflurane was inhaled and the target-controlled anesthesia system (TCI) was used to administer propofol and remifentanil to maintain the BIS between 40 and 60 and the MAP and HR variation not exceed 20% of the baseline values.

Patients were injected with tramadol 1.0 mg/kg and azasetron (10 mg) through the intravenous line after fixed skull flap. In Group TI, after suturing the scalp, we pulled out the endotracheal tube, stopped the TCI of anesthetics to make it possible for the patient to quickly emerge from anesthesia. We then shifted the patient to supine position and used the I-gel to continue to maintain the patient's ventilation until the patient was awake and then pulled out the I-gel. In Group TT, after suturing the scalp, the patient still under general anesthesia was shifted to supine position without modification of any anesthetic drug administration. Then we continued the ventilation with the same parameters as described earlier. TCI of anesthetics were then stopped to allow the patient quickly emerge from anesthesia. Before the patient resumed spontaneous breathing and responded to simple commands, gentle manual ventilatory assistance was provided. The endotracheal tube was then removed. The criteria of pulling out the endotracheal tube or I-gel was: (1) the recovery of consciousness, muscle tension returned to normal, fist clenched strongly according to the instruction; (2) steady spontaneous breathing, $ETCO_2$ < 45 mmHg, tidal volume > 7 mL/kg; (3) the SPO_2 > 97% after stopping to receive oxygen for 5 min; (4) the frequency of spontaneous breathing < 24 times/min; (5) cough and swallowing reflex recovered. The modified observer's assessment of alertness/sedation/(MOAA/S) score reached 3 as assessed according to the criteria: (0 (asleep) = no response to painful trapezius squeeze; 1 = responding only after painful trapezius squeeze; 2 = responding only after mild prodding or shaking; 3 = responding only after name is called loudly, repeatedly, or both; 4 = Lethargic response to name spoken in normal tone; 5 (alert) = responding readily to name spoken in normal tone) [18].

2.3. Outcome Measures. Hemodynamic variables (MAP and HR), were recorded at eight time points: baseline, before dexmedetomidine infusion (T0); before anesthetic induction (T1); endotracheal tube intubation (T2); 3 min after intubation (T3); end of surgery but before awakening (Group TT) or before endotracheal tube removed (Group TI) (T4); after patients entered the PACU (T5); and throughout emergence from anesthesia at 1, 5, 15, and 30 minutes after extubation or I-gel removal (according to group assignment) (T6-9). Respiratory variables (including peak airway pressure and end-tidal carbon dioxide tension) were recorded during mechanical ventilation, and arterial blood gases were also recorded. Blood pressure elevation (Blood pressure > 140/90 mmHg or increases more than 20% value), tachycardia (HR > 100 beats/min or an increase of >30 beats/min from baseline), choking cough occurrence during the recovering period of anesthesia were recorded and timely treated. Nicardipine, or esmolol was administered at a dose where the anesthesiologist considered appropriate to maintain the patient with stable vital signs and drug doses were recorded. Choking cough reflex degree is divided into: (1) No choking cough, breathe evenly; (2) Mild choking cough, separate a choking cough; (3) Moderate choking cough, choking cough < 30 s; (4) Severe choking cough, choking cough lasts 30 s or higher. Operation time, spontaneous breathing recovery time (the time that the patients resumed breathing after stopping giving anesthetics), eye opening time (the time that the patients opened their eyes after stopping giving anesthetics), extubation or I-gel removal time (the time that extubation in Group TT or I-gel removal in Group TI), and the MOAA/S score when extubation or I-gel removal were recorded.

2.4. Blood and Sputum Processing and Analyses. Four milliliter of venous blood was collected at following time points: T0, T1, T3, T5, and T6. One drop of blood was taken to measure blood glucose level (BG). The rest was added to tubes without anticoagulant, perfectly still until the serum separation, the serum precipitated was taken with centrifugal to centrifuge at 4000 rpm in 4°C for 10 min, and then the supernatant was sucked out to place in −80°C cryogenic refrigerator to wait to test β-EP and Cor at T0, T1, T3, T5, and T6; IL-6, IL-8, TNF-α, MDA and Superoxide Dismutase (SOD) at T0 (pre-operation) and T6 (post-operation). β-EP and Cor were assayed by enzyme-linked immunosorbent assay (ELISA) (2-CAT; Elabscience Biotechnology Co., Ltd). IL-6, IL-8, TNF-α, MDA and SOD levels in plasma were measured in the Immune Surveillance Laboratory at The Research Institute at Anhui Provincial Hospital using the Immulite automated chemiluminometer (Siemens Healthcare Diagnostics, Deerfeld, IL). All assays were performed according to manufacturer's instructions.

2.5. Statistical Analysis. The demographic characteristics were compared using a two-sample t test for continuous data. The χ^2 test was used to analyze categorical variables. Data are presented as Mean ± SD, Mean ± SEM or as count (%). Student I test and ANOVA were used for unpaired quantitative variables. All reported P values were two-sided, and P values less than 0.05 were considered significant. The statistical analyses were performed with SPSS Statistics 13.0 software.

3. Results

Flow diagram of patient recruitment was shown in Figure 1.

Patient and procedural characteristics of both groups are shown, respectively, in Table 1. There were no significant differences between groups at baseline.

No differences were found at baseline measurements of HR and MAP between the two groups. Both the groups had significant reduction in MAP and HR from their respective baseline values till the end of the surgery, however, patients in Group TI had a greater fall in comparison to Group TT over the time period of the observation. Of note, MAP

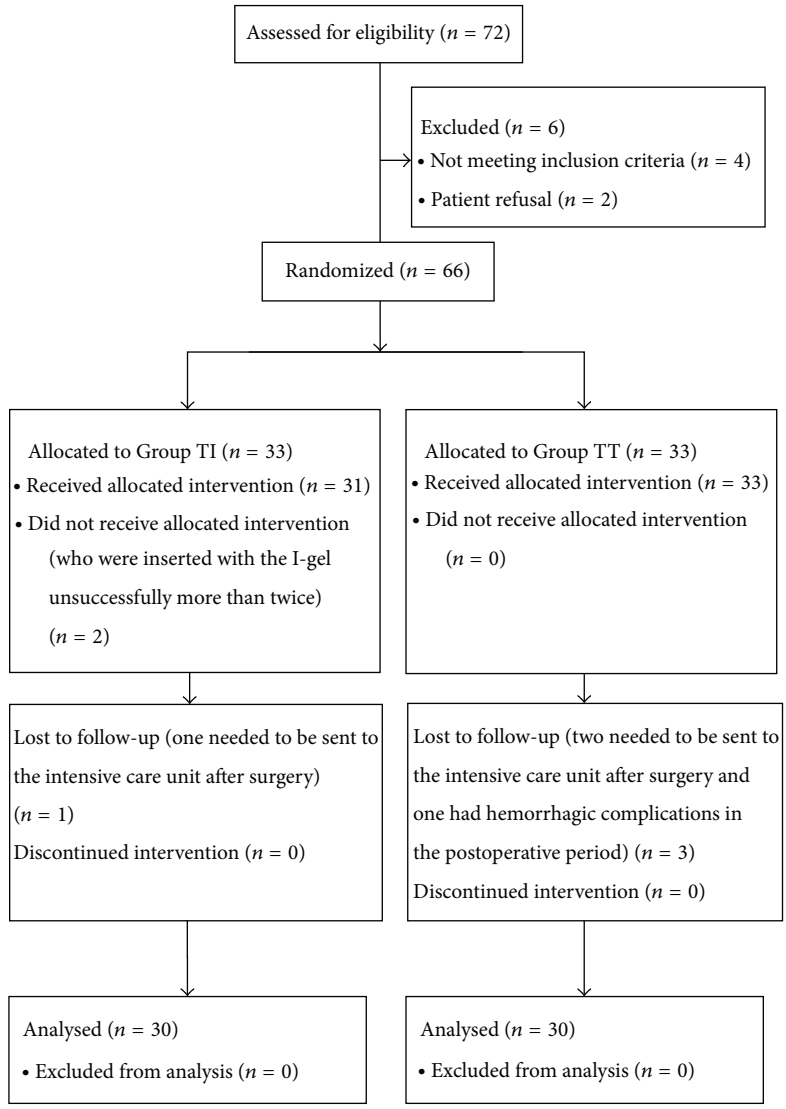

Figure 1: Flow diagram of patient recruitment.

and HR on emergence from anesthesia in Group TT were significantly higher than that at baseline (highest of the significant $P < 0.0001$). Intergroup comparison of MAP and HR at similar time intervals during intraoperative period, Group TI had a lower MAP and HR, especially at the time of endotracheal tube intubation ($P < 0.05$). Similarly, Group TI had lower MAP and HR on emergence from anesthesia in PACU than those in Group TT. The highest mean between-group difference was 12.73 mmHg and 22.0 beats/min ($P < 0.0001$). Most of differences were narrowed 30 minutes after extubation or I-gel removal (Figure 2).

Ppeak, $ETCO_2$, PaO_2 and $PaCO_2$ were comparable and within normal limits in both groups. Although the above-mentioned respiratory parameters tended to be more optimal in Group TT during intraoperative period, the differences did not reach statistical significant ($P > 0.05$). At 1 and 30 minutes after emergence, $PaCO_2$ were (38.9 ± 0.95 mmHg) and (38.3 ± 0.89 mmHg) in Group TI in comparison to (41.6 ± 2.39 mmHg) and (40.3 ± 1.68 mmHg) in Group TT, and the differences were significant between groups at both time points ($P < 0.0001$ and $P = 0.0011$, resp.) (Figure 3(c)). Similarly, PaO_2 at 1 min (152.6 ± 20.52 mmHg) and 30 min (137.3 ± 22.24 mmHg) in Group TI were significantly higher than those (119.5 ± 17.19 mmHg and 119.6 ± 21.65 mmHg, resp. at 1 min and 30 min) in Group TT ($P = 0.0002$ and $P = 0.0407$, resp.) (Figure 3(d)).

Plasma β-EP concentration varied greatly. Mean concentration of β-EP was lower during the whole procedure than at baseline in both groups ($P < 0.0001$). Only at 1 minute after extubation, the β-EP concentration in Group TI became higher than that in Group TT ($P = 0.037$) (Figure 4(a)). Also, Plasma Cor concentration was lower during intraoperative period than at baseline in both groups ($P < 0.0001$), but it slowly began to rise on emergence from anesthesia and reached its highest value at 1 minute after extubation or I-gel removal, and was higher than its baseline values, respectively,

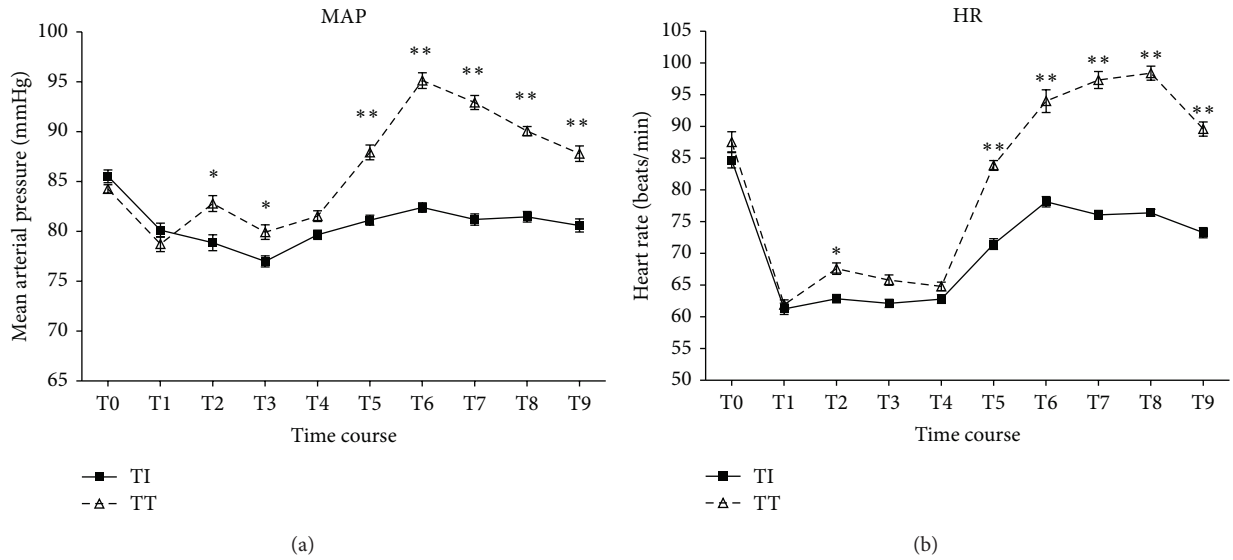

Figure 2: Changes in mean hemodynamic variables in patients with a tracheal tube intubation (Group TT) or an I-gel facilitated endotracheal tube intubation (Group TI) during the study; bars indicate the SEM. Both groups had significant reduction in MAP and HR from their respective baseline values till the end of the surgery. Patients in Group TI had a greater fall in comparison to Group TT over the time period of the observation ($P < 0.0001$). During emergence from anesthesia, MAP and HR in Group TT were significantly higher than that at baseline ($P < 0.0001$). And the intergroup differences were also significant ($^{*}P < 0.05$; $^{**}P < 0.0001$). Baseline (T0); before anesthetic induction (T1); endotracheal tube intubation (T2); 3 min after intubation (T3); end of surgery but before awakening (Group TT) or before endotracheal tube removed (Group TI) (T4); after patients entered the PACU (T5); and throughout emergence from anesthesia at 1, 5, 15, and 30 minutes after extubation or I-gel removal (according to group assignment) (T6-9).

Table 1: Subject and procedure characteristics.

Characteristic	Treatment groups		
	Group TT ($n = 30$)	Group TI ($n = 30$)	P value
Age (years)	49 (8)	48 (7)	0.774
Gender (M/F)	18/12	14/16	0.747
Weight (kg)	64 (8)	67 (6)	0.206
Height (cm)	163 (8)	163 (7)	0.867
Procedures			
Cerebellar hemisphere tumors	6 (20%)	4 (13%)	NS
Cerebellar vermis tumor	2 (7%)	2 (7%)	NS
Cerebellopontine angle tumors	6 (20%)	6 (20%)	NS
Fourth ventricle tumor	3 (10%)	3 (10%)	NS
Acoustic neuroma	10 (33%)	13 (43%)	NS
Slope tumor	3 (10%)	2 (7%)	NS
Duration of surgery (min)	335 (20)	338 (23)	0.696

Values are given as Mean ± SD, or number of patients (%).
Group TT: tracheal tube intubation group; Group TI: I-gel facilitated endotracheal tube intubation group.

in Group TT and Group TI ($P < 0.0001$ and $P = 0.0008$, resp.). Intergroup comparison, Group TT had higher Cor concentration at 3 min after intubation ($P = 0.036$) and 1 minute after extubation ($P = 0.016$) (Figure 4(b)). BG level was lower during intraoperative period than at baseline in both groups ($P < 0.0001$), it also slowly began to rise to close to baseline on emergence from anesthesia, however, the differences were not significant ($P > 0.05$). The percent increase of BG tended to be higher in Group TT as compared to that in Group TI ($P = 0.004$) (Figure 4(c)).

Plasma concentrations of IL-6, IL-8, and TNF-α during pre-operation and post-operation are displayed in Figure 5. IL-8 level was decreased over time in both groups. IL-6 and TNF-α were decreased in Group TI, but increased in Group TT. Intergroup comparison, there were no differences in both experimental groups during pre-operation. However, IL-6 and TNF-α were significant lower in Group TI post-operatively. ($P = 0.0186$ and $P = 0.0273$) (Figures 5(a) and 5(c)).

MDA and SOD levels were decreased over time in both groups, but Group TI had a significant decrease of MDA ($P = 0.0384$, post-operation versus pre-operation). Between-group comparison, MDA levels were significantly higher ($P = 0.0409$) in Group TT during post-operation (Figure 6(a)). SOD activity was greater in Group TI during post-operation. However, no significant difference in SOD levels was observed between the groups ($P = 0.6263$) (Figure 6(b)).

As shown in Table 2, spontaneous breathing recovery time and eye opening time were shorter in Group TI, but the differences were not significant ($P = 0.084$ and $P = 0.426$). I-gel removal time in Group TI (22.0 ± 3.0) in comparison to extubation time in Group TT (19.0 ± 1.0) was significantly difference ($P < 0.001$). However, the MOAA/S score was significantly higher in Group TI at the time of I-gel removal ($P = 0.032$).

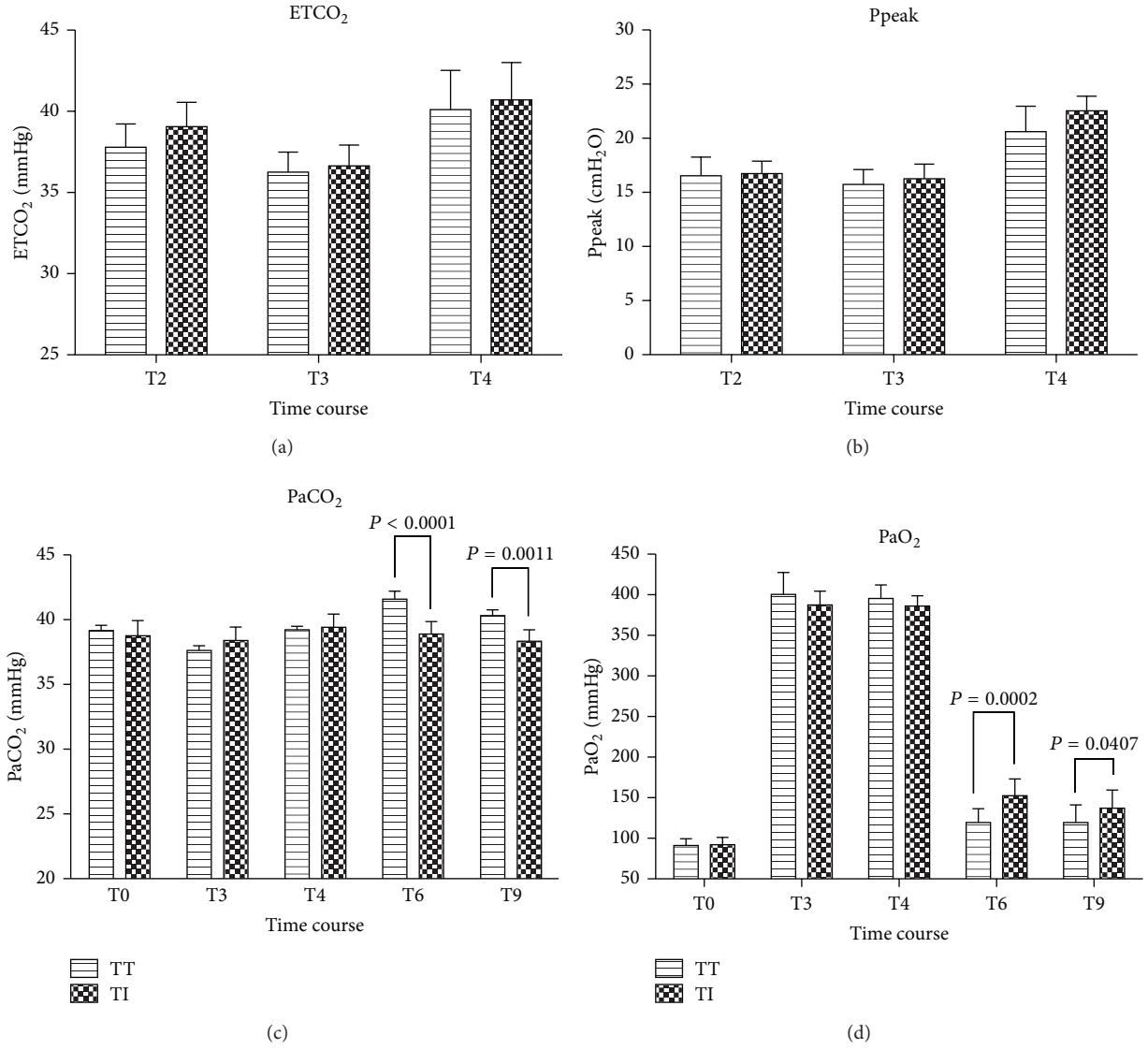

Figure 3: Changes in $ETCO_2$, Ppeak, $PaCO_2$, and PaO_2 in patients with a tracheal tube intubation (Group TT) or an I-gel facilitated endotracheal tube intubation (Group TI) over a period of time. Results are expressed as Mean ± SD. No significant difference in $ETCO_2$ and Ppeak over time. During emergence, $PaCO_2$ and PaO_2 were better in Group TI than those in Group TI, and the differences were significant. Baseline (T0); endotracheal tube intubation (T2); 3 min after intubation (T3); end of surgery but before awakening (Group TT) or before endotracheal tube removed (Group TI) (T4); and throughout emergence from anesthesia at 1 and 30 minutes after extubation or I-gel removal (according to group assignment) (T6, 9).

Table 2: Spontaneous breathing recovery time, eye opening time, extubation or I-gel removal time, and MOAA/*S* score.

Characteristic	Treatment groups		
	Group TT (n = 30)	Group TI (n = 30)	P value
Spontaneous breathing recovery time (min)	9.0 (1.3)	8.0 (1.5)	0.084
Eye opening time (min)	11.0 (1.5)	10.0 (2.1)	0.426
Extubation or I-gel removal time (min)	19 (1.0)	22 (3.0)	<0.001
MOAA/*S* score: 5 (alert)/4/3/2/1/0 (asleep)	0/6/20/4/0/0	4/14/12/0/0/0	0.032

Values are given as Mean ± SD.
Group TT: tracheal tube intubation group; Group TI: I-gel facilitated endotracheal tube intubation group.

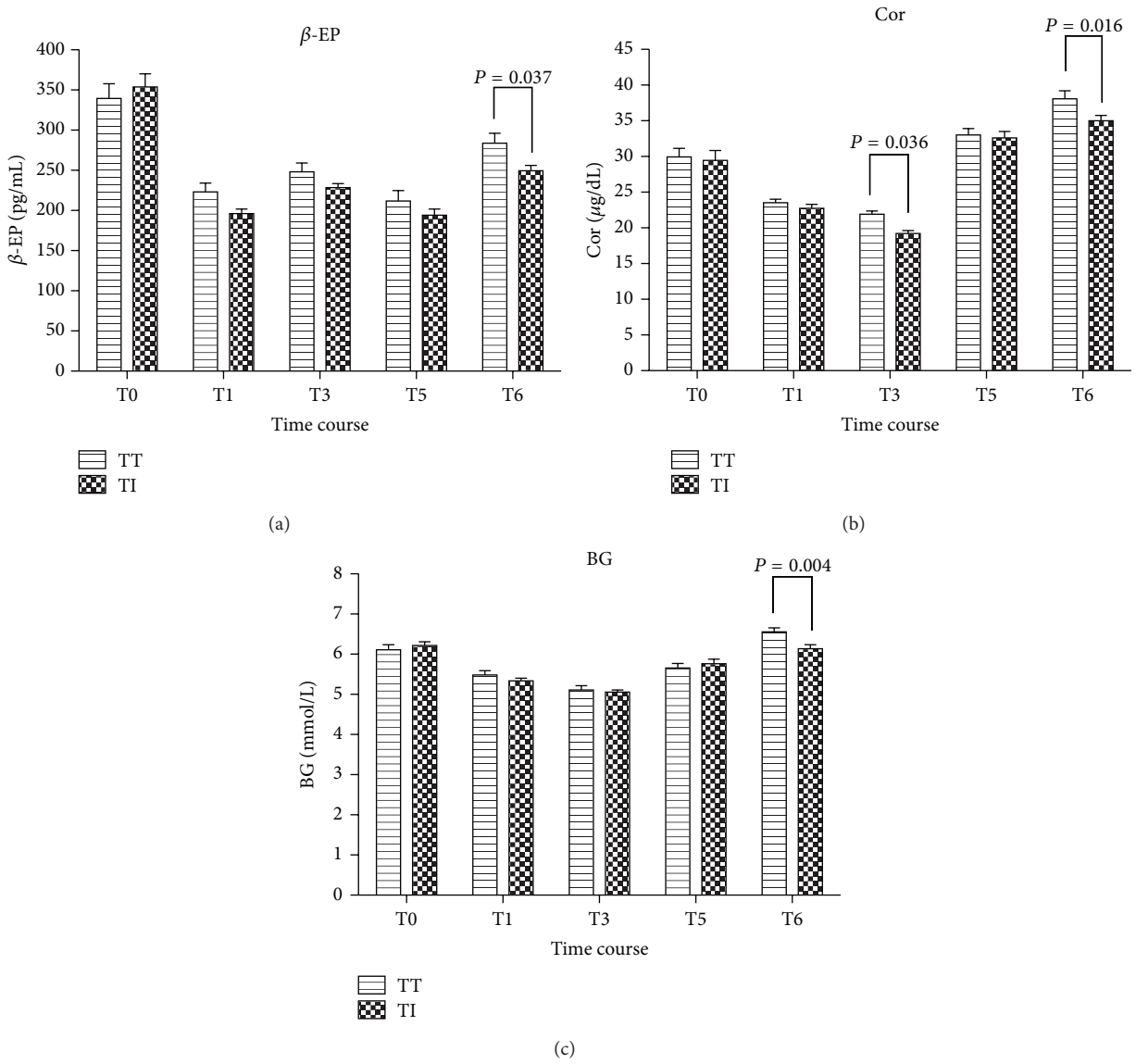

Figure 4: Changes in plasma β-EP and Cor concentrations and BG in patients with a tracheal tube intubation (Group TT) or an I-gel facilitated endotracheal tube intubation (Group TI) during the study. Results are expressed as Mean ± SD. Mean concentration was lower during intraoperative period than at baseline in both groups ($P < 0.0001$). They began to rise during emergence, and the Cor concentration even higher than that of baseline (Group TT, $P < 0.0001$; Group TI, $P = 0.0008$). The percent increase tended to be higher in Group TT ($P < 0.05$). Baseline (T0); before anesthetic induction (T1); 3 min after intubation (T3); after patients entered the PACU (T5); and throughout emergence from anesthesia at 1 minute after extubation or I-gel removal (according to group assignment) (T6).

Mild choking cough occurred in 12 of 30 patients (40%), moderate choking cough were 6 (20%), and severe choking cough was 1 (3%) in Group TT and only 3 mild choking cough patients (10%) in Group TI ($P < 0.001$). Blood pressure and heart rate increase in Group TT as compared to Group TI. Patients that needed vasoactive drugs for at least once preoperatively are 13 (43.3%) in Group TT versus 2 (6.7%) in Group TI ($P < 0.001$). All Group TT patients known to have controlled chronic hypertension before surgery required pharmacological intervention whereas only one of the 5 known chronically hypertensive patients in Group TI required treatment (Table 3).

No patient in Group TI had hemorrhagic complications during the postoperative period, but one excluded from the study in Group TT due to hemorrhagic complications.

4. Discussion

I-gel laryngeal mask airway in combination of tracheal intubation for patients undergoing posterior fossa surgery not only ensured the normal ventilation during intraoperative, but also reduced the hemodynamic impact of intubation and emergence from anesthesia in our study in terms of MAP and HR reduction, the main outcome measure. The incidence of

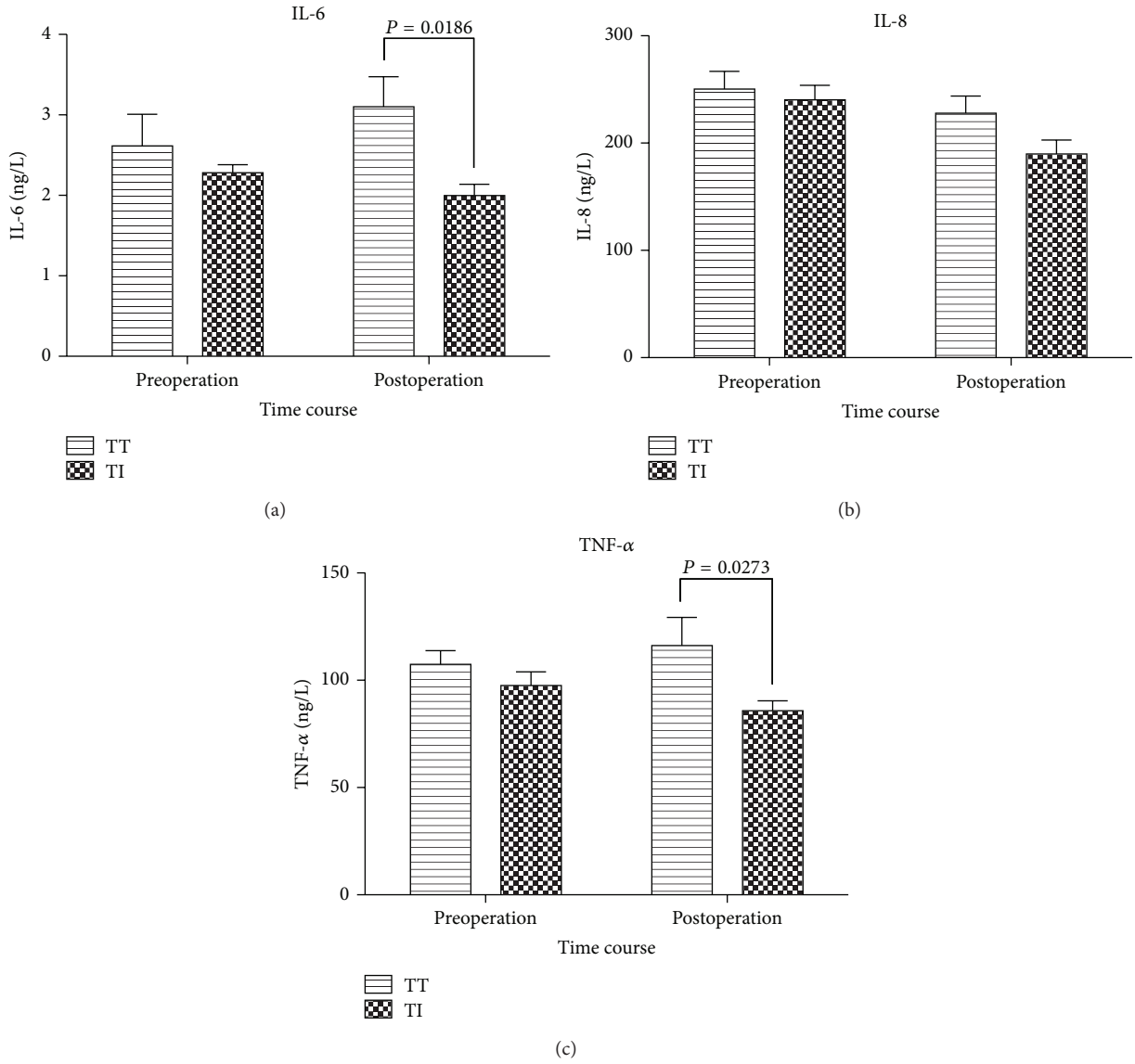

Figure 5: Changes in plasma IL-6, IL-8 and TNF-α concentration in Group TT and Group TI. Values are given as Mean ± SEM. Group TT, tracheal tube intubation group; Group TI, I-gel facilitated endotracheal tube intubation group.

coughing was also lower with I-gel use. As far as we know, this is the first study to compare the effects of I-gel in combination of tracheal intubation for posterior fossa surgery patients, who are particularly susceptible to hemodynamic changes.

Anesthesiologists had to pay more attention to the unattenuated hemodynamic responses, caused by orotracheal intubation, which is an extremely invasive procedure performed at induction of anesthesia. According to Kovac's study about hemodynamic responses to laryngoscopy and endotracheal intubation, laryngoscopy has the maximal increase in BP, and endotracheal intubation has the maximal increase of HR [19]. During conventional laryngoscopy, the maximum force transmitted by a laryngoscope blade onto the base of the tongue is considered to be exceptionally invasive [19], and this stimulation even may be as high as approximately 40 Newtons [20, 21]. This is also verified in our study, the hemodynamic variables as well as MAP and HR were lower in Group TI during intubation. We inserted the endotracheal tube through the I-gel's air duct under the guidance of the Flexible Intubation Videoscope in Group TI. We used the properly seated I-gel as a conduit for endotracheal tube, which can reduce adverse cardiovascular responses due to the avoidance of such a strong stimulus to laryngeal tissues [22, 23]. Moreover, Cros et al. [24] confirmed that tracheal intubation through the ILMA can be used in patients with a difficult airway, and allow for continuous ventilation and oxygenation during tracheal intubation attempts. Also the use of Flexible Intubation Videoscope, reduced the intubation time and improved the accuracy of intubation.

Although the highest mean intergroup difference of 12.73 mmHg in MAP and 22.0 beats/min in HR during emergence from anesthesia may not seem numerically impressive,

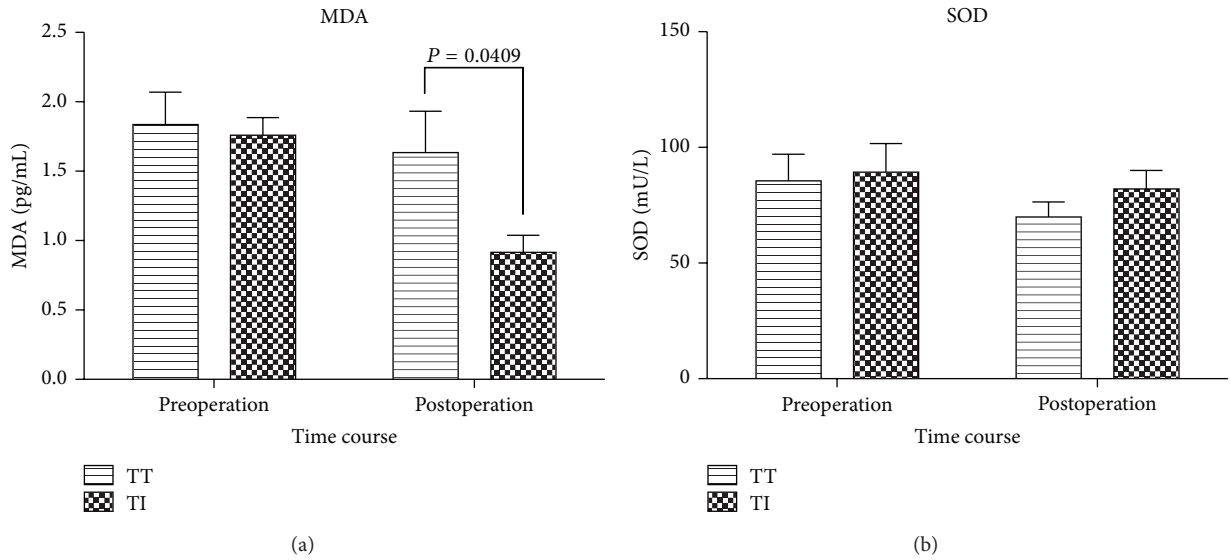

Figure 6: Changes in plasma MDA and SOD concentrations in Group TT and Group TI. Values are given as Mean ± SEM. Group TT, tracheal tube intubation group; Group TI, I-gel facilitated endotracheal tube intubation group.

Table 3: Adverse events during the procedure.

Adverse events	Treatment groups		P value
	Group TT ($n = 30$)	Group TI ($n = 30$)	
No choke to cough	11 (37%)	27 (90%)	<0.001
Mild choking cough	12 (40%)	3 (10%)	<0.001
Moderate choking cough	6 (20%)	0	1.000
Severe choking cough	1 (3%)	0	1.000
Hypertension	15 (50%)	3 (10%)	<0.001
Tachycardia	5 (17%)	0	1.000
Use of vasoactive drugs	13 (43.3%)	2 (6.7%)	<0.001

Values are given as number of subjects (%).
Group TT: tracheal tube intubation group; Group TI: I-gel facilitated endotracheal tube intubation group.

it would be clinically significant in these posterior fossa surgery patients. We continuously evaluated all our patients for hypertension and tachycardia, and whenever it was identified it was treated with a standard protocol. Nevertheless, most patients in Group TT developed MAP close to 100 mmHg and HR over 100 beats/min, and intergroup differences were statistically significant and as such 43.3% of Group TT patients needed treatments with vasoactive drugs that had probably blunted a more severe rise in blood pressure. On the contrary, only 6.7% patients (2 out of total of 30 patients) in Group TI required vasoactive drug treatment. The 6.5-fold greater need for vasoactive drugs in Group TT reflected a higher incidence of blood pressure surges, which are events that increase the risk of postoperative intracranial hemorrhage. Therefore, we are confident that the differences were also clinically relevant in this setting. In Group TI, after having sutured the scalp, we pulled out the endotracheal tube, stopped the TCI of anesthetics to make the patient could quickly emerge from anesthesia in the operation room. This does attenuate hemodynamic responses, oxygen consumption and stress hormone concentrations as compare with patients in Group TT that were associated with delayed awakening until later in the post anesthesia care unit. Such hemodynamic changes have been reported to be a kind of incentive for intracranial bleeding and cerebral edema. According to a retrospective study of Basali, the incidence of cerebral hemorrhage was 0.77% after craniotomy, and 62% of patients with this complication had developed hypertension in the immediate postoperative period [25]. And other reports have also linked the prior history of hypertension to postoperative hematoma [26]. Our results indicate that in such patients, it can attenuate the rise in hemodynamic responses during emergence from anesthesia by pulling out the endotracheal tube before shifted the patient to supine position and then using the I-gel to continue to maintain the patient's ventilation, as less vasoactive agents were needed in this subgroup. All Group TT patients known to have a controlled history of chronic hypertension before surgery needed pharmacological intervention during emergence but only one of the 5 known controlled-chronically hypertensive patients in Group TI required treatment. Our findings are consistent with those of previous researches of anesthesia convalescence [27], even though we did not design to recruit enough patients to detect differences in the subgroup of patients with controlled chronic hypertension. We think that our results could suggest that the beneficial effects of patients awakening with an I-gel in place would be particularly beneficial in the subgroup of patients with chronic hypertension undergoing craniotomy especially posterior fossa surgery that doctors often fixed the patients' head with the head frame.

Numerous studies have explored methods to reduce the effects of extubation on systemic hemodynamic response. Drugs such as diltiazem/nicardipine [28], esmolol [29],

fentanyl [30], dexmedetomidine [31] and lidocaine [32] have been used for this purpose. Remifentanil is the most commonly administration in neurosurgery, which has been suggested as a strategy to smooth emergence generally, and enhance analgesia effect and subsequently reduce hemodynamic impairment during emergence. However, it must be carefully titrated to avoid neurological depression, as well as respiratory depression that may lead to hypercapnia and further hyperemia; otherwise, it may abolish the beneficial effect of hemodynamic control [33]. Smith et al. [34] advocated that postoperative patients with general anesthesia in neurosurgery should be pulled the endotracheal tube under deep anesthesia to avoid the cardiovascular stress reaction. However, the residual effect of sedative, analgesic, and muscle relaxants could lead to insufficient alveolar ventilation, the accumulation of carbon dioxide and hypoxia. Therefore, this method is not suitable for posterior fossa surgery patients. Some scholars [13, 35] also advocated pulling out the endotracheal tube and then making use of the LMA to maintain ventilation at the end of neurosurgery, but the two operations increased the risk of momentary loss of control of the airway. Also, some airway obstruction and the aspiration of gastric content may occur while the airway is unprotected, and we must maintain an adequate depth of anesthesia to ensure the LMA inserting successfully that may delay the patients' awakening. However, patients with anticipated or known difficult airway or at high risk of bronchial aspiration mustn't be recommended to use such replacement techniques [36].

The LMA has been used successfully in some neurosurgical procedures, such as ventriculoperitoneal shunt [37], lumbar spine microsurgery [38], and awake craniotomy [39]. In our study, we also successfully used I-gel combined with endotracheal tube in 30 patients undergoing posterior fossa surgery. It had less effect on hemodynamic response when I-gel was inserted, and also had more stable hemodynamics by the way of inserting the endotracheal tube through the I-gel's air duct under the guidance of the Flexible Intubation Videoscope than that of inserting the tracheal tube using a direct laryngoscope. Although the inner diameter of the trachea was less in Group TI than that of Group TT, there were no significant difference of $ETCO_2$, Ppeak, PaO_2 and $PaCO_2$ during intraoperative period between the groups. On the contrary, PaO_2 and $PaCO_2$ were better in Group TI than Group TT at 1 min and 30 min after extubation.

Plasma β-EP and Cor concentrations and BG level were lower during intraoperative period than at baseline in both groups. It indicated that general anesthesia could partly limit the perception of stimuli from injury and have little effect on the endocrine and physiological functions. Plasma β-EP and Cor concentrations and BG level began to rise, some of them even higher than that of baseline during emergence from anesthesia, and the percent increase tended to be higher in Group TT. It showed that the stress reaction at the time of extubation was greater than that of the intubation, and also the strongest point during the whole process. I-gel combined with endotracheal tube can also reduce the stress reaction level both during intubation and extubtion.

IL-6 is an endogenous pyrogen, which exerts multiple effects that are both beneficial and destructive to CNS cells. IL-8 is a chemokine produced mainly by macrophages and epithelial cells and functions to attract neutrophils towards inflammation sites. TNF-α is one of the central mediators of tissue inflammation and proinflammatory during the acute phase of CNS inflammatory. The inflammatory reaction and oxidative stress did not significantly change over time in both groups, which may be explained by the use of dexmedetomidine and propofol. Several studies have reported both dexmedetomidine and propofol could attenuate the inflammation and oxidative stress [40–42]. In our study, there was a significant plasma IL-6, TNF-α and MDA decrease during post-operative period in Group TI and a slight increase in reported hemodynamic can be partially explained by the expected increase in hemodynamic after extubtion. Group TT had a higher IL-6, TNF-α and MDA levels with a significant increase in hemodynamic during emergence from anesthesia. The decrease of SOD in both groups could be because of the decrease in antioxidant status. And the decrease of MDA in both groups may be due to the use of anesthetics that has antioxidant property.

In our study, the high incidence of cough in Group TT was in contrast with the incidence of 3.6%, which reported in another recent research of patients emerging from anesthesia after craniotomy [43]. This can be explained by our detailed and strict recording criteria of any occurrence of cough during the awakening process. The cough incidence rates in our study were 10% and 63%, respectively, for I-gel and endotracheal tube. We used the I-gel for its' better seal of the airway, good evacuation of gastroesophageal contents, simply guided insertion and especially for its' high tolerance [44]. There were no serious adverse reactions, such as cough, elevated blood pressure, and tachycardia when removal the I-gel in Group TI, and also the patients were very clear for neurosurgeon to do early neurological assessment.

The current study has a number of limitations. It was a randomized, but not double-blinded trial. We arranged an independent observer recorded most of the variables identified, but the observer may clearly identify which device was used. We must also note the small effect of nicardipine on increasing HR, because a certain degree of the observed increase in that variable. In order to reduce its influence on HR, we used esmolol at the appropriate time. In this case, we will not record it as the usage of vasoactive drug. We used the I-gel for about five hours during the surgery, but we simply observed whether the patients had such complications as hoarseness, throat pain, and the damage of the contact parts during the recovery period, we did not have a systematic study and follow-up like Taheri et al. [45]. However, according to our observation, there were no serious complications in Group TI.

In conclusion, I-gel combined with endotracheal tube for ventilation can be effective in preventing the cardiovascular response, attenuating inflammatory and oxidative response, reducing adverse events risk, and improving the quality of anesthesia during intubation and extubation in posterior fossa surgery. Use of the I-gel in this way may be of special interest in patients with a difficult airway or a history of chronic hypertension. It also may provide a novel path for neurosurgical anesthesia airway management.

Conflict of Interests

The authors declare that there is no conflict of interests regarding the publication of this paper.

Acknowledgments

The authors would like to thank Professor Chaoshi Niu and Wanhai Ding, Department of Neurosurgery, for their help in designing and conducting the study, and Hang Dong, Department of Clinical laboratory, for his help in detecting plasma β-endorphin (β-EP), cortisol (Cor) concentrations, IL-6, IL-8, TNF-α, MDA, and SOD. The authors are grateful for the enthusiastic support of the nurses of the PACU at Southern District of Anhui Provincial Hospital. This study was supported by the international cooperation fund (no. 1503062021), Department of International Cooperation of Science and Technology, Bureau of Science and Technology of Anhui province.

References

[1] N. Bruder and P. Ravussin, "Recovery from anesthesia and postoperative extubation of neurosurgical patients: a review," *Journal of Neurosurgical Anesthesiology*, vol. 11, no. 4, pp. 282–293, 1999.

[2] N. Bruder, D. Pellissier, P. Grillot, and F. Gouin, "Cerebral hyperemia during recovery from general anesthesia in neurosurgical patients," *Anesthesia and Analgesia*, vol. 94, no. 3, pp. 650–654, 2002.

[3] J. P. Desborough, "The stress response to trauma and surgery," *British Journal of Anaesthesia*, vol. 85, no. 1, pp. 109–117, 2000.

[4] S. V. More, H. Kumar, I. S. Kim, S.-Y. Song, and D.-K. Choi, "Cellular and molecular mediators of neuroinflammation in the pathogenesis of Parkinson's disease," *Mediators of Inflammation*, vol. 2013, Article ID 952375, 12 pages, 2013.

[5] G. Chen, J. Shi, Z. Hu, and C. Hang, "Inhibitory effect on cerebral inflammatory response following traumatic brain injury in rats: a potential neuroprotective mechanism of N-Acetylcysteine," *Mediators of Inflammation*, vol. 2008, Article ID 716458, 8 pages, 2008.

[6] R. Kazmierski, P. Guzik, W. Ambrosius, A. Ciesielska, J. Moskal, and W. Kozubski, "Predictive value of white blood cell count on admission for in-hospital mortality in acute stroke patients," *Clinical Neurology and Neurosurgery*, vol. 107, no. 1, pp. 38–43, 2004.

[7] P. Hans and V. Bonhomme, "Why we still use intravenous drugs as the basic regimen for neurosurgical anaesthesia," *Current Opinion in Anaesthesiology*, vol. 19, no. 5, pp. 498–503, 2006.

[8] M. Klimek, J. W. Hol, S. Wens et al., "Inflammatory profile of awake function-controlled craniotomy and craniotomy under general anesthesia," *Mediators of Inflammation*, vol. 2009, Article ID 670480, 8 pages, 2009.

[9] M. Maes, C. Song, A. Lin et al., "The effects of psychological stress on humans: increased production of pro-inflammatory cytokines and a Th1-like response in stress-induced anxiety," *Cytokine*, vol. 10, no. 4, pp. 313–318, 1998.

[10] L. Perelló-Cerdà, N. Fàbregas, A. M. López et al., "ProSeal laryngeal mask airway attenuates systemic and cerebral hemodynamic response during awakening of neurosurgical patients: a randomized clinical trial," *Journal of Neurosurgical Anesthesiology*, 2014.

[11] D. J. Kelly, M. Ahmad, and S. J. Brull, "Preemptive analgesia II: recent advances and current trends," *Canadian Journal of Anesthesia*, vol. 48, no. 11, pp. 1091–1101, 2001.

[12] A. Suzuki and H. Ogawa, "A new technique of extubation using laryngeal mask in the neurosurgical anesthesia," *Masui*, vol. 46, no. 7, pp. 994–996, 1997.

[13] T. Umegaki, K. Murao, T. Asai, and K. Shingu, "Insertion of a laryngeal mask airway before removal of a nasotracheal tube in a patient after anterior spine surgery," *Japanese Journal of Anesthesiology*, vol. 55, no. 4, pp. 451–453, 2006.

[14] F. Kang, J. Li, X. Chai, J. Yu, H. Zhang, and C. Tang, "Comparison of the I-gel laryngeal mask airway with the LMA-supreme for airway management in patients undergoing elective lumbar vertebral surgery," *Journal of Neurosurgical Anesthesiology*, vol. 27, no. 1, pp. 37–41, 2015.

[15] R. M. Levitan and W. C. Kinkle, "Initial anatomic investigations of the I-gel airway: a novel supraglottic airway without inflatable cuff," *Anaesthesia*, vol. 60, no. 10, pp. 1022–1026, 2005.

[16] B. Richez, L. Saltel, F. Banchereau, R. Torrielli, and A. M. Cros, "A new single use supraglottic airway device with a noninflatable cuff and an esophageal vent: an observational study of the i-gel," *Anesthesia and Analgesia*, vol. 106, no. 4, pp. 1137–1139, 2008.

[17] J. A. Ludeña, J. J. A. Bellas, V. L. Pérez, A. C. García, and R. A.-R. Carbonell, "Placement of a bronchial blocker through the I-gel supraglottic airway device for single-lung ventilation: preliminary study," *Revista Española de Anestesiología y Reanimación*, vol. 57, no. 8, pp. 532–535, 2010.

[18] J. H. Ryu, S. W. Lee, J. H. Lee, E. H. Lee, S. H. Do, and C. S. Kim, "Randomized double-blind study of remifentanil and dexmedetomidine for flexible bronchoscopy," *British Journal of Anaesthesia*, vol. 108, no. 3, pp. 503–511, 2012.

[19] A. L. Kovac, "Controlling the hemodynamic response to laryngoscopy and endotracheal intubation," *Journal of Clinical Anesthesia*, vol. 8, no. 1, pp. 63–79, 1996.

[20] R. H. Hastings, E. D. Hon, C. Nghiem, and E. A. Wahrenbrock, "Force, torque, and stress relaxation with direct laryngoscopy," *Anesthesia and Analgesia*, vol. 82, no. 3, pp. 456–461, 1996.

[21] R. H. Hastings, E. D. Hon, C. Nghiem, and E. A. Wahrenbrock, "Force and torque vary between laryngoscopists and laryngoscope blades," *Anesthesia and Analgesia*, vol. 82, no. 3, pp. 462–468, 1996.

[22] M. Kahl, L. H. J. Eberhart, H. Behnke et al., "Stress response to tracheal intubation in patients undergoing coronary artery surgery: direct laryngoscopy versus an intubating laryngeal mask airway," *Journal of Cardiothoracic and Vascular Anesthesia*, vol. 18, no. 3, pp. 275–280, 2004.

[23] Y. Hirabayashi, M. Hiruta, T. Kawakami et al., "Effects of lightwand (Trachlight) compared with direct laryngoscopy on circulatory responses to tracheal intubation," *British Journal of Anaesthesia*, vol. 81, no. 2, pp. 253–255, 1998.

[24] A. M. Cros, F. Maigrot, and D. Esteben, "Fastrach laryngeal mask and difficult intubation," *Annales Francaises d'Anesthesie et de Reanimation*, vol. 18, no. 10, pp. 1041–1046, 1999.

[25] A. Basali, E. J. Mascha, L. Kalfas, and A. Schubert, "Relation between perioperative hypertension and intracranial hemorrhage after craniotomy," *Anesthesiology*, vol. 93, no. 1, pp. 48–54, 2000.

[26] M. A. Seifman, P. M. Lewis, J. V. Rosenfeld, and P. Y. K. Hwang, "Postoperative intracranial haemorrhage: a review," *Neurosurgical Review*, vol. 34, no. 4, pp. 393–407, 2011.

[27] D. Bhattacharya, S. Ghosh, T. Chaudhuri, and S. Saha, "Pressor responses following insertion of laryngeal mask airway in patients with controlled hypertension: comparison with tracheal intubation," *Journal of the Indian Medical Association*, vol. 106, no. 12, pp. 787–810, 2008.

[28] T. Tsutsui, "Combined administration of diltiazem and nicardipine attenuates hypertensive responses to emergence and extubation," *Journal of Neurosurgical Anesthesiology*, vol. 14, no. 2, pp. 89–95, 2002.

[29] A. L. Kovac and A. Masiongale, "Comparison of nicardipine versus esmolol in attenuating the hemodynamic responses to anesthesia emergence and extubation," *Journal of Cardiothoracic and Vascular Anesthesia*, vol. 21, no. 1, pp. 45–50, 2007.

[30] Y.-C. Yoo, S. Na, J.-J. Jeong, E.-M. Choi, B.-E. Moon, and J.-R. Lee, "Dose-dependent attenuation by fentanyl on cough during emergence from general anesthesia," *Acta Anaesthesiologica Scandinavica*, vol. 55, no. 10, pp. 1215–1220, 2011.

[31] R. N. Soliman, A. R. Hassan, A. M. Rashwan, and A. M. Omar, "Prospective, randomized study to assess the role of dexmedetomidine in patients with supratentorial tumors undergoing craniotomy under general anaesthesia," *Middle East Journal of Anesthesiology*, vol. 21, no. 3, pp. 325–334, 2011.

[32] N.-K. Hung, C.-T. Wu, S.-M. Chan et al., "Effect on postoperative sore throat of spraying the endotracheal tube cuff with benzydamine hydrochloride, 10% lidocaine, and 2% lidocaine," *Anesthesia and Analgesia*, vol. 111, no. 4, pp. 882–886, 2010.

[33] J. H. Lee, B.-N. Koo, J.-J. Jeong, H.-S. Kim, and J.-R. Lee, "Differential effects of lidocaine and remifentanil on response to the tracheal tube during emergence from general anaesthesia," *British Journal of Anaesthesia*, vol. 106, no. 3, pp. 410–415, 2011.

[34] W. D. Smith, R. C. Dutton, and N. T. Smith, "Measuring the performance of anesthetic depth indicators," *Anesthesiology*, vol. 84, no. 1, pp. 38–51, 1996.

[35] I. H. Kalfas and J. R. Little, "Postoperative hemorrhage: a survey of 4992 intracranial procedures," *Neurosurgery*, vol. 23, no. 3, pp. 343–347, 1988.

[36] M. Popat, V. Mitchell, R. Dravid, A. Patel, C. Swampillai, and A. Higgs, "Difficult Airway Society Guidelines for the management of tracheal extubation," *Anaesthesia*, vol. 67, no. 3, pp. 318–340, 2012.

[37] S. S. Kumar, N. Chaterjee, and S. Kamath, "LMA and ventriculoperitoneal shunt surgery: is it the ideal airway?" *Journal of Neurosurgical Anesthesiology*, vol. 21, no. 1, article 66, 2009.

[38] A. M. López, R. Valero, P. Hurtado, P. Gambs, M. Pons, and T. Anglada, "Comparison of the LMA supreme with the LMA Proseal for airway management in patients anaesthetized in prone position," *British Journal of Anaesthesia*, vol. 107, no. 2, pp. 265–271, 2011.

[39] S. Gadhinglajkar, R. Sreedhar, and M. Abraham, "Anesthesia management of awake craniotomy performed under asleep-awake-asleep technique using laryngeal mask airway: report of two cases," *Neurology India*, vol. 56, no. 1, pp. 65–67, 2008.

[40] Y. Wu, Y. Liu, H. Huang et al., "Dexmedetomidine inhibits inflammatory reaction in lung tissues of septic rats by suppressing TLR4/NF- B pathway," *Mediators of Inflammation*, vol. 2013, Article ID 562154, 9 pages, 2013.

[41] L. Xianbao, Z. Hong, Z. Xu, Z. Chunfang, and C. Dunjin, "Dexmedetomidine reduced cytokine release during postpartum bleeding-induced multiple organ dysfunction syndrome in rats," *Mediators of Inflammation*, vol. 2013, Article ID 627831, 7 pages, 2013.

[42] M. Mathy-Hartert, G. Deby-Dupont, P. Hans, C. Deby, and M. Lamy, "Protective activity of propofol, Diprivan and intralipid against active oxygen species," *Mediators of Inflammation*, vol. 7, no. 5, pp. 327–333, 1998.

[43] G. Citerio, A. Pesenti, R. Latini et al., "A multicentre, randomised, open-label, controlled trial evaluating equivalence of inhalational and intravenous anaesthesia during elective craniotomy," *European Journal of Anaesthesiology*, vol. 29, no. 8, pp. 371–379, 2012.

[44] C. Hughes, K. Place, S. Berg, and D. Mason, "A clinical evaluation of the i-gel supraglottic airway device in children," *Paediatric Anaesthesia*, vol. 22, no. 8, pp. 765–771, 2012.

[45] A. Taheri, F. Hajimohamadi, H. Soltanghoraee, and A. Moin, "Complications of using laryngeal mask airway during anaesthesia in patients undergoing major ear surgery," *Acta Otorhinolaryngologica Italica*, vol. 29, no. 3, pp. 151–155, 2009.

Hindawi Publishing Corporation
Mediators of Inflammation
Volume 2015, Article ID 238041, 7 pages
http://dx.doi.org/10.1155/2015/238041

Clinical Study

Intravenous Infusion of Dexmedetomidine Combined Isoflurane Inhalation Reduces Oxidative Stress and Potentiates Hypoxia Pulmonary Vasoconstriction during One-Lung Ventilation in Patients

Rui Xia,[1] Jinjin Xu,[2] Hong Yin,[1] Huozhi Wu,[3] Zhengyuan Xia,[4,5,6] Daiwei Zhou,[7] Zhong-yuan Xia,[2] Liangqing Zhang,[5,6] Haobo Li,[5,6] and Xiaoshan Xiao[7]

[1]*Department of Anesthesiology, First Affiliated Hospital, Yangtze University, Jingzhou 434000, China*
[2]*Department of Anesthesiology, Wuhan University Renmin Hospital, Wuhan 430060, China*
[3]*Department of Cardiothoracic Surgery, Fifth Affiliated Hospital of Zunyi Medical College, Zhuhai 519100, China*
[4]*Department of Anesthesiology, The Second Affiliated Hospital & Yuying Children's Hospital of Wenzhou Medical University, Wenzhou, Zhejiang 325000, China*
[5]*Department of Anesthesiology, Affiliated Hospital of Guangdong Medical College, Zhanjiang, Guangdong 524001, China*
[6]*Department of Anesthesiology, The University of Hong Kong, Hong Kong*
[7]*Department of Anesthesiology, Guangdong No. 2 Provincial People's Hospital, Guangdong Provincial Emergency Hospital, Guangzhou, Guangdong 510317, China*

Correspondence should be addressed to Zhengyuan Xia; zhengyuan_xia@yahoo.com and Xiaoshan Xiao; gd177mzk@163.com

Received 7 January 2015; Accepted 13 February 2015

Academic Editor: Huang-Ping Yu

Inhalation anesthetic isoflurane inhibits hypoxia pulmonary vasoconstriction (HPV), while dexmedetomidine (Dex) could reduce the dose of isoflurane inhalation and potentiate HPV, but the mechanism is unclear. Inhibition of reactive oxygen species (ROS) production can favor HPV during one-lung ventilation (OLV). Similarly, nitric oxide (NO), an important endothelium-derived vasodilator in lung circulation, can decrease the regional pulmonary vascular resistance of ventilated lung and reduce intrapulmonary shunting. We hypothesized that Dex may augment HPV and improve oxygenation during OLV through inhibiting oxidative stress and increasing NO release. Patients undergoing OLV during elective thoracic surgery were randomly allocated to either isoflurane + saline (NISO, $n = 24$) or isoflurane + dexmedetomidine (DISO, $n = 25$) group. Anesthesia was maintained with intravenous remifentanil and inhalational isoflurane (1.0–2.0%), with concomitant infusion of dexmedetomidine 0.7 $\mu g kg^{-1} h^{-1}$ in DISO and saline 0.25 $mL\,kg^{-1}h^{-1}$ in NISO group. Hemodynamic variables or depth of anesthesia did not significantly differ between groups. Administration of Dex significantly reduced Qs/Qt and increased PaO_2 after OLV, accompanied with reduced lipid peroxidation product malondialdehyde and higher levels of SOD activity as well as serum NO (all $P < 0.05$ DISO versus NISO). In conclusion, reducing oxidative stress and increasing NO release during OLV may represent a mechanism whereby Dex potentiates HPV.

1. Introduction

With the popularity of video-assisted thoracic surgery, the requirement for one-lung ventilation (OLV) has been increasing. OLV is used to provide a good surgical field and protect normal lungs from hemorrhage or abscess caused by affected lung [1]. However, OLV can induce ventilation-perfusion mismatch and pulmonary arteriovenous shunt in the nonventilated lung that can cause hypoxemia [2]. Hypoxic pulmonary vasoconstriction (HPV) is an important protective mechanism by which blood flow is diverted from the nonventilated lung toward a better ventilated region, thereby

maintaining adequate arterial oxygenation [3]. Inhalational anesthetic sevoflurane and isoflurane have been shown to inhibit HPV and thereby increase hypoxemia [4]. Dextral dexmedetomidine (Dex) is a new highly selective alpha2-adrenergic receptor agonist which has been increasingly used both in the intensive care unit and also perioperatively as an adjunct to general anesthesia. Dex has been shown to reduce the dose of the inhalational and intravenous anesthetics [5, 6] and to reduce anti-inflammatory properties against sepsis induced lung injury [7] and in bleeding-induced multiple organ dysfunction syndrome in rats [8]. Our recent study showed that intravenous infusion of Dex combined with inhalation of isoflurane potentiated HPV and thereby improved oxygenation during OLV [9]. However, the underlying mechanism remains to be elucidated.

Dex can induce vasoconstriction by activating alpha2-adrenoreceptor at a dose dependent manner [10]. It was reported that Dex even at a concentration 5 to 15 times lower than the clinically recommended plasma target concentration (0.4 to 1.2 ng/mL) could induce vasoconstriction [11]. Also, Dex at the clinical concentration can decrease the redistribution of pulmonary blood flow from the ventilated to the non-ventilated lung [9]. How did Dex maintain or augment the small pulmonary arteries contraction in the nonventilated lung and/or induce vasodilation in the ventilated lung? The ventilated lung should have the same alpha2- adrenoreceptors as the nonventilated lung in a specific person. This suggests that Dex may have conferred its effects through mechanisms other than a direct vasoconstriction modulator by activation of alpha2-adrenoceptor agonist.

Current evidence suggests that reactive oxygen species (ROS) and oxidative stress play a fundamental role in the regulation of HPV [12, 13]. Hypoxia is monitored by the pulmonary arteries smooth muscle cells (PASMCs) [14, 15]: during hypoxia, inhibition of ROS production and changes in the ratios of cytosolic reducing cofactors (GSH/GSSG, NADH/NAD^+, and NADPH/$NADP^+$) within human PASMCs activate voltage-gated K^+ channels in PASMCs, resulting in membrane depolarization and opening of L-type Ca^{2+} channels, which increases intracellular Ca^{2+} concentration and then elicits compensatory pulmonary artery constriction in hypoxic lung. Although inhibition of ROS production favors HPV during acute hypoxia, clinical studies found that during one-lung ventilation systematic lipid peroxidation product malondialdehyde (MDA) level was significantly increased which indicates increased oxidative stress [16]. During one-lung ventilation, ROS can be produced from multiple sources including mechanical ventilation, surgical trauma, manipulated lung tissue, and hyperoxia in ventilated lung [17]. Hypoxia also damps the levels of endogenous antioxidant enzyme superoxide dismutase (SOD) [18, 19], which plays an important role in balancing ROS generation and the overall tissue antioxidant capacity. Therefore, decreased SOD activity aggravates oxidative stress, which alleviates HPV effect. Studies found that Dex can decrease oxidative stress during pneumoperitoneum and strengthen the antioxidant defense system [20]. Whether Dex can inhibit oxidative stress during one-lung ventilation and whereby potentiates HPV effect is unclear.

Nitric oxide (NO) is an important endothelium-derived relaxing factor in lung circulation [21], which is produced mainly from human pulmonary endothelial cells (PAECs) in the pulmonary circulation by endothelial nitric oxide synthase (eNOS). Studies found that inhalation of nitric oxide can decrease the regional pulmonary vascular resistance of ventilated lung area, decrease intrapulmonary shunting, and improve arterial oxygenation [22, 23]. However, Takemoto et al. reported that chronic hypoxia is associated with a decrease in eNOS mRNA and protein expression in human PAECs [24]. Alpha2-adrenergic receptor agonist can activate NO production [25]. However, it is unknown whether Dex can activate NO production and decrease intrapulmonary shunting during one-lung ventilation in patients.

Therefore, the current study was designed to test the hypothesis that Dex can inhibit oxidative stress and increase NO production, whereby decreasing intrapulmonary shunting and improving arterial oxygenation in patients under one-lung ventilation.

2. Methods

2.1. General Information. After approval of the institutional ethical committee and written informed consent, 60 male patients (40–60 years old, ASA I~II, 50~73 kg, 151~175 cm high) undergoing elective thoracic surgery were included in the study. The clinical trial registration number is Chic TROIR-15005784. Exclusion criteria were renal insufficiency, liver dysfunction or ischemic or valvular heart disease, long-term alcohol, opioid, or sedative hypnotic drug addiction and dependency history, and neuropsychiatric diseases.

2.2. Group Division. All patients were randomly divided after induction of general anaesthesia into two groups, intravenous infusion of the Dex combined with isoflurane inhalation (DISO group) and the intravenous infusion of normal saline with isoflurane inhalation (ISO group), 30 patients in each group. Both the patients and the anaesthesiologists were blinded to the identity of the study drug (Dex or saline placebo). Study drug (Dex) or placebo was prepared in a 50 mL syringe without identification marked by specialized staff, who does not take part in the process of anaesthesia and the research.

2.3. Anaesthesia. Routine monitoring was established on all patients including ECG, noninvasive blood pressure (NIBP), and SPO_2. Central vena catheterization, radial artery cannulation and module, and electrodes monitor for bispectral index (BIS, Aspect Medical Systems) were also performed in all patients. Anaesthesia was induced with intravenous midazolam 2 mg, fentanyl 4 ug/kg, propofol 2 mg/kg, and vecuronium 0.1 mg/kg. A left-side double-lumen tube was inserted and correct position was assured by auscultation and by fiberoptic bronchoscopy before and after the patient was in the lateral decubitus position. Intermittent positive pressure ventilation (IPPV), mechanical ventilation, was used during

one-lung ventilation with tide volume (TV) 8 mL/kg, respiratory rate (RR) 12 bpm, I : E = 1 : 2, FiO2 100%. After bronchial intubation was positioned, patients in DISO group received intravenous infusion of Dex (D-dexmedetomidine liquid, Jiangsu Hengrui Medicine Co., Ltd., production, 100 ug/mL, diluted with normal saline to 50 mL) at 1.0 $ug{\cdot}kg^{-1}{\cdot}h^{-1}$ over 10 minutes, which was then reduced to 0.7 $ug{\cdot}kg^{-1}{\cdot}h^{-1}$ and maintained throughout the study; patients in NISO group were given intravenous infusion of 0.25 $mL{\cdot}kg^{-1}{\cdot}h^{-1}$ saline, and it was reduced to 0.18 $mL{\cdot}kg^{-1}{\cdot}h^{-1}$ 10 minutes later. During maintenance of anesthesia, all patients were given isoflurane 1.0 to 2.0%, intravenous infusion of remifentanil 0.1~0.2 $ug{\cdot}kg^{-1}{\cdot}min^{-1}$, and rocuronium to maintain the BIS between 40 to 60. Supplemental vasoactive drugs were used to maintain hemodynamic stability, and the doses of vasoactive drugs (atropine, ephedrine, and urapidil) used in two groups were recorded.

2.4. Monitoring. Pulmonary function tests and arterial blood gas analysis for all patients were performed before operation. Arterial blood gases were drawn; central venous blood gas, heart rate (HR), mean artery blood pressure (MAP), BIS values, and intrapulmonary shunt according to the formula Qs/Qt = [(Cc′O2 a CaO2)/(Cc′O2 a CvO2)] × 100% [26] were recorded at 15 minutes during two-lung ventilation (TLV) (TLV-15) and after 10, 20, 30, and 40 min of OLV (OLV-10, OLV-20, OLV-30, and OLV-40). Drager PM8030 was used to measure the concentrations of isoflurane in the inhalation gas (FiIso) and in the exhaled gas (EEIso).

2.5. Plasma SOD Activity and MDA Level. Blood sample was collected at TLV-15 and OLV-10, OLV-20, OLV-30, and OLV-40 minutes, respectively, and then plasma was separated by centrifugation. Plasma SOD activity and MDA level were measured by using specific reagents according to the protocols provided by the manufacturer (Nanjing, Jiancheng Bioengineering Institute, China) as described [27, 28], in which the xanthine oxidase method was used for the detection of SOD activity while the thiobarbituric acid was used as substrate for the detection of MDA [29].

2.6. Serum NO Concentration. Blood sample was collected at TLV-15 and OLV-30 minutes, respectively, and then serum was separated by centrifugation. Total NO concentration was determined using an indirect method based on measurement of nitrite concentration in serum according to Griess's method [30].

2.7. Statistical Analysis. The data were expressed as mean ± standard deviation ($\overline{x} \pm s$). SPSS 13.0 statistical software was used for analysis. The data that meet the analysis of variance between groups comparison were analyzed by ANOVA; pairwise comparison between groups was analyzed by SNK test; one-lung ventilation blood gas analysis of data over time was analyzed by repeated measures analysis of variance. A P value less than 0.05 was considered statistically significantly different.

Table 1: General characteristics and preoperative data.

	DISO group (n = 25)	NISO group (n = 24)
Age (yr)	55 ± 12	56 ± 11
Gender (M/F)	17/8	16/8
Weight (kg)	61 ± 12	60 ± 14
Height (cm)	167 ± 5	165 ± 7
ASA physical status (I/II)	3/22	2/22
Preoperative blood gas		
pH	7.42 ± 0.02	7.41 ± 0.03
PaO_2 (mmHg)	79.7 ± 13.7	79.5 ± 14.1
$PaCO_2$ (mmHg)	35.5 ± 3.7	34.9 ± 4.1
Hb (g/L)	119.5 ± 13.8	120.5 ± 12.5
Preoperative pulmonary function		
FEV_1 (%)	79 ± 17	81 ± 16
FVC (%)	86 ± 14	87 ± 11
FEV_1/FVC (%)	83 ± 13	80 ± 10

FEV_1: forced expiratory volume in one second; FVC: forced vital capacity; Hb: hemoglobin. There is no statistic difference between groups.

3. Results

60 patients were enrolled in the study. 11 patients were excluded from analysis (six in NISO and five in DISO group): in group NISO, 3 patients had BIS value over the range while another 3 cases had SpO2 less than 90% during one-lung ventilation; in group DISO, 2 cases had BIS value over the range and 3 cases had SpO2 less than 90%. Therefore, data from 49 patients were statistically analyzed in this study: 25 in group DISO and 24 in group NISO.

Patients' characteristics are presented in Table 1. There were no differences among groups regarding age, weight, height, ASA physical status, preoperative blood gas, and preoperative pulmonary function.

As shown in Table 2, the values for pH, Hb, $PaCO_2$, SaO_2, and $ScvO_2$ did not differ significantly between groups. Initiation of OLV caused a significant decrease in PaO_2 during conversion from TLV to OLV in both groups and PaO_2 reached its lowest value at OLV-30 min. The decrease in PaO_2 in group DISO was less severe as compared to NISO during OLV ($P < 0.05$). However, there was no hypoxemia (too low PaO_2) recorded in both groups. On changing from TLV to OLV, Qs/Qt% increased significantly in both groups and peaked at OLV-30 min, but the increase of Qs/Qt% in group DISO was less severe as compared with group NISO ($P < 0.05$, Table 2). Heart rate was significantly slower in group DISO than that in group NISO ($P < 0.05$). However, MAP and the use of vasoactive drugs were not significantly different between the two groups ($P > 0.05$) (Table 2).

BIS values were similar throughout the studied period in each group and between the two groups (Figure 1). FETIso was significantly lower in group DISO throughout the study as compared with group NISO ($P < 0.05$, Figure 2).

The plasma MDA level was about 10% higher in group NISO than in group DISO at TLV-15 min but it was not statistically different ($P > 0.05$, Table 3). On changing from

Table 2: Perioperative time-course changes of blood gas variables in DISO group ($n = 25$) and NISO group ($n = 24$) ($\overline{x} \pm s$).

Parameters	Group	TLV-15 min	OLV-10 min	OLV-20 min	OLV-30 min	OLV-40 min
pH	DISO	7.37 ± 0.04	7.38 ± 0.03	7.39 ± 0.04	7.40 ± 0.03	7.39 ± 0.04
	NISO	7.37 ± 0.04	7.38 ± 0.03	7.39 ± 0.04	7.40 ± 0.03	7.39 ± 0.04
Hb (mg/L)	DISO	118.5 ± 10.7	116.9 ± 12.5	117.5 ± 11.6	116.1 ± 14.2	115.3 ± 12.5
	NISO	117.4 ± 12.4	117.0 ± 12.3	116.9 ± 14.3	115.9 ± 12.7	115.1 ± 13.4
Qs/Qt (%)	DISO	11.5 ± 1.8	23.5 ± 2.9[ab]	25.3 ± 2.3[ab]	27.1 ± 2.1[ab]	23.5 ± 2.2[ab]
	NISO	12.0 ± 1.1	28.1 ± 2.5[a]	30.1 ± 2.0[a]	31.9 ± 1.9[a]	27.7 ± 2.0[a]
$PaCO_2$ (mmHg)	DISO	34.8 ± 3.2	35.0 ± 3.1	35.1 ± 3.9	35.3 ± 4.1	35.1 ± 3.3
	NISO	35.2 ± 3.1	35.7 ± 4.5	36.0 ± 3.7	35.7 ± 4.0	35.5 ± 4.2
SaO_2 (%)	DISO	99.7 ± 0.1	99.0 ± 1.2	98.7 ± 0.3	98.4 ± 0.8	99.3 ± 0.5
	NISO	99.7 ± 0.4	98.9 ± 0.7	98.4 ± 1.1	97.5 ± 1.5	99.2 ± 0.6
$ScvO_2$ (%)	DISO	84.9 ± 9.1	84.5 ± 8.5	83.5 ± 6.9	82.2 ± 9.2	84.4 ± 5.9
	NISO	84.5 ± 8.5	83.6 ± 7.1	81.7 ± 7.3	80.7 ± 9.4	82.7 ± 5.5
HR (beats/min)	DISO	66.3 ± 9.2[b]	65.5 ± 13.1[b]	67.5 ± 12.1[b]	68.7 ± 11.2[b]	67.6 ± 11.3[b]
	NISO	77.5 ± 10.5	78.2 ± 12.8	78.7 ± 13.3	81.5 ± 14.1	78.4 ± 14.3
MAP (mmHg)	DISO	78.9 ± 17.2	77.2 ± 12.5	76.1 ± 10.5	75.0 ± 16.2	76.6 ± 13.4
	NISO	81.1 ± 15.7	79.1 ± 14.2	79.1 ± 14.7	77.5 ± 17.1	77.9 ± 15.3
PaO_2 (mmHg)	DISO	457.5 ± 85.2	258.6 ± 68.6[ab]	198.5 ± 68.3[ab]	185.6 ± 73.2[ab]	209.6 ± 85.1[ab]
	NISO	461.5 ± 87.5	223.5 ± 89.7[a]	165.2 ± 75.3[a]	151.3 ± 68.5[a]	171.6 ± 88.9[a]

[a] $P < 0.05$ versus TLV-15 min; [b] $P < 0.05$ versus NISO group.

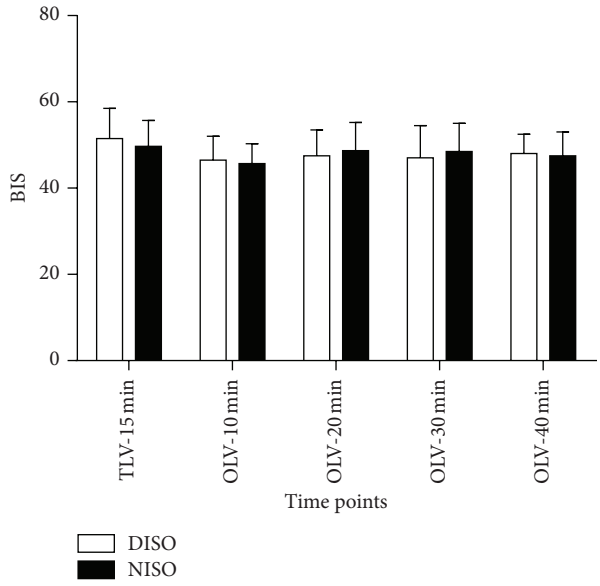

Figure 1: Perioperative time-course alterations of the bispectral index (BIS) in DISO group and NISO group. The values were measured as follows: 15 min after two-lung ventilation (TLV-15), 10 min after one-lung ventilation (OLV-10 min), 20 min after one-lung ventilation (OLV-20 min), 30 min after one-lung ventilation (OLV-30 min), and 40 min after one-lung ventilation (OLV-40 min). Data are presented as median (interquartile range).

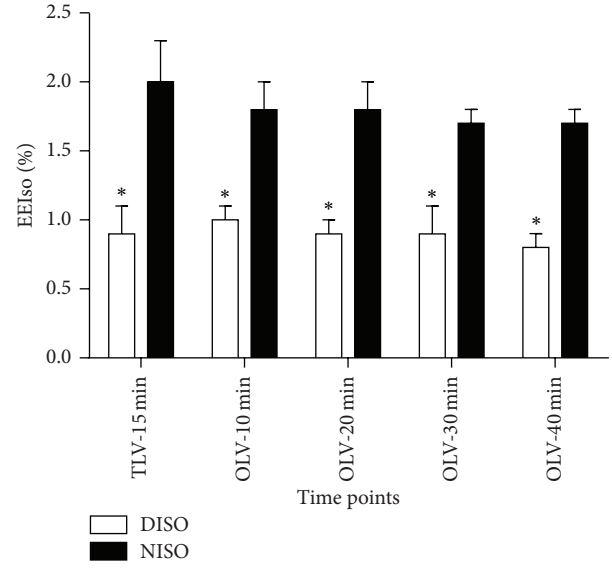

Figure 2: Perioperative time-course alterations of the end-expiratory isoflurane concentration (EEIso) in DISO group and NISO group. The values were measured as follows: 15 min after two-lung ventilation (TLV-15), 10 min after one-lung ventilation (OLV-10 min), 20 min after one-lung ventilation (OLV-20 min), 30 min after one-lung ventilation (OLV-30 min), and 40 min after one-lung ventilation (OLV-40 min). Data are presented as median (interquartile range). $^*P < 0.05$ intergroup comparison between group DISO and group NISO.

TLV to OLV, the MDA level significantly increased further in group NISO at OLV-30 min ($P < 0.05$ versus TLV-15 and versus DISO, Table 3), while MDA level did not significantly increase in group DISO. Concomitant with the change of MDA level, plasma SOD activity was significantly decreased in group NISO at OLV-30 min, which was remarkably lower than that in group DISO ($P < 0.05$, Table 3), while there was

Table 3: Changes in MDA level, SOD activity, and NO concentration in DISO group and NISO group ($\bar{x} \pm s$).

	Group	TLV-15 min	OLV-30 min
MDA (umol/L)	DISO ($n = 25$)	16.9 ± 1.7	17.5 ± 1.2^{b}
	NISO ($n = 24$)	18.3 ± 1.7	21.0 ± 1.7^{a}
SOD (ug/mL)	DISO ($n = 25$)	1.9 ± 0.2	1.8 ± 0.3^{b}
	NISO ($n = 24$)	1.9 ± 0.1	1.6 ± 0.2^{a}
NO (ug/mL)	DISO ($n = 25$)	1.9 ± 0.3	$2.3 \pm 0.3^{a;b}$
	NISO ($n = 24$)	1.9 ± 0.4	1.8 ± 0.1

[a] $P < 0.05$ versus TLV-15 min; [b] $P < 0.05$ versus NISO group.

no significant change in SOD activity in group DISO after OLV.

We have observed the changes of Qs/Qt% and PaO_2 at 5 different time points from TLV-15 min to OLV-40 min and found that, on changing from TLV to OLV, Qs/Qt% increased significantly in both groups and peaked at OLV-30 min while PaO_2 reached its lowest value at OLV-30 min in both groups. These results suggested that the time point of OLV-30 min may be the key moment for NO releasing, so we detected serum NO at the time point of OLV-30. There was no significant difference in serum NO concentration between two groups at TLV-15 min. After conversion from TLV to OLV-30 min, the serum NO concentration was significantly increased in group DISO ($P < 0.05$, Table 3), but it did not change significantly in group NISO ($P > 0.05$, Table 3), and the values of NO content at OLV-30 min was significantly higher in DISO than in NISO group.

4. Discussion

The use of intravenous infusion Dex combined inhalation isoflurane in comparison with isoflurane alone can attenuate the increase in shunt fraction and improve PaO2 in patients undergoing OLV, but the mechanism is unclear. In the current study, we further revealed that plasma MDA level remarkably increased and SOD activity decreased in isoflurane group accompanied with decreased NO concentration, while Dex-isoflurane combination significantly decreased MAD level, maintained SOD activity, and increased serum NO content during OLV. The results support our hypothesis that Dex at clinical dose combined with isoflurane can inhibit oxidative stress and increase NO release compared with volatile anesthetics alone, whereby reducing shunt fraction and improving oxygenation during one-lung ventilation.

The effect of DEX on HPV during OLV is likely dose dependent. Kernan et al. recently reported that Dex administered at a loading dose of 0.3 μg/kg and an infusion rate of 0.3 μg/kg/h did not affect HPV and oxygenation, although the PaO2/FiO2 ratio in patients receiving Dex was relatively higher [31]. However, in our previous [9] and current study, Dex at a higher loading dose of 1 μg/kg and an infusion of 0.7 μg/kg/h, combined isoflurane, significantly limited the increase in pulmonary shunt and the decrease in PaO2 in one-lung ventilated patients, compared with isoflurane alone group. In the current study, DEX-isoflurane treatment decreased plasma MDA content and kept SOD activity, an indication of attenuation of oxidative stress and improvement in the endogenous antioxidative capacity. Furthermore, Dex-isoflurane treatment increase serum NO content, an important endothelium-derived vasodilation factor. These results suggested that DEX should be provided at a dose sufficient to prevent oxidative stress.

ROS are important messengers produced in response to changes in oxygen tension and contribute to the regulation of acute HPV during hypoxia [12, 13]. Mehta et al. have shown that under sustained hypoxic conditions (1–4 hours), ROS production was decreased in nonventilation lung [14]. Consistent with Cheng et al. [16], in current study we found that plasma MDA levels were significantly increased and important antioxidant enzyme SOD activity was decreased in patients during one-lung ventilation (OLV), accompanied with increased shunt fraction and decreased PaO2, which indicates that the increased oxidative stress may impair the protective effect of HPV. Yamaguchi et al. found that, in the presence of high level of ROS and reduced endogenous SOD, HPV was considerably suppressed in the isolated rabbit lung but was restored after adding exogenous SOD in the perfusate [32]. Together with above results, our findings that Dex decreased MDA level and maintained SOD activity, concomitant with decreased shunt fraction and increased PaO2, suggested that inhibition of oxidative stress and restore antioxidant defense system may be important mechanisms whereby DEX can augment HPV during one-lung ventilation.

The decrease in shunt fraction in the Dex group occurred in conjunction with increase in nitric oxide concentration in the serum, which suggests that the changes in shunt fraction may be particularly caused by increased nitric oxide, an important endothelium-derived relaxing factor. Mam et al. found that nitroprusside caused less relaxation in the pulmonary arteries in hypoxic than in normoxic rats, suggesting decreased responsiveness of vascular smooth muscle cells (VSMCs) to vasodilators [33]. Hakim et al. found nitric oxide did not affect pulmonary vasoconstriction in hypoxia rat lung [34]. Therefore, we postulated that increased serum nitric oxide mainly affects the arteriovenous in the ventilated lung. It has been reported that inhalation of nitric oxide (iNO) decreases the regional pulmonary vascular resistance of ventilated lung area, decreases intrapulmonary shunting, and improves arterial oxygenation [23, 24], while Minamishima et al. [35] and Lang Jr. et al. [36] found that inhalation of nitric oxide can increase serum nitrite and nitrate (NO), and NO may be the most likely candidate for transducing the iNO stimulus to the organs. Therefore, all above results suggested that serum NO may play an important role in improving arterial oxygenation in ventilated lung. It is reported that Dex can induce vasodilation through activation NO synthase (NOS) [37, 38]. In the current study, Dex significantly increased serum NO concentration, concomitant with decreased shunt fraction and increased PaO2, which indicates that Dex may have induced vasodilation in the ventilated lung by enhancing NO release. In the current study isoflurane did not inhibit NO activation after OLV, while studies found that volatile anesthetics inhibit the NO-mediated relaxation in many

vascular beds [39, 40], which may partly explain why volatile anesthetics inhibit HPV.

In conclusion, intravenous infusion of the dexmedetomidine along with isoflurane inhalation during OLV inhibits oxidative stress and increases NO concentration, which may represent a mechanism whereby dexmedetomidine attenuates intrapulmonary shunt and improves arterial oxygenation during one-lung ventilation in patients.

Conflict of Interests

The authors have no potential conflict of interests to declare.

Authors' Contribution

Rui Xia and Jinjin Xu contribute equally to this study.

Acknowledgment

This study was supported by the NSFC grants (81301621).

References

[1] J. H. Campos, "Current techniques for perioperative lung isolation in adults," *Anesthesiology*, vol. 97, no. 5, pp. 1295–1301, 2002.

[2] W. Karzai and K. Schwarzkopf, "Hypoxemia during one-lung ventilation: prediction, prevention, and treatment," *Anesthesiology*, vol. 110, no. 6, pp. 1402–1411, 2009.

[3] A. M. Evans and J. P. Ward, "Hypoxic pulmonary vasoconstriction—invited article," in *Arterial Chemoreceptors*, vol. 648 of *Advances in Experimental Medicine and Biology*, pp. 351–360, 2009.

[4] J. Y. Y. Wang, G. N. Russell, R. D. Page, M. Jackson, and S. H. Pennefather, "Comparison of the effects of sevoflurane and isoflurane on arterial oxygenation during one lung ventilation," *British Journal of Anaesthesia*, vol. 81, no. 6, pp. 850–853, 1998.

[5] R. Mariappan, H. Ashokkumar, and B. Kuppuswamy, "Comparing the effects of oral clonidine premedication with intraoperative dexmedetomidine infusion on anesthetic requirement and recovery from anesthesia in patients undergoing major spine surgery," *Journal of Neurosurgical Anesthesiology*, vol. 26, no. 3, pp. 192–197, 2014.

[6] J. A. Tan and K. M. Ho, "Use of dexmedetomidine as a sedative and analgesic agent in critically ill adult patients: a meta-analysis," *Intensive Care Medicine*, vol. 36, no. 6, pp. 926–939, 2010.

[7] C. Zhou, Y. Wu, Y. Liu et al., "Dexmedetomidine inhibits inflammatory reaction in lung tissues of septic rats by suppressing TLR4/NF-κB pathway," *Mediators of Inflammation*, vol. 2013, Article ID 562154, 9 pages, 2013.

[8] L. Xianbao, Z. Hong, Z. Xu, Z. Chunfang, and C. Dunjin, "Dexmedetomidine reduced cytokine release during postpartum bleeding-induced multiple organ dysfunction syndrome in rats," *Mediators of Inflammation*, vol. 2013, Article ID 627831, 7 pages, 2013.

[9] R. Xia, H. Yin, Z. Y. Xia, Q. J. Mao, G. D. Chen, and W. Xu, "Effect of intravenous infusion of dexmedetomidine combined with inhalation of isoflurane on arterial oxygenation and intrapulmonary shunt during single-lung ventilation," *Cell Biochemistry and Biophysics*, vol. 67, no. 3, pp. 1547–1550, 2013.

[10] E. S. W. Wong, R. Y. K. Man, P. M. Vanhoutte, and K. F. J. Ng, "Dexmedetomidine induces both relaxations and contractions, via different α_2-adrenoceptor subtypes, in the isolated mesenteric artery and aorta of the rat," *Journal of Pharmacology and Experimental Therapeutics*, vol. 335, no. 3, pp. 659–664, 2010.

[11] P. Talke, E. Lobo, and R. Brown, "Systemically administered alpha2-agonist-induced peripheral vasoconstriction in humans," *Anesthesiology*, vol. 99, no. 1, pp. 65–70, 2003.

[12] P. Ariyaratnam, M. Loubani, and A. H. Morice, "Hypoxic pulmonary vasoconstriction in humans," *BioMed Research International*, vol. 2013, Article ID 623684, 8 pages, 2013.

[13] S. L. Archer, H. L. Reeve, E. Michelakis et al., "O_2 sensing is preserved in mice lacking the gp91 phox subunit of NADPH oxidase," *Proceedings of the National Academy of Sciences of the United States of America*, vol. 96, no. 14, pp. 7944–7949, 1999.

[14] J. P. Mehta, J. L. Campian, J. Guardiola, J. A. Cabrera, E. K. Weir, and J. W. Eaton, "Generation of oxidants by hypoxic human pulmonary and coronary smooth-muscle cells," *Chest*, vol. 133, no. 6, pp. 1410–1414, 2008.

[15] S. A. Gupte and M. S. Wolin, "Oxidant and redox signaling in vascular oxygen sensing: implications for systemic and pulmonary hypertension," *Antioxidants and Redox Signaling*, vol. 10, no. 6, pp. 1137–1152, 2008.

[16] Y.-D. Cheng, Y. Gao, H. Zhang, C.-J. Duan, and C.-F. Zhang, "Effects of OLV preconditioning and postconditioning on lung injury in thoracotomy," *Asian Journal of Surgery*, vol. 37, no. 2, pp. 80–85, 2014.

[17] P. Misthos, S. Katsaragakis, N. Milingos et al., "Postresectional pulmonary oxidative stress in lung cancer patients. The role of one-lung ventilation," *European Journal of Cardio-thoracic Surgery*, vol. 27, no. 3, pp. 379–383, 2005.

[18] B. Zhang, W. Niu, D. Xu et al., "Oxymatrine prevents hypoxia- and monocrotaline-induced pulmonary hypertension in rats," *Free Radical Biology and Medicine*, vol. 69, pp. 198–207, 2014.

[19] O. F. Araneda and M. Tuesta, "Lung oxidative damage by hypoxia," *Oxidative Medicine and Cellular Longevity*, vol. 2012, Article ID 856918, 18 pages, 2012.

[20] B. Cekic, S. Geze, G. Ozkan et al., "The effect of dexmedetomidine on oxidative stress during pneumoperitoneum," *BioMed Research International*, vol. 2014, Article ID 760323, 5 pages, 2014.

[21] J. Subramani, M. D. M. Leo, K. Kathirvel et al., "Essential role of nitric oxide in sepsis-induced impairment of endothelium-derived hyperpolarizing factor-mediated relaxation in rat pulmonary artery," *European Journal of Pharmacology*, vol. 630, no. 1–3, pp. 84–91, 2010.

[22] H. Sahebjami, "Inhaled nitric oxide for the adult respiratory distress syndrome," *The New England Journal of Medicine*, vol. 329, no. 3, pp. 206–207, 1993.

[23] T. Grubb, J. H. M. Frendin, A. Edner, P. Funkquist, G. Hedenstierna, and G. Nyman, "The effects of pulse-delivered inhaled nitric oxide on arterial oxygenation, ventilation-perfusion distribution and plasma endothelin-1 concentration in laterally recumbent isoflurane-anaesthetized horses," *Veterinary Anaesthesia and Analgesia*, vol. 40, no. 6, pp. e19–e30, 2013.

[24] M. Takemoto, J. Sun, J. Hiroki, H. Shimokawa, and J. K. Liao, "Rho-kinase mediates hypoxia-induced downregulation of endothelial nitric oxide synthase," *Circulation*, vol. 106, no. 1, pp. 57–62, 2002.

[25] A. V. Maltsev, Y. M. Kokoz, E. V. Evdokimovskii, O. Y. Pimenov, S. Reyes, and A. E. Alekseev, "Alpha-2 adrenoceptors and imidazoline receptors in cardiomyocytes mediate counterbalancing effect of agmatine on NO synthesis and intracellular calcium handling," *Journal of Molecular and Cellular Cardiology*, vol. 68, pp. 66–74, 2014.

[26] P. G. Roe and J. G. Jones, "Analysis of factors which affect the relationship between inspired oxygen partial pressure and arterial oxygen saturation," *British Journal of Anaesthesia*, vol. 71, no. 4, pp. 488–494, 1993.

[27] W. Yao, G. Luo, G. Zhu et al., "Propofol activation of the Nrf2 pathway is associated with amelioration of acute lung injury in a rat liver transplantation model," *Oxidative Medicine and Cellular Longevity*, vol. 2014, Article ID 258567, 9 pages, 2014.

[28] K. X. Liu, T. Rinne, W. He, F. Wang, and Z. Xia, "Propofol attenuates intestinal mucosa injury induced by intestinal ischemia-reperfusion in the rat," *Canadian Journal of Anesthesia*, vol. 54, no. 5, pp. 366–374, 2007.

[29] S. Lei, W. Su, H. Liu et al., "Nitroglycerine-induced nitrate tolerance compromises propofol protection of the endothelial cells against TNF- α: the role of PKC- β_2 and nadph oxidase," *Oxidative Medicine and Cellular Longevity*, vol. 2013, Article ID 678484, 9 pages, 2013.

[30] S. Lei, H. Li, J. Xu et al., "Hyperglycemia-induced protein kinase C β2 activation induces diastolic cardiac dysfunction in diabetic rats by impairing caveolin-3 expression and Akt/eNOS signaling," *Diabetes*, vol. 62, no. 7, pp. 2318–2328, 2013.

[31] S. Kernan, S. Rehman, T. Meyer, J. Bourbeau, N. Caron, and J. D. Tobias, "Effects of dexmedetomidine on oxygenation during one-lung ventilation for thoracic surgery in adults," *Journal of Minimal Access Surgery*, vol. 7, no. 4, pp. 227–231, 2011.

[32] K. Yamaguchi, K. Asano, T. Takasugi et al., "Modulation of hypoxic pulmonary vasoconstriction by antioxidant enzymes in red blood cells," *American Journal of Respiratory and Critical Care Medicine*, vol. 153, no. 1, pp. 211–217, 1996.

[33] V. Mam, A. F. Tanbe, S. H. Vitali, E. Arons, H. A. Christou, and R. A. Khalil, "Impaired vasoconstriction and nitric oxide-mediated relaxation in pulmonary arteries of hypoxia- and monocrotaline-induced pulmonary hypertensive rats," *Journal of Pharmacology and Experimental Therapeutics*, vol. 332, no. 2, pp. 455–562, 2010.

[34] T. S. Hakim, A. Pedoto, D. Mangar, and E. M. Camporesi, "Nitric oxide plays a minimal role in hypoxic pulmonary vasoconstriction in isolated rat lungs," *Respiratory Physiology and Neurobiology*, vol. 189, no. 1, pp. 93–98, 2013.

[35] S. Minamishima, K. Kida, K. Tokuda et al., "Inhaled nitric oxide improves outcomes after successful cardiopulmonary resuscitation in mice," *Circulation*, vol. 124, no. 15, pp. 1645–1653, 2011.

[36] J. D. Lang Jr., X. Teng, P. Chumley et al., "Inhaled NO accelerates restoration of liver function in adults following orthotopic liver transplantation," *Journal of Clinical Investigation*, vol. 117, no. 9, pp. 2583–2591, 2007.

[37] J. Feldman, L. Fellmann, and P. Bousquet, "The central hypotensive effect induced by α2-adrenergic receptor stimulation is dependent on endothelial nitric oxide synthase," *Journal of Hypertension*, vol. 26, no. 5, pp. 1033–1036, 2008.

[38] A. Snapir, P. Talke, J. Posti, M. Huiku, E. Kentala, and M. Scheinin, "Effects of nitric oxide synthase inhibition on dexmedetomidine-induced vasoconstriction in healthy human volunteers," *British Journal of Anaesthesia*, vol. 102, no. 1, pp. 38–46, 2009.

[39] Y. Vulliemoz, "The nitric oxide-cyclic 3′,5′-guanosine monophosphate signal transduction pathway in the mechanism of action of general anesthetics," *Toxicology Letters*, vol. 100-101, pp. 103–108, 1998.

[40] M. M. Arriero, L. Muñoz Alameda, A. López-Farré et al., "Sevoflurane reduces endothelium-dependent vasorelaxation: role of superoxide anion and endothelin," *Canadian Journal of Anesthesia*, vol. 49, no. 5, pp. 471–476, 2002.